STAGNATION-POINT SOLUTIONS FOR INVISCID, RADIATING SHOCK LAYERS

A thesis presented

by

Walter B. Olstad

to

The Division of Engineering and Applied Physics

in partial fulfillment of the requirements

for the degree of

Doctor of Philosophy

in the subject of

Applied Mathematics

Harvard University

Cambridge, Massachusetts

April 1966

ACKNOWLEDGMENT

The author wishes to express his sincere appreciation to his research supervisor Professor Howard W. Emmons for his guidance, criticism, and encouragement throughout the course of study. Thanks are also due the author's employer, the National Aeronautics and Space Administration, Langley Research Center, for their financial support while the author was in residence and for their support of the research and preparation of the thesis.

Grateful thanks are also extended to Mrs. Jane T. Kemper, who programed the solutions of chapter III and to Mrs. Barbara M. Buchanan, who typed the final manuscript.

Appreciation is also due the author's wife, Helen, for her patience and encouragement throughout the entire period of graduate study.

TABLE OF CONTENTS

Chapter | Page

LIST OF FIGURES

Figure Page

CHAPTER I

INTRODUCTION

As the exploration of space progresses from the near earth environment to the moon and the planets of the solar system, study of the atmospheric entry of objects in excess of escape velocity (about 11 km/sec) becomes necessary. In addition to stuides concerning manmade objects, there is considerable interest in the entry of meteoroids into the earth's atmosphere at velocities from 20 to 70 km/sec. At these large speeds radiant energy transfer is an important factor governing the behavior of the hot shock layer gas enveloping the object.

Consequently, a number of investigators have addressed themselves to the problem of the radiating shock layer. The first analyses assumed that the flow processes were uneffected by (or uncoupled from) the transfer of energy by radiation (see for example refs. 1 and 2). Thermodynamic and flow properties were calculated neglecting radiation. The radiant energy flux was then calculated from measured or theoretically determined optical properties for these conditions. While this approach provides acceptable engineering estimates at speeds less than escape velocity, it is not sufficient to describe the effects of radiation at higher speeds. The next step was to take into account the loss of energy from the shock layer due to radiation. This cooling of the shock layer tends to reduce the emergent radiant energy flux. This reduction is often termed "radiation decay." Radiation decay was studied by a number of authors (see, for example, refs. 3-8). All of the cited works, with the exception of reference 8, used the transparent approximation*, which neglects absorption within the shock layer, and assumed that the radiation cooling of the shock layer gas was small and did not influence the mass transport. The process of absorption by a gray** gas was studied in reference 8. However, the flow model used in that investigation only roughly approximates the flow in the stagnation region of a shock layer. Consequently, the analysis was unable to describe details of conditions in the shock layer or to provide reliable quantitative results.

Perhaps the most ambitious analysis to appear to date is the work of Howe and Viegas (ref. 9). They obtained numerical solutions to the integrodifferential system of equations governing the flow in the stagnation region including the effects of radiation decay, absorption by a gray gas, viscosity, and surface mass injection. An indication of the complexity of this numerical approach is the reported computation time for a single example of 5 hours on the IBM 7090 electronic digital computer.

---

*So called because the shock layer gas is considered to be transparent to its own radiation.

**A gray gas is one for which the optical properties are independent of the photon energy or wavelength.

All of the works discussed above are restricted to velocities less than about 20 km/sec, although the work of Howe and Viegas was so restricted simply because they did not choose to make calculations for higher velocities. Fay, Moffatt, and Probstein (ref. 10) undertook an analysis of meteoroid entry, in the speed range of 20 to 70 km/sec. Since they were interested only in obtaining upper bound estimates of radiant heating, they ignored radiation decay and absorption (except that they did not allow the radiant energy flux to exceed the black-body limit) both of which can be quite important at these speeds.

While the existing studies (which include many works in addition to those cited) have contributed much to the qualitative and quantitative understanding of the physical processes taking place in radiating shock layers, a great amount of work remains. For example, parametric studies of absorption in a realistic shock layer flow are lacking, the effects of surface reflectivity have been generally ignored, and there have been no reported attempts (at least in the knowledge of this investigator) to study shock layer gases with nongray optical properties.*

The investigation reported herein was undertaken to provide a parametric study of the influence of radiation on blunt objects large and small, travelling at speeds up to 70 km/sec. The approach

---

*Lick (ref. 11) and Greif (ref. 12) considered nongray optical properties in their studies of combined radiation and conduction. Their results indicated that nongray effects can be significant.

has been to seek simple approximate solutions where available in the hope that they would lead to a better understanding of the physical processes involved. The parameters to be studied include the radiation cooling parameter ϵ, which characterizes the relative importance of radiation as an energy transport mechanism compared to convection, the Bouguer number, which indicates the importance of absorption in radiant transport, the surface reflectivity, indicative of the ability of the surface of the object to accept the incident radiant energy flux, and the spectral variation of the absorption coefficient. (There is no single quantity or even group of quantities which characterizes the important effect of spectral variation on the flow.) Definitions of these parameters and their role in influencing the flow will be discussed in greater detail in subsequent chapters.

In order to facilitate this investigation without sacrificing physical significance, analysis is limited to the stagnation region and the following conditions are assumed to apply: (1) the shock layer gas is in local thermodynamic and chemical equilibrium, (2) the body geometry is axisymmetric, (3) there is no mass addition to the flow from the body surface, (4) the thicknesses of the shock and the viscous boundary layer are small in comparison to the shock standoff distance, and (5) absorption in the free stream ahead of the object is negligible.

In this investigation, solutions will be obtained for four limiting cases of the radiation cooling parameter and the Bouguer number. The first of these, which is presented in chapter III, is a small perturbation expansion in the radiation cooling parameter ϵ valid when the influence of radiation is small. The second solution, presented in chapter IV, holds when the shock layer is optically thin. This solution is presented as a small perturbation expansion in the Bouguer number. A solution valid when the shock layer is optically thick (Bouguer number $\gg 1$) and the final solution, which is restricted to the case when radiation is the principal mode of energy transport within the shock layer, are presented in chapters V and VI, respectively. The first and second solutions have been formulated to include the effects of nongray radiation. The third and fourth solutions are restricted to the gray case. In each of the four limiting cases, it is possible to approximate the governing integro-differential system of equations by a purely differential system which leads to a singular perturbation problem.

The results obtained by means of the various approximations are combined in chapter VII to give the radiant heat transfer rate and an estimate of the effect of radiation on the convective heating rate at the stagnation points of blunt objects traversing a gray model earth atmosphere. The effects of the nongray character of air on these results is discussed.

CHAPTER II. STAGNATION MODEL FOR A RADIATING SHOCK LAYER

A. Fundamental Equations of Radiation Gas Dynamics

Prior to setting up a particular flow model for the problem at hand, it is desirable to examine briefly the fundamental equations of radiation gas dynamics. An excellent discussion of these equations has been presented by Goulard in the volume "High Temperature Aspects of Hypersonic Flow" (ref. 13), and the reader is referred to this work for a more detailed exposition.

In the first chapter, it was indicated that the studies of this paper are limited to the steady flow of gases in local thermodynamic and chemical equilibrium. In addition, the effects of radiation pressure and radiation energy density are ignored. These effects are important only when the radiant energy flux is extremely large as it is deep in the interior of a stellar atmosphere. Finally, the presence of external forces, such as gravity and electromagnetic forces, are neglected. With these restrictions in mind, the conservation equations for a radiating gas can be written

$$\left(\rho u_i\right)_{,i} = 0 \qquad \text{(Continuity)} \qquad (2.1)^*$$

---

*The double subscript notation is employed.

$$\rho u_j\, u_{i,j} = p_{,i} + \tau_{ij,j} \qquad \text{(Momentum)} \tag{2.2}$$

$$\rho u_i\, h_{t,i} = -\left(u_j\, \tau_{ij}\right)_{,j} - q^C_{i,i} - q^R_{i,i} \qquad \text{(Energy)} \tag{2.3}$$

where the quantity h_t is the total specific enthalpy of the gas

$$h_t = h + \frac{1}{2} u_i\, u_i \tag{2.4}$$

The static specific enthalpy h includes the chemical energy of the gas in terms of the heats of formation of the various gaseous species.

An expression relating the thermodynamic variables is needed to complete the set of equations. A convenient form is

$$h \equiv h(p,\rho) \tag{2.5}$$

The molecular transfer processes are represented by the classical expressions

$$\tau_{ij} = \mu\left(u_{i,j} + u_{j,i}\right) + \left(\mu' - \frac{2}{3}\mu\right) \delta_{ij}\, u_{k,k} \tag{2.6}$$

$$q^C_i = -k_{eff}\, T_{,i} \tag{2.7}$$

The quantity k_{eff} is an effective coefficient of heat conduction which includes the effects of energy transport by molecular collisions and by the diffusion of reacting species. These two processes can be lumped together like this only when the conditions of local thermodynamic and chemical equilibrium hold (see ref. 14).

The radiant energy flux vector q_i^R is defined in terms of the radiation intensity J_λ.

$$q_i^R \equiv \int_0^\infty q_{\lambda i}^R \, d\lambda, \quad q_{\lambda i}^R \equiv \int_{4\pi} J_\lambda \, l_i \, d\omega \qquad (2.8)$$

and is the rate of flow of radiant energy per unit area across an element of area whose normal points in the ith direction. The quantity l_i is the direction cosine between the direction of a single beam of intensity J_λ and the ith direction. J_λ can be determined from the conservation equation of radiation transfer

$$\frac{dJ_\lambda}{ds} = -\rho\beta_\lambda\left(J_\lambda - \frac{j_\lambda}{\beta_\lambda}\right) \qquad (2.9)$$

where β_λ is the mass extinction coefficient. It is composed of the mass absorption coefficient κ_λ and the mass scattering coefficient σ_λ

$$\beta_\lambda = \kappa_\lambda + \sigma_\lambda \qquad (2.10)$$

The ratio of mass emission coefficient j_λ to the mass extinction coefficient β_λ is often called the source function $S_\lambda = j_\lambda / \beta_\lambda$.

For nonscattering media in a state of local thermodynamic equilibrium $\left(\sigma_\lambda = 0\right)$, the source function reduces to the Planck function

$$B_\lambda = \frac{2hc^2}{\lambda^5}\left(e^{hc/\lambda kT} - 1\right)^{-1} \tag{2.11}$$

provided that the mass absorption coefficient κ_λ includes the effects of induced emission. Here h and k are the Planck and Boltzmann constants, respectively, and c is the speed of light. Throughout the remainder of this paper, it is assumed that the gas in the shock layer is nonscattering. This assumption is reasonable as the number of large solid particles which might scatter radiation is expected to be negligible in the shock layer. A few such particles might exist in the cooler regions of the boundary layer adjacent to the body surface as a result of "spalling" of this surface. However, their presence could be accounted for, if necessary, by changing the effective reflectivity of the body surface.

At the extremely high shock layer temperatures for which the gas is multiply ionized and free electrons are plentifully, Thomson scattering can become important. For example, Kivel and Mayer (ref. 15) show that scattering cannot be neglected when the temperature reaches 350,000° K at densities less than about 0.01 of the sea level value.

For the nonscattering case the intensity of radiation at a point M in the direction $\vec{s}$ follows from a formal integration of equation (2.9)

$$J_\lambda^{(s)}(M) = \int_{P=Q}^{M} B_\lambda(P)\exp\left(-\tau_{\lambda,MP}\right) d\tau_{\lambda,MP} + J_\lambda^{(s)}(Q)\exp\left(-\tau_{\lambda,MQ}\right) \tag{2.12}$$

where

$$\tau_{\lambda,MP} = \int_{P}^{M} \rho\kappa_\lambda \, ds$$

is the "optical thickness"* or "optical path length"* along the beam between the points M and P. P is a "running" point on the beam between point M and the boundary point Q.

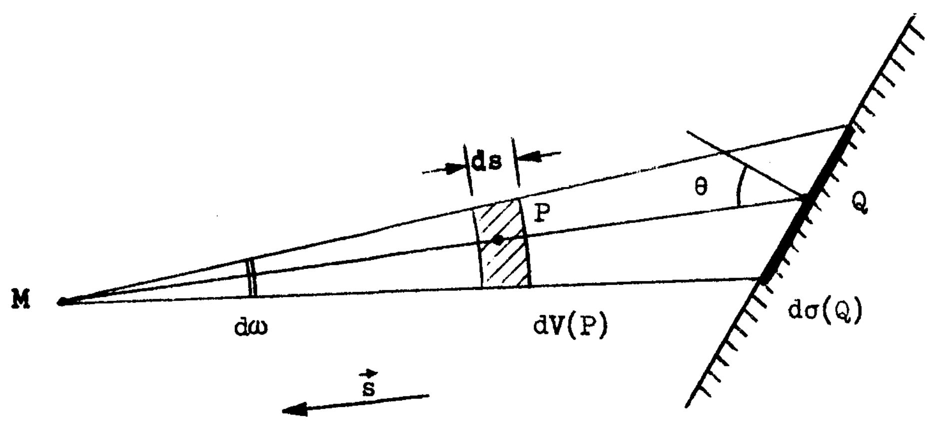

*Although the terms "optical thickness" and "optical path length," long established in astrophysical literature, seem to imply a dimension of length the quantity $\tau_{\lambda,MP}$ is dimensionless and is indicative of the number of photon mean free path lengths in the physical distance between M and P.

The quantity $J_{\lambda}^{(s)}(Q)$ represents the contribution to the intensity at point M from the boundary and, in general, includes emission from the surface, reflection from the boundary of radiation originating from within the region, and transmission through the boundary of radiation originating from without the region.

The integral term represents the summation of the contributions from all points P along the beam reduced by the attenuating factor $\exp(-\tau_{\lambda,MP})$ which acounts for absorption by the intervening matter.

The divergence of the radiation flux vector can be found with the aid of solution (2.12) with the result

$$q_{i,i}^{R} = 4\left(\rho\kappa_P\right)_M \sigma T_M^4 - \int_0^\infty \left(\rho\kappa_\lambda\right)_M \int_V \left(\rho\kappa_\lambda B_\lambda\right)_P \frac{\exp\left(-\tau_{\lambda,MP}^{(s)}\right)}{\overline{MP}^2} dV(P)d\lambda$$
$$- \int_0^\infty \left(\rho\kappa_\lambda\right)_M \int_A J_\lambda (Q) \frac{\exp\left(-\tau_{\lambda,MQ}\right)}{\overline{MQ}^2} \cos\theta \, ds(Q)d\lambda \qquad (2.13)$$

The integrations over the volume V of the gas and the area A of the bounding surface include only those portions of the volume and surface which are visible to an observer stationed at point M.

B. Stagnation Flow Model

The study of three-dimensional flow of compressible gas in the vicinity of the forward face of a blunt body cannot be reduced via transformation to the study of an equivalent one-dimensional system as can be done in the incompressible case. However, available numerical solutions (see for example refs. 15-18) indicate that for all practical purposes a reduction from a three-dimensional to a nearly equivalent one-dimensional problem can be carried out in the stagnation region. The reason that this simplification can be applied is that the flow behind a strong bow shock is nearly incompressible in the stagnation region. Also the various thermodynamic properties are nearly independent of the lateral or radial coordinate. While the same arguments apply in the stagnation region of a radiating shock layer, it is not possible to postulate the existance (even approximately) of a one-dimensional solution solely on this basis. Some additional assumption is required regarding the effect of the far-field on the radiant heat flux and its divergence. This effect, of course, cannot be obtained a priori as it depends on the solution to the entire flow field. Fortunately, the shock layer is thin and only a small portion of the radiant energy emitted by gas removed from the stagnation region actually passes through the stagnation region. If absorption is small, only a small portion of this is absorbed in the stagnation region. If, on the other hand, absorption is large, the beam is greatly attenuated when it reaches the stagnation region leaving only a small portion of the energy which started the journey to be absorbed in the stagnation region. The divergence of the radiant flux is influenced only by the amount of energy absorbed and emitted. Consequently, the far-field effect on the divergence of the radiant flux is a result of that small portion of radiant energy originating in the far-field and absorbed in the stagnation region. In the transparent and optically thick limits, this effect of the far field vanishes.

It would appear from the above discussion that a stagnation model for a radiating gas can be postulated as long as the assumptions concerning the far-field are not grossly unrealistic. In what follows, a particular stagnation model will be formulated and an estimate of the inaccuracy resulting from the assumption concerning the far field will be obtained.

A schematic of the flow in the stagnation region of a blunt body is shown below

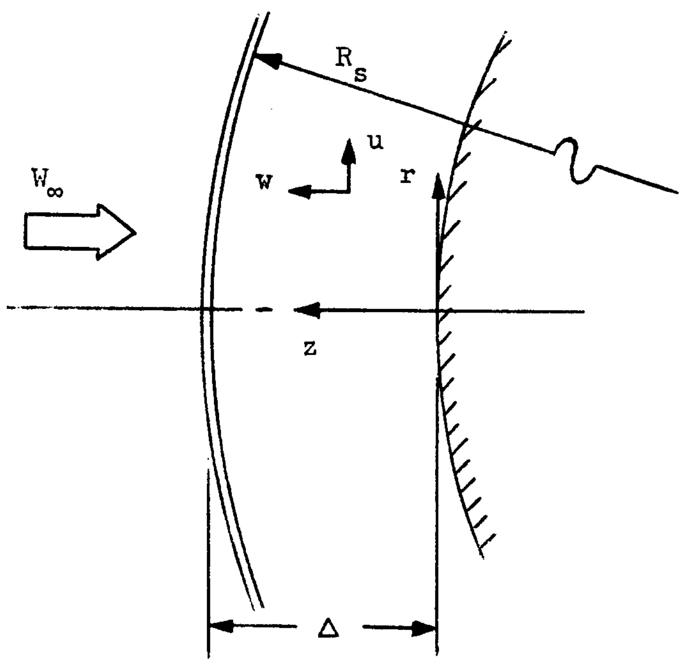

At very high speeds, the ratio of the shock standoff distance Δ to the shock radius R_s is very much smaller than one (a typical value is 0.05). Under these conditions, the geometry of the stagnation region closely resembles a plane parallel gas slab. In addition, the enthalpy in the shock layer varies slowly with respect to r/Δ so that the stagnation region may be approximately represented by a gas slab in which the thermodynamics as well as the geometry is one-dimensional.

As a result of the above considerations, the model described below has been chosen to represent the flow of a radiating gas in the stagnation region of a blunt object. The model consists of an axially symmetric flow impinging upon an infinite flat plate normal to the stream direction. At a plane which is parallel to the plate and a distance Δ in front of it, the gas is suddenly raised to a total specific enthalpy of $\frac{1}{2} W_\infty^2$. The plate is held at a constant temperature T_w. A sketch illustrating the geometry of the flow model is shown below.

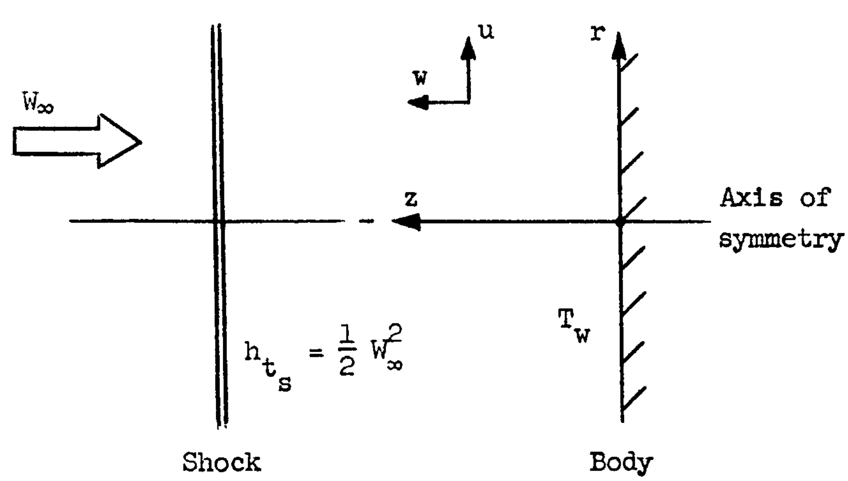

The general equations of motion (eqs. (2.1) and (2.3)) when specialized to the asisymmetric geometry become

$$\frac{\partial}{\partial r}(\rho u r) + \frac{\partial}{\partial z}(\rho w r) = 0 \tag{2.14}$$

$$\rho u \frac{\partial u}{\partial r} + \rho w \frac{\partial u}{\partial z} = - \frac{\partial p}{\partial r} + \frac{\partial \tau_{rr}}{\partial r} + \frac{\partial \tau_{rz}}{\partial z} + \frac{\tau_{rr} - \tau_{\theta\theta}}{r} \tag{2.15}$$

$$\rho u \frac{\partial w}{\partial r} + \rho w \frac{\partial w}{\partial z} = - \frac{\partial p}{\partial z} + \frac{\partial \tau_{zz}}{\partial z} + \frac{\partial \tau_{rz}}{\partial r} + \frac{\tau_{rz}}{r} \tag{2.16}$$

$$\begin{aligned} \rho u \frac{\partial h_t}{\partial r} + \rho w \frac{\partial h_t}{\partial z} = &- \frac{\partial q_r}{\partial r} - \frac{q_r}{r} - \frac{\partial q_z}{\partial z} + \frac{\partial}{\partial r}\left(u\tau_{rr} + w\tau_{rz}\right) \\ &+ \frac{1}{r}\left(u\tau_{rr} + w\tau_{rz}\right) + \frac{\partial}{\partial z}\left(u\tau_{rz} + w\tau_{zz}\right) \end{aligned} \tag{2.17}$$

where q_r and q_z are the r- and z-components, respectively, of the heat flux vector which includes, conduction, diffusion of reacting species, and radiation. The stress components are given by the expressions

$$\tau_{rr} = 2\mu \frac{\partial u}{\partial r} + \left(\mu' - \frac{2}{3}\mu\right)\left(\frac{\partial u}{\partial r} + \frac{\partial w}{\partial z} + \frac{u}{r}\right) \tag{2.18}$$

$$\tau_{zz} = 2\mu \frac{\partial w}{\partial z} + \left(\mu' - \frac{2}{3}\mu\right)\left(\frac{\partial u}{\partial r} + \frac{\partial w}{\partial z} + \frac{u}{r}\right) \tag{2.19}$$

$$\tau_{\theta\theta} = 2\mu \frac{u}{r} + \left(\mu' - \frac{2}{3}\mu\right)\left(\frac{\partial u}{\partial r} + \frac{\partial w}{\partial z} + \frac{u}{r}\right) \tag{2.20}$$

$$\tau_{zr} = \mu\left(\frac{\partial w}{\partial r} + \frac{\partial u}{\partial z}\right) \tag{2.21}$$

The equation of state is

$$h \equiv h(p,\rho) \tag{2.22}$$

In order to completely specify the problem, a consistent set of boundary conditions must be provided. The kinematical conditions on the velocity are

$$w(r,0) = 0 \tag{2.23}$$

$$\rho(r,\Delta)w(r,\Delta) = -\rho_\infty W_\infty \tag{2.24}$$

The first of these conditions restricts the analysis to one for which there is no injection from the surface of the object. When gas injection is important, it is necessary to replace the zero on the right-hand side of equation (2.23) with w_w, the normal velocity of the gas at the wall. The second condition was obtained from continuity across the normal shock at the stagnation point. A third kinematical condition is introduced here in order to relate the standoff distance Δ to the variation of the tangential velocity along the surface $z = \Delta$. This variation in velocity is taken to be equal to that behind the near normal portion of a spherical shock, that is

$$u(r,\Delta) = W_\infty \cos\beta \approx W_\infty \frac{r}{R_s} \tag{2.25}$$

where β is the local inclination of the shock from the free stream direction and R_s is the radius of the spherical shock.

The dynamical "no-slip" condition at the surface is

$$u(r,0) = 0 \tag{2.26}$$

The conditions on the enthalpy and pressure are

$$h_t\ (r,\Delta) = \frac{1}{2} W_\infty^2 \tag{2.27}$$

$$h_t\ (r,0) = h_w \tag{2.28}$$

$$p(r,\Delta) = \rho_\infty W_\infty^2 (1 - X) \left[1 - \left(\frac{r}{R_s}\right)^2\right] \tag{2.29}$$

where $X = \rho_\infty / \rho(0,\Delta)$ is the density ratio across the normal shock. Condition (2.27) comes from the conservation of energy across a strong normal shock and does not take into account absorption in the free stream of radiant energy emitted by the shock layer. Condition (2.28) restricts the analysis to those conditions at which a temperature "jump" or discontinuity is not present at the body surface. Such a "jump" can occur only when the molecular mean free path in the gas is not negligible in comparison to the characteristic length of the domain (in this case, the thickness of the thermal boundary layer). Condition (2.29) is the pressure distribution behind the near normal portion of a spherical shock of radius R_s.

In addition to the boundary conditions listed above, boundary conditions on the radiant energy flux must be specified. These conditions are:

(1) The boundary at $z = \Delta$ (which corresponds to a bow shock) is transparent.

(2) There is no radiant energy transfer from the free stream to the shock layer.

(3) The boundary at $z = 0$ (which corresponds to the body surface) is cold and reflects diffusely and independently of wavelength a fraction r_w of the incident radiation.

The statement (contained in condition (3)) that the body surface is cold means that emission from the body surface has a negligible influence on the gas in the shock layer. When the hot (temperatures in excess of 10,000° K) shock layer is optically thin emission from the relatively cool (temperatures less than 4,000° K) body surface may be comparable to emission from the shock layer gas. However, because the shock layer is optically thin very little of the radiant energy emitted at the body surface will be absorbed by the shock layer gas. On the other hand, when absorption in the shock layer is important the shock layer gas emission will approach the black-body value corresponding to the high shock layer temperature. Since black-body radiation is proportional to the fourth power of temperature the gas emission from an optically thick layer will greatly exceed the emission from the body surface. Thus whenever the body surface temperatures are small compared to the shock layer gas temperatures the influence of emission from the body surface on the shock layer gas is unimportant.

Prior to assuming that the shock layer is one-dimensional it is necessary to specify whether the body surface reflects diffusely, specularly, or in some combination of the two. However, in a one-dimensional system this specification is superfluous because the difference in effect of the two types of reflectivity vanishes. Since the surface reflectivity of most solid materials at high temperatures varies little with the wavelength, the assumption that the surface reflectivity is independent of wavelength provides a simplification in the analysis without sacrificing physical significance.

It can be seen from the definition of the total enthalpy

$$h_t = h + \frac{1}{2}\left(u^2 + w^2\right)$$

and the boundary conditions (2.24) and (2.27) that the magnitude of the kinetic energy in the shock layer is order χ^2 compared with the static specific enthalpy. For a strong shock, which is the only case of interest here, 0.05 is a typical value for χ, the density ratio across the shock. As a consequence of the above the kinetic energy terms will be neglected in the subsequent analysis. The viscous dissipation terms (the last three terms on the right-hand side of equation (2.17)) will also be neglected because only kinetic energy is dissipated through the action of the viscous forces.

It is desired that the solutions to the one-dimensional model represent, as closely as possible, the phenomena in the stagnation region of a blunt body. For simplicity, the blunt body geometry, flow field, and thermodynamic properties are considered to be axially symmetric about the stagnation streamline. Expanding the solutions for the real blunt body problem in terms of the radial coordinate r and arguing on physical grounds that $w(r,z)$, $p(r,z)$, $\rho(r,z)$, and $h(r,z)$ are even functions of r while $u(r,z)$ is odd, gives

$$\begin{aligned} w &= w^{(0)}(z) + O(r^2) \\ u &= ru^{(1)}(z) + O(r^3) \\ p &= p^{(0)}(z) + O(r^2) \\ \rho &= \rho^{(0)}(z) + O(r^2) \\ h &= h^{(0)}(Z) + O(r^2) \end{aligned} \tag{2.30}$$

In addition, the heat flux components will have the form

$$\begin{aligned} q_z &= q_z^{(0)}(z) + O(r^2) \\ q_r &= rq_r^{(1)}(z) + O(r^3) \end{aligned} \tag{2.31}$$

Neglecting terms of order r^2 and higher restricts the solutions to the vicinity of the stagnation point. Since stagnation region solutions are desired, it will be assumed that the solutions in the plane parallel model have the functional forms of equations (2.30) and (2.31) truncated after the linear term in r. For these assumed forms, the continuity equation (2.14) requires

$$\rho u = r g'(z)$$
$$\rho w = -2g(z) \tag{2.32}$$

That portion of the heat flux due to conduction and diffusion of reaction species is proportional to the enthalpy gradient, that is

$$q_z{}^c \sim \frac{dh}{dz}, \quad q_r{}^c \sim \frac{dh}{dr}$$

From conservation of energy across the near normal portion of a strong spherical shock

$$h \sim \frac{1}{2} W_\infty^2 \left[1 - \frac{1}{2} \left(\frac{r}{R_s} \right)^2 \right]$$

Thus

$$q_z{}^c \sim \frac{1}{2} W_\infty^2 / \Delta, \quad q_r{}^c \sim \frac{1}{2} W_\infty^2 \left(\frac{\Delta}{R_s} \right)^2 \Big/ \Delta$$

Comparing terms that appear in the energy equation one finds that

$$\left(\frac{\partial q_r{}^c}{\partial r} + \frac{q_r{}^c}{r} \right) \Big/ \frac{\partial q_z{}^c}{\partial z} \sim \left(\frac{\Delta}{R_s} \right)^2 \ll 1$$

Thus, the terms containing $q_r{}^c$ can be neglected in the formulation of the stagnation flow model.

If the shock layer is optically thick, that is the photon mean free path is very small compared to the shock standoff distance, the radiation flux terms take on the same form as the conduction terms* and $\partial q_r^R / \partial r + q_r^R / r$ may be neglected. On the other hand, if the gas is not optically thick, this simple order of magnitude analysis no longer suffices because the divergence of the radiant energy flux depends not only on local conditions, but on conditions throughout all of the shock heated gas which can be seen by an observer located at the point in question.

Calculations were made of the divergence of the radiant flux for a gray isothermal gas in a shock layer formed by two concentric spherical surfaces with a standoff distance to shock radius ratio of 0.05. A sketch showing the volume of gas which contributes to the radiant flux at a point on the stagnation streamline is shown below.

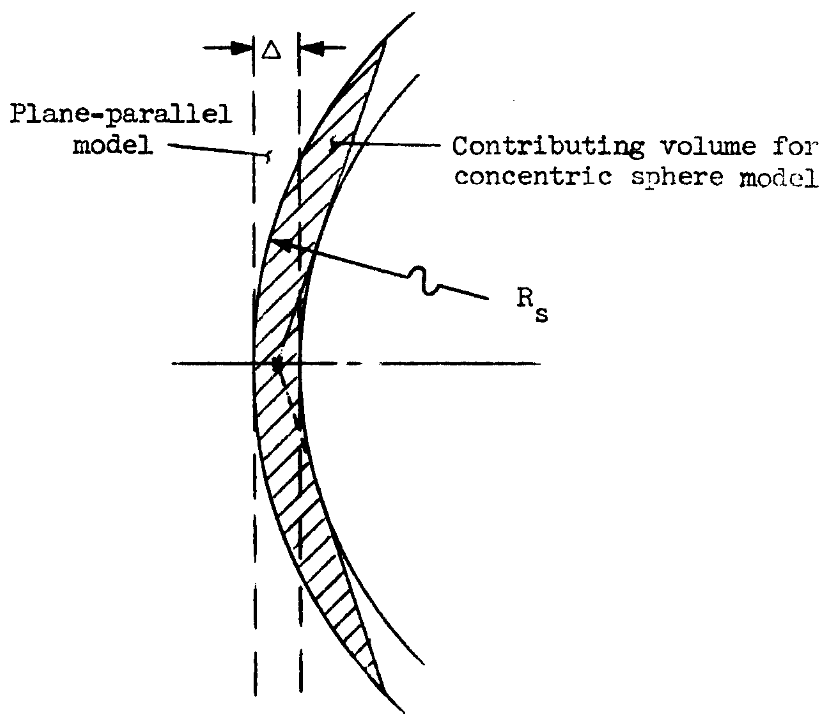

*According to the Rosseland or diffusion approximation.

The largest difference between this result and the divergence of the radiant flux for a plane-parallel layer occurred adjacent to the wall for an optical thickness of about 0.13. The difference amounted to 2.2 percent of the value for the plane-parallel layer.

A second set of calculations was made to determine the effect of a nonuniform enthalpy distribution, in the lateral direction, on the magnitude of the divergence of the radiant flux. The enthalpy distribution was given by

$$h(r) = \begin{cases} h(0)\left[1 - \frac{1}{2}\left(\frac{\Delta}{R_s}\right)^2 \left(\frac{r}{\Delta}\right)^2\right], & \text{for } r \leq \sqrt{2}R_s \\ 0, \text{ for } r > \sqrt{2}R_s \end{cases} \tag{2.33}$$

This expression approximately corresponds to the enthalpy distribution in the shock layer about a spherical body. The absorption coefficient was assumed to vary as the third power of the enthalpy* and the shock standoff distance to shock radius ratio, Δ/R_s, was chosen to be 0.05. A comparison of calculations for a plane-parallel layer in which the enthalpy was assumed to vary according to equation (2.33) and of calculations for a plane-parallel layer in which the lateral enthalpy distribution was uniform (i.e., $h(r) = h(0)$) indicated that the largest difference in the magnitude of the

---

*This variation is consistent with the correlations of the optical properties of air to be discussed in a subsequent section of this chapter.

divergence of the radiant flux occurred for a shock layer optical thickness of about 0.1. This difference amounted to 2.8 percent of the value for the uniform distribution. These results are independent of the value of $h(0)$.

Since the errors in the divergence of the radiation flux for the one-dimensional shock layer due to the separate effects of geometry and nonuniform lateral distribution of enthalpy are small, their combined effect should be given approximately by the sum of the separate effects. That is, the maximum error due to the combined effects of geometry and nonuniform lateral distribution is probably not much greater than 5 percent for $\Delta/R_s = 0.05$. This, of course, does not imply that the final results for the enthalpy (for example) would be in error by 5 percent but only that one term in the energy equation is in error by 5 percent. In any event, the results of the calculations mentioned above are considered to give sufficient justification for choosing the plane-parallel layer as a model for the stagnation region of a blunt body.

The expression for the radiant energy flux is more seriously affected by the plane-parallel layer assumption than is the divergence. For example, Koh (ref. 19) has computed the radiant flux at the wall for an isothermal shock layer formed by two concentric spheres. For a shock standoff distance to body nose radius ratio of 0.05 and a vanishingly small value of optical thickness the result is about 17 percent less than for a plane-parallel isothermal layer of equal optical thickness. This difference decreases with increasing optical thickness. Koh also computed the effect of nonuniform lateral enthalpy distribution using an assumed enthalpy distribution similar to that given by equation (2.33). He found that the flux at the wall for the nonuniform distribution was about 1.5 percent less than that for an isothermal layer for a shock standoff distance to shock radius ratio $\Delta/R_s = 0.05$ and a vanishingly small optical thickness. As expected, the difference decreases as the optical thickness increases.

It is apparent from Koh's results, that an accurate estimate to the rate of radiant heat transfer to the stagnation point cannot be obtained through the use of the plane-parallel layer approximation unless some correction factor, which takes into account the actual geometry of the shock layer, is employed. However, because this investigation is concerned with obtaining a general understanding of the problem of radiating shock layers rather than specific numerical results, such a correction factor will not be used herein.

At this point, it is convenient to introduce the variable transformation

$$\eta = \int_0^z \rho dz \tag{2.34}$$

The new variable η is often called the Dorodnitsyn variable. Under this transformation, the normal and tangential velocity components become

$$w = -2f(\eta)\,\frac{dz}{d\eta} \tag{2.35a}$$

$$u = rf'(\eta) \tag{2.35b}$$

The two momentum equations (eqs. (2.15) and (2.16)) take the form

$$\left[\rho\, f''(\eta)\right]' + 2f(\eta)\, f''(\eta) - \left[f'(n)\right]^2 = \frac{1}{\rho r}\,\frac{\partial p}{\partial r} \tag{2.36}$$

and

$$\begin{aligned} &\rho\mu f''(\eta) - 2\rho\left[\mu\left(f'(\eta) - \frac{1}{\rho}\,\rho'(\eta)\, f(\eta)\right)\right]' \\ &+ \rho\left[\left(\mu' - \frac{2}{3}\,\mu\right)\frac{1}{\rho}\,\rho'(\eta)\, f(\eta)\right]' - 2f(\eta)\, f'(\eta) \\ &+ \frac{2}{\rho}\,\rho'(\eta)\left[f(\eta)\right]^2 = +\,\frac{1}{2}\,\rho p'(\eta) \end{aligned} \tag{2.37}$$

An order of magnitude analysis of equation (2.37) indicates that $p'(\eta)$ is order X or Re^{-1}, whichever is larger. Since both X and Re^{-1} are very small compared to unity equation (2.37) will be replaced by the simple approximate expression

$$p'(\eta) = 0 \tag{2.38}$$

Thus, the pressure is a function of r only. In particular, the strong shock relations for the near normal portion of a spherical shock give

$$p(r) = \rho_\infty\, W_\infty^{\,2}\,(1 - X)\left[1 - \left(\frac{r}{R_s}\right)^2\right] + O\left(r^4\right) \tag{2.39}$$

To first-order in r

$$\frac{1}{r}\frac{\partial p}{\partial r} = -2\rho_\infty W_\infty{}^2 (1 - X)\frac{1}{R_s{}^2}$$

so that equation (2.36) becomes

$$\left[\rho\mu f''(\eta)\right]' + 2f(\eta)\, f''(\eta) - \left[f'(\eta)\right]^2 = -\frac{2\rho_\infty W_\infty{}^2 (1 - X)}{\rho R_s{}^2} \tag{2.40}$$

Under the foregoing assumptions and the coordinate transformation, the energy equation (eq. (2.17)) becomes

$$-2f(\eta)\, h'(\eta) + q'(\eta) = 0 \tag{2.41}$$

The boundary conditions are

$$f(0) = 0 \tag{2.42}$$

$$f'(0) = 0 \tag{2.43}$$

$$f\left(\eta_\Delta\right) = \frac{1}{2}\rho_\infty W_\infty \tag{2.44}$$

$$f'\left(\eta_\Delta\right) = \frac{W_\infty}{R_s} \tag{2.45}$$

$$h(0) = h_w \tag{2.46}$$

$$h\left(\eta_\Delta\right) = \frac{1}{2} W_\infty{}^2 \tag{2.47}$$

where

$$\eta_\Delta = \int_0^\Delta \rho dz \tag{2.48}$$

The heat flux term $q(\eta)$ in the energy equation (2.41) is composed of a combined conduction and diffusion term

$$q^c(\eta) = -\rho k T'(\eta) = -\frac{\rho\mu}{Pr} h'(\eta) \tag{2.49}$$

and a radiation term

$$\begin{aligned} q^R(\eta) = -2\pi \int_0^\infty \Bigg\{ & \int_{\tau_\lambda}^{\tau_{\lambda_\Delta}} B_\lambda\left(t_\lambda\right) E_2\left(t_\lambda - \tau_\lambda\right) dt_\lambda \\ & - \int_0^{\tau_\lambda} B_\lambda\left(t_\lambda\right) E_2\left(\tau_\lambda - t_\lambda\right) dt_\lambda \\ & -2r_w E_3\left(\tau_\lambda\right) \int_0^{\tau_{\lambda_\Delta}} B_\lambda\left(t_\lambda\right) E_2\left(t_\lambda\right) dt_\lambda \Bigg\} d\lambda \end{aligned} \tag{2.50}$$

This radiation term is representative of the case of a plane-parallel geometry with a transparent wall (shock) and a cold wall, which reflects diffusely and independently of wavelength a fraction r_w of the incident radiation, separated by a nonscattering, nongray gas. The variable τ_λ is called the "optical path length" and is defined by the expression

$$\tau_\lambda = \int_0^z \rho\kappa_\lambda \, dz = \int_0^\eta \kappa_\lambda \, d\eta \qquad (2.51)$$

Expression (2.50) was specialized from the more general expression of Goulard (ref. 1). Goulard derived the expression for the radiant flux in a plane parallel geometry with arbitrary reflecting, absorbing, and emitting walls separated by a nonscattering, nongray gas. His expression was restricted to isotropically emitting and diffusely reflecting surfaces and hence, so is equation (2.50). However, this restriction is of little consequence in this problem because emission from the wall will be neglected (the wall is cold) and there is no difference in effect between specular and diffuse reflection in the one-dimensional case.

The first term in equation (2.50) represents the radiant energy flux passing through the plane τ_λ = const. and which originated in the region between this plane and the shock at $\tau_\lambda = \tau_{\lambda_\Delta}$. This radiant flux has been attenuated by partial absorption in the intervening gas. The second term represents the radiant energy flux passing through the plane τ_λ = const. and which originated in the region between this plane and the wall at $\tau_\lambda = 0$. This flux has also been attenuated by partial absorption in the intervening gas. The last term represents the radiant flux passing through the plane τ_λ = const. and which was reflected from the wall and attenuated by the intervening absorbing gas.

Substituting the expressions for the energy flux equations (2.49) and (2.50) into the energy equation (2.41) gives

$$2f(\eta)\, h'(\eta) + \left[\frac{\rho\mu}{Pr} h'(\eta)\right]' + I\left[\eta\right] = 0 \tag{2.52}$$

where the divergence of the radiant flux is represented by the integral term

$$\begin{aligned} I\left[\eta\right] = &-4\pi\, \kappa_P(\eta)\, B(\eta) \\ &+ 2\pi \int_0^\infty \kappa_\lambda(\eta) \left\{ \int_0^{\eta_\Delta} \kappa_\lambda(\eta')\, B_\lambda(\eta')\, E_1\left(\left|\tau_\lambda(\eta) - \tau_\lambda(\eta')\right|\right) d\eta' \right. \\ &\left. + 2r_w\, E_2\left(\tau_\lambda(\eta)\right) \int_0^{\eta_\Delta} \kappa_\lambda(\eta')\, B_\lambda(\eta')\, E_2\left(\tau_\lambda(\eta')\right) d\eta' \right\} d\lambda \end{aligned} \tag{2.53}$$

The final step in the derivation is to reduce the equation to nondimensional form. For this purpose, the following set of nondimensional quantities is introduced

$$\begin{aligned} &\eta = \rho_s\, \Delta_A\, \bar{\eta}, \quad f(\eta) = \frac{1}{2}\, \rho_\infty W_\infty f(\bar{\eta}), \quad h(\eta) = \frac{1}{2}\, W_\infty^{\ 2}\, \bar{h}(\eta) \\ &\frac{\rho\mu}{Pr} = \left(\frac{\rho_s\, \mu_s}{Pr_s}\right) \mathcal{F}_1(\bar{h}), \quad \rho\mu = \left(\rho_s\, \mu_s\right) \mathcal{F}_2(\bar{h}), \quad \rho^{-1} = \rho_s^{-1} \mathcal{F}_3(\bar{h}) \\ &I\left[\eta\right] = 2\sigma T_s^{\ 4}\, \kappa_{P_s}\, \bar{I}\left[\bar{\eta}\right], \quad \kappa_\lambda(\eta) = \kappa_{P_s}\, \bar{\kappa}_\lambda(\bar{\eta}), \quad \tau_\lambda(\eta) = k_P\, \bar{\tau}_\lambda(\bar{\eta}) \\ &B_\lambda(\eta) = \frac{\sigma T_s^{\ 4}}{\pi}\, \bar{B}_\lambda(\bar{\eta}), \quad a^2 = 8\left(\frac{1 - X}{X}\right)\left(\frac{\Delta_A}{R_s}\right)^2 \end{aligned} \tag{2.54}$$

$$Pr_s = \frac{\mu_s \, c_{p_s}}{k_s}, \quad Re_s = \frac{\rho_\infty \, W_\infty \, \Delta_A}{\mu_s}, \quad Pe_s = Pr_s \, Re_s$$

$$\Gamma = \frac{4\sigma T_s^4}{\rho_\infty \, W_\infty^3}, \; k_P = \rho_s \, \kappa_{P_s} \, \Delta_A, \quad \epsilon = k_P \, \Gamma \tag{2.54}$$

The subscripts ∞ and s indicate conditions evaluated in the undisturbed free stream and immediately behind the shock, respectively. The quantity Δ_A is the shock standoff distance for the nonradiating (or adiabatic) shock layer. The property variations represented by $\mathfrak{F}_1$, $\mathfrak{F}_2$, and $\mathfrak{F}_3$ are functions of $\bar{h}$ only as the gas is in local thermodynamic and chemical equilibrium and the pressure has been assumed constant throughout the stagnation region. The quantities Pr_s, Re_s, and Pe_s are the Prandtl, Reynolds, and Peclet numbers, respectively, based on conditions immediately behind the shock. The parameters Γ, k_P, and ϵ are the inverse of the Boltzmann number, the Bouguer number, and the radiation cooling parameter, respectively. These parameters are fundamental to the study of radiation gas dynamics and have been discussed by a number of investigators (see, for example, refs. 21 and 22).

Substituting the above listed nondimensional quantities into equations (2.40), (2.42) through (2.47), (2.52), and (2.53) yields the nondimensional system governing the flow in the stagnation region of a blunt body traveling at hypersonic speeds.

$$\bar{f}(\bar{\eta})\ \bar{h}'(\bar{\eta}) + Pe_s^{-1}\left[\mathcal{J}_1(\bar{h})\ \bar{h}(\bar{\eta})\right]' + \epsilon \bar{I}\left[\bar{\eta}\right] = 0 \qquad (2.55)$$

$$2Re_s^{-1}\left[\mathcal{J}_2(\bar{h})\ \bar{f}''(\bar{\eta})\right]' + 2\bar{f}(\bar{\eta})\ \bar{f}''(\bar{\eta}) - \left[\bar{f}(\bar{\eta})\right]^2 + a^2\mathcal{J}_3(\bar{h}) = 0 \qquad (2.56)$$

$$\bar{f}(0) = 0 \qquad (2.57)$$

$$\bar{f}'(0) = 0 \qquad (2.58)$$

$$\bar{f}\left(\bar{\eta}_\Delta\right) = 1 \qquad (2.59)$$

$$\bar{f}'\left(\bar{\eta}_\Delta\right) = \frac{2}{X}\left(\frac{\Delta_A}{R_s}\right) = \frac{a}{\sqrt{2X(1 - X)}} \qquad (2.60)$$

$$\bar{h}(0) = \bar{h}_w = \frac{1}{2} W_\infty^2\ h_w \qquad (2.61)$$

$$\bar{h}\left(\bar{\eta}_\Delta\right) = 1 \qquad (2.62)$$

where $\bar{\eta}_\Delta$ is the value of the nondimensional Dorodnitsyn variable at the shock. This quantity is determined from the expression

$$\frac{\Delta}{\Delta_A} = \int_0^{\bar{\eta}_\Delta} \bar{h}(\bar{\eta})d\bar{\eta} \qquad (2.63)$$

The integral term $\bar{I}\left[\bar{\eta}\right]$ is given by the expression.

$$\bar{I}\left[\bar{\eta}\right] = -2\bar{\kappa}_P(\bar{\eta})\ \bar{B}(\bar{\eta})$$

$$+ k_P \int_0^{\infty} \bar{\kappa}_\lambda(\bar{\eta}) \left\{ \int_0^{\bar{\eta}_\Delta} \bar{\kappa}_\lambda(\bar{\eta}')\ \bar{B}_\lambda(\bar{\eta}')\ E_1\left(k_P \left|\bar{\tau}_\lambda(\bar{\eta}') - \bar{\tau}_\lambda(\bar{\eta})\right|\right) d\bar{\eta}' \right. \tag{2.64}$$

$$\left. + 2r_w\ E_2\left(k_P\ \bar{\tau}_\lambda(\bar{\eta})\right) \int_0^{\bar{\eta}_\Delta} \bar{\kappa}_\lambda(\bar{\eta}')\ \bar{B}_\lambda(\bar{\eta}')\ E_2\left(k_P\ \bar{\tau}_\lambda(\bar{\eta}')\right) d\bar{\eta}' \right\} d\lambda$$

In two chapters (V and VI) of this paper, it will be convenient to express the energy equation in terms of the optical path length as independent variable. In both cases the optical properties of the gas will be assumed to be independent of wavelength. In this event, the energy equation (less the thermal conductivity term) becomes

$$\bar{f}(\bar{\tau})\ \bar{h}'(\bar{\tau}) + \epsilon\bar{I}\left[\bar{\tau}\right] = 0 \tag{2.65}$$

where

$$\bar{I}\left[\bar{\tau}\right] = \frac{1}{\bar{\kappa}(\bar{\eta})}\ \bar{I}\left[\bar{\eta}\right] = -2\bar{B}(\bar{\tau})$$

$$+ k_P \left\{ \int_0^{\bar{\tau}_\Delta} \bar{B}(\bar{t})\ E_1\left(k_P \left|\bar{\tau} - \bar{t}\right|\right) d\bar{t} \right. \tag{2.66}$$

$$\left. + 2r_w\ E_2\left(k_P\ \bar{\tau}\right) \int_0^{\bar{\tau}_\Delta} \bar{B}(\bar{t})\ E_2\left(k_P\ \bar{t}\right) d\bar{t} \right\}$$

Throughout the remainder of this paper, the bars over the nondimensional variables will be dropped. This should not lead to any confusion because only the nondimensional form of the governing equations will be employed.

C. The Divergence of the Radiant Flux

The nondimensional form of the divergence of the radiant flux is

$$\epsilon I\left[\eta\right] = -2\epsilon\kappa_P(\eta)\ B(\eta)$$

$$+ \epsilon k_P \int_0^\infty \kappa_\lambda(\eta)\left\{\int_0^{\eta_\Delta} \kappa_\lambda(\eta')\ B_\lambda(\eta') E_1\Big(k_P \left|\tau_\lambda(\eta) - \tau_\lambda(\eta')\right|\Big) d\eta'\right.$$

$$\left. + 2r_w\ E_2\Big(k_P\ \tau_\lambda(\eta)\Big) \int_0^{\eta_\Delta} \kappa_\lambda(\eta')\ B_\lambda(\eta')\ E_2\Big(k_P\ \tau_\lambda(\eta')\Big) d\eta'\right\} d\lambda \qquad (2.67)$$

The first term on the right-hand-side of this expression is the local emission term which represents the rate at which energy is emitted per unit volume of gas at the location η. The integration over all wavelengths λ has been performed for this term with the aid of the definition of the Planck mean mass absorption coefficient (see below). The second and third terms represent the rate at which radiant energy is absorbed per unit volume at the location η.

It is the presence of the second and third terms which so greatly complicate the radiation problem. These terms are integral expressions. In addition, their presence makes it impossible to define a wavelength averaged absorption coefficient by which the wavelength dependence might be eliminated. The importance of these terms is indicated by the magnitude of the Bouguer number k_p which is the ratio of the shock standoff distance for a nonradiating shock layer to the photon mean free path evaluated at conditions immediately behind the shock.

The radiation cooling parameter ϵ is a ratio of the rate of energy loss per unit area by radiation from both sides of a non-absorbing isothermal layer of gas of thickness Δ_A to the rate at which kinetic energy enters the shock layer per unit area of shock surface. Alternatively, the parameter ϵ may be interpreted as the ratio of the radiationless standoff distance to the decay length where the decay length is the length required by an element of gas to lose all the energy it possessed upon emerging from the normal shock if it loses this energy by radiating (without reabsorbing) at a constant rate. This parameter modifies the entire radiation term and thus, acts as a measure of the relative efficiency of radiation compared to convection as energy transport mechanisms within the shock layer. In addition, the surface reflectivity r_w and the wavelength dependence of the absorption coefficient influence the character of the radiation terms and will be considered as parameters in this study.

Most investigators who have studied problems in which a term similar to $I[\eta]$ appears have assumed that the gas and its surroundings are gray, that is the optical properties are independent of wavelength. This allows the integration over frequency to be performed analytically. Accurate results can be achieved in the two extreme cases of optically thin $\left(\tau_\Delta \ll 1\right)$ and optically thick $\left(\tau_\Delta \gg 1\right)$ gases. When the gas is optically thin at all wavelengths, the gray absorption coefficient is correctly given by the Planck mean mass absorption coefficient

$$\kappa_P = \frac{\pi}{\sigma T^4} \int_0^\infty \kappa_\lambda B_\lambda \, d\lambda \tag{2.68}$$

Where κ_λ is the monochromatic mass absorption coefficient and the weighting function B_λ is the Planck black-body function. When the gas is optically thick at all wavelengths, the gray absorption coefficient, in the interior of the gas, is correctly given by the Rosseland mean mass absorption coefficient

$$\kappa_R = \left(\int_0^\infty \frac{\partial B_\lambda}{\partial T} \, d\lambda\right) \Bigg/ \left(\int_0^\infty \kappa_\lambda^{-1} \frac{\partial B_\lambda}{\partial T} \, d\lambda\right) \tag{2.69}$$

Near a radiation boundary or in regions of rapid (with respect to the optical path length) variations in thermodynamic properties the Rosseland mean is not valid. At intermediate values of optical depth, no single mean absorption coefficient, which depends only on local thermodynamic conditions can be defined. In fact, as has been pointed out by Krook (ref. 23) it would be necessary to define an infinite number of such mean coefficients. This, of course, does not preclude the possibility of defining approximate mean coefficients under these conditions.

Stone (ref. 24) introduced a model in which the monochromatic absorption coefficient was a step function of frequency with the size of the steps independent of the geometry or thermodynamics of the system. By means of this method, the integral over all wavelengths is reduced to a finite series. Carrier and Averrett (ref. 25) considered an absorption coefficient with only two steps, one of which was very much larger than the other. Both of the papers noted above were concerned with Milne's problem of a stellar atmosphere in radiative equilibrium. Lick (ref. 11) and later Grief (ref. 12) studied the problem of one-dimensional energy transfer between two walls separated by a radiating and conducting gas. A picket fence model, which is a specialization of the step function model, for the absorption coefficient was used. Krook (ref. 26) derived expressions by means of the P-L-K perturbation procedure for a slightly nongray gas. The solution represents a perturbation to the gray gas solution. Rhyming (ref. 27) considered wave propagation in a simple dissociating flow of a radiating gas where the absorption coefficient was given as a Gaussian function of the frequency.

However, even with the above simple models for the absorption coefficient, the term $I[\eta]$ retains an integral character and the solution to the set of e uation is still very difficult to obtain. Numerical procedures are extremely tedious. For example, it was pointed out in reference 9 that the time to obtain solutions on the IBM 7090 to a similar (though not idential) set of equations with the gray gas assumption ranged from 20 minutes to 5 hours. As a result of this difficulty, several approximate analytical methods have been derived in order to reduce this term to purely differential form. One such technique is the Milne-Eddington approximation (ref. 28), the derivation of which has been based on physical considerations, but which may also be thought of as a substitute kernal approximation (ref. 29). The integral terms can then be eliminated by means of a double differentiation (for a gray gas only). Of course, this increases the order of the differential equation by two. This technique has been used by a number of authors in the study of the dynamics of radiating gases (see for example, refs. 30 and 31).* Barbier (ref. 28) introduced the method of expanding the source function in a Taylor series about the zero of the argument of the exponential integral kernal, $E_1\left(\left|\tau_\lambda(\eta) - \tau_\lambda(\eta')\right|\right)$. Because the kernal function has a logarithmic singularity at the zero of its argument, the integral over the first few terms of the series should provide a good approximation. The resulting integrals can then be evaluated analytically and the equation becomes purely differential in character. Yoshikawa and Chapman (ref. 8), Thomas (ref. 33), and Viskanta (ref. 34) all used the method of Barbier to different degrees of approximation.

---

*Traugott (ref. 32) has introduced a "method of moments" in order to reduce the integral term to differential form. This method may be taken to any degree of approximation desired (not without a considerable sacrifice in simplicity however). The first approximation is identical to the Milne-Eddington approximation. Traugott's higher approximations can also be obtained by a substitute kernal method similar to that of Krook (ref. 29).

When more than the constant term in the Taylor series is retained, it may become necessary to introduce additional boundary conditions. In fact, it may not be enough to merely specify a new condition, it may be necessary to modify the existing conditions as well so that in the limit as the parameter $N = k\kappa/4\sigma T_o^3$ (for example) tends to zero, the solution will approach the proper pure radiation solution.* Apparently, this point was overlooked by Viskanta. In his paper, Viskanta blamed the failure of his pure radiation solutions for a finite optical thickness to exhibit a temperature jump at the wall on a premature truncation of the Taylor series expansion of the source function $B(\tau)$. Actually, this failure was a result of improperly specifying the boundary conditions.

The diffusion approximation for optically thick gases has been used extensively in astrophysics and gas dynamics. Probstein (ref. 35) has shown how to extend the usefulness of this approximation to gas layers of finite optical thickness by means of radiation slip boundary conditions. It is not at all clear, however, that these slip conditions can be used in the problem of this paper because of the presence of the convection term $\rho w dh/dz$.

---

*This parameter, which appears in the literature concerning energy transport by radiation and conduction, represents the relative importance of conduction compared to radiation. When N tends to zero radiation is the dominant mode of energy transport.

The optically thin approximation of hot gases, in which absorption is neglected in comparison to emission has also been used extensively in gas dynamics. As Thomas (ref. 33) has pointed out, this approximation is not valid in those portions of the gas which are considerably cooler than the remainder of the gas.

In this paper, the integral term $I[\eta]$ will be reduced to algebraic or differential form through the use of various approximations similar to those described above. The manner in which this is to be accomplished will depend on the order of magnitude of the parameters ϵ and k_p and will be discussed in detail in the next four chapters. Whenever possible, the gas will be treated as nongray.

D. The Inviscid Shock Layer

As was pointed out in chapter I, the studies of this paper will be concerned only with those cases for which the thicknesses of the wall boundary layers due to the presence of viscosity and thermal conductivity are very much less than the shock standoff distance. For a nonradiating gas, the shock layer can be separated into an outer inviscid and nonheat conducting region and an inner viscous and heat conducting region or boundary layer. Considerable simplication will result if a similar separation can be achieved in the case of a radiating gas. As will be shown, such a separation can be obtained when the boundary is either optically thin or optically thick. Only the former situation will be considered herein. The method of separation follows the procedures delineated by Van Dyke (ref. 36). Mathematical details are presented in appendix A.

It is shown in the appendix that the significant parameter which determines the extent of the boundary layer is the inverse square root of the Péclet number, $Pe^{-1/2}$. The zero-order in $Pe^{-1/2}$ system of equations which governs the flow in the inviscid region is

$$f_o(\eta)\, h_o'(\eta) + \epsilon I_d\left[\eta\right] = 0 \tag{2.70}$$

$$2f_o(\eta)\, f_o''(\eta) - \left[f_o'(\eta)\right]^2 + a^2 \mathcal{J}_3(h) = 0 \tag{2.71}$$

$$f_o(0) = 0 \tag{2.72}$$

$$f_o\left(\eta_\Delta\right) = 1 \tag{2.73}$$

$$f_o'\left(\eta_\Delta\right) = \frac{2}{X}\left(\frac{\Delta_A}{R_s}\right) = \frac{a}{\sqrt{2X(1-X)}} \tag{2.74}$$

$$h_o\left(\eta_\Delta\right) = 1 \tag{2.75}$$

The dependent variables $f_o(\eta)$ and $h_o(\eta)$ are the asymptotic values of $f(\eta)$, the nondimensional stream function, and $h(\eta)$, the nondimensional enthalpy, respectively as $Pe^{-1/2}$ approaches zero.

In the boundary layer, the zero-order system of equations is

$$\left[\mathcal{J}_1(i_o)i_o'(\xi)\right]' + g_o(\xi)i_o'(\xi) + \epsilon J_o\left[\xi\right] = 0 \qquad (2.76)$$

$$2Pr_s\left[\mathcal{J}_2\, i_o\, g_o''(\xi)\right]' + 2g_o(\xi)g_o''(\xi) - \left[g_o'(\xi)\right]^2 + a^2\mathcal{J}_3\left(i_o\right) = 0 \qquad (2.77)$$

$$g_o(0) = 0 \qquad (2.78)$$

$$g_o'(0) = 0 \qquad (2.79)$$

$$\lim_{\xi\to\infty} g_o'(\xi) = f_o'(0) \qquad (2.80)$$

$$\lim_{\xi\to\infty} i_o(0) = h_w \qquad (2.81)$$

$$i_o(\xi) = h_o(0) \qquad (2.82)$$

The independent variable ξ is the "stretched" boundary layer coordinate defined by the relation

$$\xi = Pe^{1/2}\,\eta \qquad (2.83)$$

The dependent variables $g(\xi)$ and $i(\xi)$ are defined by the expressions

$$i(\xi) = h(\eta) \qquad (2.84)$$

$$g'(\xi) = f'(\eta) \qquad (2.85)$$

in the boundary layer as $Pe^{-1/2}$ approaches zero.

The quantities $I_o\left[\eta\right]$ and $J_o\left[\xi\right]$ are terms of zero-order in the expansion of $I\left[\eta\right]$, the divergence of the radiant flux vector, for the inviscid and boundary layer regions, respectively. The derivation of these quantities is presented in appendix A. The results are listed below

$$
\begin{aligned}
I_o\left[\eta\right] = & -2\kappa_P\left[h_o(\eta)\right]B\left[h_c(\eta)\right] \\
& + k_P \int_0^\infty \kappa_\lambda\left[h_o(\eta)\right]\left\{\int_0^{\eta_\Delta} \kappa_\lambda\left[h_o(\eta')\right]B_\lambda\left[h_o(\eta')\right]E_1\left(k_P\left|\tau_\lambda(\eta) - \tau_\lambda(\eta')\right|\right)d\eta'\right. \\
& \left. + 2r_w E_2\left(k_P\,\tau_\lambda(\eta)\right)\int_0^{\eta_\Delta} \kappa_\lambda\left[h_o(\eta')\right]B_\lambda\left[h_o(\eta')\right]E_2\left(k_P\,\tau_\lambda(\eta')\right)d\eta'\right\}d\lambda
\end{aligned}
\tag{2.36}
$$

and

$$
\begin{aligned}
J_o\left[\xi\right] = & -2\kappa_P\left[i_o(\xi)\right]B\left[i_o(\xi)\right] \\
& + k_P \int_0^\infty \kappa_\lambda\left[i_o(\xi)\right]\left\{\int_0^{\eta_\Delta} \kappa_\lambda\left[h_o(\eta')\right]\ B_\lambda\left[h_o(\eta')\right]\ E_1\left(k_P\,\tau_\lambda(\eta')\right)d\eta'\right. \\
& \left. + 2r_w \int_0^{\eta_\Delta} \kappa_\lambda\left[h_o(\eta')\right]\ B_\lambda\left[h_o(\eta')\right]\ E_2\left(k_P\,\tau_\lambda(\eta')\right)d\eta'\right\}d\lambda
\end{aligned}
\tag{2.87}
$$

The integrals which appear in the second of these expressions are definite integrals. Consequently, the system of equations governing the flow in the boundary layer is a purely differential system.

It must be realized that expressions (2.86) and (2.87) are restricted to the case of an optically thin boundary layer. It is only in this case, and the case for which the boundary layer is optically thick, that a complete separation between the inviscid region and the boundary layer can be achieved. At intermediate values of optical depth, the integral term $I_o[\eta]$ is a function of the enthalpy distribution in the boundary layer in addition to being a function of the enthalpy distribution in the inviscid region so that the equations in the inviscid region and the boundary layer are coupled. The influence on the inviscid region of radiation from an optically thick boundary layer cannot be neglected. However, most of this radiation originates at the outer edge of the boundary layer. The boundary layer solution in this region is constrained by matching conditions to approach asymptotically the value of the inviscid solution at the wall. Hence, the radiation contribution to the inviscid region from the boundary layer can be obtained from the inviscid solution at the wall, leaving the inviscid solution uncoupled from the boundary layer solution.

This restriction to an optically thin boundary layer is not so severe as it might first appear. This is because the optical thickness of a boundary layer in which the absorption coefficient is the same order of magnitude as it is for shock heated air will not exceed about 0.1 at any altitude and velocity (up to km/sec) for a shock radius of 1 meter or less. In fact, the optical thickness of the boundary layer will be less than 0.1 at that point of the trajectory of a Martian or Lunar return vehicle with a shock radius of about 1 meter for which heating is a maximum even if the absorption coefficient in the boundary layer is 100 times that of shock heated air. That this should be the case is not so difficult to see when it is realized that both the optical path length and the boundary layer thickness decrease rapidly with decreasing altitude. Thus, at low altitudes where the optical path length is small and the shock layer may be optically thick, the boundary layer thickness is very small. For larger objects, the boundary layer need not be optically thin at the lower altitudes because the boundary layer thickness depends on the size of the object while the optical path length does not.

These conclusions regarding the optical thickness of the boundary layer generally concur with the observations of Fay, Moffatt, and Probstein (ref. 10). Henceforth, the discussions of this paper will be limited to the case of an optically thin boundary layer and radiation from this boundary layer will be considered to have no effect on the solution in the inviscid region of the shock layer.

If the inviscid system of equations (2.70) through (2.75) is solved for the nonradiating case $(\epsilon = 0)$ along with condition (2.65) one finds that the ratio of the shock standoff distance to the shock radius is given by the expression

$$\frac{\Delta_A}{R_s} = \frac{X}{1 + \sqrt{2X(1 - X)}} \tag{2.88}$$

Hayes (ref. 37) obtained the same result when the shock and body surfaces near the stagnation point are concentric spheres. When the shock and body surfaces are not concentric (i.e., $R_s \neq R_N + \Delta$) condition (2.88) is still approximately true over a wide range of body shapes (see, for example, refs. 38 and 39). With this result

$$a = \frac{2\sqrt{2X(1 - X)}}{1 + \sqrt{2X(1 - X)}} \tag{2.89}$$

This value for a, the constant appearing in the momentum equation (2.71), will be used throughout the remainder of this investigation.

E. Thermodynamic and Optical Property Correlations

In order to achieve meaningful results, an attempt has been made in this paper to use simple yet physically reasonable approximations to the thermodynamic and optical properties of high temperature gases. In particular, coorelation formulas were derived from the existing store of information about equilibrium air. The thermodynamic properties were obtained from reference 40, for temperature up to 100,000° K and pressures from 10^{-3} to 10^2 times atmospheric. The optical properties were obtained from a variety of sources which will be noted later.

It was noted from the data of reference 40, that both the density and temperature could be approximately represented by functions separable in the variables pressure and enthalpy. More specifically in the form $\left(\rho/\rho_o\right)^n f\left(h/RT_o\right)$. Plots of the functions $f\left(h/RT_o\right)$ for the density and temperature at various pressure levels are presented in figures 2.1 and 2.2, respectively. It is apparent from these plots that the density and temperature can adequately be represented by the expressions

$$\left(\frac{\rho}{\rho_o}\right) = 7.944\left(\frac{p}{p_o}\right)^{0.96}\left(\frac{h}{RT_o}\right)^{-1} \tag{2.90}$$

$$T = 308.8\left(\frac{p}{p_o}\right)^{0.09}\left(\frac{h}{RT_o}\right)^{0.55}, \quad {}^{o}K \tag{2.91}$$

A number of investigators (see, for example, refs. 41-45) have calculated the radiant properties of equilibrium air for temperatures up to 25,000^o K and for densities from 10^{-6} to 10^{1} Amagats. Because of the extremely complex nature of these calculations, the many physical processes which produce radiation, and the uncertain knowledge of cross sections and transition probabilities the scatter among the various calculations is often quite large. Some of the results for the Planck mean mass absorption coefficients are presented in figure 2.3.

A correlation formula can be obtained from figure 2.3 by approximating the curves of $\mathrm{Log}_{10}\, \rho\kappa_P$ versus $\mathrm{Log}_{10} T$ with straight

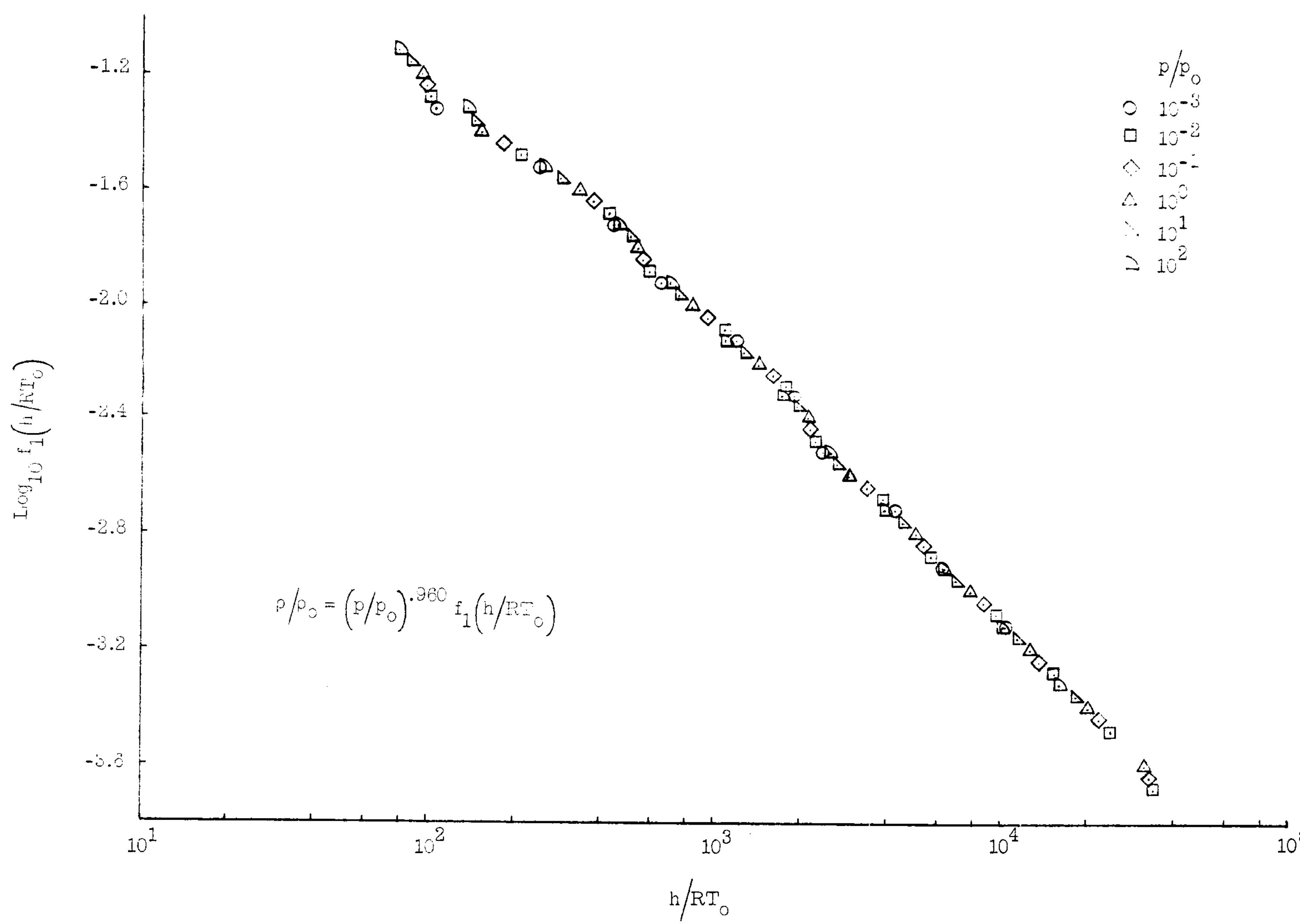

Figure 2.1.- Density correlation.

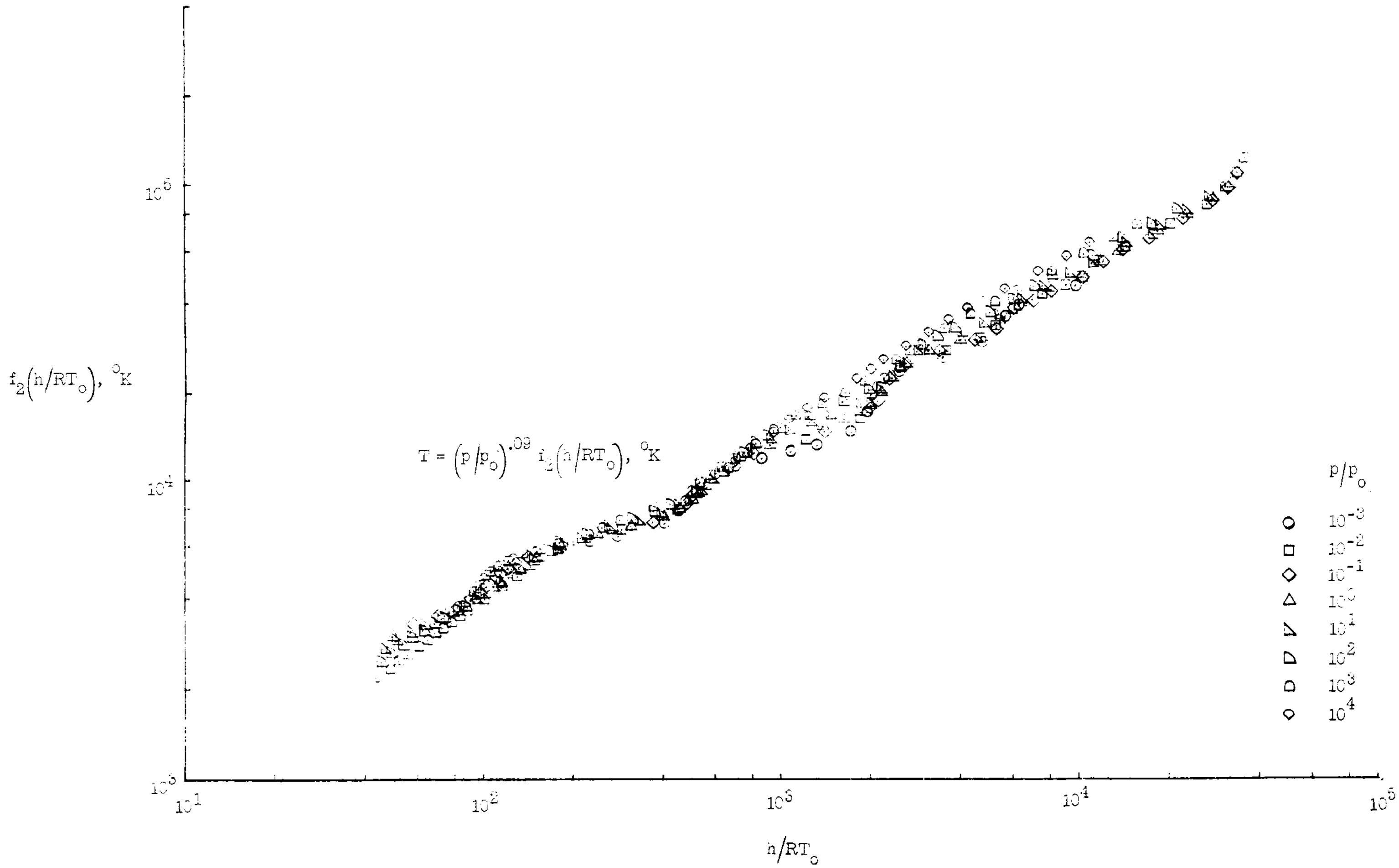

Figure 2.2.- Temperature correlation.

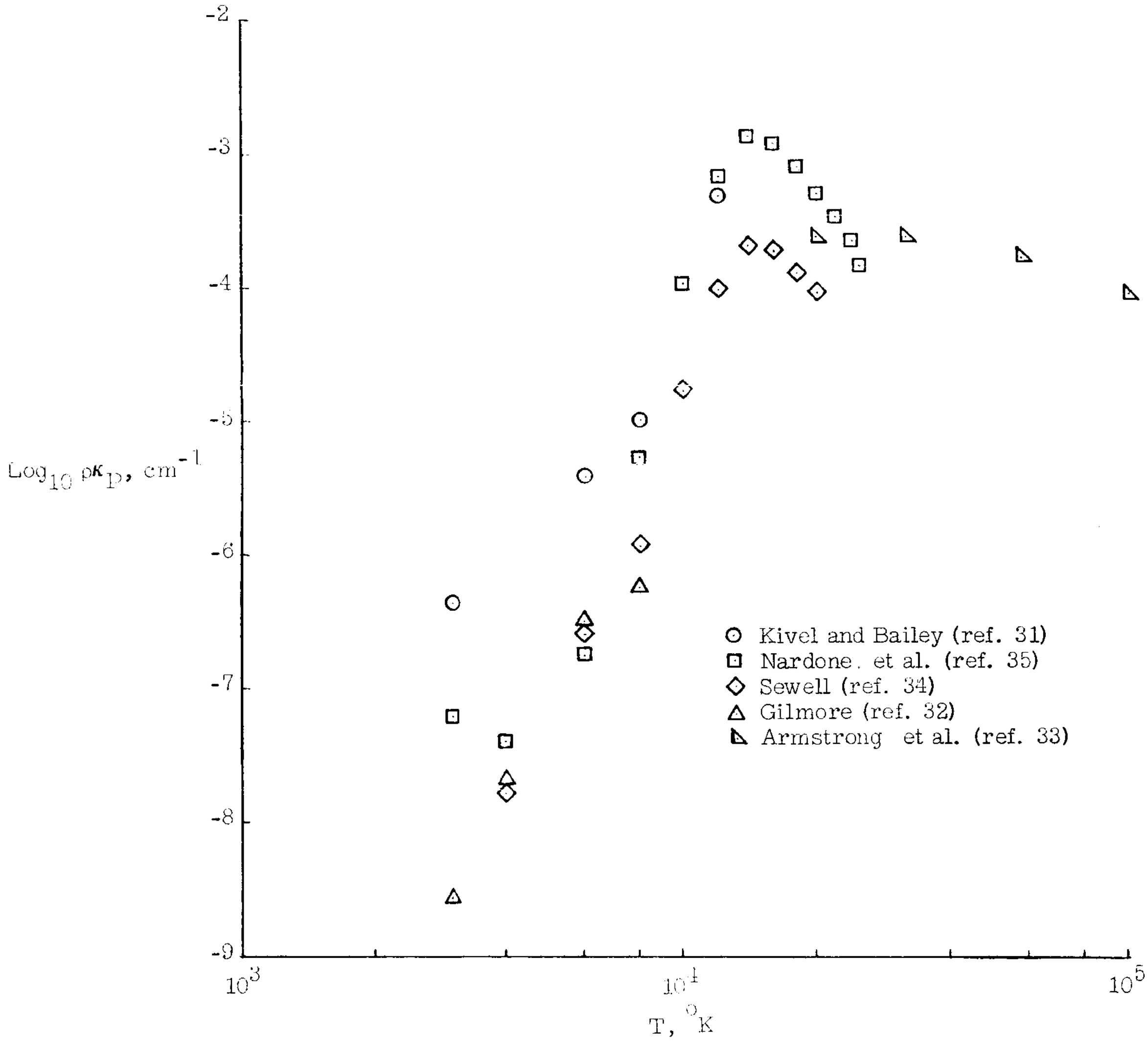

(a) $\rho/\rho_o = 10^{-3}$.

Figure 2.3.- Planck mean mass absorption coefficient correlation.

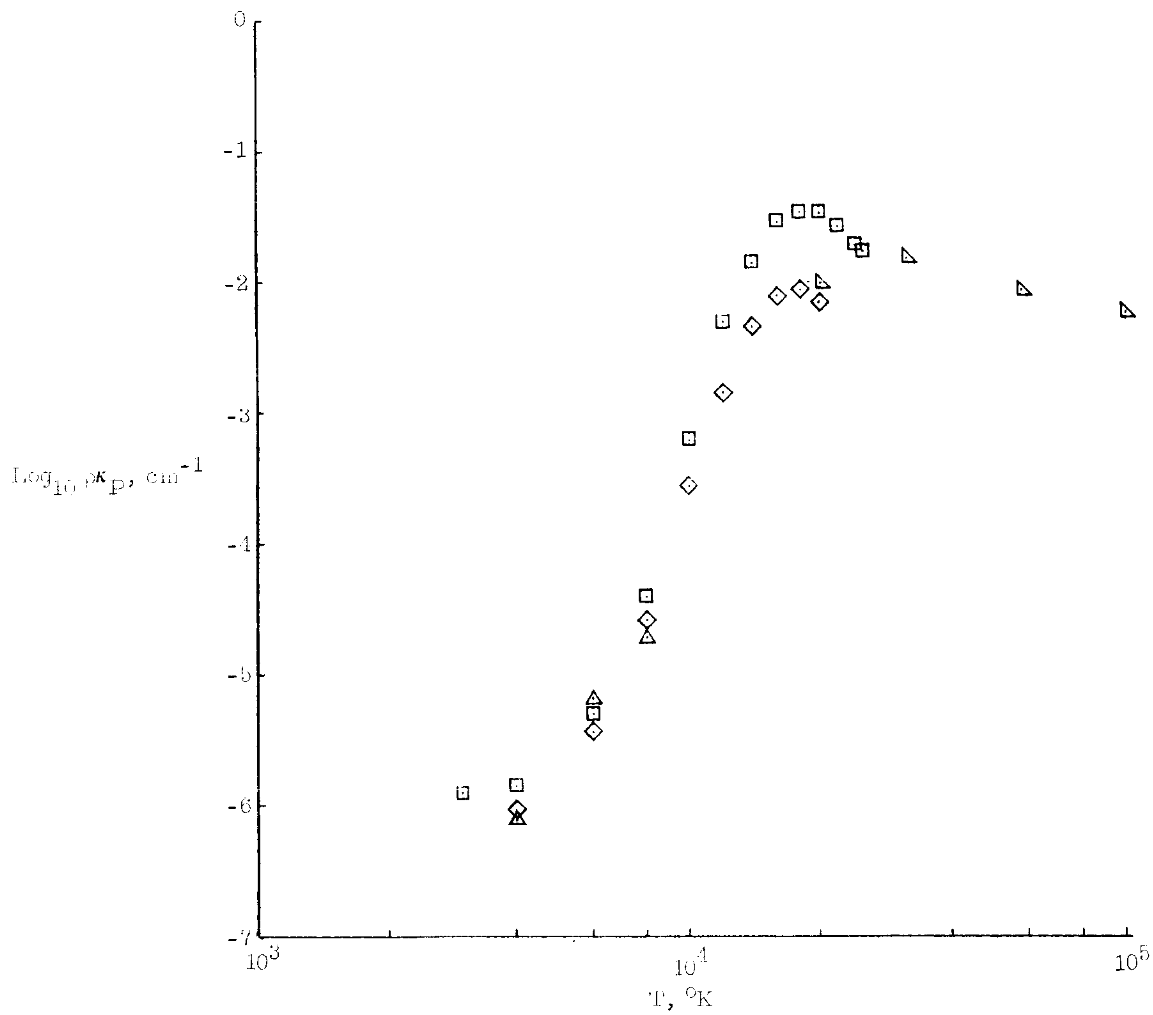

(b) $\rho/\rho_o = 10^{-2}$.

Figure 2.3.- Continued.

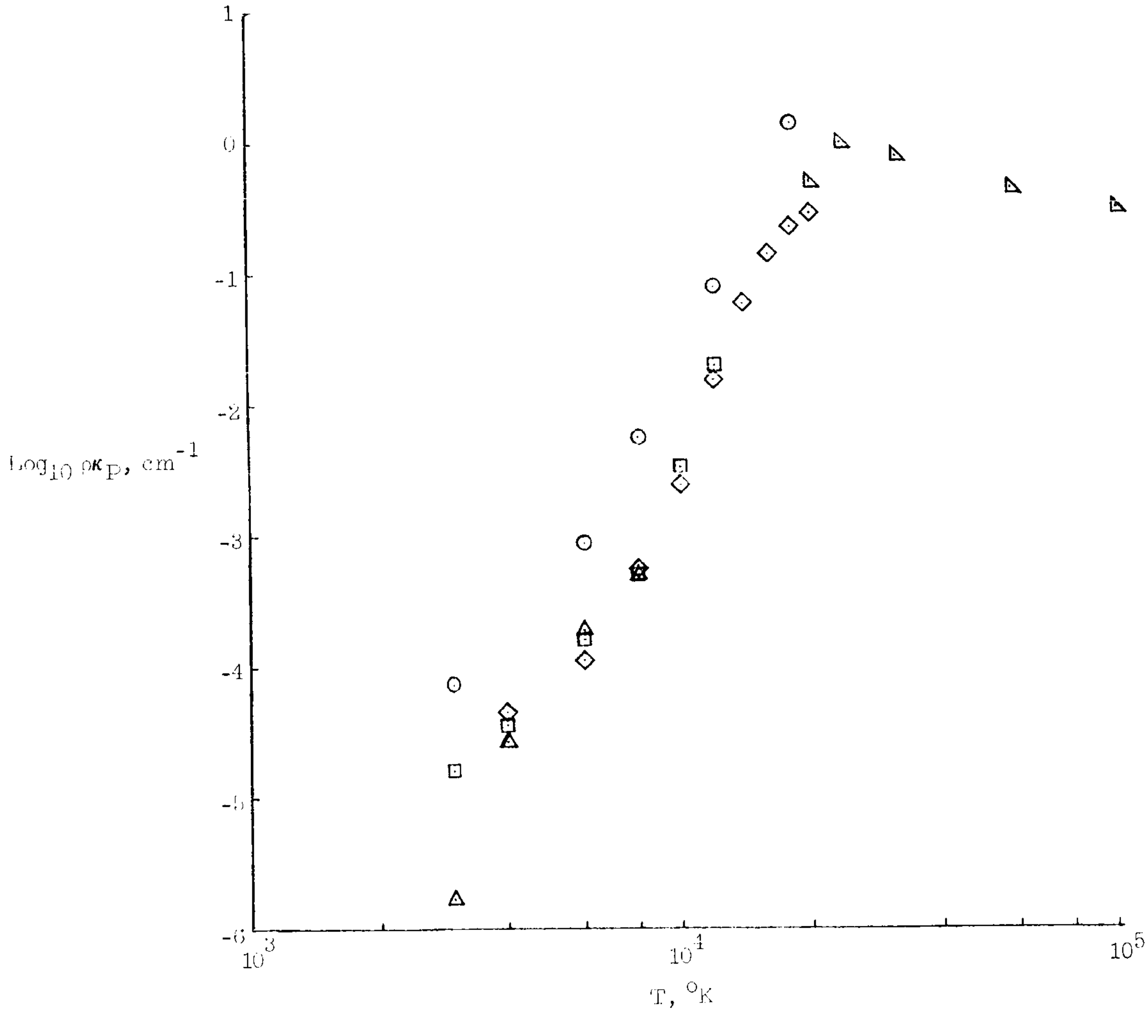

(c) $\rho/\rho_o = 10^{-1}$.

Figure 2.3.- Continued

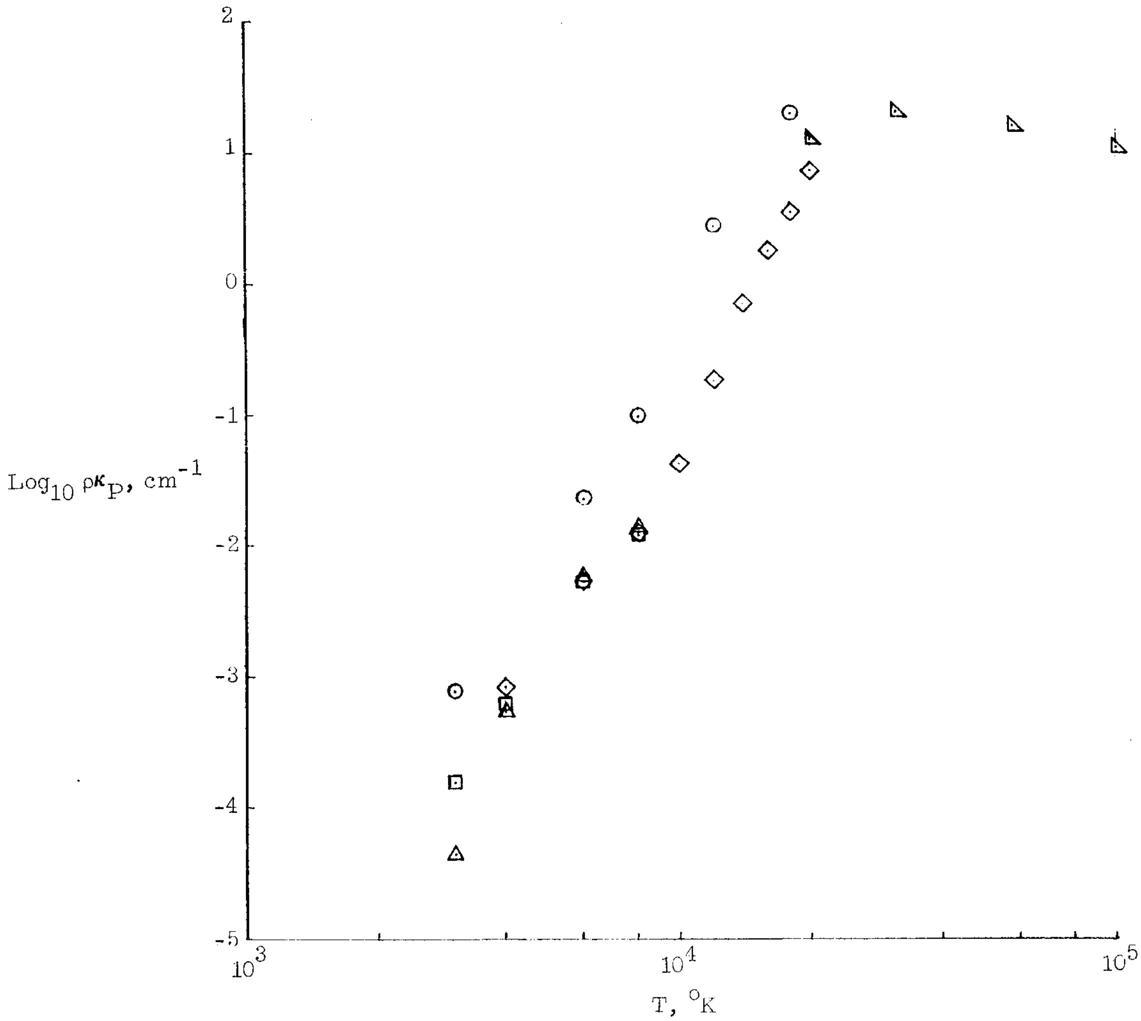

(d) $\rho/\rho_o = 10^0$.

Figure 2.3.- Continued.

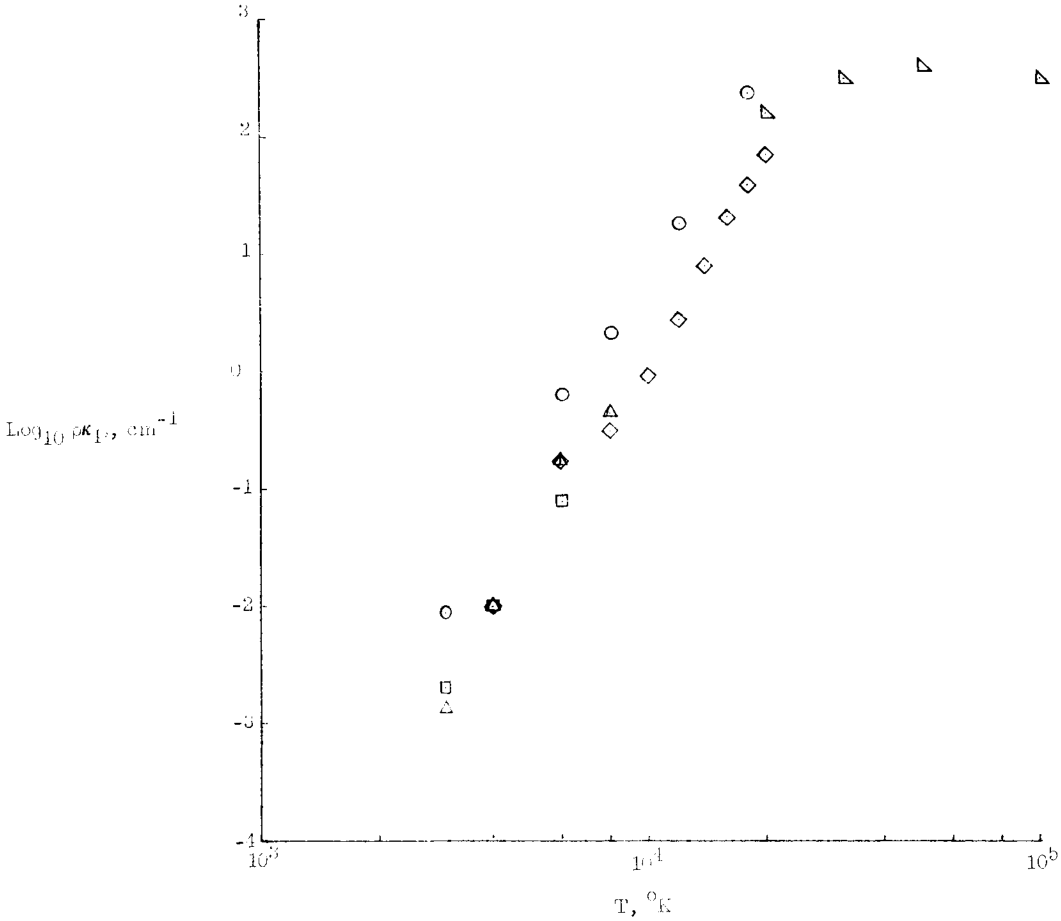

(e) $\rho/\rho_o = 10^1$

Figure 2.3.- Concluded.

lines. The resulting formula is

$$\rho\kappa_P = 7.94 \times 10^{-26} \left(\frac{\rho}{\rho_o}\right)^{3.25} T^{6.0-0.5\mathrm{Log}_{10}\frac{\rho}{\rho_o}}, \quad \mathrm{cm}^{-1} \tag{2.92}$$

This is not a particularly convenient form for use in the calculations of this paper. It is much more desirable to express the Planck mean mass absorption coefficient κ_P in terms of the pressure and enthalpy. This was done by cross-plotting the logarithm of the absorption coefficient data shown in figure 2.3 against the logatithm of the temperature at constant pressure. Straight lines were then fitted to the resulting curves. Finally, the correlation formulas (2.90) and (2.91) for density and temperature were used to obtain the formula

$$\kappa_P = 1.39 \times 10^{10}\left(\frac{p}{p_o}\right)^{-0.34-0.44\mathrm{Log}_{10}\frac{p}{p_o}} \left(\frac{h}{RT_o}\right)^{3.55-0.24\mathrm{Log}_{10}\frac{p}{p_o}}, \quad \mathrm{cm}^2/\mathrm{gm} \tag{2.93}$$

This formula is valid for temperatures up to 20,000° K at the higher pressures $\left(p/p_o = 10^{-1} \text{ to } 10^{1}\right)$ and to somewhat lower temperatures at the lower pressures (for example, when $p/p_o = 10^{-3}$ the maximum temperature at which the formula is valid is 15,000° K).

In addition to the Planck mean, it is necessary to know the spectral variation of the mass absorption coefficient. Results of some typical calculations of the monochromatic mass absorption coefficient plotted as functions of wavelength for constant temperature and pressure are presented in figure 2.4. No attempt was made to correlate these data.*

At temperatures above about 20,000° K, the information about the radiative properties is not so comprehensive. Most of what exists consists of Planck and or Rosseland mean absorption coefficients for continuum radiation. Line radiation is neglected. At these high temperatures, the radiation consists of spectral lines of the various ions which may be appreciable Stark-broadened at high electron densities, and a continuum due to free bound and free-free transitions of electrons in collisons with the ions. Since the integrated line emission is proportional to the ion density while the continuum emission is proportional to the product of ion and electron densities, the ratio of the latter to the former increases with increasing density. Thus, at the higher density levels, the continuum calculations may be adequate.

---

*It was noted from the results presented in references 45 and 46 that the functional form of the monochromatic mass absorption coefficient is approximately

$$\kappa_\lambda(h) = \sum_l \kappa_l(h)\, g_l(\lambda) \tag{2.94}$$

where the subscript refers to the lth radiating species.

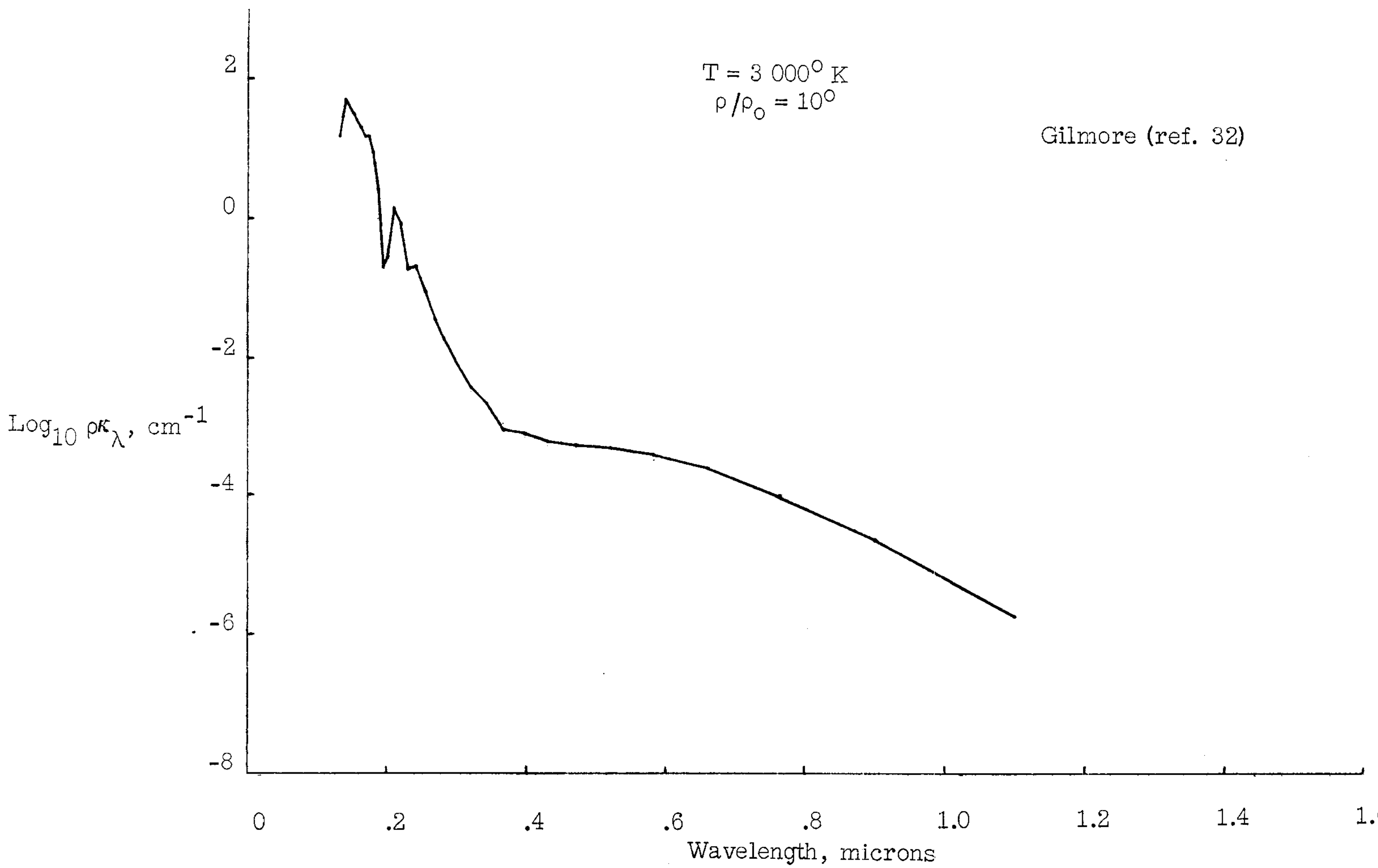

(a) $T = 3{,}000^{\circ}$ K, $\rho/\rho_o = 10^{\circ}$.

Figure 2.4.- Spectral distribution of the monochromatic mass absorption coefficient.

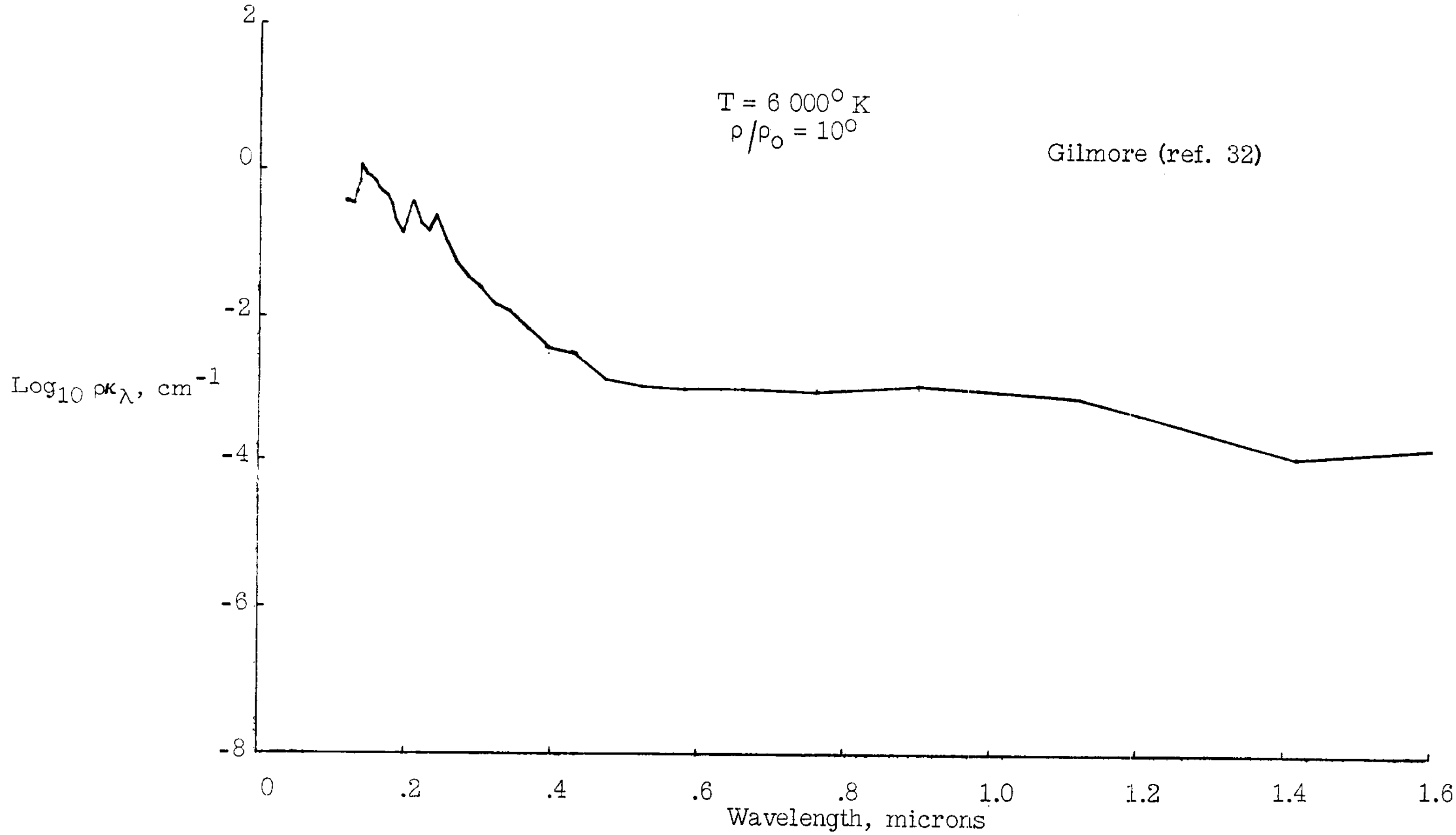

(b) $T = 6,000^\circ$ K, $\rho/\rho_o = 10^0$.

Figure 2.4.- Continued.

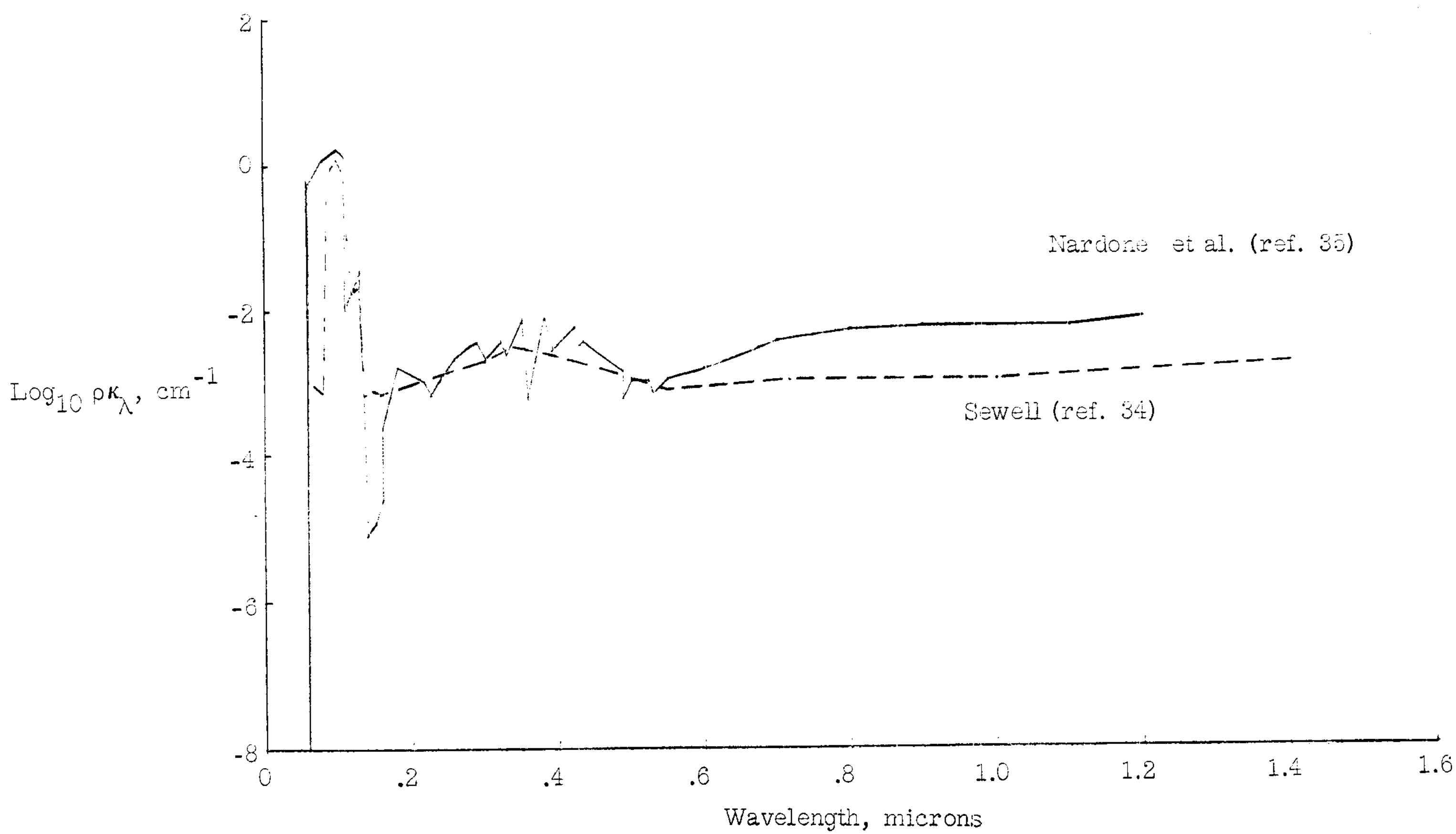

(c) $T = 10{,}000^\circ$ K, $\rho/\rho_o = 0.1$.

Figure 2.4.- Continued.

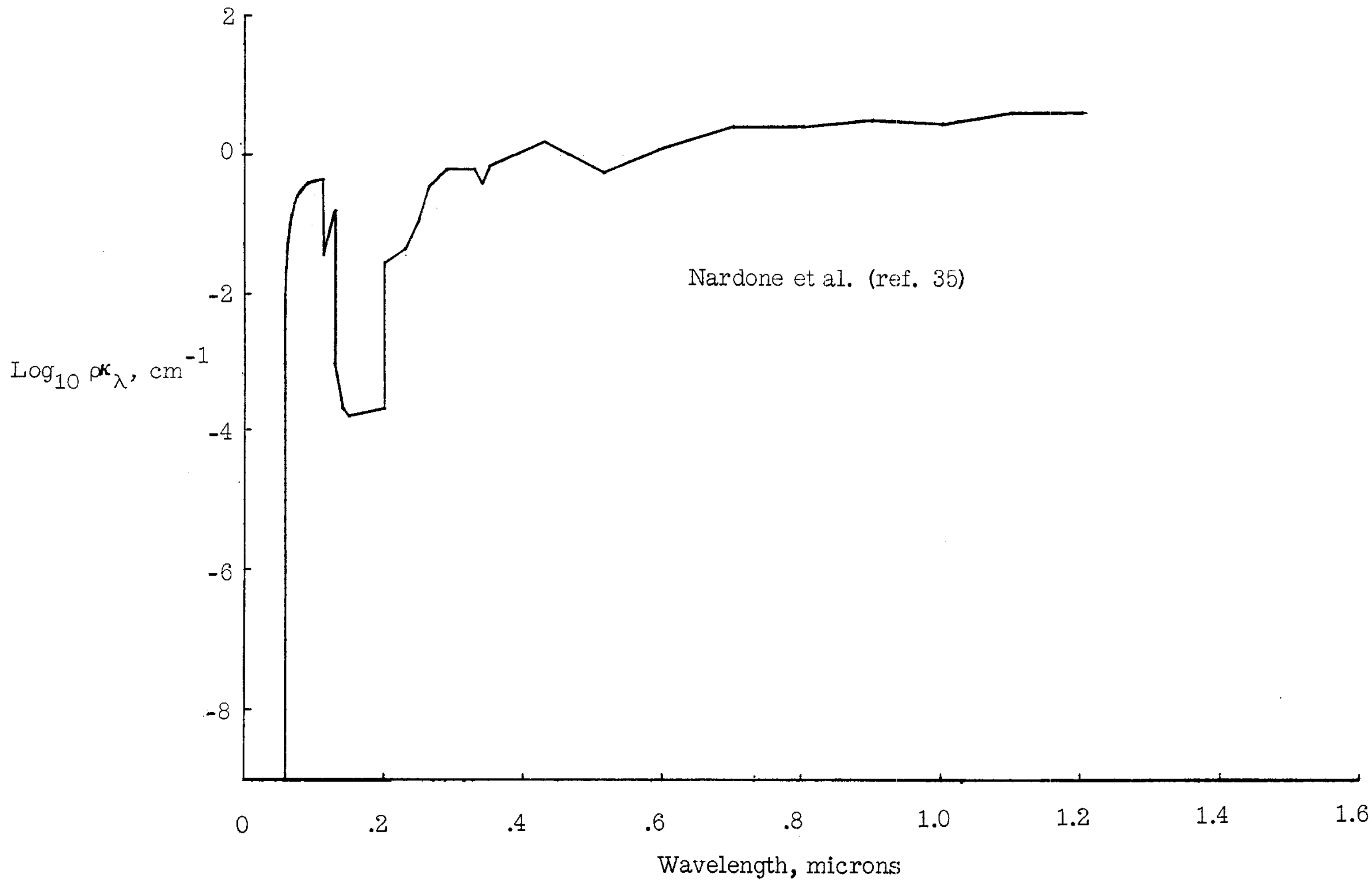

(d) $T = 25{,}000^{\circ}$ K, $\rho/\rho_o = 0.1$.

Figure 2.4.- Concluded.

The results of calculations of the Planck mean volume absorption coefficient for temperatures from 23,200° K to 100,000° K are presented in figure 2.3. These results were obtained from the paper by Armstrong et al. (ref. 43). A correlation formula was obtained from these results cross plotted in terms of constant density. The resulting formula was

$$\kappa_P = 2.95 \times 10^{19} \left(\frac{p}{p_o}\right)^{-0.055+0.011 \mathrm{Log}_{10}\left(\frac{p}{p_o}\right)} \left(\frac{h}{RT_o}\right)^{-1.217+0.065 \mathrm{Log}_{10}\left(\frac{p}{p_o}\right)}, \ \mathrm{cm}^2/\mathrm{gm} \tag{2.95}$$

This formula can be used in the range of temperatures from 30,000° K to 100,000° K.

The frequency variation of the mass absorption coefficient can be obtained for continuum radiation from the equations of Fay et al. (ref. 10). No attempt was made to obtain emperical correlations to these equations.

CHAPTER III. THE SMALL PERTURBATION SOLUTION

A. The Conventional Method

As was pointed out in chapter I, there is a flight regime of considerable importance in which the radiation cooling parameter ϵ is very much less than unity. In this regime, the energy transferred by radiation is small compared to the influx of kinetic energy across the bow shock, and it would be reasonable to expect the flow properties to be only slightly perturbed from the radiationless case. Lunev and Murzinov (ref. 4) and Goulard (ref. 5) took advantage of this and developed what amounted to first order perturbation solutions of the temperature distribution in the inviscid region of an transparent, gray gas layer. In both these papers, simplifying assumptions concerning the gas properties and flow model have been included.

In this section, the perturbation solutions will be generalized to include nongray gases with arbitrary thermodynamic and optical properties. These solutions will not be limited to shock layers of small optical thickness. Also, the solutions will be extended to second order. As will be shown, the second-order solutions can be quite important when the absorption coefficient varies rapidly with temperature.

The integrodifferential system which governs the flow in the inviscid region of the shock layer is

$$f(\eta)\ h'(\eta) + \epsilon I\left[\eta\right] = 0 \tag{3.1}$$

$$2f(\eta)\ f''(\eta) - \left[f'(\eta)\right]^2 + a^2\ h(\eta) = 0 \tag{3.2}$$

$$f(o) = 0 \tag{3.3}$$

$$f\left(\eta_\Delta\right) = 1 \tag{3.4}$$

$$f\left(\eta_\Delta\right) = 1 \tag{3.5}$$

$$f'\left(\eta_\Delta\right) = \frac{2}{X}\left(\frac{\Delta}{R_s}\right) = \frac{a}{\sqrt{2X(1 - X)}} \tag{3.6}$$

Here $f(\eta)$ and $h(\eta)$ are the nondimensional stream function and enthalpy, respectively. The quantity η_Δ is the value of the Dorodnitsyn coordinate at the location of the shock. The constant a can be expressed in terms of X, the density ratio across the shock, through expression (2.89). When the radiation cooling parameter ϵ is very small, the integral term in equation (3.1) becomes of only secondary significance throughout most of the domain of the problem.* Neglecting the integral term $I\left[\eta\right]$ reduces the problem to one in which radiation does not play a part. If, as expected when ϵ is small, the presence of radiation only slightly

---

*With the obvious exception of the region $\eta \approx 0$ where $f(\eta) \approx 0$. The difficulties presented by this exception will be discussed later.

influences the solution one can, to reasonable accuracy, evaluate $I[\eta]$ using the radiationless solution for h so that equation (3.1) becomes purely differential. Thus, when the small perturbation procedure (which roughly proceeds in the manner outlined above) is applied to this problem, the integrodifferential system is simplified to a purely differential system. In addition, as a result of the nature of the lowest order solution for the enthalpy distribution, the two differential equations become uncoupled and can be solved independently. Hence, it becomes possible to obtain analytic solutions to any order of approximation to the flow in the inviscid region of the shock layer. Details of the derivation of these solutions are presented in appendix B.

The zero-order, or radiationless, solution is simlpy

$$h_o(\eta) = 1 \tag{3.7}$$

$$f_o(\eta) = (1 - a)\eta^2 + a\eta \tag{3.8}$$

The first-order solution, which represents the effect of radiation assuming that the emissive power of the gas is independent of temperature, is

$$h_1(\eta) = \int_\eta^1 \frac{I_o[x]dx}{(1 - a)x^2 + ax} \tag{3.9}$$

$$f_1(\eta) = -\frac{1}{2}\left\{\left[2(1-a)\eta + a\right]\int_0^\eta \frac{\Phi_1(x)}{\left[(1-a)x+a\right]}\,dx\right.$$

$$\left. + \eta^2 \int_\eta^1 \frac{2(1-a)x+a}{x^2\left[(1-a)x+a\right]}\,\Phi_1(x)\,dx\right\} \tag{3.10}$$

Here x is a dummy variable of integration. The quantity $I_o[\eta]$ is given by the formula

$$I_o[\eta] = -\int_0^\infty \kappa_\lambda B_\lambda \left\{E_2\left[k_\lambda(1-\eta)\right]\right.$$

$$\left. + \left(1 - r_{o_\lambda}\right)E_2\left[k_\lambda \eta\right]\right\}d\lambda \tag{3.11}$$

The notation has been simplified somewhat in this expression by omitting the arguement h_o in the terms κ_λ and B_λ and by introducing the quantities

$$k_\lambda = k_P \kappa_\lambda \tag{3.12}$$

$$r_{o_\lambda} = r_w\left[1 - 2E_3\left(k_\lambda\right)\right] \tag{3.13}$$

Also

$$\Phi_1(\eta) = -\frac{1}{2}a^2 h_1(\eta) \tag{3.14}$$

The second-order solution takes into account the change in gas properties with changes in enthalpy. This solution is

$$h_2(\eta) = \eta_{\Delta_1} I_o\left[1\right] + \int_\eta^1 \left\{ \frac{I_1\left[x\right]}{f_o(x)} - \frac{f_1(x) I_o\left[x\right]}{f_o^2(x)} \right\} dx \tag{3.15}$$

$$\begin{aligned} f_2(\eta) = &- (1 - a)^2 \eta_{\Delta_1}^2 \eta^2 \\ &- \frac{1}{2}\left[2(1 - a)\eta + a\right] \int_o^\eta \frac{\Phi_2(x)}{\left[(1 - a)x + a\right]^2} dx \\ &- \frac{1}{2}\eta^2 \int_\eta^1 \frac{2(1 - a)x + a}{x^2\left[(1 - a)x + a\right]^2} \Phi_2(x)\, dx \end{aligned} \tag{3.16}$$

where

$$\begin{aligned} I_1\left[x\right] = h_1(\eta) &\int_o^\infty \left\{ \left[\dot{k}_\lambda B_\lambda \left\{ E_2\left[k_\lambda(1 - \eta)\right] \right. \right. \right. \\ &+ \left. \left. \left(1 - r_{o_\lambda}\right) E_2\left[k_\lambda \eta\right] \right\} - 2\kappa_\lambda \dot{B}_\lambda \right\} d\lambda \\ &+ \int_o^\infty k_\lambda \left\{ \kappa_\lambda \dot{B}_\lambda \int_o^1 h_1(x) E_1\left[k_\lambda \left|\eta - x\right|\right] dx \right. \\ &+ \dot{k}_\lambda B_\lambda \left\{ E_1\left[k_\lambda(1 - \eta)\right] \int_\eta^1 h_1(x)\, dx \right. \\ &+ \left. \left. \left(1 - r_{o_\lambda}\right) E_1\left[k_\lambda \eta\right] \int_o^\eta h_1(x) dx \right\} + r_{1_\lambda} E_2\left[k_\lambda \eta\right] \right\} d\lambda \end{aligned} \tag{3.17}$$

Here the arguement h_o is omitted in the terms $\dot{\kappa}_\lambda$ and $\dot{B}_\lambda$ and the quantity r_{1_λ} is defined by the expression

$$r_{1_\lambda} = 2r_w \left\{ \kappa_\lambda \dot{B}_\lambda \int_o^1 h_1(x) \, E_2\left(k_\lambda x\right) \, dx \right. \qquad (3.18)$$
$$\left. + \dot{\kappa}_\lambda B_\lambda E_2\left(k_\lambda\right) \int_o^1 h_1(x)dx + \eta_{\Delta_1} \kappa_\lambda B_\lambda E_2\left(k_\lambda\right) \right\}$$

Also

$$\Phi_2(\eta) = -f_1(\eta) \, f_1''(\eta) + \frac{1}{2}\left[f_1'(\eta)\right]^2 - \frac{1}{2} a^2 \, h_2(\eta) \qquad (3.19)$$

The quantities η_{Δ_o}, η_{Δ_1}, and η_{Δ_2} are given by the formulas

$$\eta_{\Delta_o} = 1 \qquad (3.20)$$

$$\eta_{\Delta_1} = \frac{1}{2} \int_o^1 \frac{\Phi_1(x)}{\left[(1 - a)x + a\right]^2} \, dx \qquad (3.21)$$

$$\eta_{\Delta_2} = (1 - a)\eta_{\Delta_1}^2 + \frac{1}{2} \int_o^1 \frac{\Phi_2(x)}{\left[(1 - a)x + a\right]^2} \, dx \qquad (3.22)$$

It can be seen upon inspection of relation (3.17) that a large value of the rate of change of the Planck mean absorption coefficient with enthalpy will lead to large values of $I_1[\eta]$. Thus, it is clear that at shock temperatures of less than about 30,000° K, for which the absorption coefficient does vary rapidly with enthalpy, the second-order solutions can become more important to the overall solution than their order in ϵ might at first indicate.

B. The P - L - K Method

As can be seen from an inspection of the expressions (3.9) and (3.15) the first order solution for the enthalpy distribution has a logarithmic singularity at the point $\eta = 0$ and the second-order solution has a singularity of greater strength at this point. As a consequence, the assumed expansion diverges as the origin is approached and the small perturbation solution is not uniformly valid throughout the domain of the problem. This divergence can lead to serious errors in the calculation of the radiant heat flux to the wall because those regions close to the wall, in which the largest errors occur, are given the most weight in the calculation. This is particularly true for shock layers which are not optically thin. Additional difficulties are encountered when attempting to specify the proper outer boundary conditions for the viscous boundary layer equations. In classical boundary layer theory, the outer boundary conditions are obtained from the values of the outer (or inviscid) solution at the wall ($\eta = 0$ in this problem). Because of the divergence of the outer solution, no finite value exists at $\eta = 0$.

In this section, the Poincare-Lighthill-Kuo perturbation of coordinate procedure* (ref. 47) is used to obtain a solution which is uniformly valid over the domain of the problem. The details of the application of this method to the problem of this paper are presented in appendix B. This method utilizes a coordinate transformation in the form of a perturbation expansion of the coordinate to remove the singularity (which caused the divergence of the conventional solution) from $\eta = 0$ to a small negative value of η which lies outside the domain of the problem. The P-L-K expansions are

$$\eta = x + \epsilon\eta_1^*(x) + \ldots \tag{3.23}$$

$$h(\eta;\epsilon) = h_o^*(x) + \epsilon h_1^*(x) + \ldots \tag{3.24}$$

$$f(\eta;\epsilon) = f_o^*(x) + \epsilon f_1^*(\eta) + \ldots \tag{3.25}$$

where x is the coordinate in the transformed plane, and the superscript * has been used to differentiate between the coefficients in the P-L-K expansion and the coefficients in the conventional expansion. Pritulo (ref. 48) has derived a general relation between the P-L-K and conventional coefficients. Adapted to this problem, the relationships become

*Variously called the P-L-K method, the P-L method, Lighthill's technique, the method of strained coordinates, and the method of perturbation of coordinates.

$$h_o^* (x) = h_o (x) \tag{3.26}$$

$$h_1^* (x) = h_1 (x) \tag{3.27}$$

$$f_o^* (x) = f_o (x) \tag{3.28}$$

$$f_1^* (x) = f_1 (x) + \eta_1^* (x) f_o' (x) \tag{3.29}$$

$$\eta_1^* (x) = -h_2 (x)/h_1' (x) \tag{3.30}$$

The second-order term $h_2 (x)$ introduces the effects of variable thermodynamic and optical properties, so it is apparent that these effects are contained in the first-order P-L-K solution.

A comparison of the P-L-K and conventional perturbation solutions for the enthalpy distribution for a constant density, transparent shock layer is presented in figure 3.1. The divergent character of the conventional solutions is apparent. Also shown on this figure is the exact analytic solution which can be obtained in this simple case. The formula for this exact solution is

$$h\left(\frac{\eta}{\eta_\Delta}\right) = \left\{1 + 4\epsilon(\gamma - 1) \log \left[\frac{1 + \left(\eta/\eta_\Delta\right)}{2\left(\eta/\eta_\Delta\right)}\right]\right\}^{-\frac{1}{\gamma-1}} \tag{3.31}$$

where γ (the exponent in the correlation formula $\kappa_p B = h^\gamma$) was taken to be 6 and the constant a (which appears in the momentum

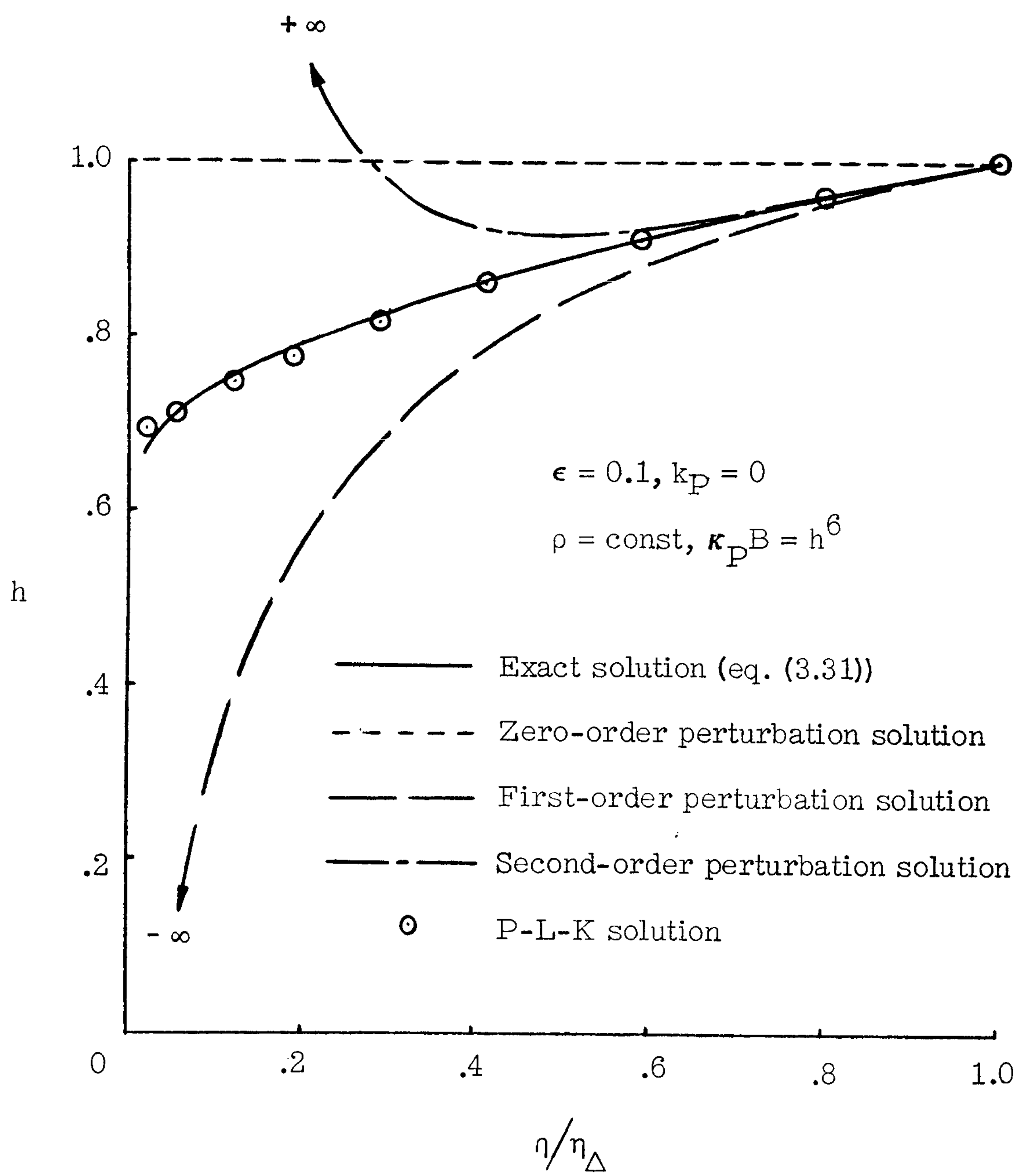

Figure 3.1.- Comparison of the P-L-K and conventional perturbation solutions.

eq. (3.2)) was taken to be 0.5. The good agreement between the P-L-K solution and the exact solution indicates that the accuracy of the P-L-K solution is probably second-order in the radiation cooling parameter ϵ throughout the domain except in the immediate neighborhood of the wall. It is clear that quantities such as the radiant heat flux at the wall, which depend upon an integration over the enthalpy distribution, will be considerably more accurate if the P-L-K solution rather than the conventional perturbation solution is used.

It should be noticed that the P-L-K solution does not lead to zero enthalpy at the wall as the exact transparent solution does. The reason for this disparity can be found in the fact that the coordinate stretching displaces the boundary with regard to both the energy and momentum equations but not by a uniform amount. Thus, a physical interpretation of the first order P-L-K solution is that the normal velocity of the flow at the boundary for the energy equation is not quite zero, and a particle approaching this boundary will reach it in a finite time before losing all its energy by radiation.

It can be shown that since the expected error in the Dorodnitsyn coordinate η in terms of the stretched coordinate x is order ϵ^2 and since the gradients in $h_1(x)$ are very large in the vicinity of the wall, the difference between the P-L-K and exact solutions at the wall lie within expected limits. Convergence to the correct solution should be attained with the addition of higher order terms to the expansion of h and η.

C. The Method of Matched Asymptotic Expansions

Van Dyke (ref. 36) has pointed out that the method of matched asymptotic expansions is applicable whenever the P-L-K method can be used. Thus, it would be interesting to formulate the solution when radiation is a small perturbation using the method of matched asymptotic expansions. Use of this method implies that the domain of the problem can be divided into at least two regions in which the governing equations take on different asymptotic forms. There must also be some overlap between adjacent regions so that a smooth transition between solutions valid in these adjacent regions can be affected. In the problem of this chapter, the regions are the "outer" region in which the conventional perturbation solutions are valid and the "inner" region in the vicinity of the wall at $\eta = 0$. The equations which describe the conditions in the outer region are simply the system (3.1) to (3.6). In order to obtain the "boundary layer" form of these equations, it is necessary to stretch the coordinate η in the vicinity of the wall. This stretching takes the nonlinear form

$$F(\xi) = \left[f(\eta)\right]^{\epsilon} \tag{3.32}$$

$$F'(\xi) = f'(\eta)$$

where ξ is the stretched boundary layer coordinate and $F(\xi)$ is the velocity function written in terms of ξ. It follows from above that

$$\frac{d\xi}{d\eta} = \epsilon\,\frac{F(\xi)}{f(\eta)} \tag{3.33}$$

and the energy and momentum equations, respectively, take the forms

$$F(\xi)H'(\xi) + \tilde{I}\left[\xi\right] = 0 \tag{3.34}$$

$$2F(\xi)F''(\xi) - \left[F'(\xi)\right] + a^2 H(\xi) = 0 \tag{3.35}$$

where

$$H(\xi) = h(\eta) \tag{3.36}$$

and

$$\tilde{I}\left[\xi\right] = I\left[\eta\right] \tag{3.37}$$

One boundary condition is available, that is

$$F(0) = 0 \tag{3.38}$$

The remaining two constants of integration can be obtained by matching the inner and outer solutions according to the matching principle put forth in reference 36.

The boundary layer system is seen to be quite complex. The energy and momentum equations remain coupled so that it is necessary to obtain a simultaneous solution to the two equations. Thus, as is often the case when the P-L-K method can be applied, its application is much simpler than the method of matched asymptotic expansions.

D. Results and Discussion

The formulas derived in the preceeding sections of this chapter were programed for numerical computation on the IBM 7094 electronic digital computer. The value of X, the density ratio across the normal shock, was fixed at a constant value of 0.06 for the calculations reported on in this and subsequent chapters. This choice is justified because X varies but little with altitude and velocity and the effects of this variation on the stagnation solutions are slight. The value $X = 0.06$ is typical for hypervelocity flight in the atmosphere of the earth.

The numerical calculations indicate that the enthalpy is a double valued function of the Dorodnitsyn coordinate η in the vicinity of the shock for large values of the Bouguer number. An examination of the governing equations failed to show the presence of any singularities which might adversely influence the solution in this region when k_P is large and ϵ small. On the other hand, the results of numerical calculations with varying mesh size seemed to rule out the possibility that the doubled valued behavior can be attributed solely to numerical inaccuracies. Consequently, it is suspected that the difficulty results from truncation of the perturbation expansion and that inclusion of higher order terms would either eliminate the problem or increase the value of k_P at which it first appears. For truncation after the second order term the conditions for validity of the solution is $\epsilon k_P < 1$.

Gray gas results

Shock layer enthalpy distributions for a gray gas with differing values of the radiation cooling parameter ϵ, the Bouguer number k_P, the variation with enthalpy of the Planck mean mass absorption coefficient $\dot{\kappa}_P$, and the reflectivity of the body surface r_w are presented in figures 3.2 to 3.4. While the gray gas assumption may not be realistic for most gases of interest, its use is felt to be justified in the study of the above listed parameters for two reasons. First, the highly complex and varied spectral structure of absorption coefficients makes a general parametric study of nongray gases impractical. Second, experience with nongray calculations indicates that the qualitative dependence of the gray results on the various parameters will carry over to most nongray cases.

The decrease in enthalpy level with increasing ϵ is illustrated in figures 3.2a to 3.2c. These results indicate that the loss of energy from the shock layer by radiation (i.e., radiation cooling) can produce a noticeable drop in enthalpy for values of ϵ as small as 0.01. The dependence of the enthalpy distribution on the Bouguer number (hence, optical thickness) is also shown in these figures. As expected an increase in the Bouguer number (or optical thickness) inhibits shock layer cooling and leads to higher values of enthalpy near the wall.

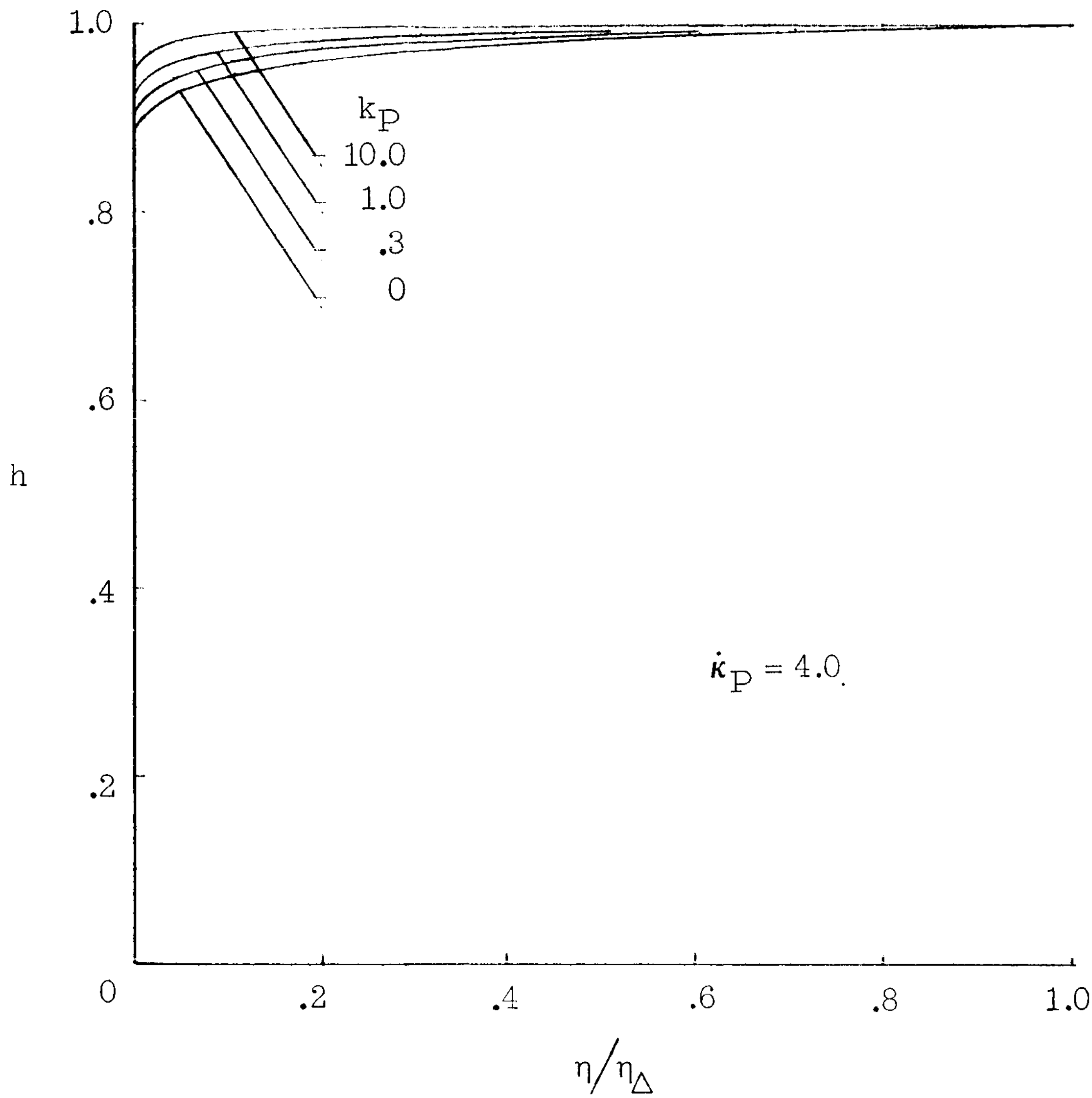

(a) $\epsilon = 0.01$.

Figure 3.2.- Effect of the parameters ϵ and k_P on the shock layer enthalpy distribution.

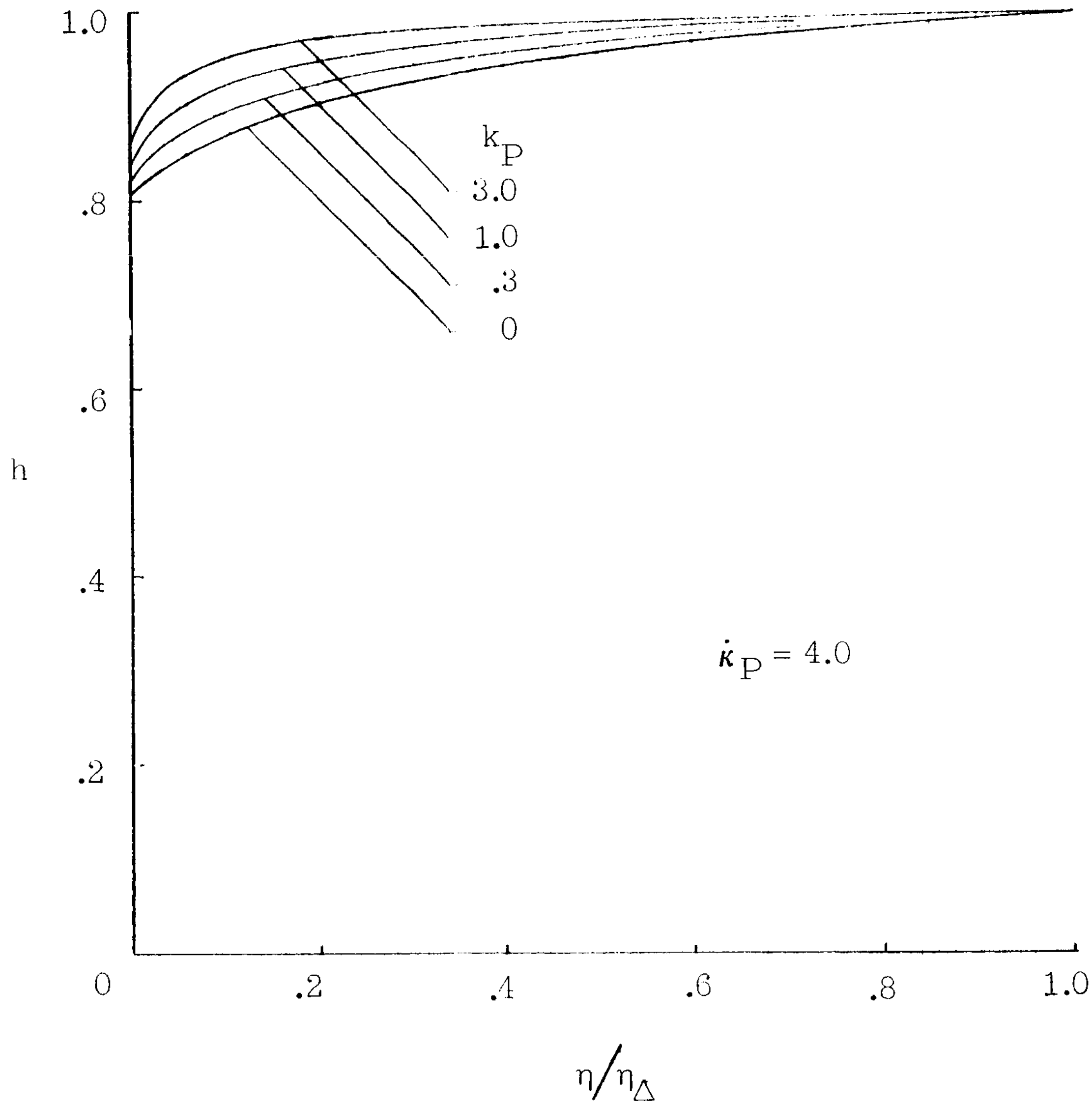

(b) $\epsilon = 0.03$.

Figure 3.2.- Continued.

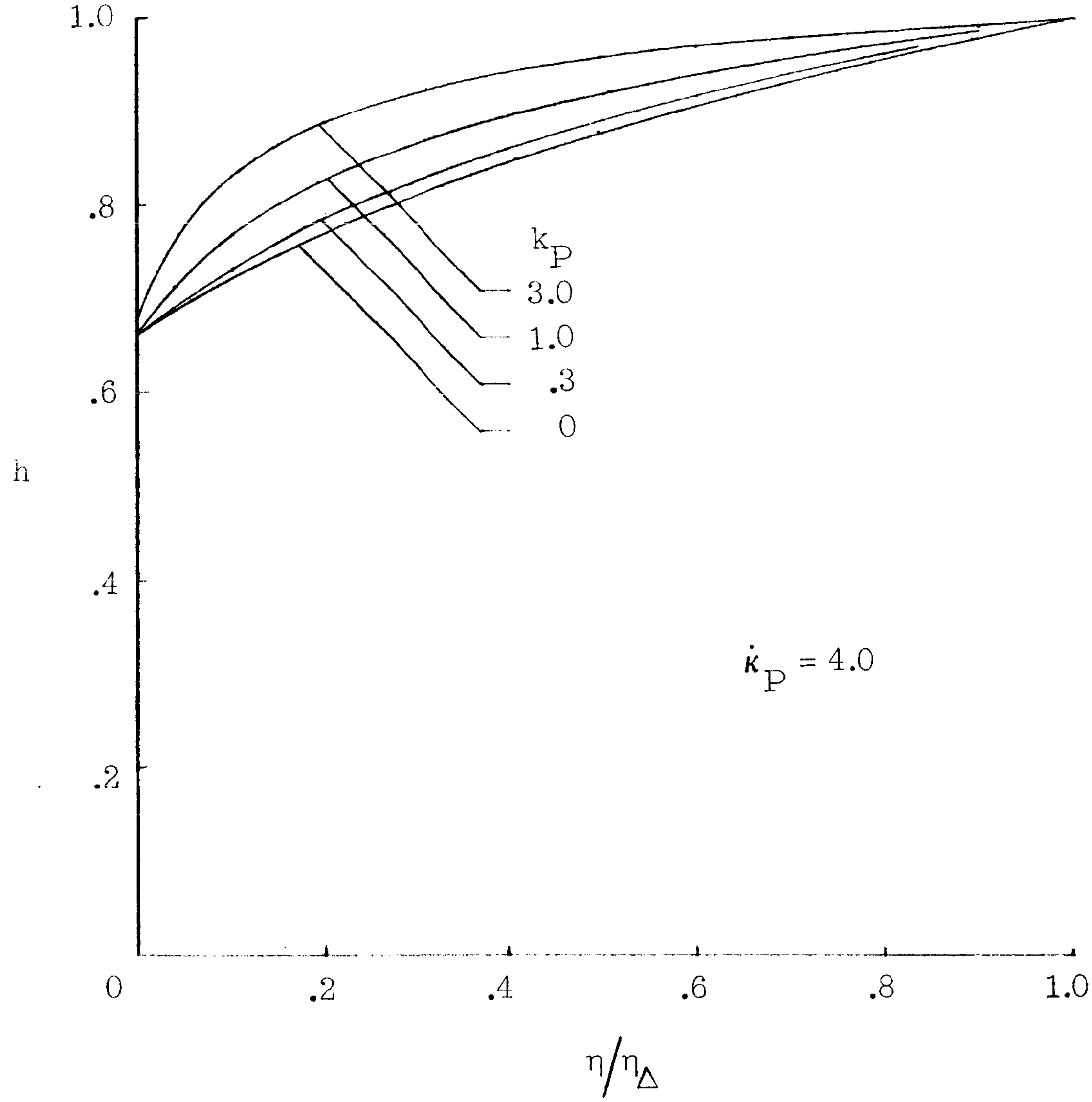

(c) $\epsilon = 0.10$.

Figure 3.2.- Concluded.

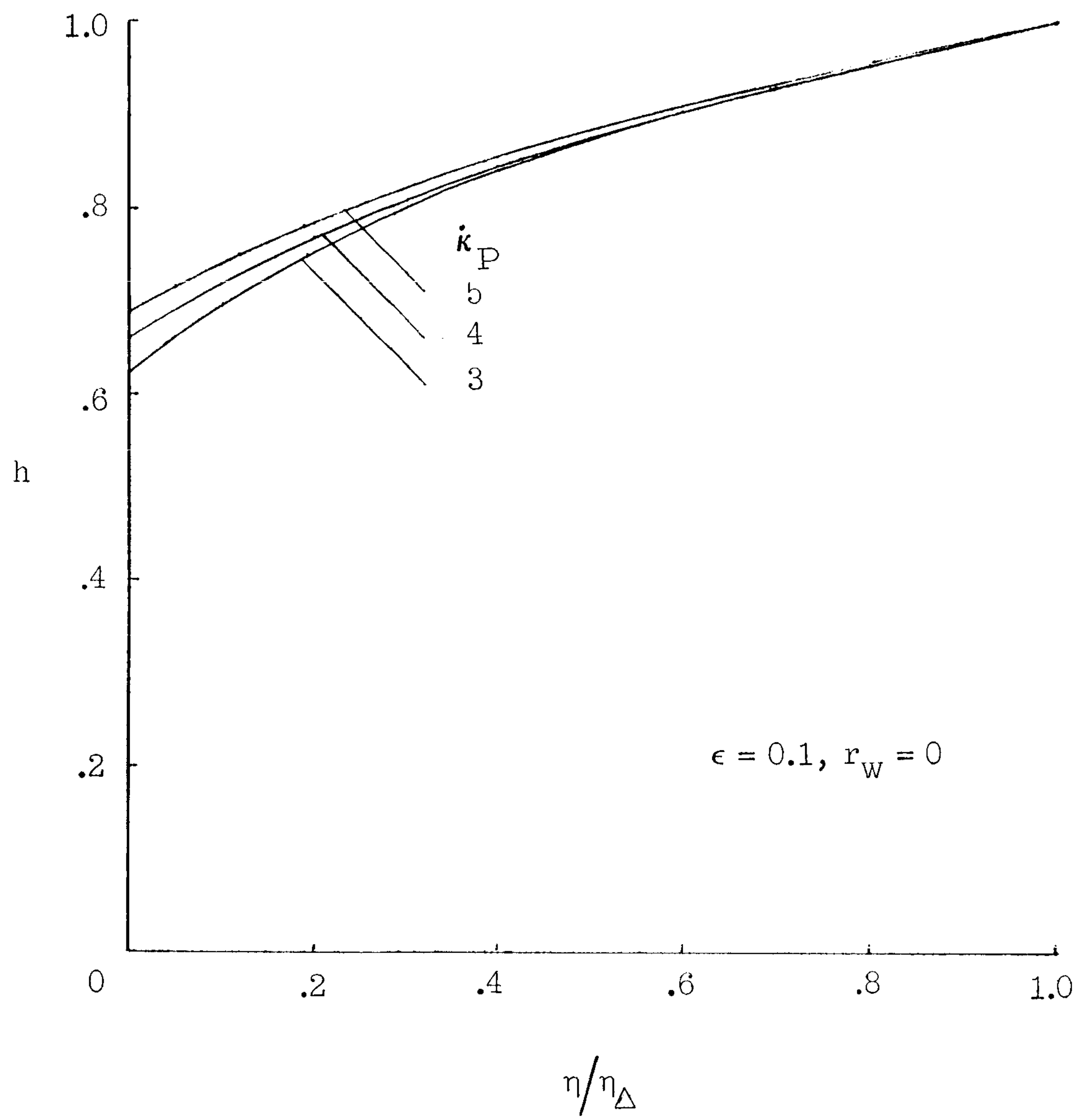

(a) $k_P = 0$.

Figure 3.3.- Effect of the enthalpy variation of the absorption coefficient on the shock layer enthalpy distribution.

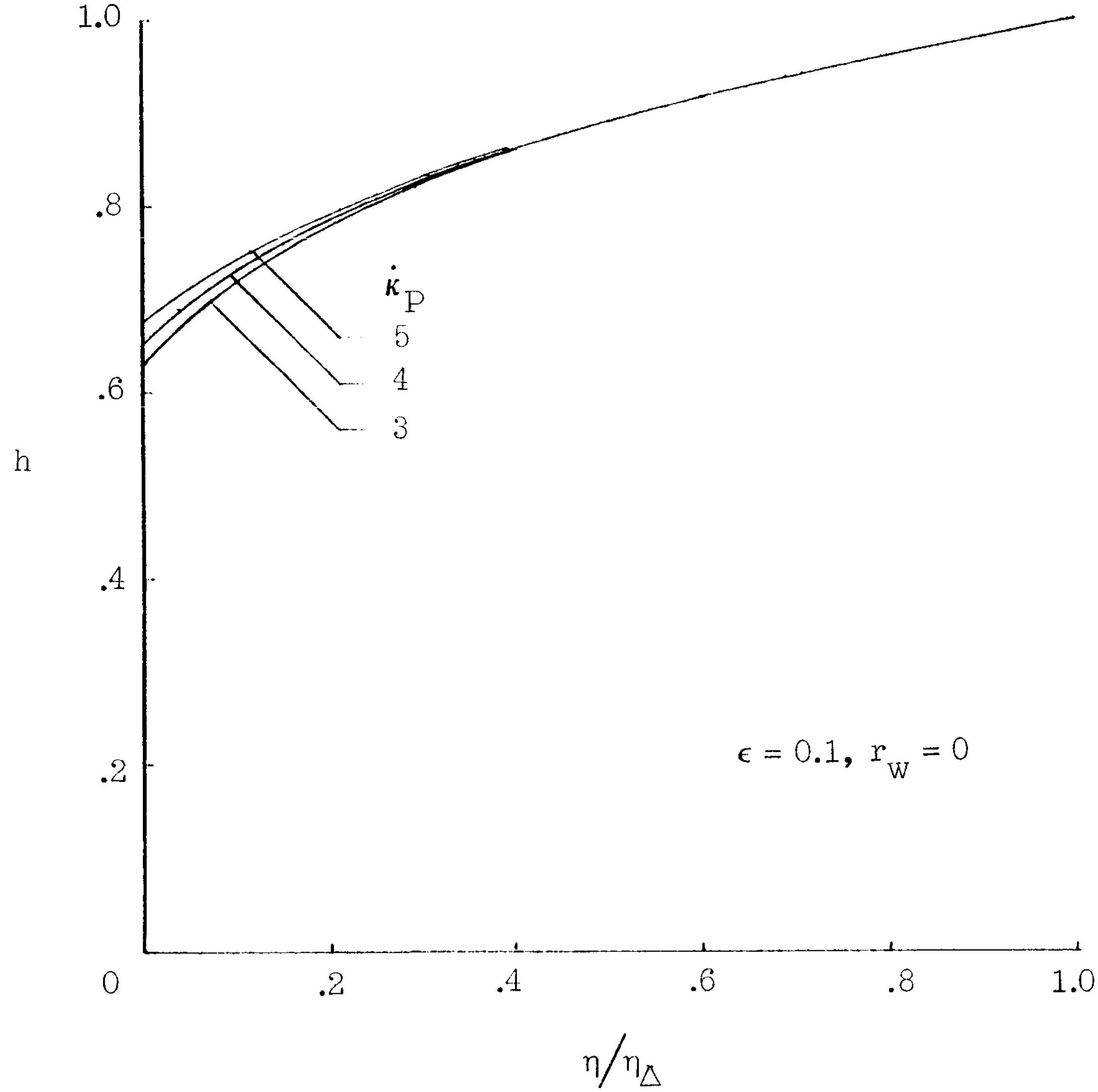

(b) $k_P = 0.3$.

Figure 3.3.- Continued.

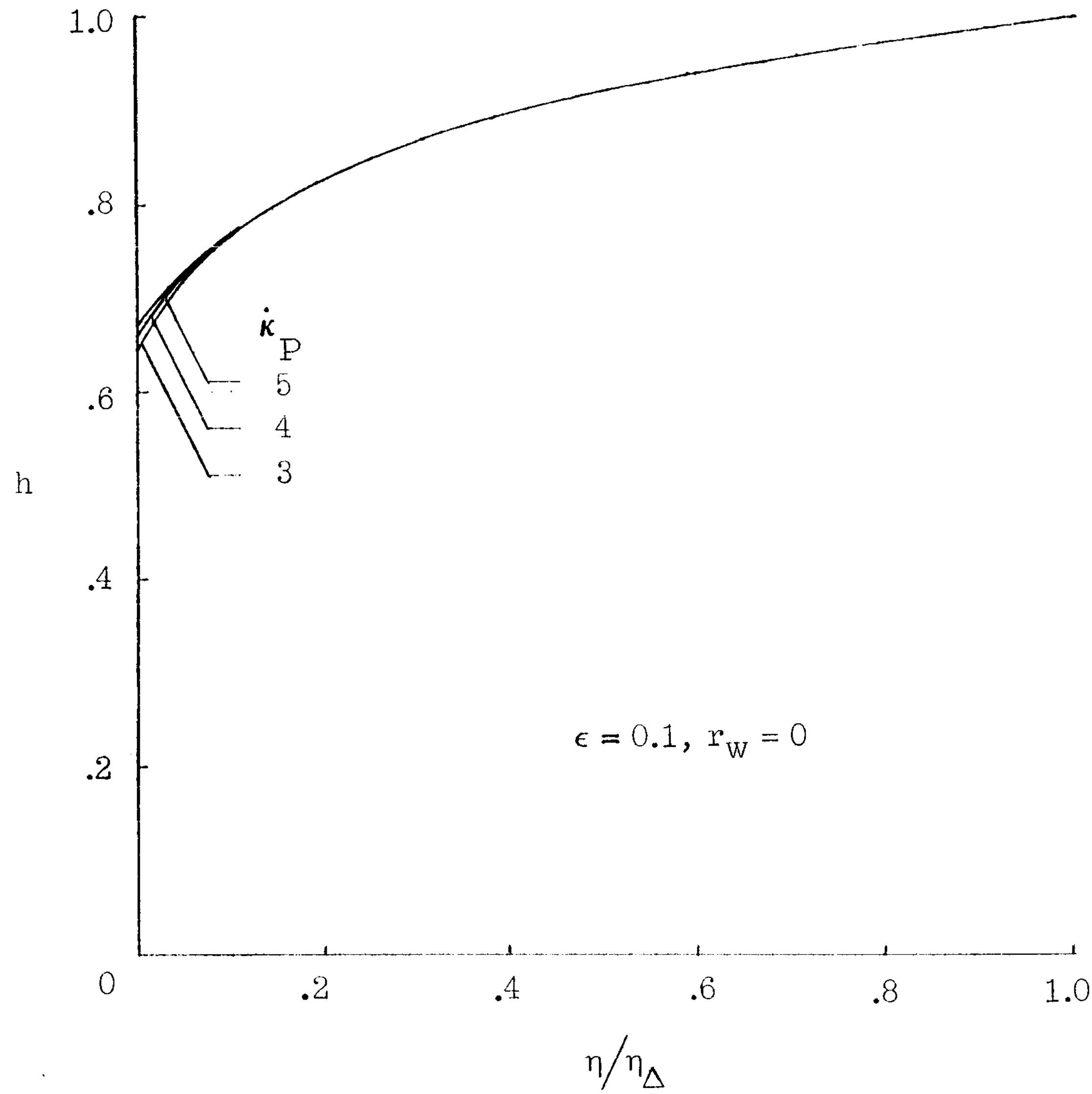

(c) $k_P = 1.0$.

Figure 3.3.- Concluded.

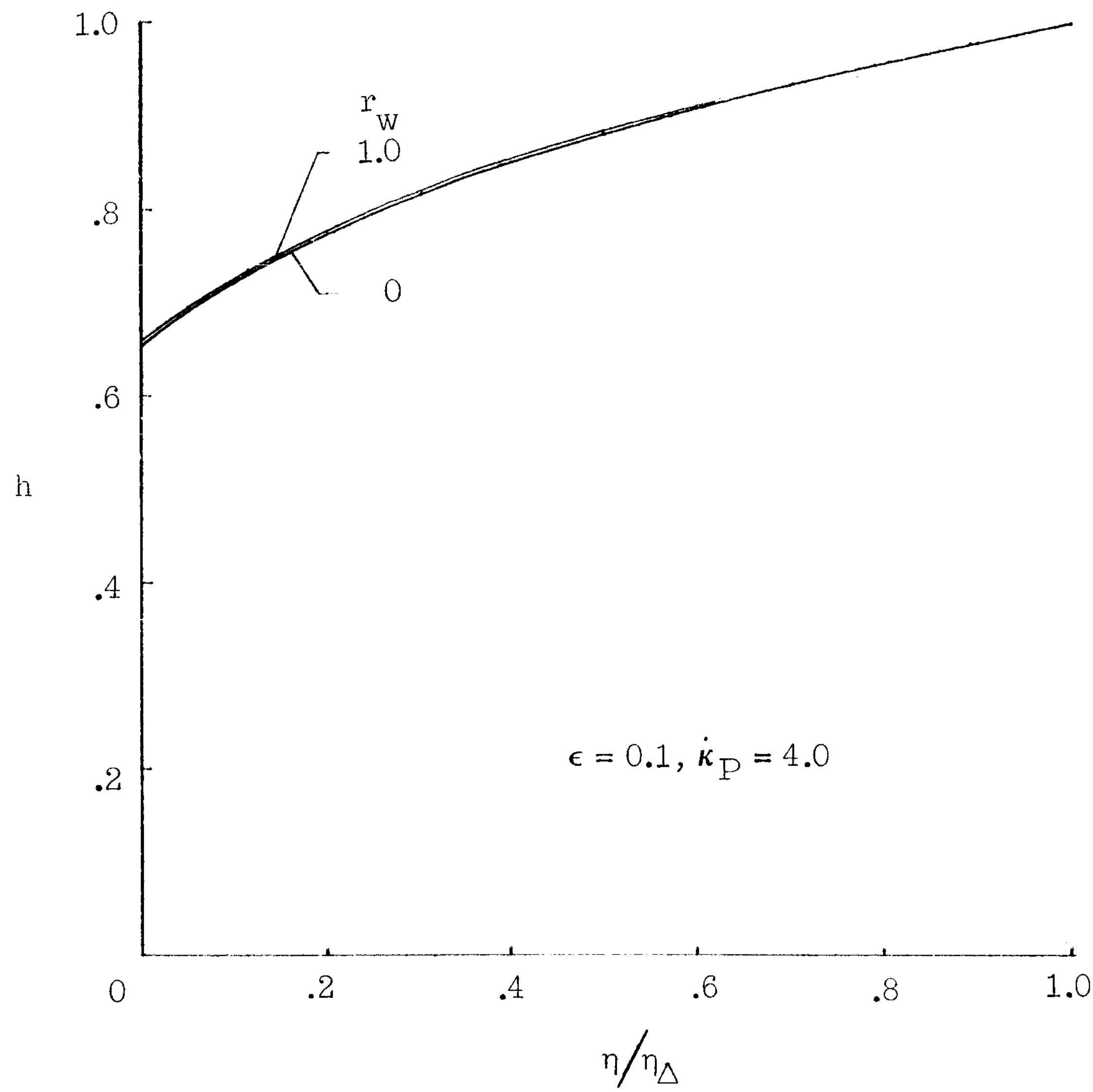

(a) $k_P = 0.1$.

Figure 3.4.- Effect of surface reflectivity on the shock layer enthalpy distribution.

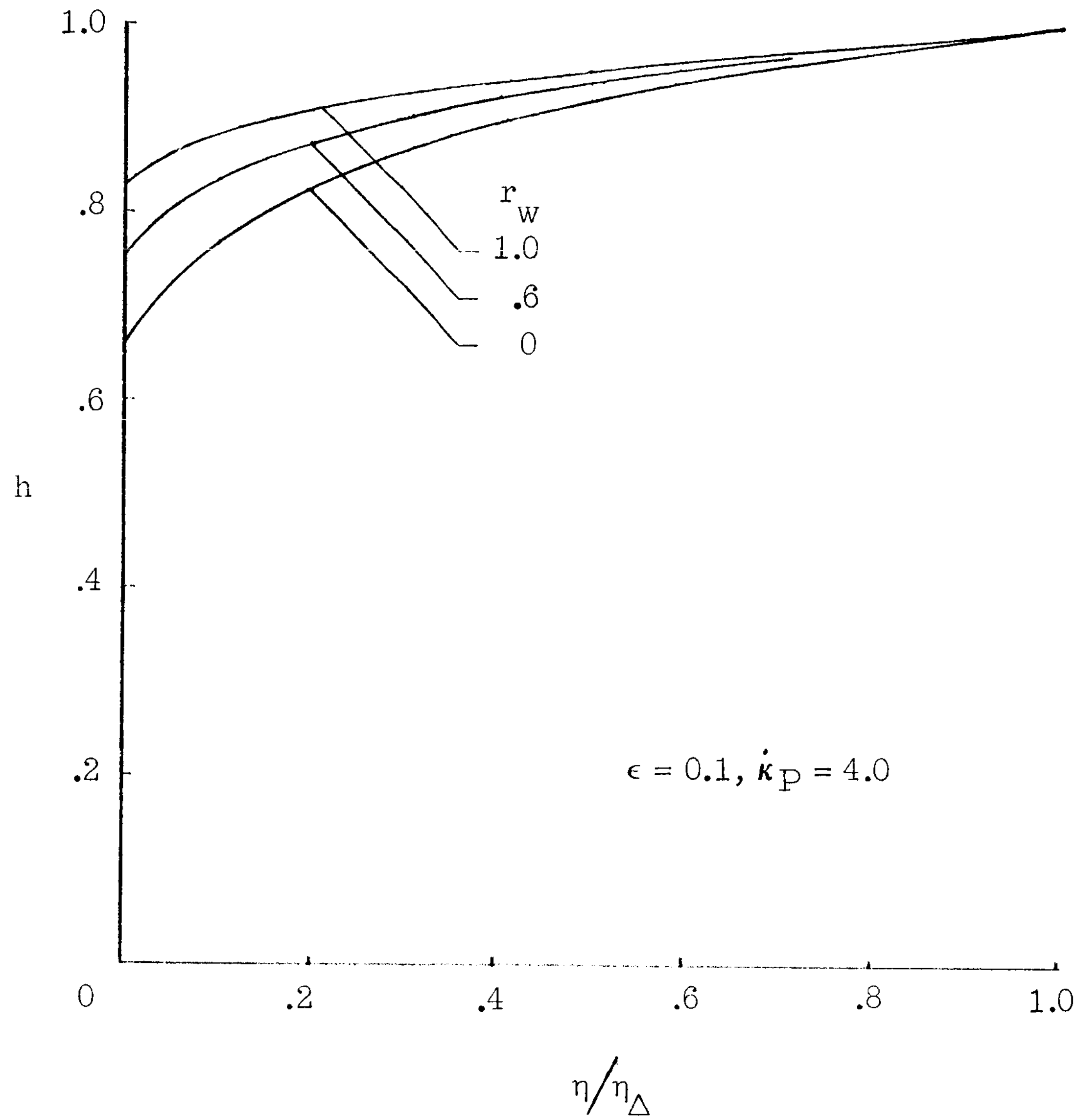

(b) $k_P = 1.0$.

Figure 3.4.- Continued.

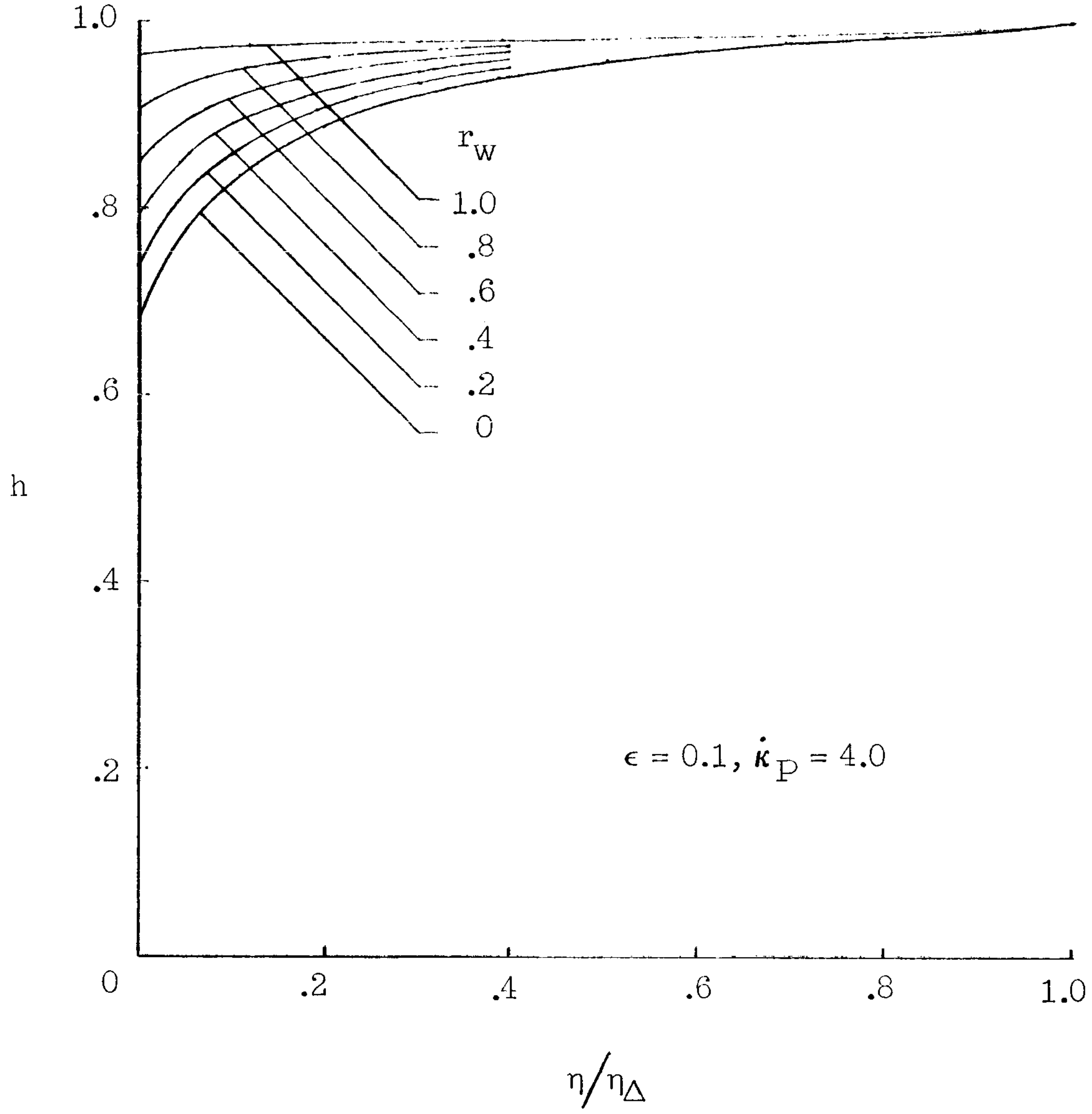

(c) $k_P = 3.0$.

Figure 3.4.- Concluded.

The variation of the enthalpy distribution with $\dot{\kappa}_P$ (the enthalpy variation of the Planck mean mass absorption coefficient) for several values of the Bouguer number k_P is shown in figures 3.3a to 3.3c. These effects are most noticeable for optically thin shock layers $\left(k_P \ll 1.0\right)$ and tend to vanish as the optical thickness increases. In a transparent layer, the rate of emission of radiant energy is proportional to the Planck mean mass absorption coefficient κ_P. Thus, gases with small values of $\dot{\kappa}_P$ (which mean larger values of κ_P when the nondimensional enthalpy is less than 1) will be cooled more than gases with large values of $\dot{\kappa}_P$. As the optical thickness increases smaller $\dot{\kappa}_P$ still implies greater emission rates but it also means greater absorption and more radiant energy available for absorption. The process of absorption tends to counteract the differences in emission rates due to differences in $\dot{\kappa}_P$. Finally, when radiation equilibrium is reached (this state is achieved in the interior of optically thick regions) the energy of the particle is independent of its optical properties. Of course, in those regions optically close to the shock and the wall the amount of radiant energy available for absorption is not so great as in the interior of the shock layer and particles in these regions cannot approach the state of radiation equilibrium (except in a region optically close to a perfectly reflecting surface). Thus, the enthalpy distribution remains dependent on the value of $\dot{\kappa}_P$ near the shock and the wall. This dependence of $\dot{\kappa}_P$ is surpressed near the shock where h is almost 1 because the values of κ_p are nearly the same dispite the differences in $\dot{\kappa}_p$.

The effect of surface reflectivity, r_w, on the shock layer enthalpy distribution is shown in figures 3.4a to 3.4c. If the shock layer gas is transparent (i.e., the gas does not absorb) surface reflectivity has no effect on the enthalpy distribution because all photons emitted by the layer escape. Whether or not a photon is absorbed or reflected by the wall is of no consequence. As the optical thickness of the layer increases the chance of capture of a photon by absorption in the layer is increased. If the surface reflectivity is increased also, the probability of capture is increased still further because many photons which might otherwise have escaped into the wall are reflected back into the layer and are once again subject to capture there. Consequently, the enthalpy level is higher near a reflecting wall than it would be near a nonreflecting wall.

It can be concluded from the above, that use of a reflecting surface will not reduce the radiant heat transfer rate from the gas to the wall by the factor $1 - r_w$ (unless, of cource, the gas is transparent) but will reduce it by some smaller fraction. This is because the radiant heat flux incident on the wall is larger when the wall is reflecting as a result of the higher enthalpy level. In addition, the rate of heat transferred to the wall by conduction will be greater, also because of the higher enthalpy level. Of course, increasing the surface reflectivity always decreases the total heat transfer rate to the wall because the higher enthalpy level must lead to an increased loss of energy by radiation through the shock in the upstream direction and by convection in a lateral direction away from the stagnation point. If the energy balance is to be maintained, the rate of heat transferred to the wall must be reduced.

The effects of variations in the parameters ϵ, k_P, $\acute{k}_P$, and r_w on the rate of radiant heat transfer to the wall (normalized by the energy influx to the shock layer, $\frac{1}{2}\rho_\infty W_\infty^3$) q_w^R are shown in figures 3.5 to 3.7. The rate of radiant heat transfer to the stagnation point was calculated with the formula

$$q_w^R = \epsilon\left(1 - r_w\right)\int_0^{\eta_\Delta} \kappa_P(\eta)\ B(\eta)\ E_2\left(k_P\ \tau(\eta)\right)d\eta \tag{3.39}$$

where the optical thickness $k_P\ \tau$ is given by

$$k_P\ \tau(\eta) = k_P \int_0^{\eta} \kappa_P(\eta)d\eta \tag{3.40}$$

The dashed curves in figure 3.5 indicate the "no decay limits" for various values of the Bouguer number. These limiting curves were computed by assuming the shock layer to be isenthalpic so that $\kappa_P(\eta) = B(\eta) = 1$. Thus, the no decay limit curves are given by the formula

$$q_w^R = \epsilon\left(1 - r_w\right)\frac{1 - 2E_3\left(k_P\right)}{2k_P} \tag{3.41}$$

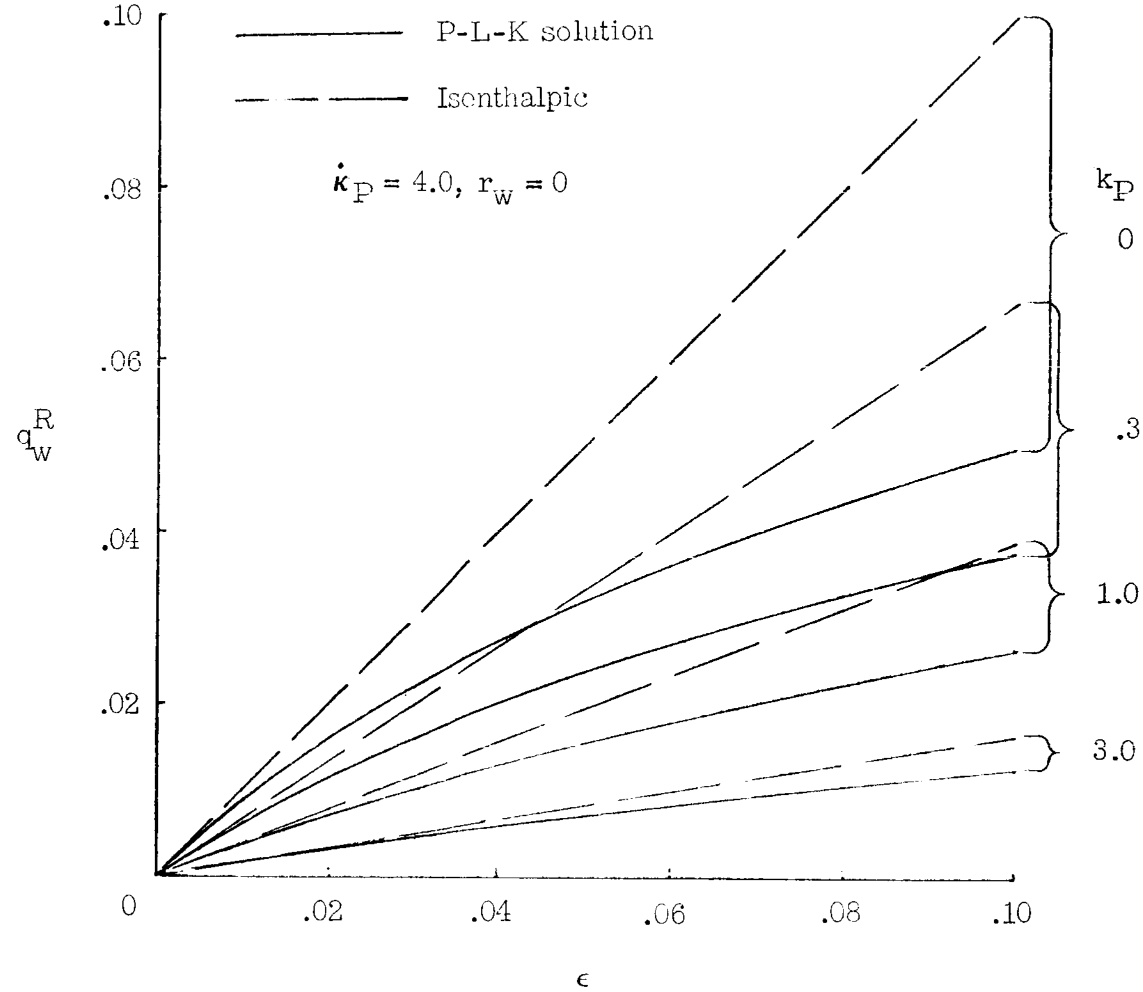

Figure 3.5.- Effect of ϵ and k_P on the rate of radiant heat transfer to the stagnation point.

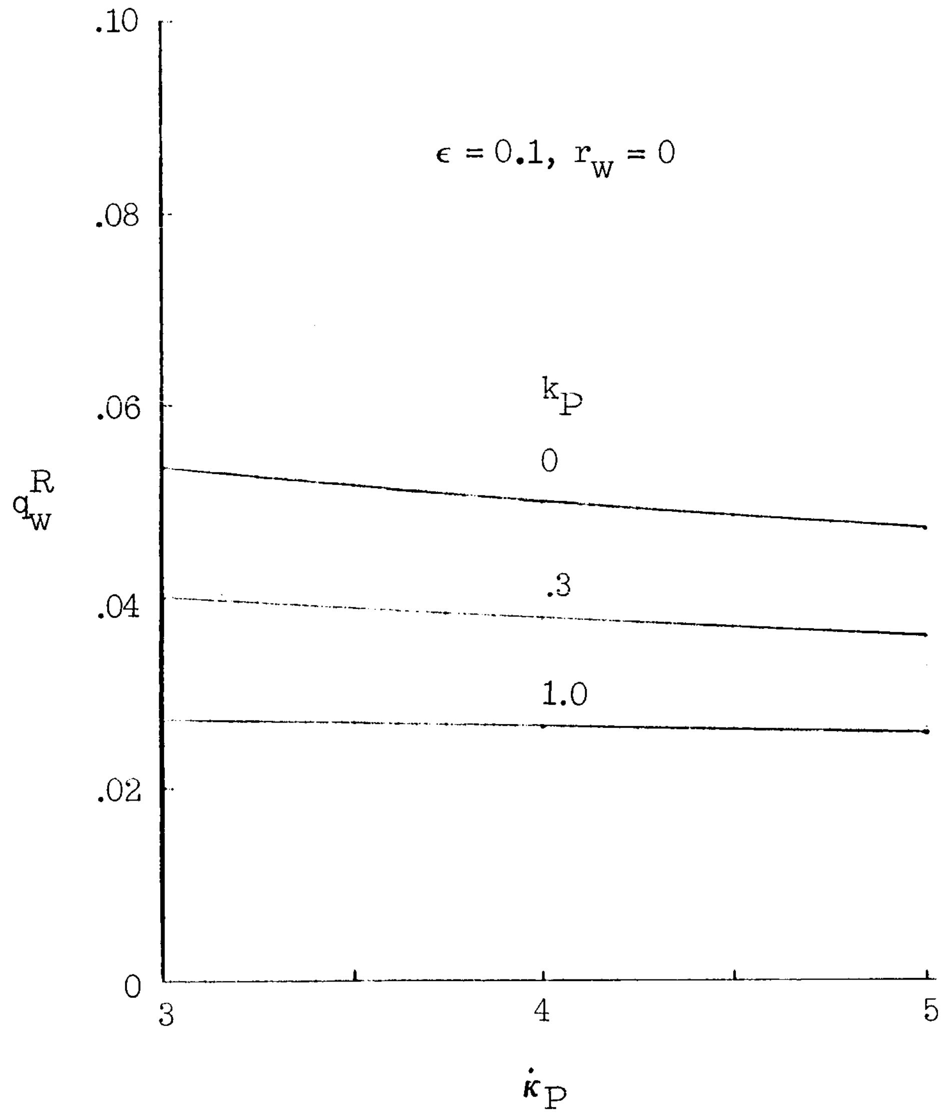

Figure 3.6.- Effect of the enthalpy variation of the absorption coefficient on the rate of radiant heat transfer to the stagnation point.

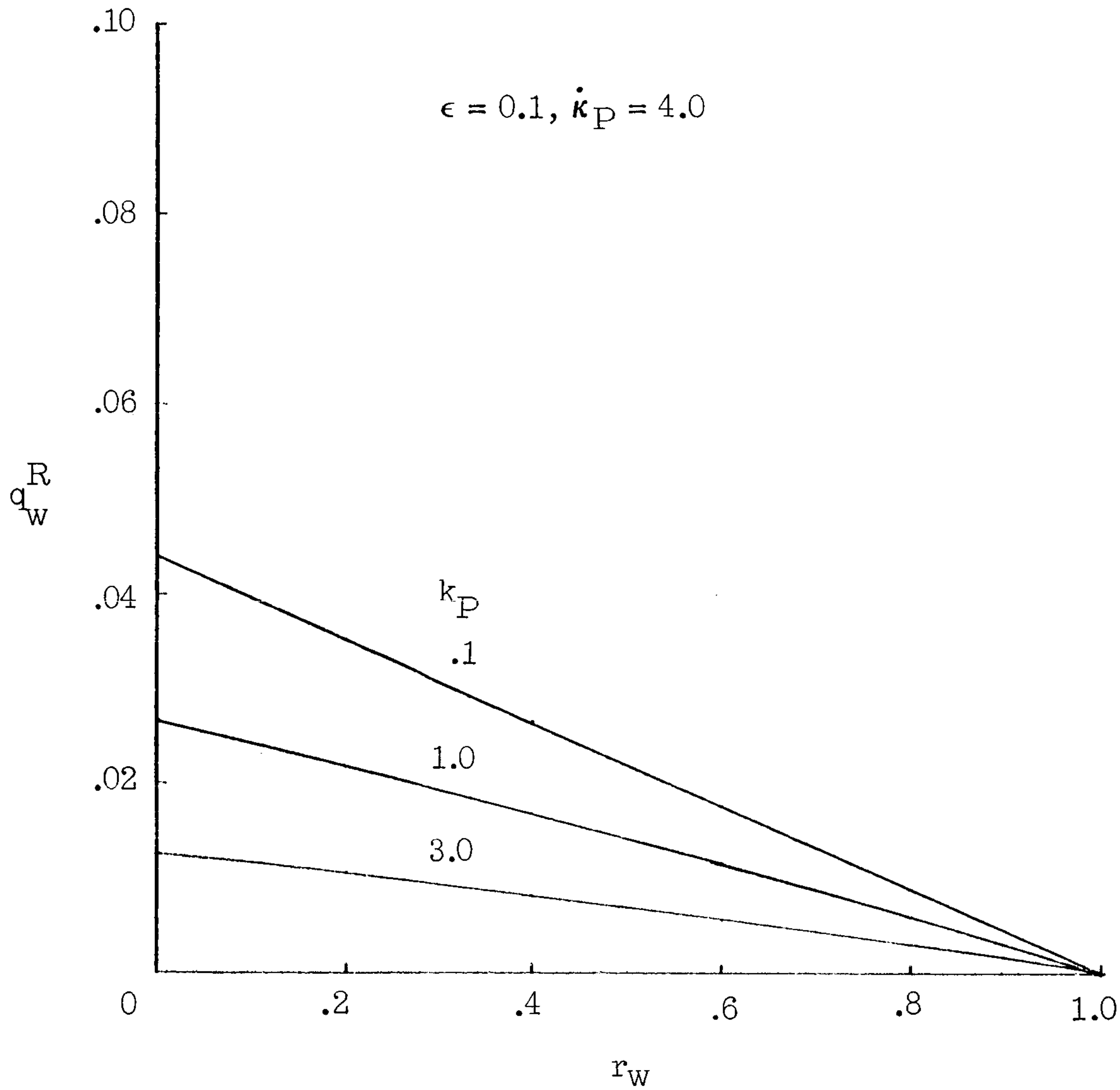

Figure 3.7.- Effect of surface reflectivity on the rate of radiant heat transfer to the stagnation point.

where $E_3(k_P)$ is the exponential integral function of third-order. This no decay approximation is often used to predict the rate of radiant heat transfer when radiation effects are small. Use of this approximation always gives an upper bound to the true value of q_w^R. A study of figure 3.5 indicates that the no decay limit curve is least accurate in predicting the rate of radiant heat transfer in the transparent case $k_P = 0$. This result is expected because the enthalpy distribution for the transparent case is the most perturbed from an isenthalpic state. Results presented in this figure also indicate the importance of absorption (as characterized by the Bouguer number k_P in reducing the rate of radiant heat transfer from the shock layer to the wall.

The results presented in figure 3.6 indicate the differences in $\dot{\kappa}_P$, the enthalpy variation of the Planck mean mass absorption coefficient, are most important when the optical thickness of the shock layer is small.

Here the radiant heat transfer to the wall is greatest for the smallest value of $\dot{\kappa}_P$. This, of course, supplements the observation (from fig. 3.3a) that radiation cooling is greatest for gases in which $\dot{\kappa}_P$ is least. The differences in radiant heat transfer to the wall brought about by differences in the value of $\dot{\kappa}_P$ tend to vanish as the optical thickness of the layer increases.

The reduction in radiant heat transfer to the wall due to surface reflectivity is shown in figure 3.7. When the shock layer is transparent, the rate of radiant heat transferred q_w^R is in the ratio

$1 - r_w$. However, as the optical thickness of the shock layer increases, the ratio becomes somewhat greater than $1 - r_w$ as predicted in an earlier discussion of this section.

The effect of the parameters ϵ, k_p, and r_w on the shock standoff distance is shown in figures 3.8 and 3.9. The quantity $\bar{\Delta}$ is the ratio of the shock standoff distance in a radiating shock layer to that in a nonradiating (or adiabatic) shock layer at the same flight conditions, and was computed with the formula

$$\bar{\Delta} = \int_0^{\eta_\Delta} h(\eta)d\eta \tag{3.33}$$

The results shown in figures 3.8 and 3.9 indicate, as expected, that a decrease in enthalpy level (with the consequent increase in density level) in a shock layer leads to a reduction in shock standoff distance.

Nongray results

It can be seen from figures 2.4 that the absorption coefficient of high temperature air depends strongly on wavelength. This is true of all other gases as well. Consequently, the assumption that the gas is gray (i.e., that the optical properties of the gas are independent of wavelength) is poor indeed, and has been resorted to so frequently in the literature only because of the resulting relative simplicity. Fortunately, the small perturbation solution derived in this chapter overcomes these difficulties by reducing the

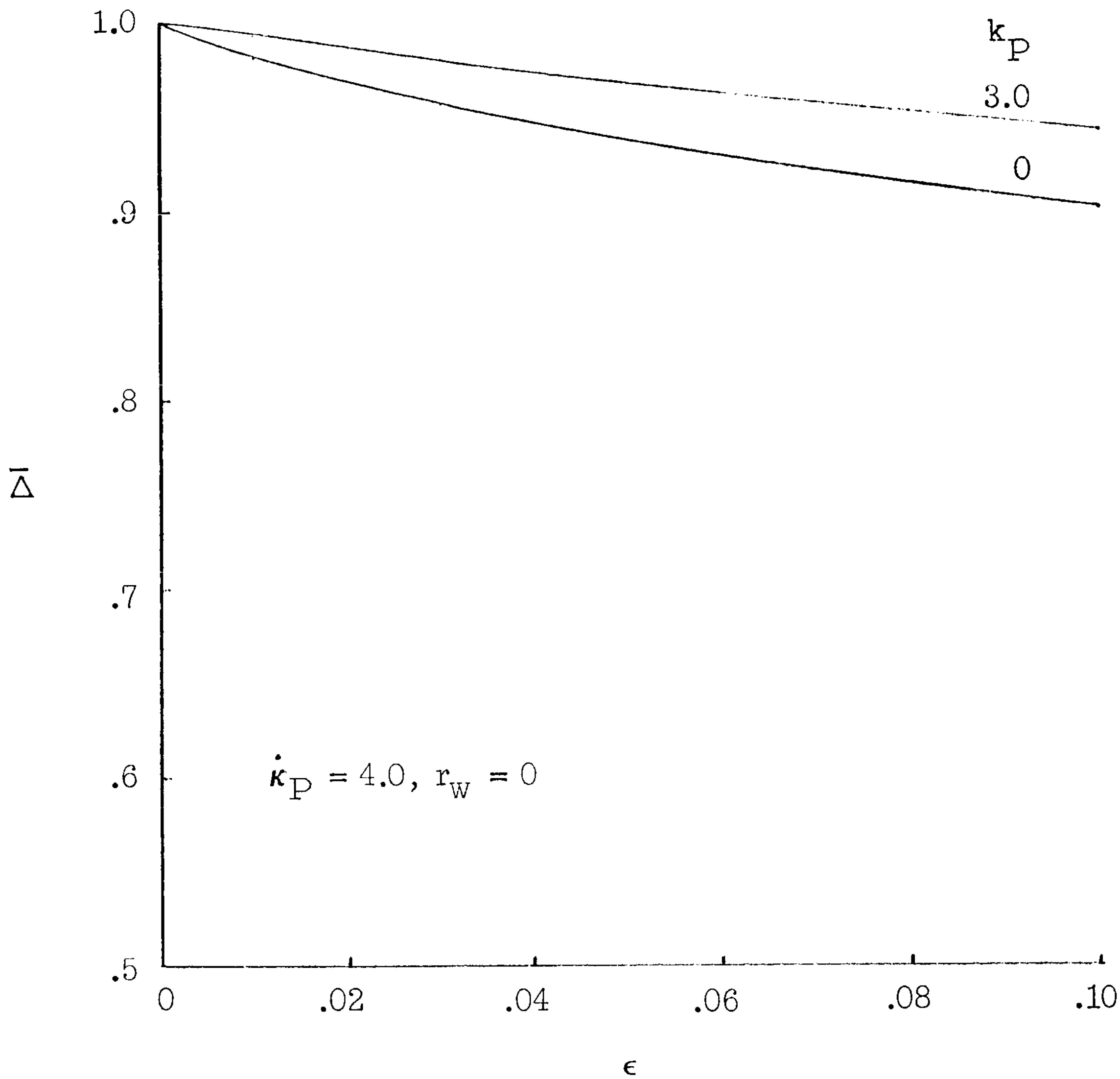

Figure 3.8.- Effect of ϵ and k_P on the shock standoff distance.

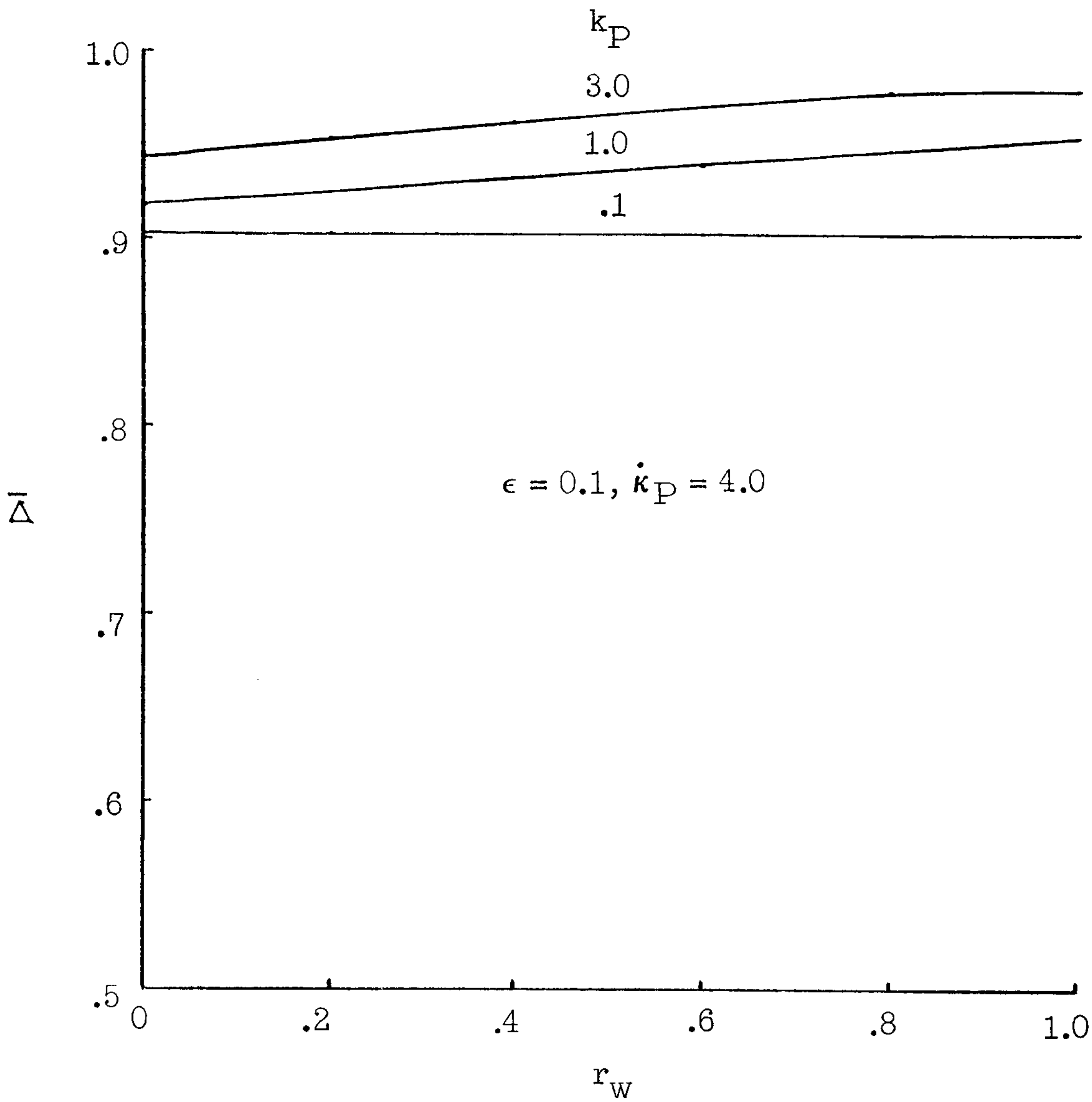

Figure 3.9.- Effect of surface reflectivity on the shock standoff distance.

absorption integrals in the divergence of the radiant flux to a form amenable to direct evaluation. Thus, one need only perform an integration over a known, albeit complicated, function of wavelength. In view of the current uncertainties, with regard to spectral distributions of gaseous absorption coefficients, it was decided to use a simplified model for the absorption coefficient of air. Consequently, the step function model shown in figure 3.10 was chosen for use in calculations to be reported on herein. The height and width of the steps were chosen so that the simple step function model provides an adequate representation of the absorption coefficient of air at a temperature of about $15{,}000^{\circ}$ K as predicted by Nardone et al. (ref. 45) and so that the Planck mean absorption coefficient of both distributions are equal. The relative heights of the nine steps located at wavelengths less than 0.113 microns were chosen to be independent of enthalpy while the tenth step which covers the wavelength interval $(0.113, \infty)$ was chosen to vary as the 1.28 power of the enthalpy. The relative heights shown in figure 3.10 are for $h = 1$, where h is the nondimensional enthalpy. The enthalpy variation of the step heights listed above is consistent with the condition that the Planck mean mass absorption coefficient is proportional to the fourth power of the enthalpy.

Shock layer enthalpy distributions were calculated using the nongray absorption coefficient model for various values of the Bouguer number, k_P. A comparison of the results of these calculations

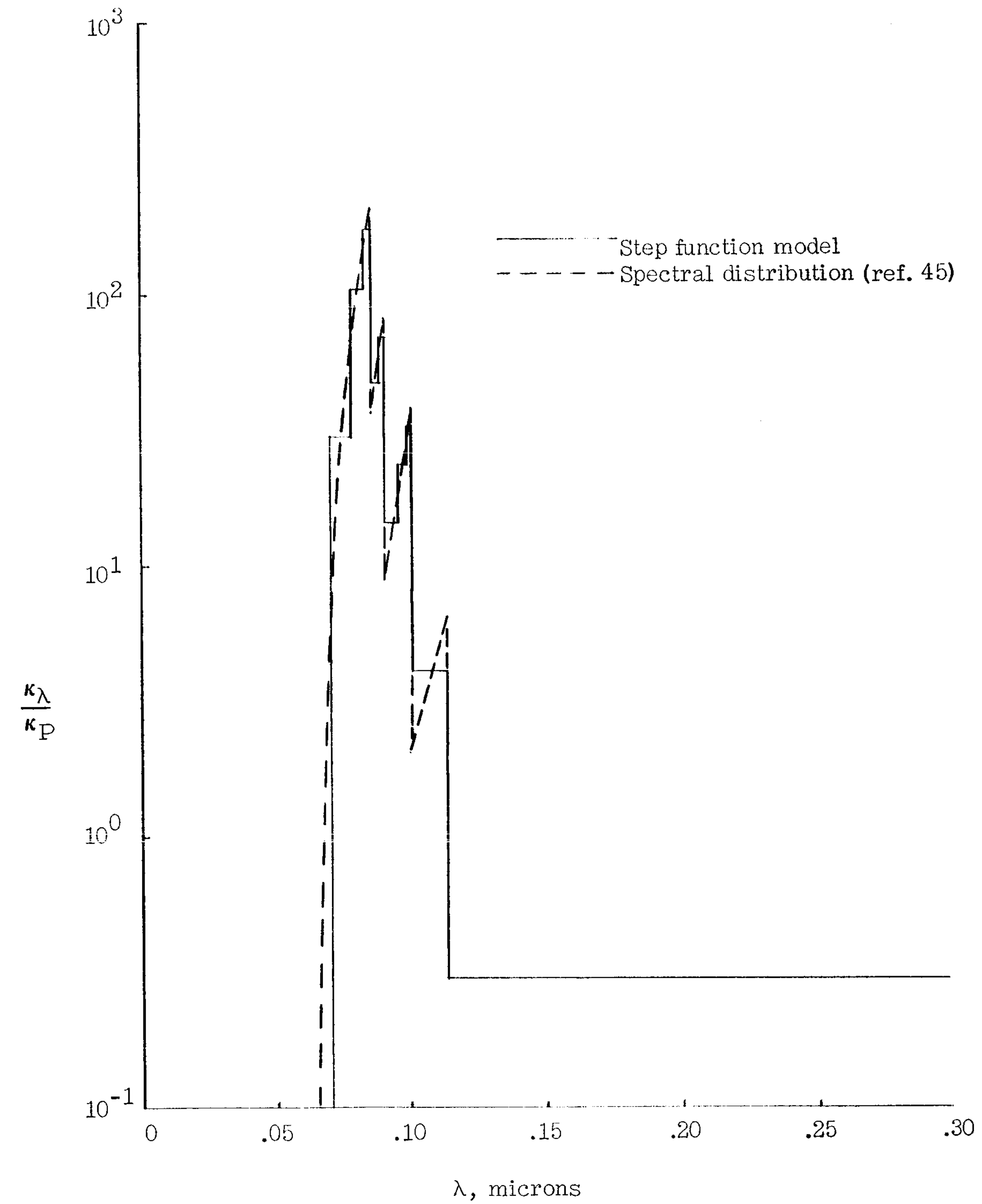

Figure 3.10.- Step function model of the mass absorption coefficient of high temperature air.

with gray calculations using the Planck mean mass absorption coefficient is presented in figures 3.11a to 3.11c.

The maximum monochromatic Bouguer number for the nongray shock layers is 186 times the Planck mean Bouguer number. When the Planck mean Bouguer number k_P is less than about 0.001 (this case is not shown) the shock layer is optically thin at all wavelengths and no perceptable difference between the nongray and the gray calculations for the enthalpy distribution can be found. When $k_P = 0.01$ the monochromatic Bouguer numbers for several of the steps are order of magnitude unity and absorption becomes important in the nongray model whereas absorption is still negligible in the gray model. As a consequence, of the above the enthalpy distribution for the nongray model lies above that for the gray model. When k_P is increased to 0.1, the disparity between the two solutions is increased still farther. In this case, absorption is very important in those regions of the spectrum for the nongray model in which much of the energy is emitted. Absorption is still of minor significance in the gray model. When $k_P = 1.0$ absorption becomes important in the gray model but still not to the extent that it is in the nongray case.

Obviously, and not unexpectedly, a gray model which uses the Planck mean mass absorption coefficient will not provide an acceptable estimate of the shock layer enthalpy distribution for a nongray gas unless that gas is optically thin at all wavelengths in which a

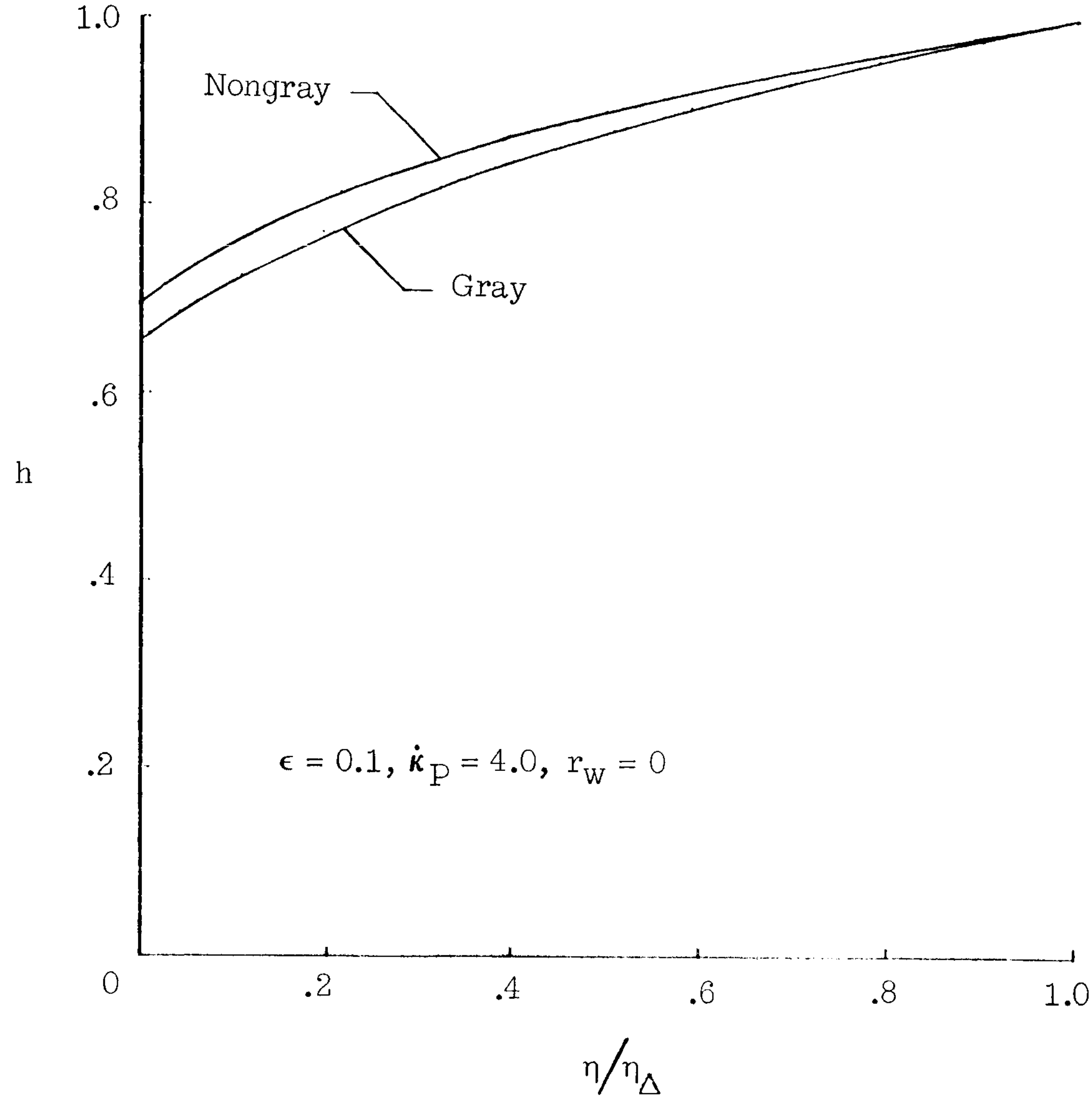

(a) $k_P = 0.01$.

Figure 3.11.- Shock layer enthalpy distribution for a nongray absorption coefficient.

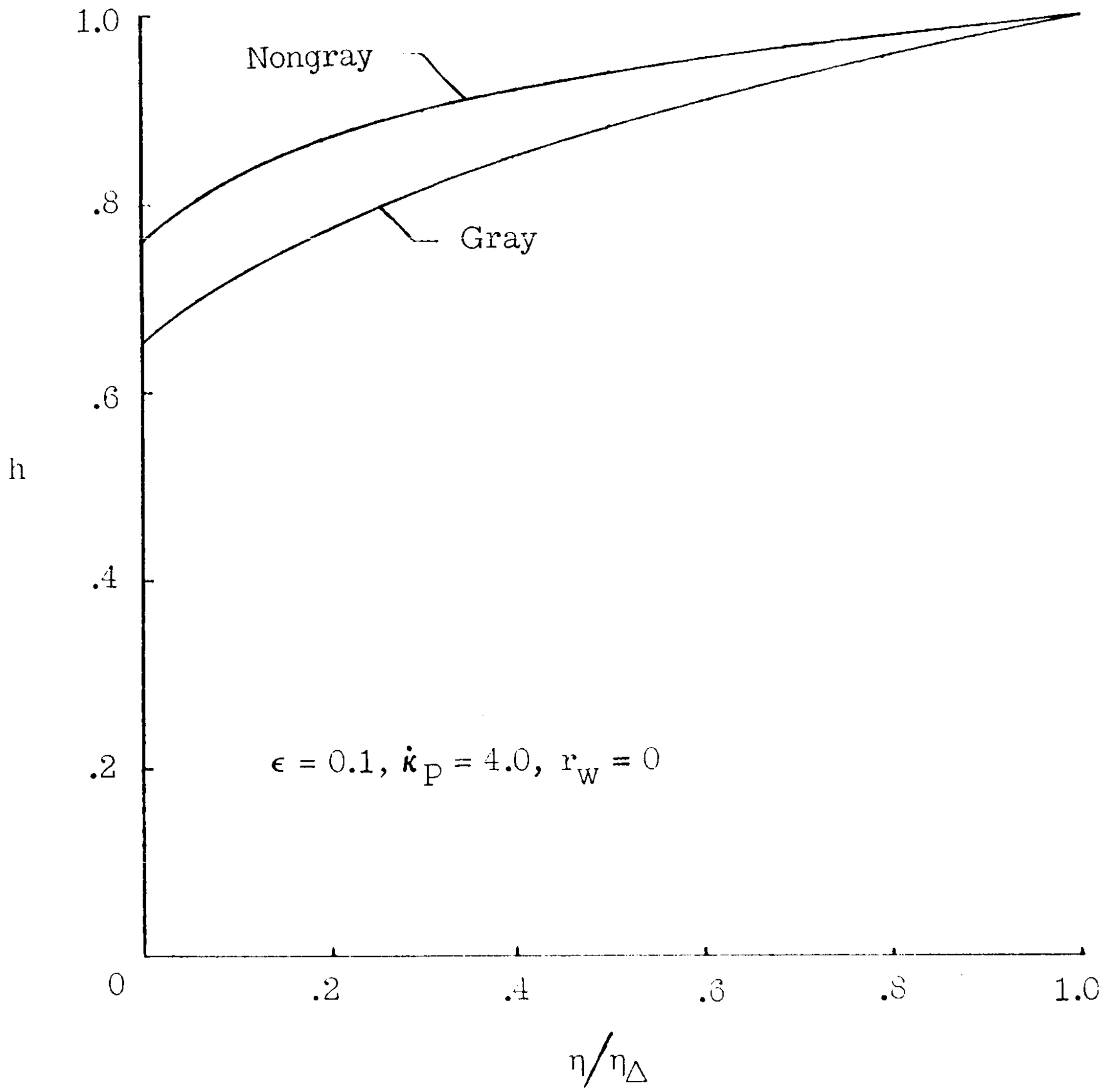

(b) $k_P = 0.1$.

Figure 3.11.- Continued.

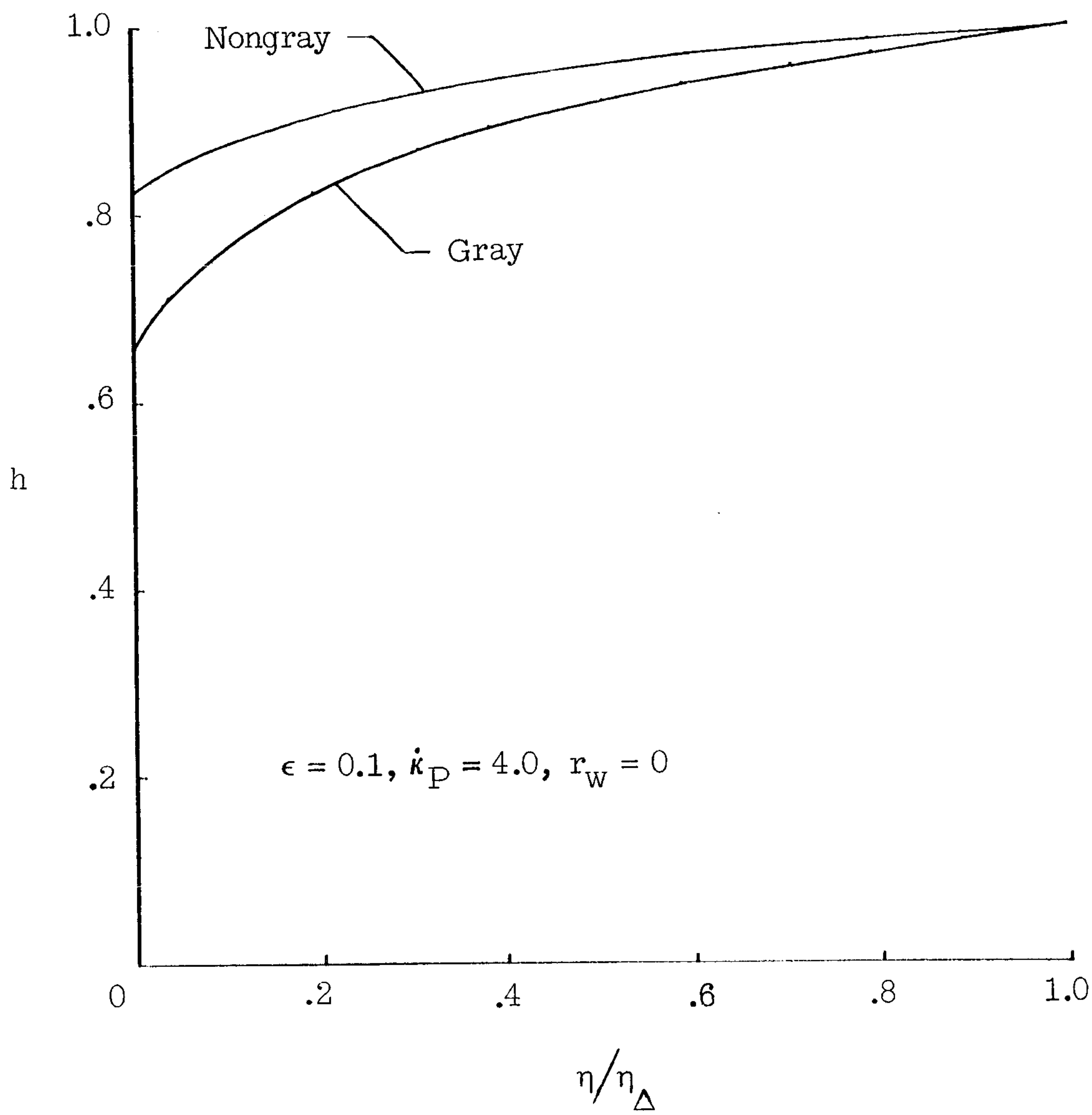

(c) $k_P = 1.0$.

Figure 3.11.- Concluded.

significant amount of radiation is transported. Nevertheless, it is very interesting, and encouraging to note that enthalpy distributions computed for the nongray models do not differ significantly in their general shape from those that can be computed for gray models. Thus, it appears that there is some wavelength averaged absorption coefficient (other than the Planck mean when absorption is important but tending toward it in the transparent limit) which will provide a good approximation to the enthalpy distribution in a nongray gas.

The rate of radiant heat transfer to the stagnation point has been calculated for nongray shock layers. The results are compared in figure 3.12 with the results of gray calculations using the Planck mean absorption coefficient. The gray approximation provides a considerable overestimate of the radiant heating even for values of the Planck mean Bouguer number as small as 10^{-3}. It is apparent from this result that the tallest steps play a very important role in the transfer of energy by radiation. This is not surprising when one considers that nearly 40 percent of the energy emitted by a particle in the shock layer is transmitted in the wavelength intervals occupied by the three tallest steps.

It can be concluded from the foregoing discussion that the effective optical thickness (or Bouguer number) of a nongray shock layer is greater than that predicted by a gray analysis using the Planck mean absorption coefficient. In order to account for this by means of average absorption coefficients, it seems proper to follow

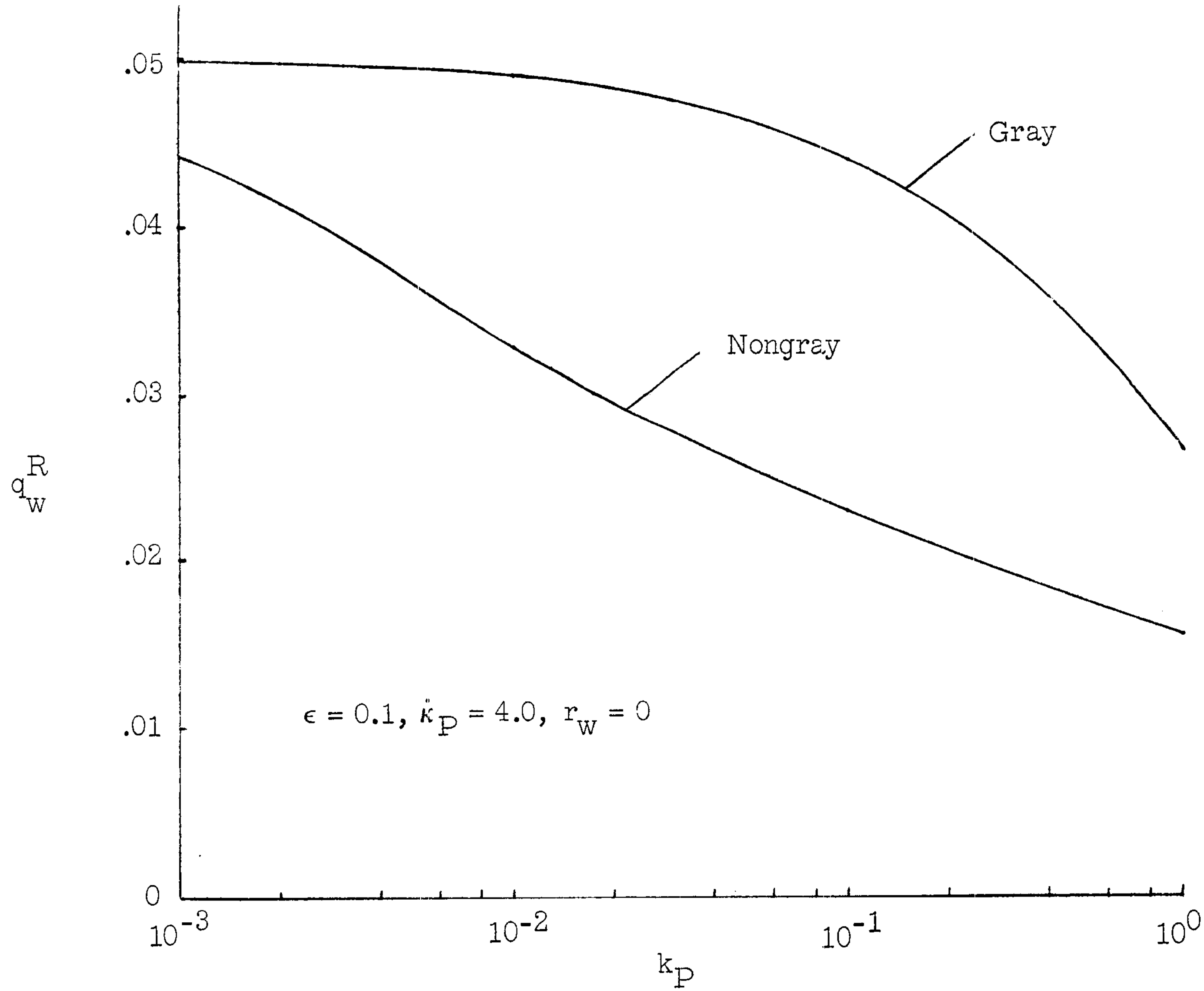

Figure 3.12.- Rate of radiant heat transfer to the stagnation point in a nongray gas.

the advice of Viskanta (ref. 49) and introduce a "mean emission coefficient" and a "mean absorption coefficient." As Viskanta pointed out, the divergence of the radiant flux is composed of two terms, one of which accounts for emission and the second for absorption of radiation in an element of volume of radiating media. In particular, for this investigation, the divergence of the radiant flux may be written (see eq. (2.67))

$$\epsilon I\left[\eta\right] = -2\epsilon \int_0^\infty \kappa_\lambda(\eta)\ B_\lambda(\eta)d\lambda + \epsilon k_P \int_0^\infty \epsilon\kappa_\lambda(\eta)\ G_\lambda(\eta)d\lambda \tag{3.34}$$

where

$$\begin{aligned} G_\lambda(\eta) = & \int_0^{\eta_\Delta} \kappa_\lambda(\eta')\ B_\lambda(\eta')\ E_1\Big(k_P\left|\tau_\lambda(\eta) - \tau_\lambda(\eta')\right|\Big)d\eta' \\ & + 2r_w\ E_2\Big(k_P\ \tau_\lambda(\eta)\Big) \int_0^{\eta_\Delta} \kappa_\lambda(\eta')\ B_\lambda(\eta')\ E_2\Big(k_P\ \tau_\lambda(\eta')\Big)d\eta' \end{aligned} \tag{3.35}$$

The first term on the right-hand side of equation (3.34) is the local emission term. The integration over wavelength can be performed for this term using the definition of the Planck mean absorption coefficient (eq. (2.68)) so that equation (3.34) becomes

$$\begin{aligned} \epsilon I\left[\eta\right] = & -2\epsilon\kappa_P(\eta)\ B(\eta) \\ & + \epsilon k_P \int_0^\infty \kappa_\lambda(\eta)\ G_\lambda(\eta)d\lambda \end{aligned} \tag{3.36}$$

Thus, the mean emission coefficient is identical to the Planck mean absorption coefficient. The mean absorption coefficient can be defined by the formula

$$\kappa_a(\eta) = \frac{\int_0^\infty \kappa_\lambda(\eta)\ G_\lambda(\eta)d\lambda}{\int_0^\infty G_\lambda(\eta)d\lambda} \tag{3.37}$$

Unfortunately, the spectral characteristics of the quantity $G_\lambda(\eta)$ which represents the amount of radiant energy incident per unit mass on an element of mass located at η, depends on the spectral characteristics of the radiating media and the boundary surfaces. Therefore, the spectral distribution of $G_\lambda(\eta)$ will not be the same as that of the Planck function $B_\lambda(\eta)$ which depends only on the temperature at η and in general $\kappa_a \neq \kappa_P$. The primary difficulty involved in the determination of the mean absorption coefficient κ_a is that the quantity $G_\lambda(\eta)$ is not known rigorously until the whole problem has been solved. This difficulty does not arise in the use of the small perturbation method of this chapter, of course, because the quantities in the equations of various order in ϵ corresponding to $G_\lambda(\eta)$ are known rigorously from the solution of the lower-order equations. In problems where $G_\lambda(\eta)$ is not known explicitly, it is hoped that it will be possible to obtain a reasonable first approximation.

CHAPTER IV

OPTICALLY THIN SHOCK LAYERS

A. The Transparent Approximation

Under certain conditions, the Bouguer number, which is indicative of the optical depth of the shock layer, is very small compared to unity. When these conditions are met, absorption is unimportant and the absorption integrals which are modified by the Bouguer number can be dropped from the expression for the divergence of the radiant flux vector (see eq. (2.86)). This leads to considerable simplification because only the local emission rate of radiant energy need be considered. All of this radiant energy is assumed to escape the shock layer and it matters not, insofar as the gas is concerned, what path it takes. Consequently, surface reflectivity will have no influence on the enthalpy distribution in the shock layer. Since only the total rate of radiant energy emitted locally is of interest the details of its spectral distribution can be ignored.

The results of the simplification is the "transparent" form of the divergence of the radiant flux vector

$$I[\eta] = -2\kappa_p(\eta)\ B(\eta) \tag{4.1}$$

Where $I[\eta]$ is the divergence of the radiant flux vector, $\kappa_p(\eta)$ is the Planck mean mass absorption coefficient, and $B(\eta)$ the Planck black-body function. The shock layer is termed transparent because the gas is transparent to its own radiation. Use of the transparent approximation reduces the governing equations from integrodifferential to purely differential form. Several investigators (see, for example, refs. 4-7) have taken advantage of this simplicity to obtain approximate analytic solutions.

B. The Optically Thin Approximation

In this paper, a distinction shall be made between the terms "transparent" and "optically thin." A layer of gas will be called transparent if none of the radiation emitted by the gas in the layer is reabsorbed. An optically thin layer is one in which a small amount of absorption does occur and the optical depth of the layer is small but not zero. In the literature, "optically thin" is often used synonymously with "transparent" as defined above.

P. D. Thomas (ref. 27) expressed concern about the validity of the transparent approximation, particularly in the highly cooled region adjacent to the cold wall. The transparent approximation is based on the assumption that emission is much greater than absorption throughout the shock layer. In regions of small enthalpy, emission no longer dominates absorption, and when radiation cooling effects are large, these regions may extend over a significant portion of the shock layer. Even when radiation cooling effects are small, the value of enthalpy adjacent to the wall tends to vanish* and absorption must become important compared to the local rate of emission. Of course, for this case, the region of nonvalidity is very small and has no appreciable effect on overall properties such as the radiant energy flux to the wall and the shock standoff distance.

Thomas sought to modify the transparent equations in order to take into account this small amount of reabsorption. He did so by expanding the Planck function $B_\lambda(t)$ which appears in the integrand of the divergence of the radiant flux vector in a Taylor series about the zero of the argument of the displacement kernal $E_1\left(k_P\left|\tau_\lambda - t_\lambda\right|\right)$. The expansion is then arbitrarily truncated after the linear term. Strictly speaking, this procedure can be used only when the Planck function varies slowly within a photon mean free path length. Obviously this criterion is not met when the shock layer is optically thin (particularly close to the wall, the region of greatest interest, where the enthalpy and hence, the Planck function varies rapidly) and some doubt must be cast on the validity of Thomas' analysis.

It would appear that the effects of small absorption could better be discovered through a straightforward expansion of the equations in terms of the Bouguer number k_P. Such a solution, up to first-order

---

*An element of gas approaching the wall requires an infinite time to reach its destination. Because of this and the fact that the rate of energy lost by radiation is proportional to a positive power of the enthalpy, the enthalpy of a transparent gas must approach zero as the particle approaches the wall.

in k_P, is presented here. In order to simplify the analysis the exponential integral functions $E_2(x)$ and $E_3(x)$ which appear in the expression for the radiant flux are replaced by the exponential functions e^{-2x} and $(1/2)e^{-2x}$, respectively. The particular form of the exponential functions was chosen so that the area under the curve of $E_2(x)$ and the approximating exponential are equal for the interval $(0, x_\Delta)$, for $x_\Delta \ll 1$, and so that the value for the radiant flux reduces to the proper value in the transparent limit. This substitute kernal approximation has been used with considerable success in a variety of problems of radiant transfer (see, for example, refs. 11, 30, 31, and 50).

Use of the substitute kernal approximation reduces the expression for the radiant flux to the form

$$q^R(\eta) = \epsilon \int_0^\infty \left\{ \int_0^{\eta_\Delta} \kappa_\lambda(\xi) B_\lambda(\xi) \mathrm{Sign}\left[\tau_\lambda(\eta) - \tau_\lambda(\xi)\right] e^{-2k_P\left|\tau_\lambda(\eta)-\tau_\lambda(\xi)\right|} d\xi \right.$$

$$\left. + r_w e^{-2k_P\tau_\lambda(\eta)} \int_0^{\eta_\Delta} \kappa_\lambda(\xi) B_\lambda(\xi) e^{-2k_P\tau_\lambda(\xi)} d\xi \right\} d\lambda \qquad (4.2)$$

The divergence of the radiant flux vector is

$$I[\eta] = 2\kappa_P(\eta)B(\eta) - 2k_P \int_C^\infty \kappa_\lambda(\eta) \left\{ \int_0^{\eta_\Delta} \kappa_\lambda(\xi) B_\lambda(\xi) e^{-2k_P\left|\tau_\lambda(\eta)-\tau_\lambda(\xi)\right|} d\xi \right.$$

$$\left. + r_w e^{-2k_P\tau_\lambda(\eta)} \int_0^{\eta_\Delta} \kappa_\lambda(\xi) B_\lambda(\xi) e^{-2k_P\tau_\lambda(\xi)} d\xi \right\} d\lambda \qquad (4.3)$$

Here the monochromatic optical depth is

$$\tau_\lambda(\eta) = \int_0^\eta \kappa_\lambda(\eta)d\eta \qquad (4.4)$$

It was seen in chapter III that an expansion of the governing equations in terms of the small parameter ϵ led to a fortuitous uncoupling of the energy and momentum equations. Unfortunately, the same is not accomplished when the expansion is performed in terms of κ_P. It is frequently pointed out in the literature (for example, refs. 4 and 6) that the coupling is quite weak.* Advantage can be taken of this situation by replacing $\mathcal{F}_3(\eta) = h(\eta)$ which appears in the momentum equation (2.71) with $\bar{h}$, the integrated average of $h(\eta)$ over the interval $\left(0, \eta_\Delta\right)$; that is,

$$\bar{h} = \frac{1}{\eta_\Delta} \int_0^{\eta_\Delta} h(\eta)d\eta \qquad (4.5)$$

(This replacement is tantamount to solving the momentum equation by the integral method with $f(\eta)$ assumed to be a quadratic function.) This approximation has the twin virtues of retaining the coupling,

---

*The solution to the momentum equation depends on the solution to the energy equation through the term $a^2 \mathcal{F}_3(\eta)$ (see eq. (2.71)) where a^2 is order of magnitude X. An analysis of equation (2.71) indicates that the contribution of this term to $f(\eta)$ is order $\sqrt{X}$. Since X is very small (typically 0.06) the effect of the solution of the energy equation to $f(\eta)$ is order 0.25.

albeit in approximate form, and greatly simplifying the solution to the energy equation.

Now the governing system of equations takes the approximate form

$$f(\eta)\ h'(\eta) + \epsilon I\left[\eta\right] = 0 \tag{4.6}$$

$$2f(\eta)\ f''(\eta) - \left[f'(\eta)\right]^2 + a^2\ \bar{h} = 0 \tag{4.7}$$

$$f(0) = 0 \tag{4.8}$$

$$f\left(\eta_\Delta\right) = 1 \tag{4.9}$$

$$f'\left(\eta_\Delta\right) = \frac{a}{\sqrt{2X(1 - X)}} \tag{4.10}$$

$$h\left(\eta_\Delta\right) = 1 \tag{4.11}$$

where $I\left[\eta\right]$ is given by equation (4.3). When the Bouguer number is very small, the absorption integrals in equation (4.3) assume a secondary significance throughout the domain of the problem. Neglecting these absorption integrals reduces the system to purely differential form. If, as expected, when the Bouguer number k_P is small, the presence of absorption only slightly influences the solution one can, to reasonable accuracy, evaluate the absorption integrals using the transparent solution for h. The perturbation expansion scheme used herein follows the general outline discussed above. Mathematical details are presented in appendix C.

The zero-order, or transparent, solution is

$$\int_{h_o}^{1} \frac{dh_o}{\kappa_P\left(h_o\right)B\left(h_o\right)} = \frac{2\epsilon\eta_{\Delta_o}}{a^*} \, ln \, \frac{(1 - a^*)x + a^*}{x} \qquad (4.12)$$

$$f_o(x) = (1 - a^*)x^2 + a^* x \qquad (4.13)$$

where

$$x = \eta/\eta_{\Delta_o} \qquad (4.14)$$

$$a^* = a\sqrt{\bar{h}_o}\ \eta_{\Delta_o} \qquad (4.15)$$

$$\eta_{\Delta_o} = \frac{1 + \sqrt{2X(1 - X)}}{1 + \sqrt{2\bar{h}_o X(1 - X)}} \qquad (4.16)$$

$$\bar{h}_o = \int_0^1 h_o(x)\ dx \qquad (4.17)$$

It was shown in chapter II that the Planck mean mass absorption coefficient normalized by its value immediately behind the shock can be adequately represented by

$$\kappa_P(h) = \begin{cases} h^{\gamma_2}, & h \geq h^* \\ C_1 h^{\gamma_1}, & h < h^* \end{cases} \qquad (4.18)$$

where $\frac{1}{2} W_\infty^2 h^*$ is the value of the enthalpy (depending on the pressure, of course) at which the value of the exponent of h changes. The constant C_1 is obtained by equating the two expressions for

$$\kappa_p(h) \quad \text{at} \quad h = h^*$$

with the result

$$C_1 = (h^*)^{\gamma_2 - \gamma_1} \tag{4.19}$$

It was also shown in chapter II that the nondimensional Planck function $B(h)$ is approximately given by the expression

$$B(h) = h^{2.2} \tag{4.20}$$

When the correlation formulas (4.18) and (4.20) are introduced into equation (4.12) the integration on the left-hand side can be carried out, and the solution for $h_o(x)$ given by the explicit formula

$$h_o(x) = \left\{ 1 + \frac{2\epsilon\left(\gamma_2 + 1.2\right)\eta\Delta_o}{a^*} \ln \frac{(1 - a^*)x + a^*}{x} \right\}^{-\frac{1}{\gamma_2 + 1.2}} \tag{4.21a}$$

for $h_o(x) \geq h^*$, and

$$h_o(x) = \left\{ (h^*)^{-\left(\gamma_2 + 1.2\right)} - \left(\frac{\gamma_1 + 1.2}{\gamma_2 + 1.2}\right) C_1 \left[(h^*)^{-\left(\gamma_1 + 1.2\right)} - 1 \right] + \frac{2\epsilon\left(\gamma_1 + 1.2\right) C_1 \eta\Delta_o}{a^*} \ln \frac{(1 - a^*)x + a^*}{x} \right\}^{-\frac{1}{\gamma_1 + 1.2}} \tag{4.21b}$$

for $h_o(x) < h^*$.

The first-order solutions which include the effects of absorption, surface reflectivity, and nongray radiation are presented below

$$h_1(x) = -2\epsilon\kappa_{P_o}(x)\, B_o(x)\left\{\eta_{\Delta_1} + \left(\frac{\eta_{\Delta_o}\,\bar{h}_1}{2\bar{h}_o}\right)\left[\left(1 - \frac{a^*\,\eta_{\Delta_o}}{1 + \sqrt{2X(1-X)}}\right)\frac{(1-x)}{(1-a^*)x + a^*} - \frac{1}{a^*}\ln\frac{(1-a^*)x + a^*}{x}\right]\right\} \tag{4.22}$$

$$+ \left(1 + r_w\right)\kappa_{P_o}(x)B_o(x)\eta_{\Delta_o}\int_0^\infty\left\{\left[\int_0^1 \kappa_{\lambda_o}(\xi)B_{\lambda_o}(\xi)\,d\xi\right]\int_{h_o}^1 \frac{\kappa_\lambda(h)\,dh}{\left[\kappa_p(h)B(h)\right]^2}\right\}d\lambda$$

$$f_1(x) = 2\,\frac{\eta_{\Delta_1}}{\eta_{\Delta_o}}\,x\left[1 - \frac{2 + \sqrt{2\bar{h}_o\,X(1-X)}}{1 + \sqrt{2\bar{h}_o\,X(1-X)}}\,x\right] \tag{4.23}$$

where

$$\eta_{\Delta_1} = -\frac{a^*\,\bar{h}_1}{4\bar{h}_o}\,\eta_{\Delta_o} \tag{4.24}$$

$$\bar{h}_1 = \frac{\bar{h}_o\displaystyle\int_0^1 h_1(X)\,dx}{\bar{h}_o + \frac{a^*}{4}\left(1 - \bar{h}_o\right)} \tag{4.25}$$

C. The P-L-K Solution

Careful inspection of the last term on the right-hand side of equation (4.22) reveals that the first-order term $h_1(x)$ displays a singular behavior near $\eta = 0$ (where h_o approaches zero). By way of illustration consider the case of a gray gas with $\kappa_p(h) = h^\gamma$ and $B(h) = h^{2.2}$. In this case the term in question is proportional to the quantity

$$h_o^{\gamma+2.2} \int_{h_o}^{1} \frac{dh}{h^{\gamma+4.4}} = \frac{h_o^{\gamma+2.2}}{\gamma + 3.4} \left[h_o^{-(\gamma+3.4)} - 1 \right] \qquad (4.26)$$

Near the wall, h_o approaches zero and equation (4.26) approaches

$$\frac{h_o^{-1.2}}{\gamma + 3.4}$$

which increases without limit. This, seemingly, anomalous behavior can be explained as follows. The first-order solution represents a gas which absorbs radiation at a rate determined by the absorption coefficient for a transparent gas* while it emits energy at a rate proportional to the derivative with respect to h_o of the emission rate for a transparent gas. Both the absorption and emission rates

---

*The magnitude of the incident radiation is independent of the amount absorbed.

tend to zero as an element of gas approaches the wall. However, the emission rate tends to zero much more rapidly than the absorption rate. The difference in the limiting behavior of these rates coupled with the infinite residence time for an element of gas in the stagnation region allows the gas element to absorb an infinite amount of energy and so the enthalpy of the gas adjacent to the wall becomes infinite.

The difficulty which has arisen as the result of the singularity can be avoided through the use of the P-L-K perturbation of coordinates procedure which transforms the coordinate in such a way that the singularity is removed from the boundary (at $x = 0$) to a point outside the domain of the problem (a slightly negative value of x). Mathematical details of the application of this method are described in appendix C. The P-L-K solutions to first order in k_P are

$$x = y + k_P\, x_1^*(y) \tag{4.27}$$

$$h(x;k_P) = h_o^*(y) \tag{4.28}$$

$$f(x;k_P) = f_o^*(y) + k_P f_1^*(y) \tag{4.29}$$

where the starred coefficients in the P-L-K expansions are related to the unstarred coefficients in the regular perturbation expansions (see ref. 48)

$$h_o^*(y) = h_o(y) \tag{4.30}$$

$$f_o^*(y) = f_o(y) \tag{4.31}$$

$$f_1^*(y) = f_1(y) + x_1^*(y)f_o'(y) \tag{4.32}$$

$$x_1^*(y) = -h_1(y)/h_o'(y) \tag{4.33}$$

D. Results and Discussion

In order to obtain some indication of the accuracy of the optically thin shock layer approximation, the results computed for a typical case are compared in figure 4.1 with the results computed by means of the small perturbation method of chapter III and the results of a numerical calculation performed by Howe and Viegas (ref. 9). The agreement among the three solutions is excellent. However, a word of caution should be interjected here in order to avoid the implication that the numerical results of Howe and Viegas represent the "exact" solution to the inviscid, plane-parallel geometry, stagnation flow model. The results of Howe and Viegas include viscosity, heat conductivity, and body curvature. The effects of curvature are expected to be quite small. The flight conditions (W_∞ = 9.75 km/sec, ps = 10 atm) were chosen to insure that the boundary layer was very thin so that "displacement" effects on the inviscid region were minimized. Finally, the thermodynamic and optical properties used by Howe and Viegas were obtained from their own correlations while the optically thin and small perturbation methods were computed using the correlations presented herein. Thus, the comparisons between the results from the methods of this paper and the numerical results of Howe and Viegas are as much, or more, checks on the validity of using

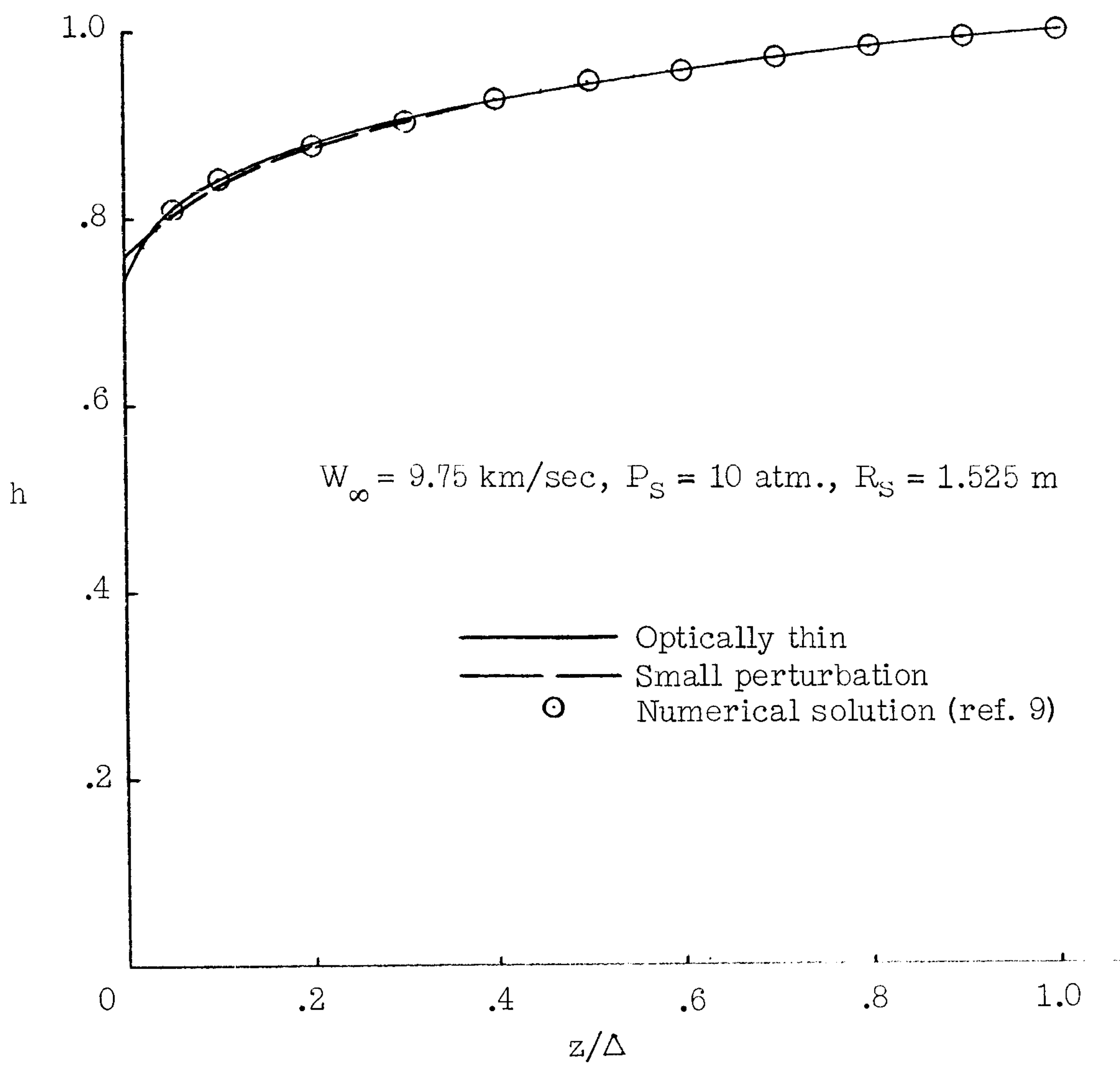

Figure 4.1.- Comparison of the optically thin and small perturbation solutions with numerical results.

the inviscid approach and checks on the similarity of two different sets of correlations as they are checks on the accuracy of the analytical methods of this paper. It is not inconceivable that erors due to the various factors mentioned tend to cancel in this example. Nevertheless, the individual errors due to the omission of viscosity, heat conductivity, and curvature and due to the difference in correlation functions are expected to be quite small so that the excellent agreement can still be interpreted as an indication of the accuracy of the methods of this and the preceding chapter.

The approximate solution derived in the preceding sections of this chapter was used to study the effects of the radiation cooling parameter, ϵ, the Bouguer number k_p, the surface reflectivity r_w, and the enthalpy dependence of the absorption coefficient on the shock layer enthalpy distribution, the rate of radiant heat transfer to the stagnation point, and the shock standoff distance. As in the previous chapter, the density ratio X across the near normal portion of the shock was fixed at a value of 0.06. In addition, all the results are limited to the case of a gray gas.

The effect of absorption on the enthalpy distribution is indicated by the curves of figure 4.2. The solid curves represent the enthalpy distributions in transparent shock layer for $\epsilon = 0.01$, 1.0, and 100. The dashed curves represent the enthalpy distributions in optically thin shock layers for the same values of the radiation cooling parameter ϵ. Values of the optical thicknesses are shown on the figure. These results show the expected trend with the enthalpy level falling as the radiation cooling parameter ϵ increases. Absorption tends to increase the enthalpy particularly in the cooler

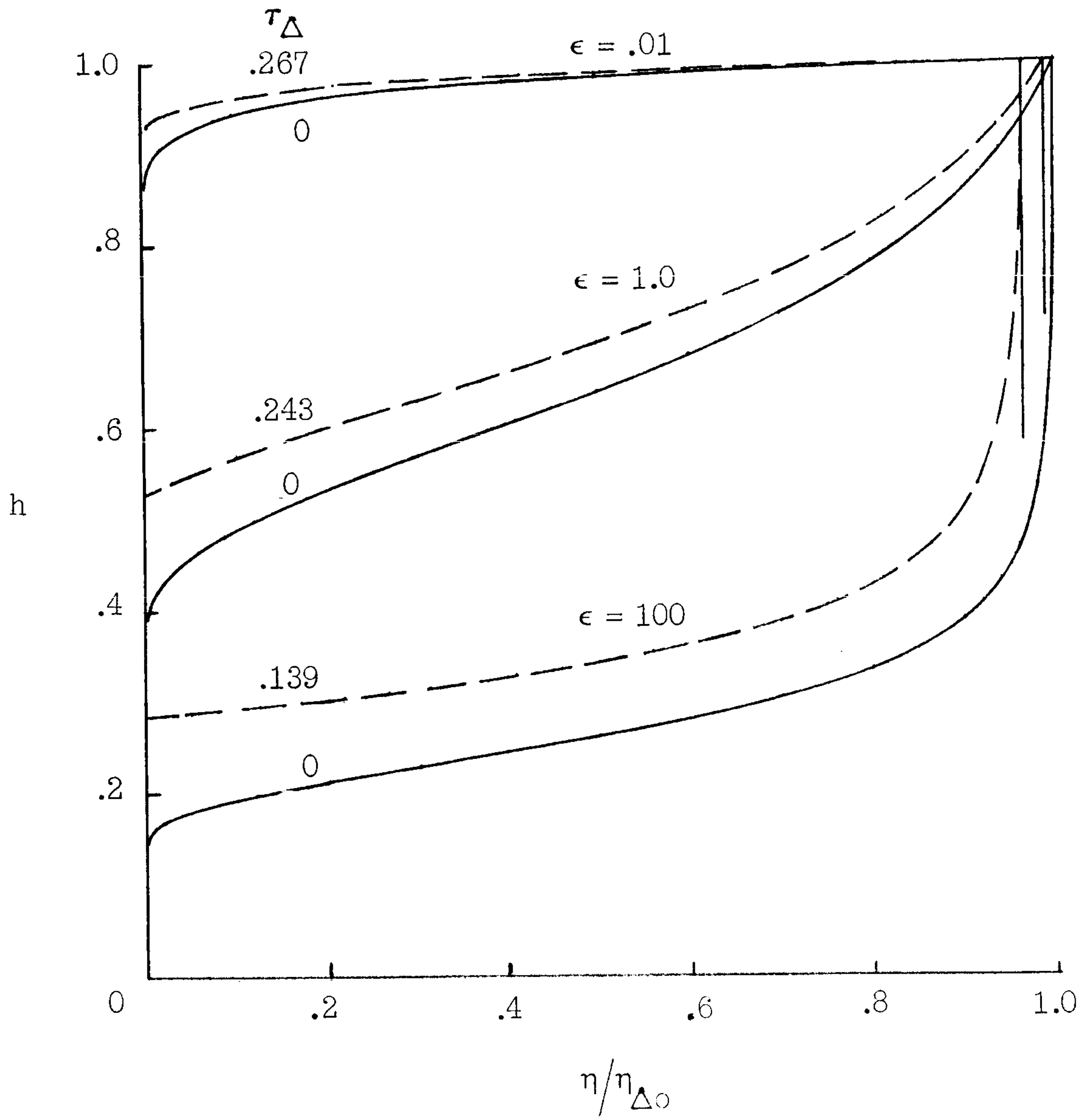

Figure 4.2.- Effect of absorption on the enthalpy distribution in an optically thin shock layer.

regions of the flow. Absorption also affects the location of the shock reducing the value of η_Δ (the location of the shock in terms of the Dorodnitsyn coordinate) because of the decreased density level. Although the value of η_Δ decreases, the shock standoff distance Δ increases with increasing optical depth.

The effect of the enthalpy dependence of the absorption coefficient on the enthalpy distribution in transparent shock layers is shown in figure 4.3. In part (a) the absorption coefficient was given by the relation $\kappa_p = h^\gamma$, where γ takes on the values 3, 4, and 5.* The value of γ determines how the rate of energy emission varies with enthalpy across the shock layer. The rate of energy loss by radiation will decrease more rapidly as the enthalpy falls if γ is large than if it is small. Consequently, the enthalpy distribution for a large value of γ lies above that for a smaller value. This, of course, is the same trend exhibited by the small perturbation solutions of the previous chapter. In part (b) the absorption coefficient is given by the relation $\kappa_p = Ch^\gamma$ where $C = (h^*)^{\gamma_2 - \gamma_1}$ and $\gamma = \gamma_1 = 4$ for $h < h^*$, and $C = 1$ and $\gamma = \gamma_2 = 1$ for $h > h^*$. This model should be used when the shock layer temperatures are in excess of about 20,000° K since at moderate altitudes h^* (the enthalpy at which the exponent γ changes value) corresponds to temperatures of approximately this value. The effects of varying

---

*These values of γ are typical for air at temperatures less than about 20,000° K (see chapter II, section E).

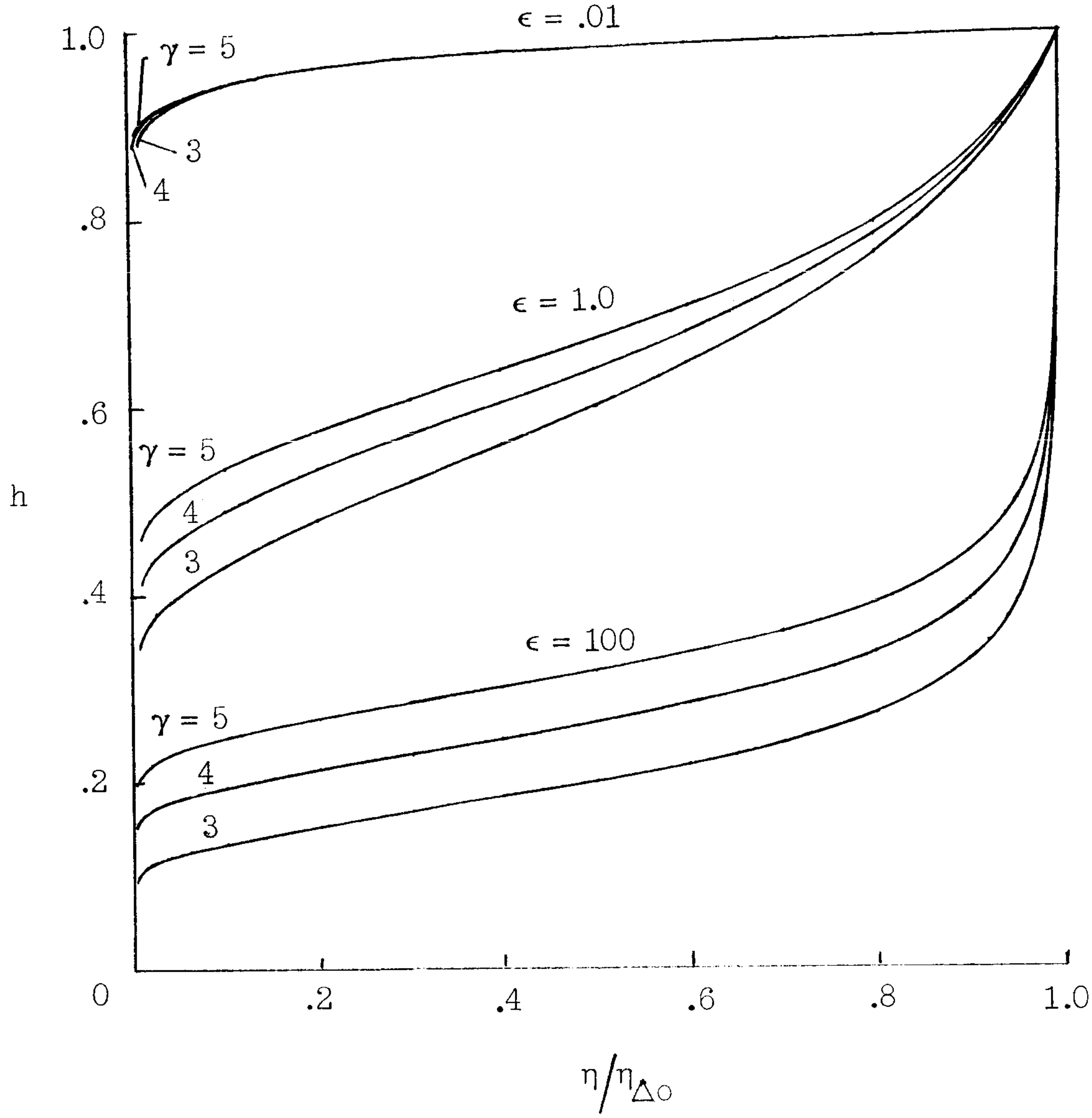

(a) Effect of γ.

Figure 4.3.- Effect of the enthalpy dependence of the absorption coefficient on the enthalpy distribution in an optically thin shock layer.

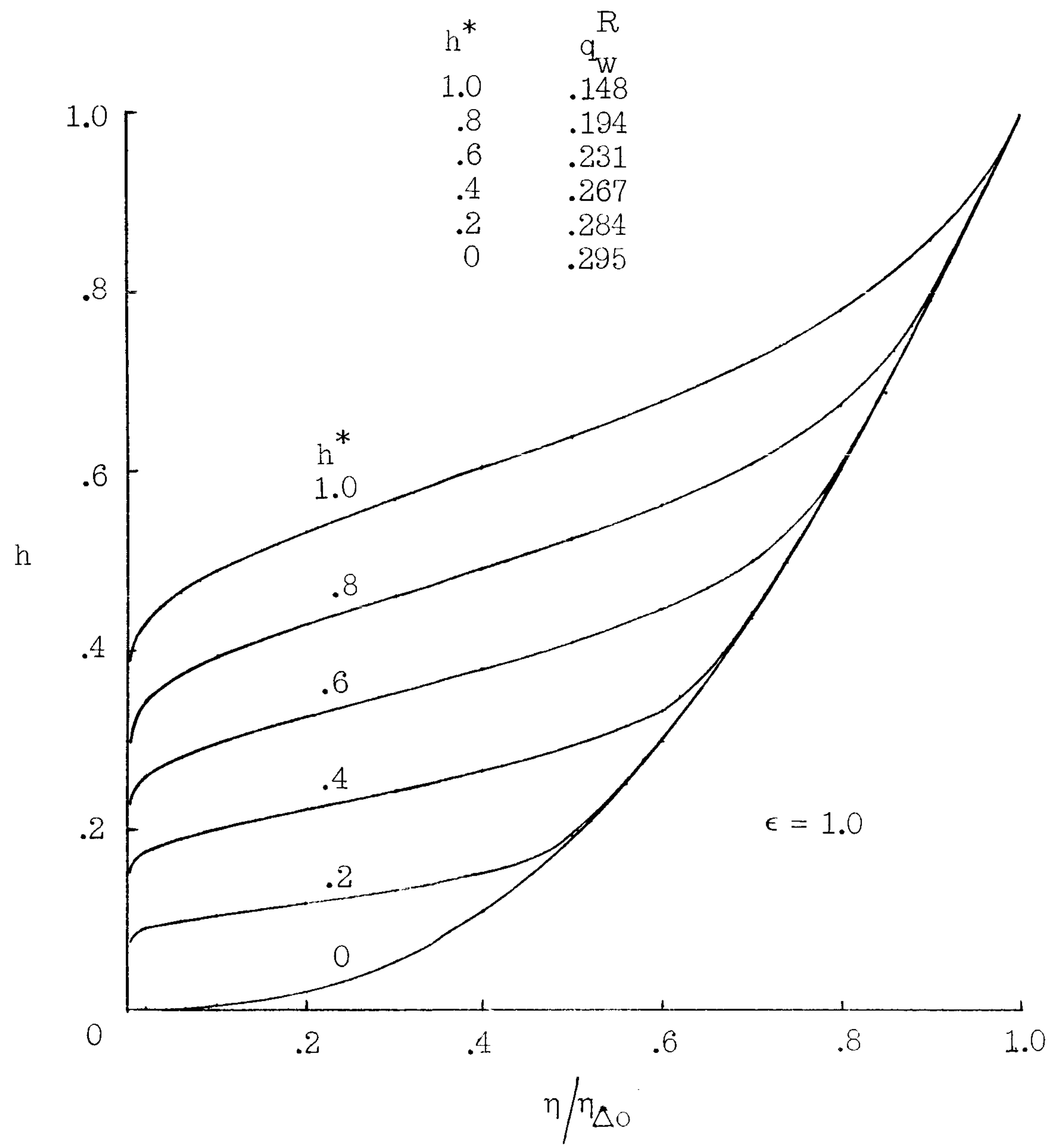

(b) Effect of h^*.

Figure 4.3.- Concluded.

h^* are shown in figure 4.3b. A decrease in h^* produces a decrease in the enthalpy level because γ takes on the smaller value (-1) throughout a greater portion of the shock layer.

The effect of surface reflectivity r_w on the enthalpy distribution is shown in figure 4.4. Of course, this effect vanishes in a transparent layer. With a small amount of absorption an increase in reflectivity brings about an increase in enthalpy level with the greatest increases occurring adjacent to the wall. These results corroborate the findings of chapter III.

The variation with the radiation cooling parameter ϵ of the rate of radiant heat transfer to the wall for various values of the Bouguer number is presented in figure 4.5. Also shown on this figure are two limit curves. One of these curves is labeled the "no decay limit" and was computed by assuming that the shock layer was isenthalpic and transparent. The second limit curve is labeled the "available energy limit" because it represents an upperbound to the radiant flux on the basis of energy balance. The amount of energy entering the shock layer per unit time per unit area of the shock surface has been normalized to unity. If all of this energy is radiated out of a transparent shock layer only one-half will be incident on the wall.

The curve labeled $k_p = 0$ shows the effect of "decay" in reducing the rate of radiant heat transfer to the wall. The remaining curves indicate the important effect of absorption (as characterized

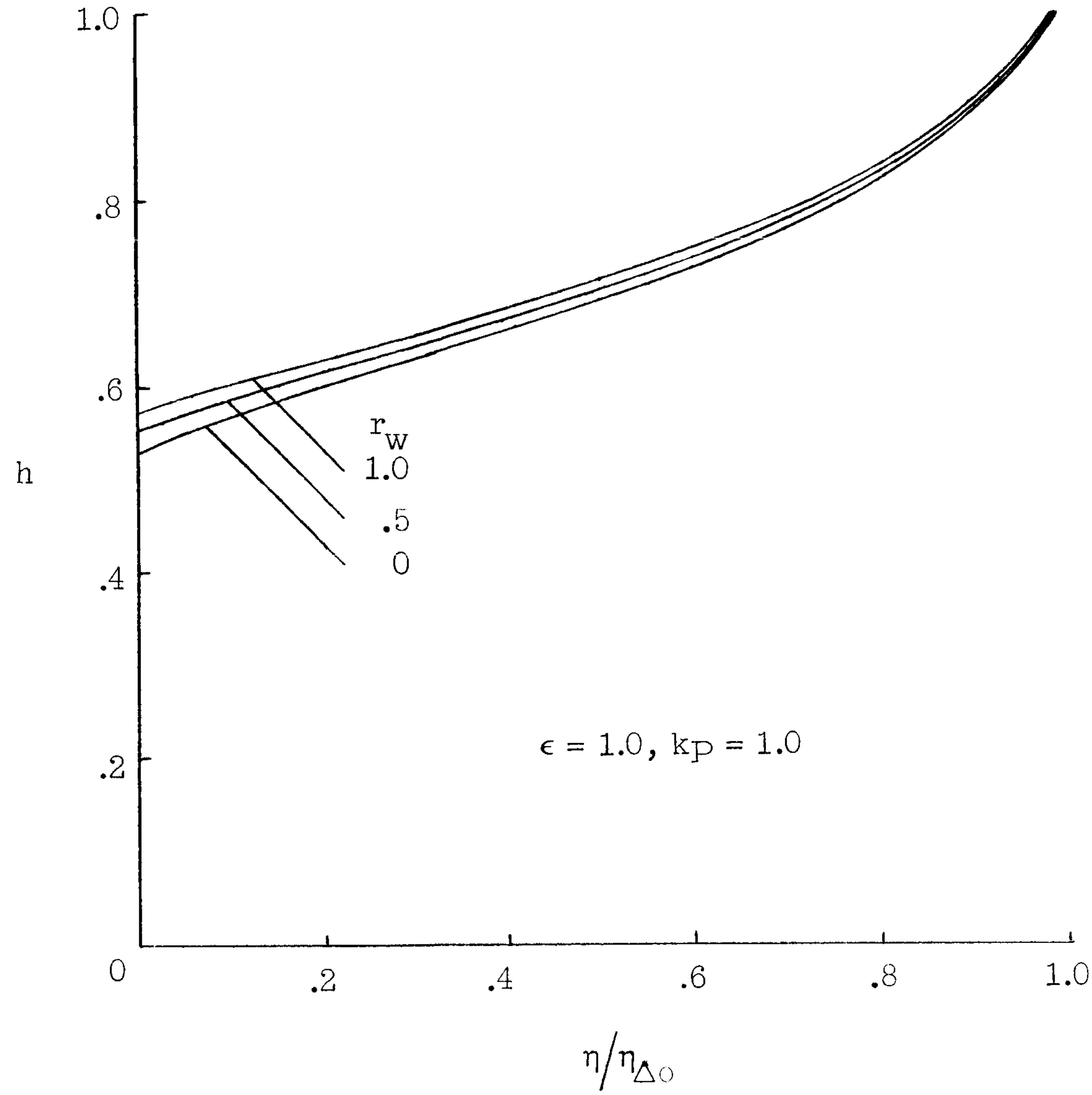

Figure 4.4.- Effect of surface reflectivity on the enthalpy distribution in an optically thin shock layer.

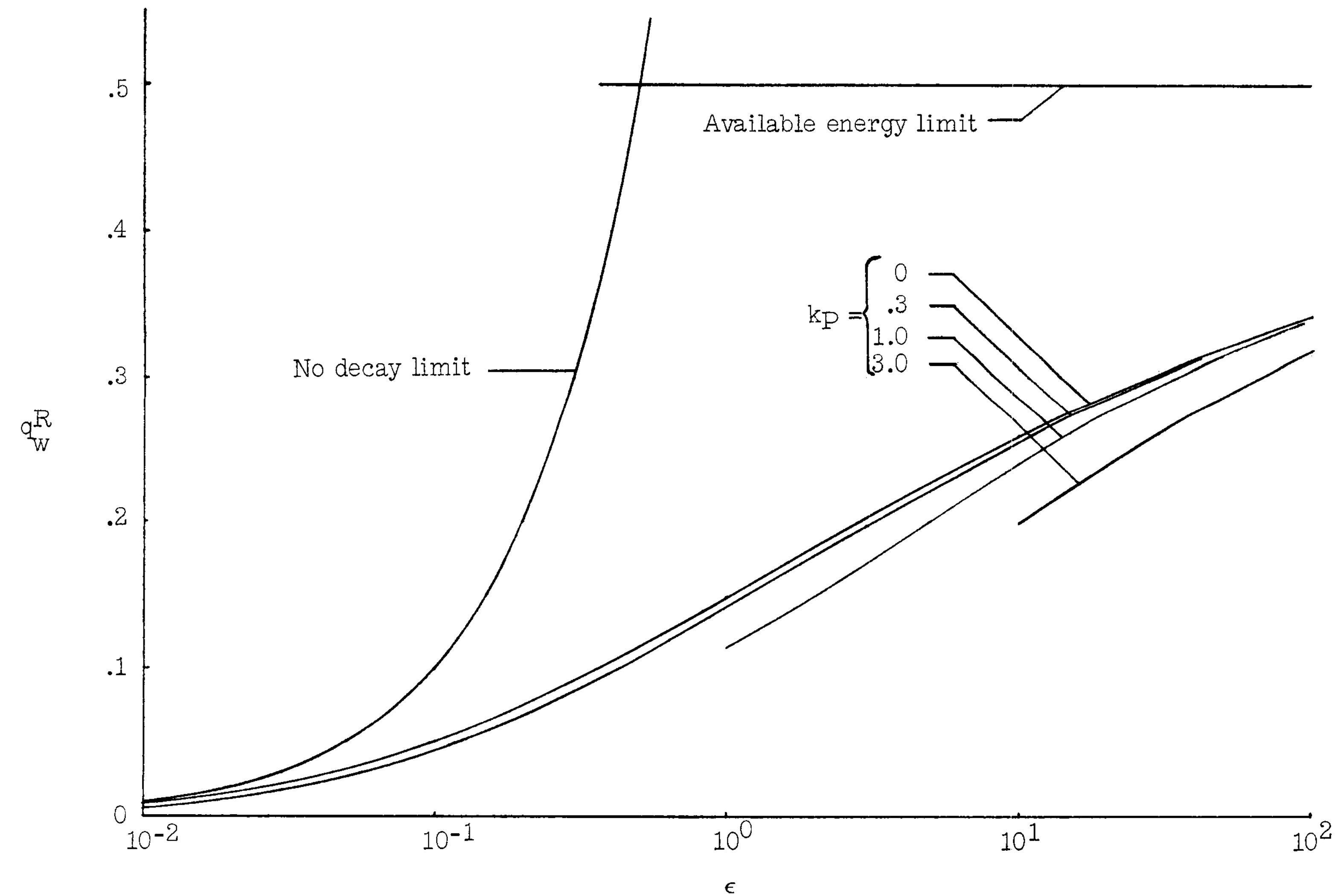

Figure 4.5.- Effect of the Bouguer number on the rate of radiation heat transfer to the stagnation point. $\gamma = 4.0$.

here by the Bouguer number k_P) in reducing the rate of radiant heat transfer to the wall. Although values of k_P presented in figure 4.5 are as large as 3, the corresponding shock layers are all optically thin $\left(k_P \tau_\Delta \ll 1\right)$.

The effect of the enthalpy dependence of the absorption coefficient on the rate of radiant heat transfer to the wall in a transparent shock layer is shown in figure 4.6. It is apparent that an increase in the exponent γ (which appears in the correlation formula $\kappa_P = h^\gamma$) magnifies the effect of decay on the rate of radiant heat transfer.

The effect of the radiation cooling parameter ϵ on the shock standoff distance for various values of the Bouguer number k_P and γ is shown in figures 4.7(a) and 4.7(b). As expected, an increase in ϵ reduces the value of $\bar{\Delta}$ (the ratio of shock standoff distances with and without radiation) for given k_P and γ because the cooling by radiation tends to increase the density level in the shock layer. Increases in k_P and γ for fixed ϵ inhibits the effect of decay on $\bar{\Delta}$ whereas these increases magnified the effects of decay on the rate of radiant heat transfer.

The variation of shock layer optical thickness $k_P \tau_\Delta$ with the radiation cooling parameter ϵ and the Bouguer number k_P is shown in figure 4.8. When the absorption coefficient varies as a positive power of the enthalpy, the shock layer optical thickness may be very much less than one even if the Bouguer number is order of magnitude one or greater provided that ϵ is sufficiently large.

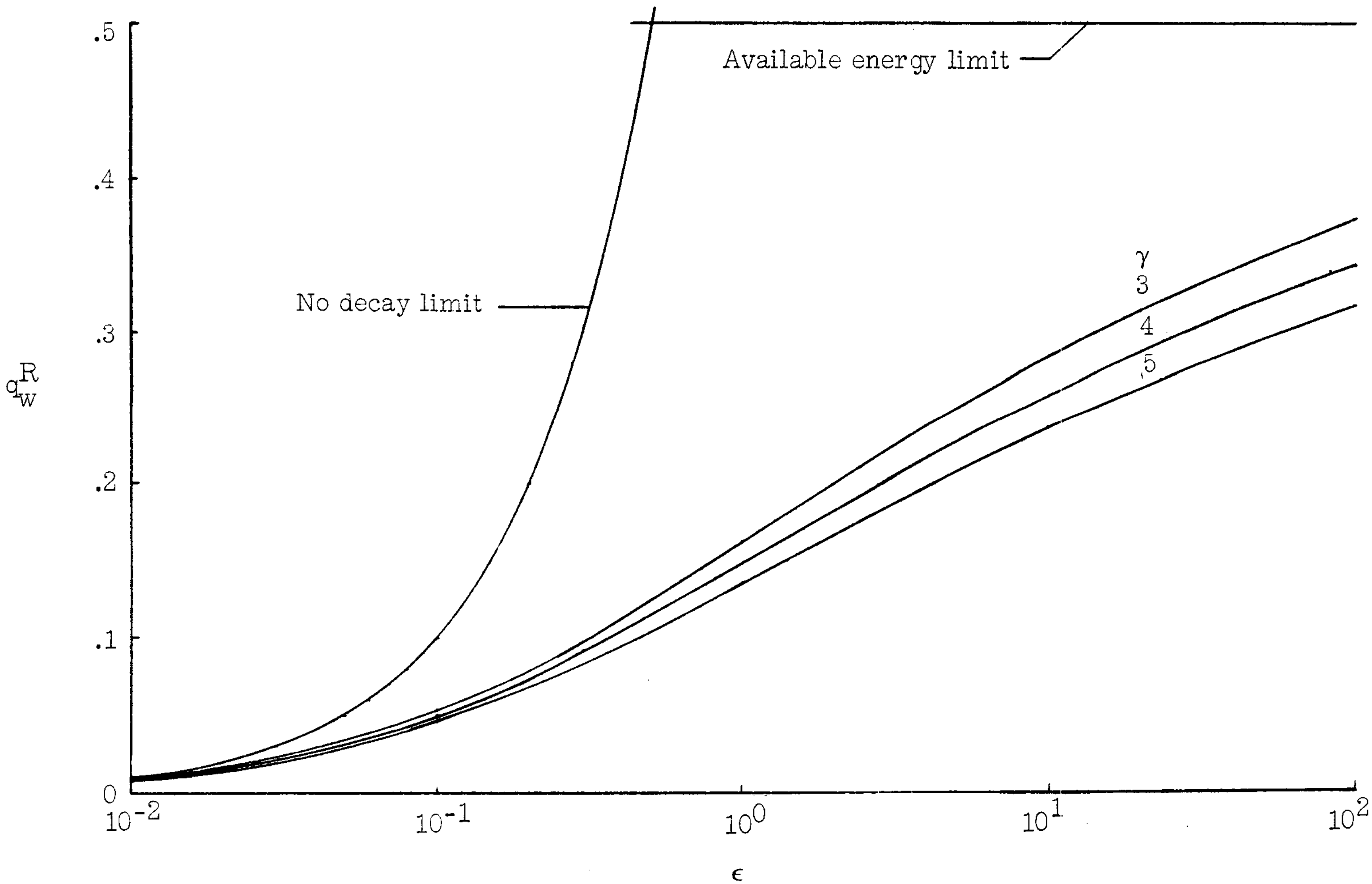

Figure 4.6.- Effect of the enthalpy dependence of the absorption coefficient on the rate of radiant heat transfer to the stagnation point.

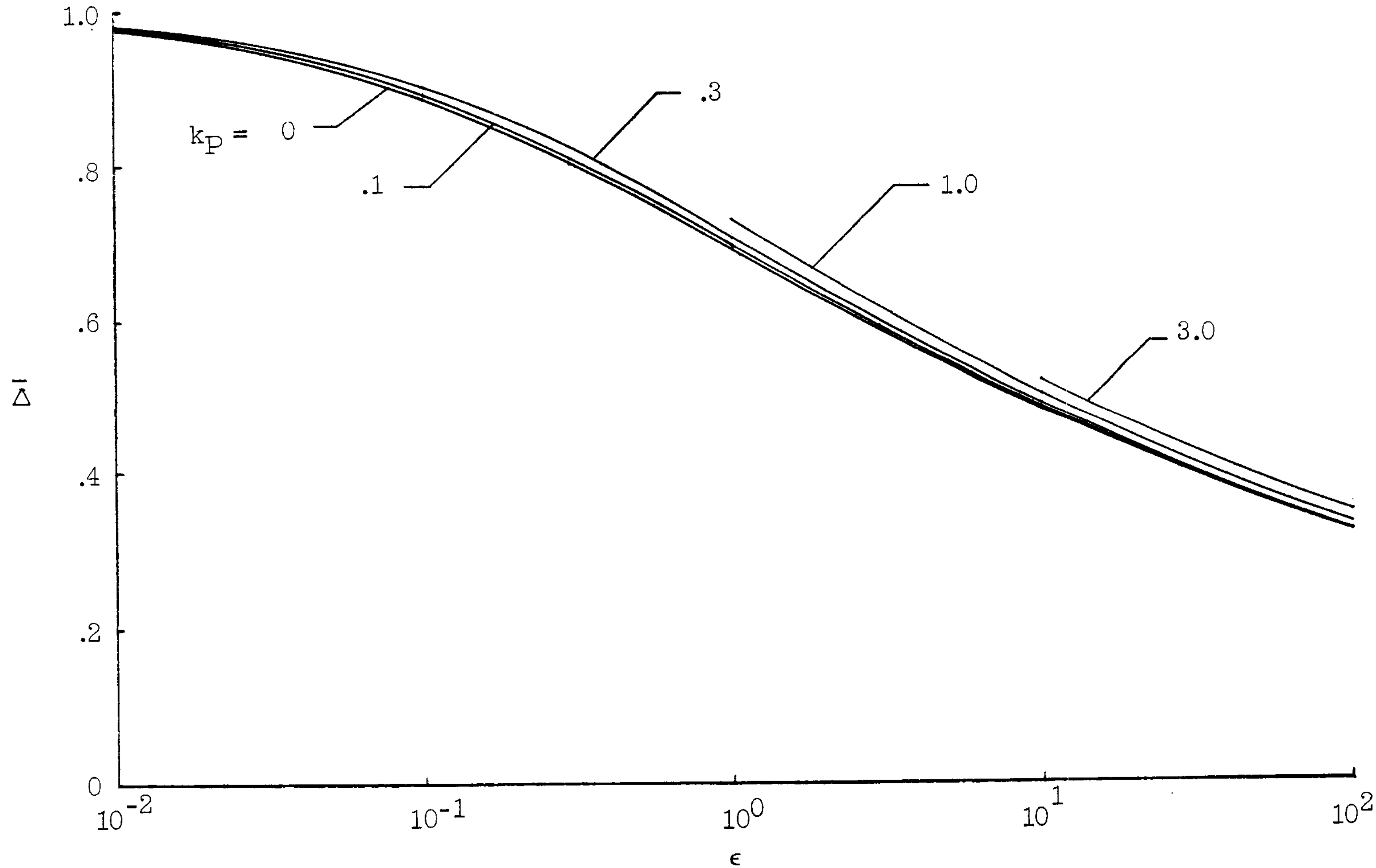

(a) Effect of k_P.

Figure 4.7.- Variation of the shock standoff distance with the radiation cooling parameter ϵ.

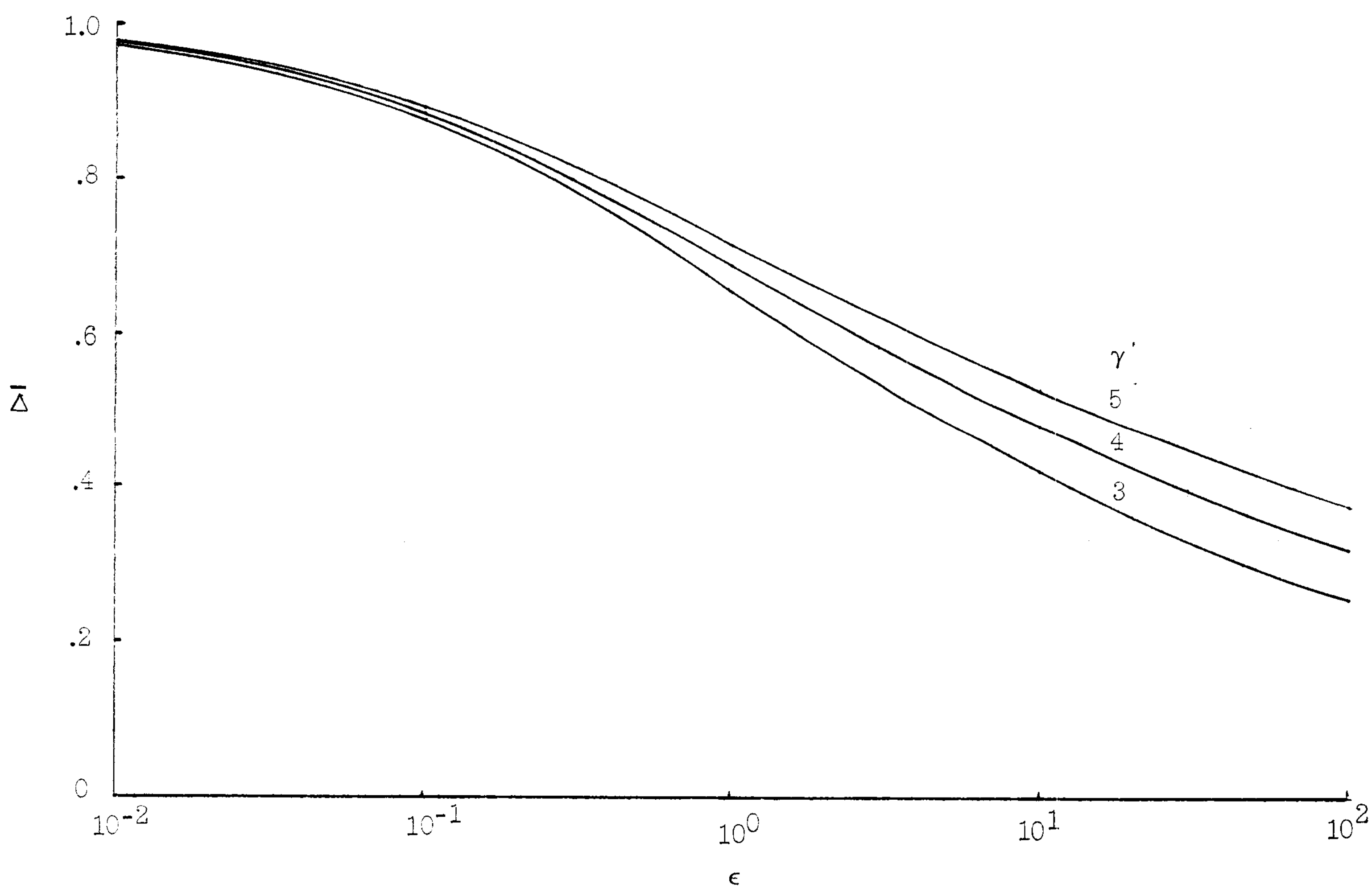

(b) Effect of γ.

Figure 4.7.- Concluded.

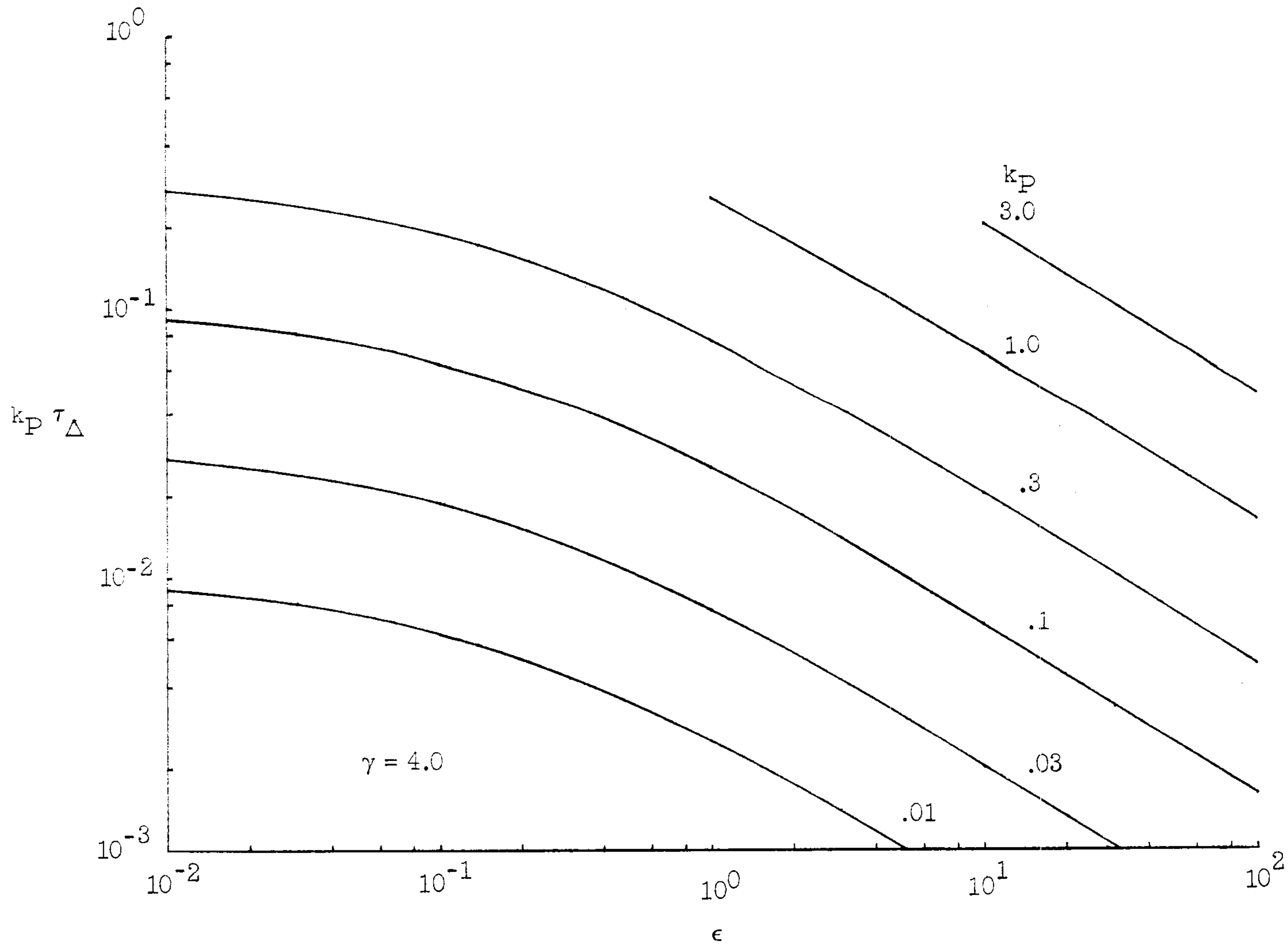

Figure 4.8.- Effect of Bouguer number on the optical thickness of an optically thin shock layer.

The criterion for the validity of the analysis presented in this chapter is that the optical depth of the shock layer be much smaller than one for those wavelength regions in which a significant amount of radiant energy is transported. It has been shown herein, for the case of a gray gas for which the absorption coefficient is proportional to a positive power of the enthalpy, that this condition is always less restrictive than the condition that the Bouguer number, k_P, is very much less than one. However, for the more realistic case of a nongray gas the criterion stated above is generally more restrictive than the condition $k_P \ll 1$. In mathematical terms the criterion implies the inequality

$$2\left(1 + r_w\right)k_P \int_0^\infty \kappa_\lambda(\eta)\left\{\int_0^{\eta_\Delta} \kappa_\lambda(\xi)\, B_\lambda(\xi)\, d\xi\right\} d\lambda \ll 1 \qquad (4.34)$$

The quantity on the left-hand side of the inequality is the first-order term in the expansion of $I\left[\eta\right]$, the divergence of the radiant flux vector, in terms of the Bouguer number, k_P. When both κ_λ and B_λ are proportional to a positive power of the enthalpy an upper-bound to the aforementioned quantity can be obtained by replacing $\kappa_\lambda(\eta)$, $\kappa_\lambda(\xi)$, and $B_\lambda(\xi)$ by their values at $\eta = \eta_\Delta$, immediately behind the shock. The result is

$$2\left(1 + r_w\right)k_P\, \eta_\Delta \int_0^\infty \kappa_\lambda^2\left(\eta_\Delta\right) B_\lambda\left(\eta_\Delta\right) d\lambda \qquad (4.35)$$

If the same substitution is used for a gray gas the result is simply

$$2\left(1 + r_w\right)k_P \, \eta_\Delta \tag{4.36}$$

because $\kappa_\lambda\left(\eta_\Delta\right)$ and $\int_0^\infty B_\lambda\left(\eta_\Delta\right)d\lambda$ are both identically equal to 1. When the nongray step function model for the absorption coefficient of air, which was used in chapter III (see fig. 3.10), is used to evaluated the quantity (4.35) the result is about 60 times greater than the corresponding gray quantity (4.36). Thus, the criterion for the validity of the optically thin analysis, in this nongray example, is

$$60 \; k_P \ll 1$$

for small values of the radiation cooling parameter ϵ. For larger values the criterion could probably be relaxed somewhat $\left(\text{for example } 60 \; k_P \; \tau_\Delta \ll 1\right)$. As a result of this criterion the practical applicability of the optically thin analysis (and consequently of all transparent analyses) is seriously restricted.

CHAPTER V

THE OPTICALLY THICK SHOCK LAYER

A. The Optically Thick Approximation

A qualitative description of the optically thick shock layer has been given by Goulard (ref. 5). He pointed out that this layer is characterized by an isothermal region between two thin boundary layers adjacent to the shock and the wall. The boundary layer immediately behind the shock is a result of the cooling of the hot gas by radiation through the transparent shock. Because radiation travels only a short distance before being absorbed in an optically thick layer, this energy loss is restricted to a narrow region which extends approximately a photon mean free path. Once this initial adjustment in energy has occurred the gas particle is carried into the interior of the shock layer by the flow where convection is the dominant mode of energy transport. In this region, the enthalpy of the gas is essentially constant. As the particle nears the cold wall, moving ever more slowly as it does so, convection becomes of decreasing importance and energy transfer by radiation begins to assume the major role. Finally, in the immediate vicinity of the wall all of the energy transport proceeds by means of radiation. When the emissive power in the interior (or isothermal portion) of the shock layer is large the take-over by radiation occurs at greater distances from the wall than if the emissive power is small. Thus, the thickness of the wall boundary layer depends not only on the optical thickness of the shock layer but on the emissive power of the gas as well.

While the shock layer is optically thick, the boundary layer behind the shock is not and so the Rosseland or diffusion approximation so commonly used in the study of optically thick gases cannot be applied in this region. The Rosseland approximation is valid only in regions of an opaque gas which are at great optical distances from all radiation boundaries (a perfectly reflecting barrier is not a radiation boundary) and in which the thermodynamic and optical properties do not vary greatly within a photon mean free path. Neither of these conditions are met in the shock boundary layer.

The conditions of validity for the Rosseland approximation might hold throughout much of the wall boundary layer if the emissive power of the gas is sufficiently large. However, the approximation must break down optically close to the wall. The use of a temperature jump boundary condition as suggested by several investigators (refs. 25, 51, and 52) has proven successful in problems of radiant and combined radiant and conductive energy transport. Whether or not this concept can be applied with equal success to problems of combined radiant and convective energy transport has not, as yet, been demonstrated. In a region optically close to a radiation boundary the temperature predicted through the use of the Rosseland approximation and a slip boundary condition represents not the temperature of the molecules of the gas, but a sort of average photon temperature. The convective heat flux depends on the molecular temperature. Thus, it is not clear that the slip boundary condition can be used in a problem of combined radiant and convective energy transport. There is a basis for optimism when considering the problem of this chapter, however, in that the convective flux may be negligible compared to the radiant flux optically close to the wall.

In order to arrive at a solution to the problem of the optically thick shock layer, the substitute kernal approximation, introduced in the previous chapter, will be used. It will be shown that in the interior of the shock layer and close to the wall, but not in the shock boundary layer, this method is equivalent to using the Rosseland approximation with slip boundary conditions. The use of this approximation will restrict the analysis to gray gases.*

B. The Substitute Kernal Approximation

In this and the subsequent chapter, it will be convenient to rewrite the energy equation (equation 2.70 of chapter II) with the optical path length τ as the independent variable, that is

$$f(\tau)\ h'(\tau) + \epsilon I[\tau] = 0 \tag{5.1}$$

*This restriction is not a condition for application of these approximations, but has been invoked here to avoid the considerable additional complication that relaxation of this restriction would incur.

Here, f is the nondimensional stream function, h the nondimensional enthalpy, and ϵ the radiation cooling parameter. The divergence of the radiant flux vector, $I[\tau]$ is given by the expression

$$I[\tau] = \frac{1}{\kappa(\eta)} I[\eta] = -2B(\tau) E_2(0) + k_P \int_0^{\tau_\Delta} B(t) E_1\left(k_P|\tau - t|\right)dt$$

$$+ 2k_P r_w E_2\left(k_P\tau\right) \int_0^{\tau_\Delta} B(t) E_2\left(k_P t\right) dt \qquad (5.2)$$

where τ is the nondimensional absorption coefficient, B the nondimensional Planck black-body function, k_P the Bouguer number, r_w the reflectivity of the wall (at $\tau = 0$), τ_Δ the value of the optical path length at the shock, and E_1 and E_2 the exponential integral functions of first- and second-order, respectively.

In order to simplify the analysis the substitute kernal approximation will be used. For the optically thick shock layer, the appropriate substitution for $E_2(x)$ is found to be $(3/4)\ e^{-(3/2)x}$. This substitution satisfies the conditions that the areas under the two functions over the domain $0 \leq x \leq \infty$ are equal and that the expression for the radiant flux approach the Rosseland expression as x increases without limit.

If the expression for the radiation flux is differentiated twice with respect to τ the integral terms can be eliminated with the result

$$I''[\tau] - \frac{9}{4} k_P^2 \, I[\tau] = - \frac{3}{2} B''(\tau) \tag{5.3}$$

The energy equation (5.1) can then be used to eliminate $I[\tau]$.

$$\left[f(\tau) \; h'(\tau)\right]'' - \frac{9}{4} k_P^2 \, f(\tau) \; h'(\tau) = \frac{3}{2} \epsilon B''(\tau) \tag{5.4}$$

This alternate form of the energy equation is a third-order nonlinear ordinary differential equation the solution of which must satisfy the condition $h(1) = 1$. Two additional constants of integration are introduced by the solution of (5.4). These constants are determined by satisfying appropriate physical conditions or by satisfying the original integrodifferential equation (5.1).

An expression for the flux of radiant energy which enters the wall can be obtained quite simply. The expression for the flux incident on the wall is

$$\frac{q_w^R}{1 - r_w} = \frac{3}{4} \epsilon \int_0^{\tau_\Delta} B(t) \; e^{-\frac{3}{2} k_P t} \, dt$$

When the integrodifferential form of the energy equation (5.1) is evaluated at $\tau = 0$, it becomes (since $f(0) = 0$ is a boundary condition)

$$B(0) - \frac{3}{4} k_P \left(1 + r_w\right) \int_0^{\tau_\Delta} B(t) \; e^{-\frac{3}{2} k_P t} \, dt = 0$$

Thus the flux entering the wall can be written in terms of the value of the black-body emissive power of the gas adjacent to the wall, that is

$$q_w^R = \left(\frac{1 - r_w}{1 + r_w}\right) \frac{\epsilon}{k_P} B(0) \tag{5.5}$$

C. Boundary Layer Analysis

In terms of the substitute kernal approximation, the complete differential system governing the flow in the stagnation region of a radiating shock layer is

$$\left[f(\tau)h'(\tau)\right]'' - \frac{3}{2}\epsilon B''(\tau) - \frac{9}{4}k_P^2 f(\tau)h'(\tau) = 0 \tag{5.6}$$

$$2f(\eta)f''(\eta) - \left[f'(\eta)\right]^2 + a^2 h(\eta) = 0 \tag{5.7}$$

$$f(0) = 0 \tag{5.8}$$

$$f\left(\eta_\Delta\right) = 1 \tag{5.9}$$

$$f'\left(\eta_\Delta\right) = \frac{a}{\sqrt{2X(1 - X)}} \tag{5.10}$$

$$h\left(\tau_\Delta\right) = 1 \tag{5.11}$$

$$f(\tau)h'(\tau) + \epsilon\left\{\frac{9}{8}k_P \int_0^{\tau_\Delta} B(t)e^{-\frac{3}{2}|t - \tau|k_P}\,dt - \frac{3}{2}B(\tau) + \frac{9}{8}k_P r_w e^{-\frac{3}{2}k_P\tau} \int_0^{\tau_\Delta} B(t)e^{-\frac{3}{2}k_P t}\right\}dt = 0 \tag{5.12}$$

When the optical thickness of the shock layer is such that $k_P^2 \gg 1$ and $k_P^2 \gg \epsilon$ equation (5.6) becomes asymptotic to the equation

$$f(\tau)h'(\tau) = 0 \tag{5.13}$$

Thus, the enthalpy approaches a constant. It can be shown by attempting to satisfy equation (5.12) as a condition, that this solution is valid only at large optical distances from both the shock and the wall (unless it is a perfectly reflecting wall). It also becomes clear that the value of this constant, hereafter denoted h_2, cannot be determined without knowledge of the shock boundary layer.

If the enthalpy throughout most of the shock layer is constant with a value h_2, the density will be constant also with a value ρ_2. In this case, the momentum equation may be easily solved with the result

$$f(\eta) = 1 - a\eta_\Delta \sqrt{\frac{\rho_2}{\rho_s}} \left(\frac{\eta}{\eta_\Delta}\right)^2 + a\eta_\Delta \sqrt{\frac{\rho_2}{\rho_s}} \left(\frac{\eta}{\eta_\Delta}\right) \tag{5.14}$$

A first approximation to the shock standoff distance is

$$\frac{\Delta}{R_s} = \frac{(\rho_s/\rho_2)X}{1 + \sqrt{2(\rho_s/\rho_2)X(1 - X)}} = \frac{h_2 X}{1 + \sqrt{2h_2 X(1 - X)}} \tag{5.15}$$

In addition to the region of constant enthalpy in the interior of the layer, there are two thermal boundary layers; one immediately behind the shock and the other adjacent to the wall.

The forms that the energy equation assumes in these boundary layers can be determined by means of conventional boundary layer techniques. In the vicinity of the shock the "stretched" coordinate

$$\xi = \left(\tau_\Delta - \tau\, k_P\right) \tag{5.16}$$

is introduced. Close to the shock the quantity $f(\tau)$ is slowly varying and may be adequately represented by the first term in the Taylor expansion about $\xi = 0$, that is

$$f(\xi) \approx f\left(\eta_\Delta\right) = 1 \tag{5.17}$$

Substitution of equation (5.16) and equation (5.17) into the energy equation (5.6) gives the shock boundary layer equation

$$h''(\xi) + \frac{3}{2}\frac{\epsilon}{k_P} B'(\xi) - \frac{9}{4} h(\xi) = \text{Const} \tag{5.18}$$

Solution of this equation is complicated by the nonlinear term $(3/2)\,\frac{\epsilon}{k_P} B'(\xi)$. If ϵ is at least an order of magnitude less than k_P, this term can be neglected and the solution to equation (5.18) easily found. This solution is

$$h(\xi) = \left(1 - h_2\right)e^{-\frac{3}{2}\xi} + h_2 \tag{5.19}$$

The constant h_2 can be determined by writing an energy balance across the shock boundary layer. This energy balance is

$$1 = h_2 + \frac{3}{4}\frac{\epsilon}{k_P}\int_0^\infty B(\xi)e^{-\frac{3}{2}\xi}\,d\xi \tag{5.20}$$

When $\epsilon \ll k_P$ condition (5.20) reduces to

$$h_2 \approx 1 - \frac{1}{2}\frac{\epsilon}{k_P}$$

and it is apparent that h_2 approaches one and the boundary layer ceases to exist. Thus, there cannot be a shock boundary layer with a thickness characterized solely by the optical path length in the gas.

An approximate solution to the boundary layer equation (5.18) can be obtained if the nonlinear term $(3/2)\frac{\epsilon}{k_P}B'(\xi)$ is replaced by an appropriate linear term, for example

$$\frac{3}{2}\frac{\epsilon}{k_P}B'(\xi) \approx \frac{3}{2}\frac{\epsilon}{k_P}\frac{d}{d\xi}\left[\bar{B} + \dot{\bar{B}}h(\xi)\right] = \frac{3}{2}\frac{\epsilon}{k_P}\dot{\bar{B}}h'(\xi)$$

where the constant $\dot{\bar{B}}$ is arbitrary and represents a mean variation of the black body emissive power B with h over the range of values of h encountered in the shock boundary layer. The linearized version of equation (5.18) has the simple solution

$$h(\xi) = \left(1 - h_2\right)e^{-\omega_1\xi} + h_2 \tag{5.21}$$

where

$$\omega_1 = \frac{3}{4}\frac{\epsilon}{k_P}\dot{\bar{B}}\left[1 + \sqrt{1 + 4/9\left(\frac{\epsilon}{k_P}\dot{\bar{B}}\right)^2}\,\right] \tag{5.22}$$

where ϵ/k_P is very much less than unity this solution reduces to equation (5.20). When ϵ/k_P is very much larger than unity, the solution takes the form

$$h(\xi) = \left(1 - h_2\right)e^{-\frac{\epsilon}{k_P}\dot{\bar{B}}\xi} + h_2 \tag{5.23}$$

and, in this limit, the thickness of the shock boundary layer is determined by the parameter ϵ^{-1} instead of simply k_P^{-1}. Thus, the shock boundary layer can be very much thinner than a photon mean free path if the black body radiative power behind the shock is large. This effect was shown by Heaslet and Baldwin (ref. 31) in their study of radiation resisted shock waves. Simply stated it means that a particle starting immediately behind the shock loses energy at such a rapid rate by means of radiation that it is substantially cooled in the time that it takes to travel only a small portion of a photon mean free path.

A value for the constant $\dot{\bar{B}}$ can be obtained from the condition

$$\left(1 - h_2\right)\omega_1^2 - \frac{3}{2}\frac{\epsilon}{k_P}\left(1 - h_2\right)\omega_1 - \frac{9}{4}\left(1 - h_2\right) = 0 \tag{5.24}$$

This condition was derived by integration of the nonlinear energy equation (5.18) between the limits zero and infinity and substitution into the result of the linearized solution (5.21). In addition, the correlation formula $B = h^{\delta}$ was used. It was shown in chapter II that $\delta \approx 2.2$. However, the ensuing analysis will be greatly simplified, without any significant loss in accuracy, by setting $\delta = 2$.

A second condition is required to uniquely determine the enthalpy distribution in the shock layer. The energy balance relation (5.20) evaluated with the aid of the linearized solution provides this condition, which is

$$2\left[h_2^2 - \frac{2k_P}{\epsilon}\left(1 - h_2\right)\right]\omega_1^2 + \left[1 + 2h_2 - \frac{6k_P}{\epsilon}\left(1 - h_2\right)\right]\omega_1 + \left[1 - \frac{2k_P}{\epsilon}\left(1 - h_2\right)\right] = 0 \tag{5.25}$$

The quantity ω_1 can be eliminated between the conditions (5.24) and (5.25) resulting in an expression for h_2 the enthalpy level in the interior of the shock layer, as a function of ϵ/k_P. The result of this calculation is presented in figure 5.1.

The thickness of the shock boundary layer (in terms of optical path length) is characterized by the parameter $\left(\omega_1 k_P\right)^{-1}$. A plot of ω_1 as a function of ϵ/k_P is presented in figure 5.2.

As has been indicated previously, there is also a thermal boundary layer due to radiation adjacent to the wall. If this boundary layer is thin, which shall be assumed, herein, the dimensionless stream function $f(\tau)$ may be represented by the first few terms of its McLaurin expansion

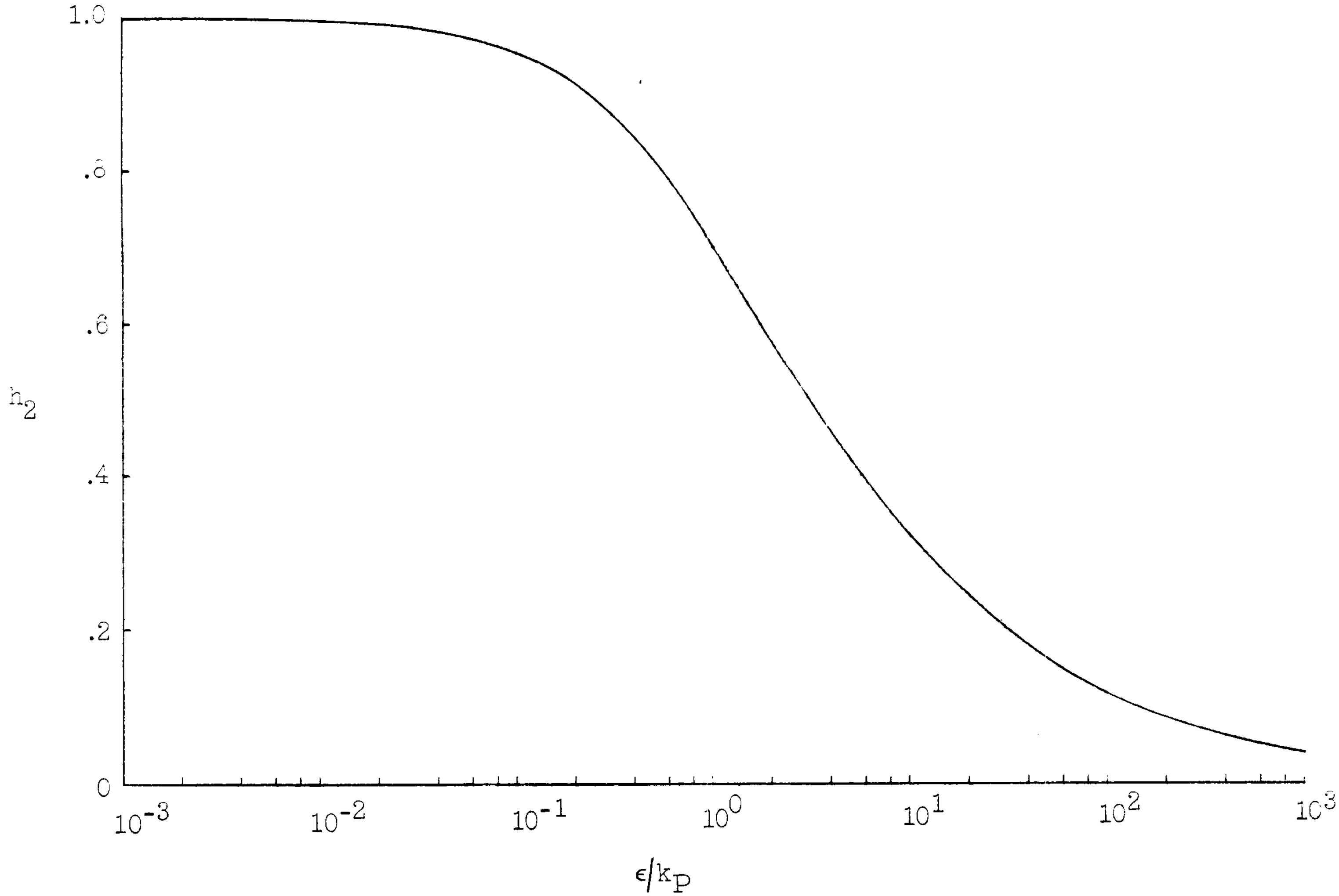

Figure 5.1.- Variation of h_2 with ϵ/k_p.

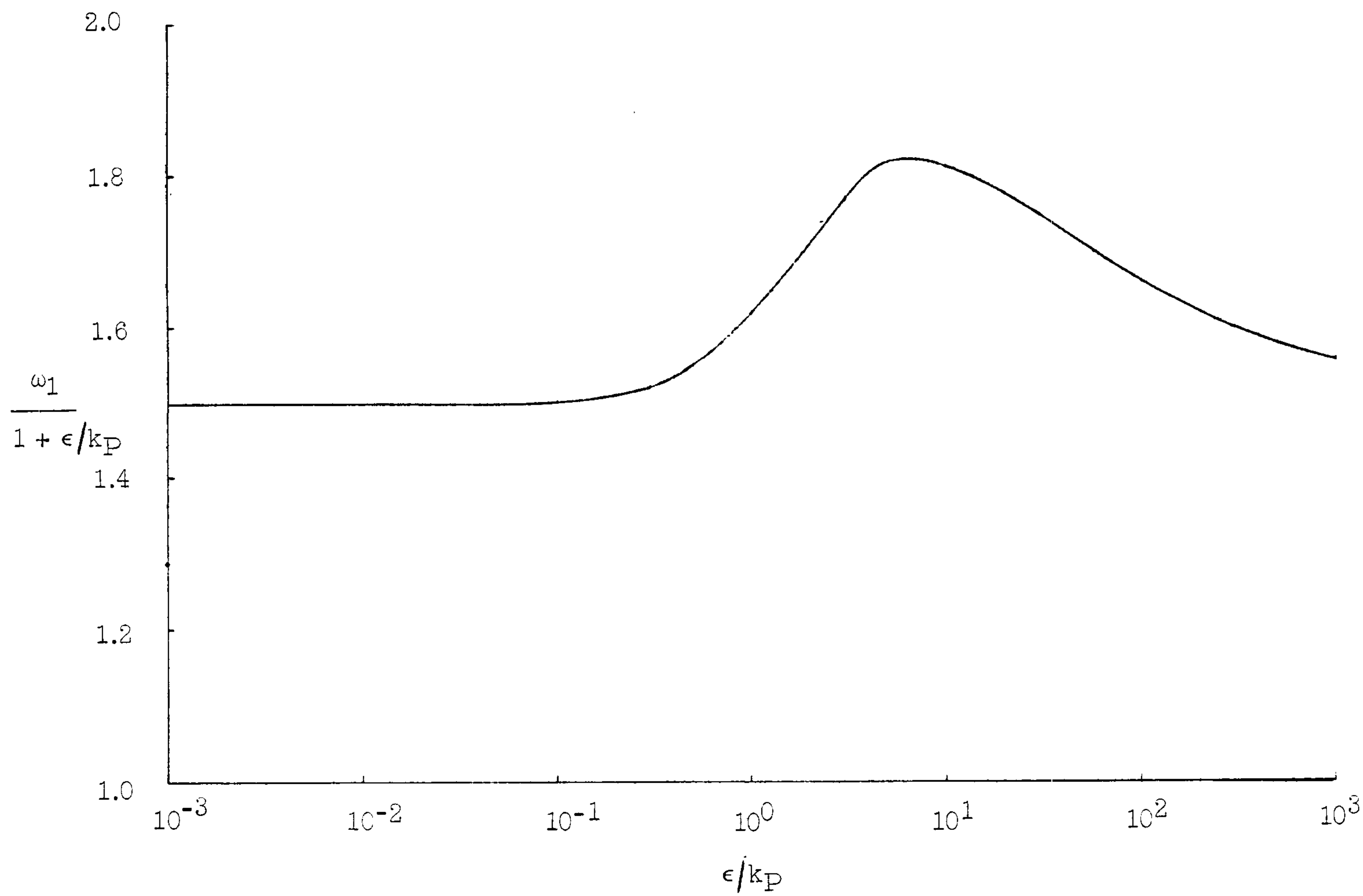

Figure 5.2.- Variation of ω_1 with ϵ/k_P

$$f(\tau) \approx f(o) + \tau f'(o)$$

Employing the kinematic boundary condition (5.8) and the asymptotic solution for $f(\eta)$ Equation (5.14) one finds

$$f(\tau) \approx \frac{a\eta_\Delta}{\kappa(o)\sqrt{h_2}}\,\tau \approx \frac{2\sqrt{2X(1-X)}}{\kappa(o)\left[\sqrt{h_2} + \sqrt{2X(1-X)}\right]}\,\tau = b\tau \qquad (5.26)$$

Of the several approximations introduced in the analysis of this chapter this is perhaps the poorest because the requirement that the wall boundary layer be thin with respect to the optical path length τ does not necessarily imply that it is thin with respect to either the Dorodnitsyn coordinate η or the geometric coordinate z.

Substituting this expression into the energy equation (5.6), introducing the "stretched" coordinate

$$\zeta = \tau k_P^{1/2} \qquad (5.27)$$

and neglecting terms of order $k_P^{1/2}$ yields the boundary layer equation

$$B''(\zeta) + \frac{3}{2}\left(\frac{k_P}{\epsilon}\right) b\zeta\, h'(\zeta) = 0 \qquad (5.28)$$

In general, equation (5.28) is nonlinear and does not possess an analytic solution. A simple approximate analytic solution can be obtained by replacing the quantity $h'(\zeta)$ with $\dot{\bar{h}}B'(\zeta)$, where $\dot{\bar{h}}$ is an as yet undetermined constant. This substitution reduces equation (5.28) to the linearized form

$$B''(\zeta) + 2\omega_2 \zeta B'(\zeta) = 0 \tag{5.29}$$

where

$$\omega_2 = \frac{3}{4}\left(\frac{k_P}{\epsilon}\right)b\dot{\bar{h}} \tag{5.30}$$

The solution to equation (5.29) is easily found with the result

$$B(\zeta) = B_w + \left(B_2 - B_w\right)\mathrm{erf}\left(\sqrt{\omega_2}\ \zeta\right) \tag{5.31}$$

The quantities B_w, the nondimensional black body emissive power of the gas adjacent to the wall, and ω_2 (because it contains the arbitrary constant $\dot{\bar{h}}$) are still unknown. One condition for evaluating these quantities can be obtained by integrating the nonlinear boundary layer equation (5.28) with respect to ζ between the limits zero and infinity. In performing this integration, it is convenient to eliminate the term $B''(\zeta)$ in equation (5.28) with equation (5.29). Then it is found that

$$\dot{\bar{h}} = \frac{h_2 - h_w}{B_2 - B_w} = \frac{1}{h_2 + h_w} \tag{5.32}$$

Here B_2 is the nondimensional black-body emissive power of the gas in the interior of the shock layer and h_w is the nondimensional enthalpy of the gas adjacent to the wall. The last equality in expression (5.32) holds because it has been assumed that $B = h^2$.

The second condition is obtained by evaluating the integral condition (5.12) at $\tau = 0$. Written in terms of the boundary layer coordinate ζ this condition becomes

$$B_w = \frac{3}{4} k_P^2 \left(1 + r_w\right) \int_0^\infty B(\zeta) e^{-\frac{3}{2} k_P^{1/2} \zeta} d\zeta \tag{5.33}$$

Substitution of the linearized solution for $B(\zeta)$ into equation (5.33) and integration yields

$$B_w = \frac{\left(1 + r_w\right) e^{\frac{9k_P}{16\omega_2}} \operatorname{erfc} \sqrt{\frac{9k_P}{16\omega_2}}}{\left(1 - r_w\right) + \left(1 + r_w\right) e^{\frac{9k_P}{16\omega_2}} \operatorname{erfc} \sqrt{\frac{9k_P}{16\omega_2}}} B_2 \tag{5.34}$$

Equations (5.30) and (5.32) can be used to eliminate ω_2 from equation (5.34) yielding a transcendental equation for the value of the black body emissive power at the wall B_w.

The variation of B_w as a function of the radiation cooling parameter to Bouguer number ratio, ϵ/k_P for various values of k_P and the exponent γ (from the correlation formula $\kappa = h^\gamma$) is shown in figure 5.3. This curve has particular significance because the ratio of radiant heat transfer to the cold wall is directly related to B_w through expression (5.5). The variation of the quantity ω_2 (eq. (5.30) with these same parameters is presented in figure 5.4.

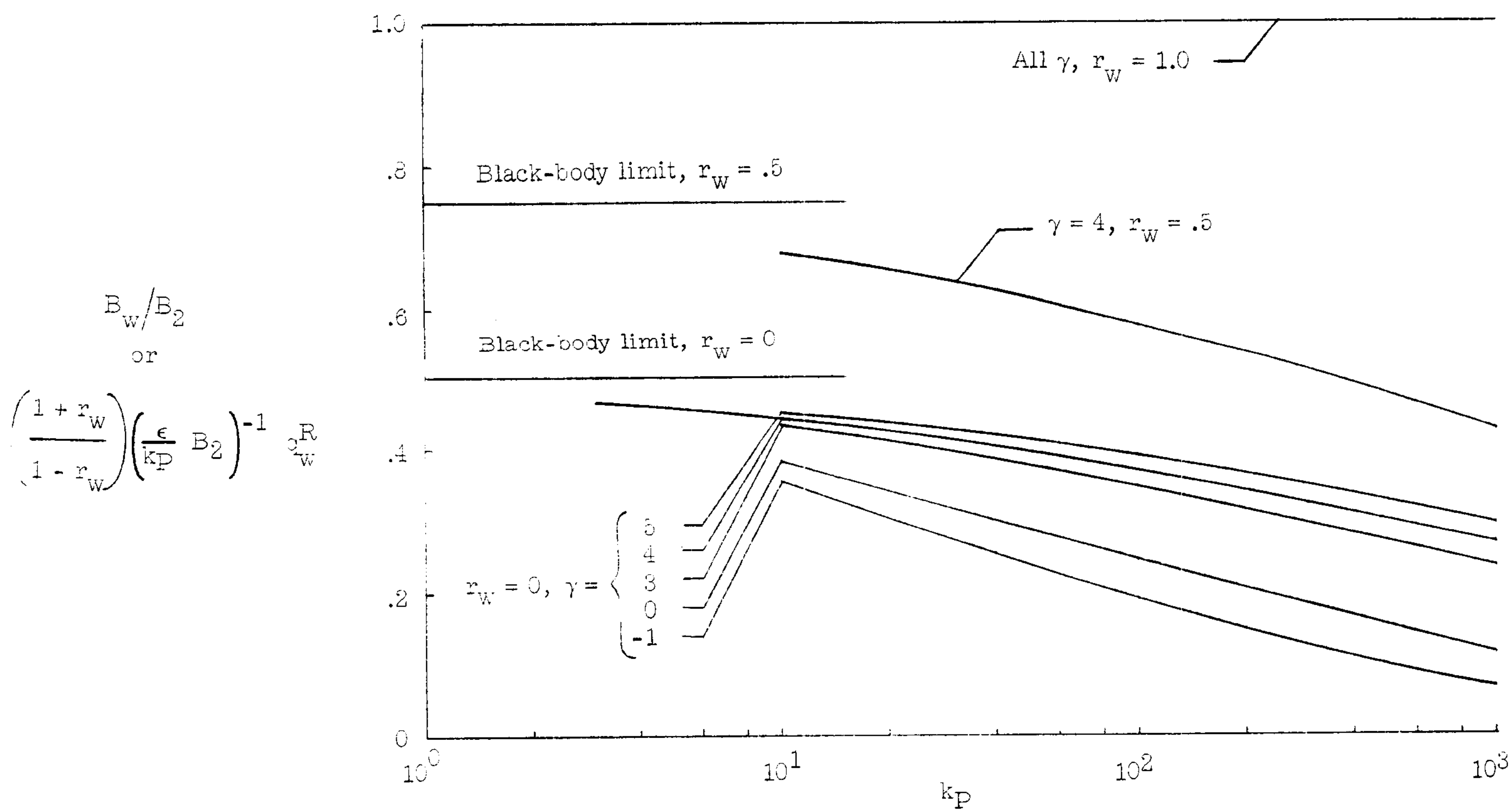

(a) $\epsilon/k_P = 0.01$, $B_2 = 0.9900$.

Figure 5.3.- Variation of B_w/B_2 with k_P for various values of γ and r_w.

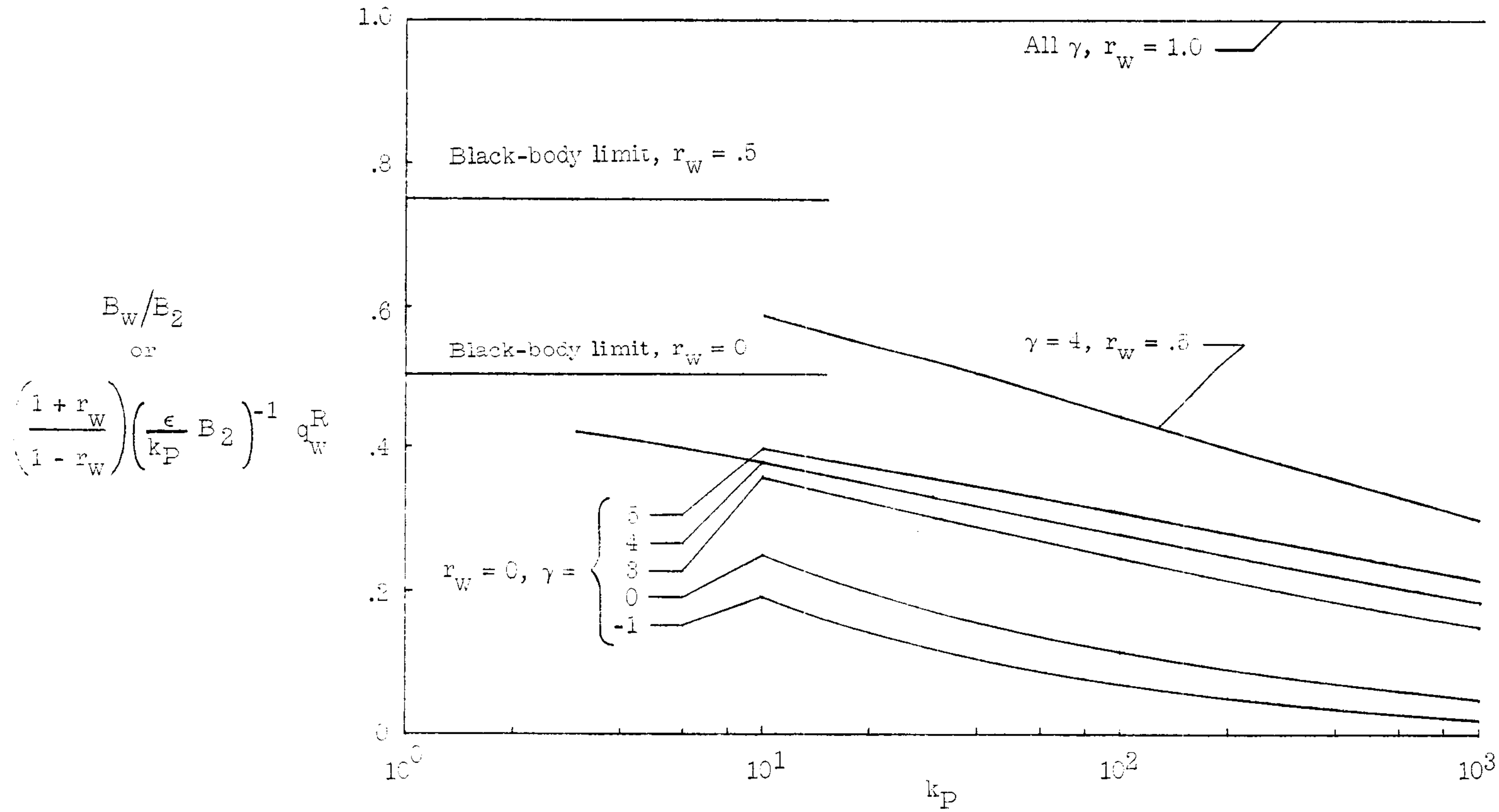

(b) $\epsilon/k_P = 0.1$, $B_2 = 0.9080$.

Figure 5.3.- Continued.

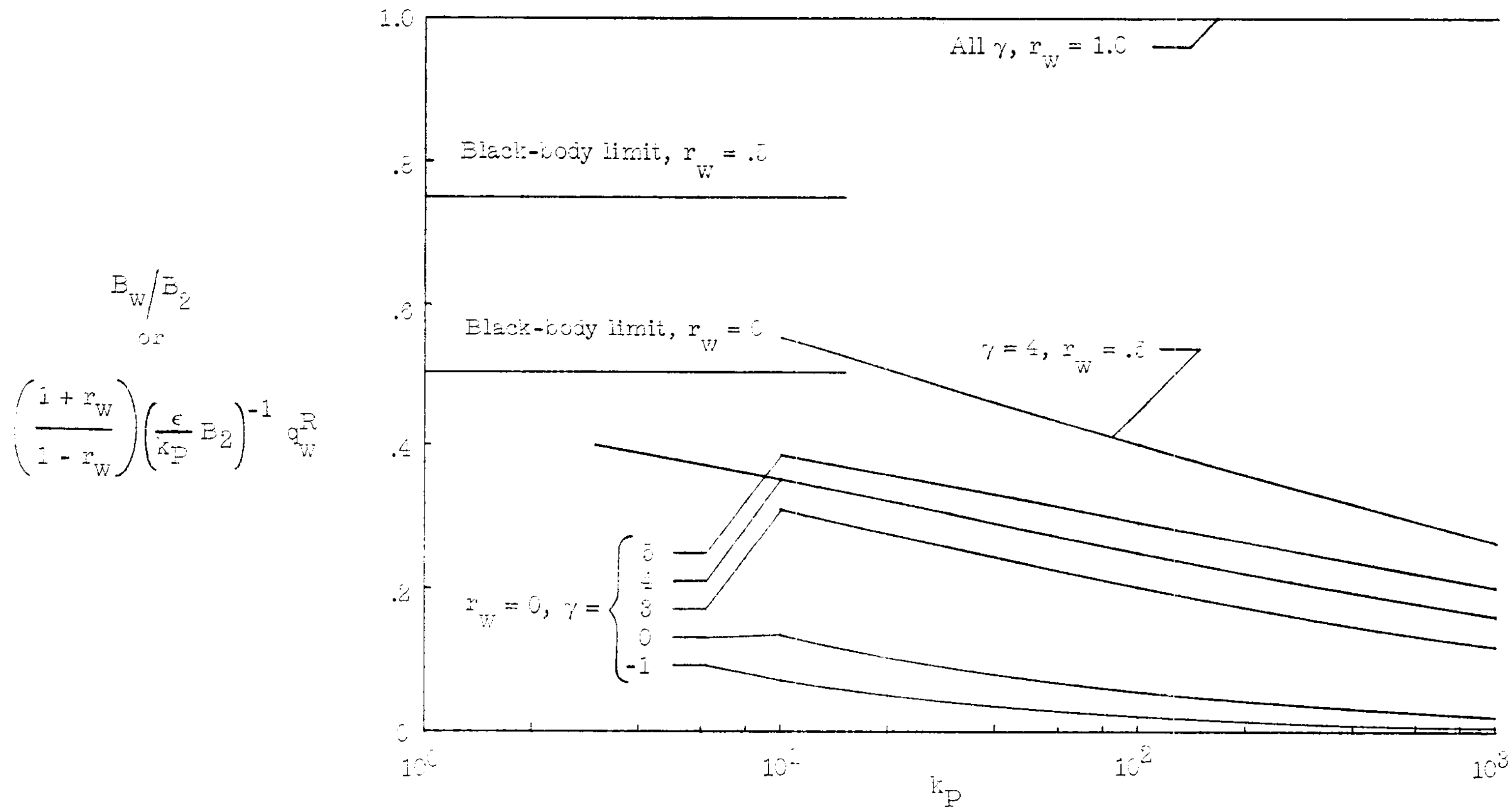

(c) $\epsilon/k_P = 1.0, B_2 = 0.4896$.

Figure 5.3.- Continued.

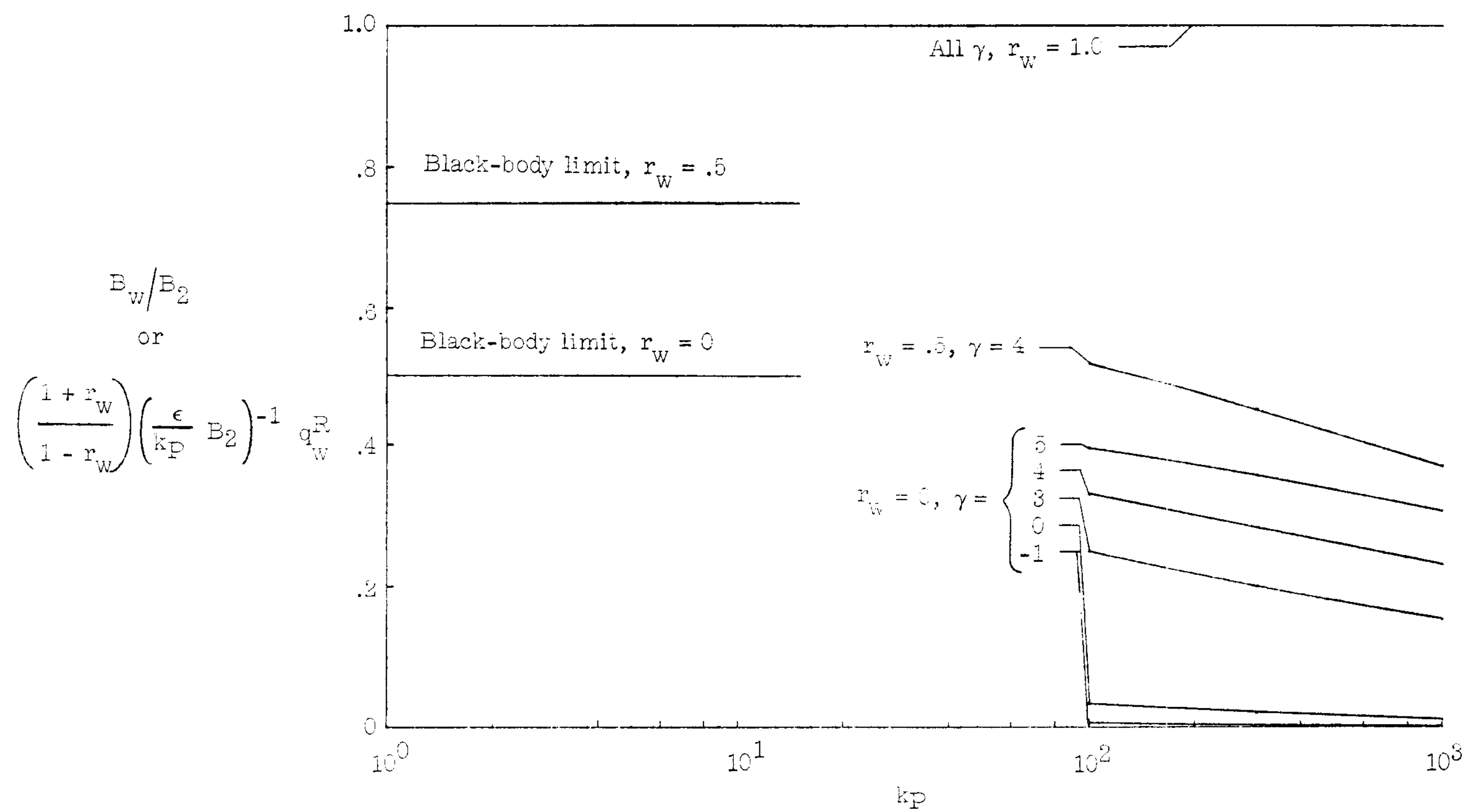

(d) $\epsilon/k_P = 10$, $B_2 = 0.1036$.

Figure 5.3.- Concluded.

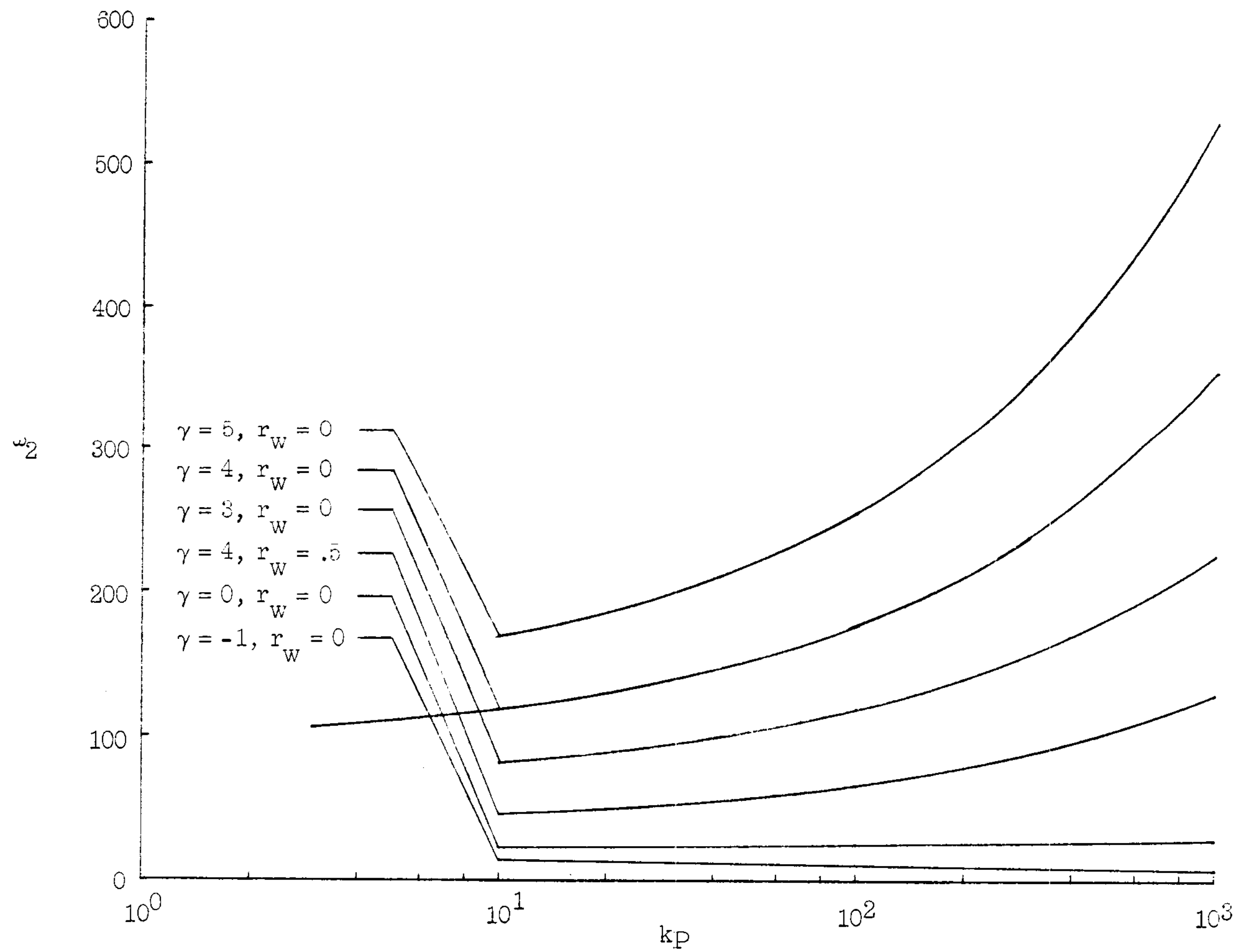

(a) $\epsilon/k_P = 0.01$.

Figure 5.4.- Variation of ω_2 with k_P for various values of γ and r_w.

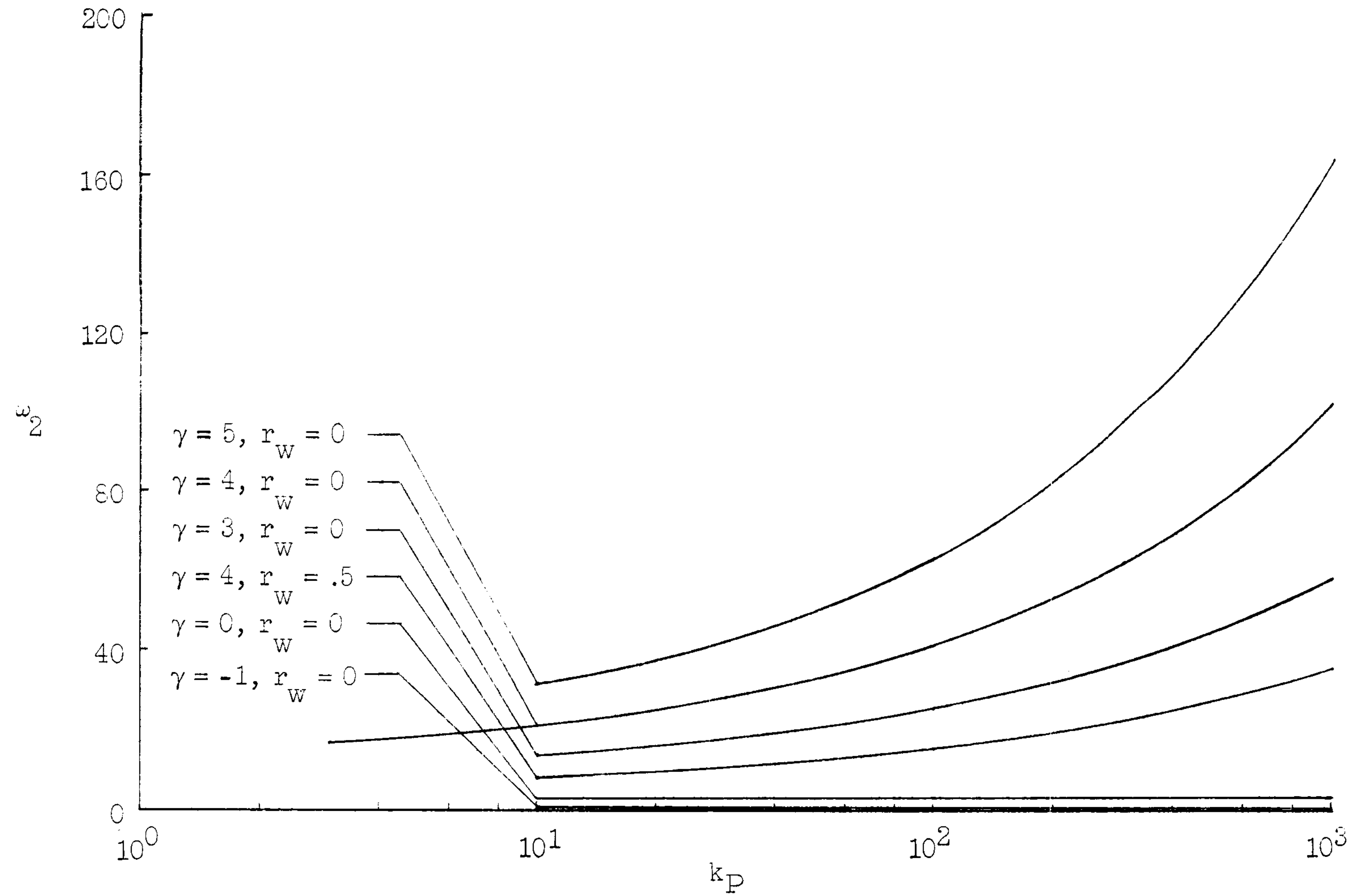

(b) $\epsilon / k_P = 0.1$.

Figure 5.4.- Continued.

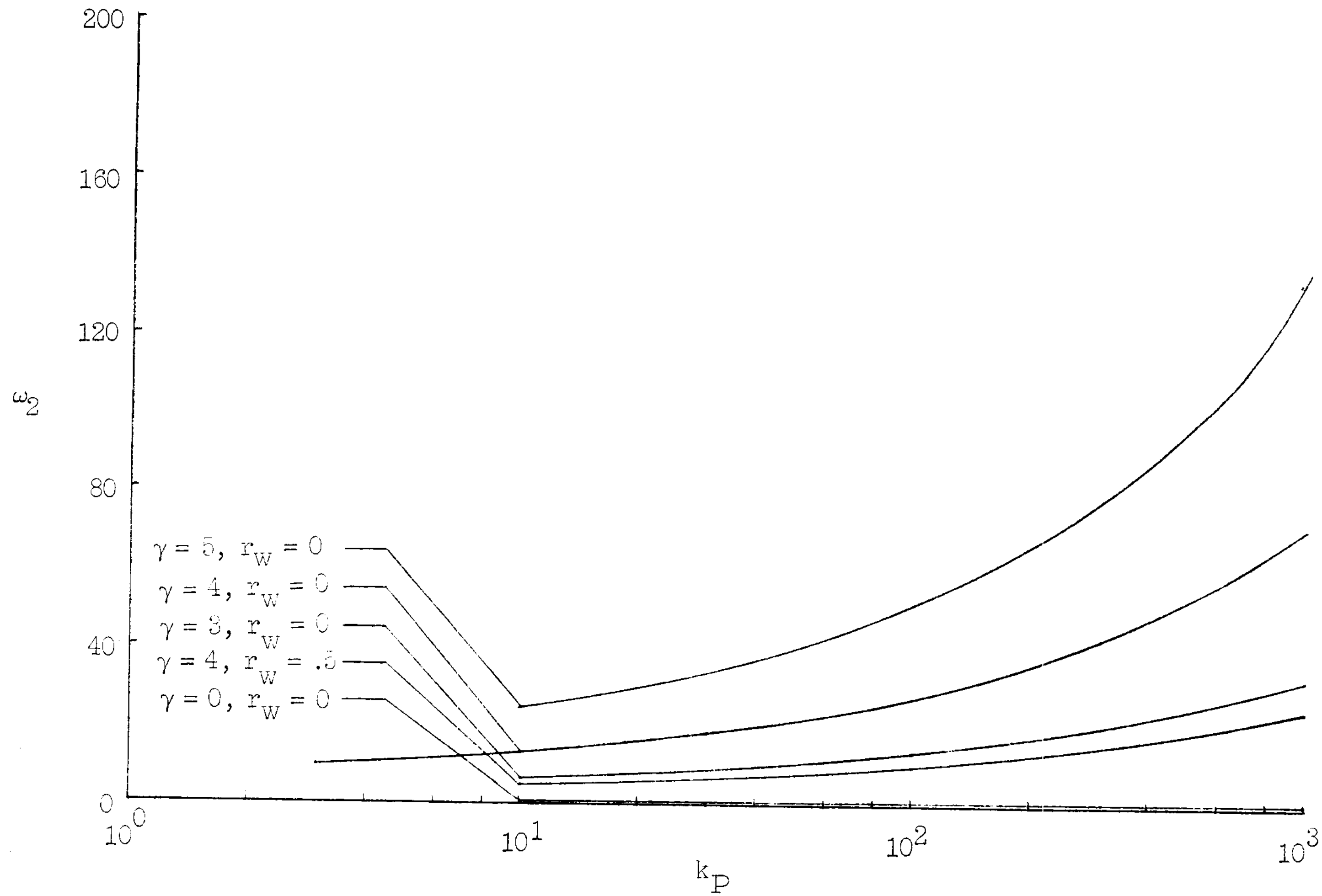

(c) $\epsilon / k_P = 1.0.$

Figure 5.4.- Continued.

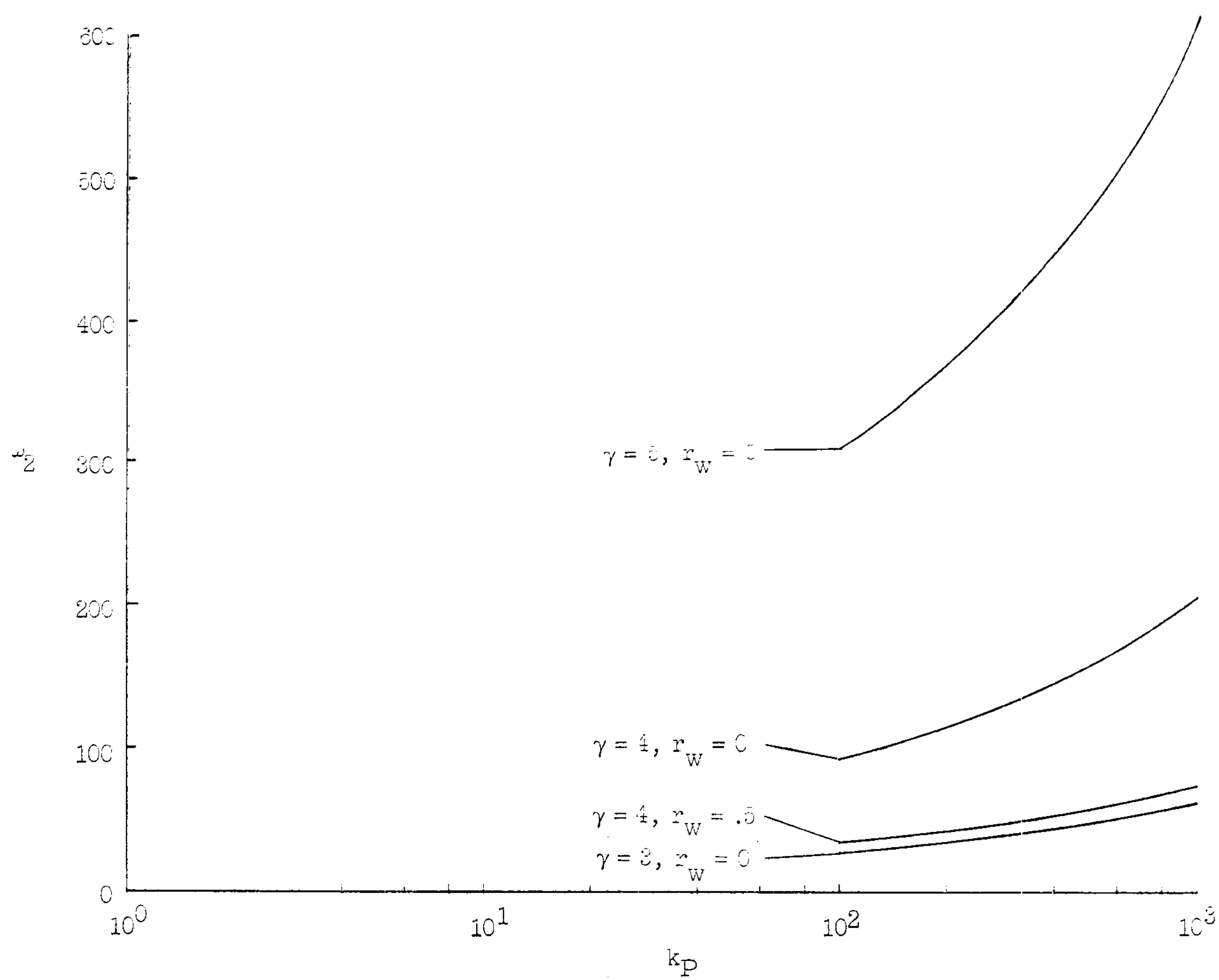

(d) $\epsilon/k_P = 10.$

Figure 5.4.- Concluded.

D. The Rosseland Approximation

The Rosseland or diffusion approximation is frequently used in the study of problems in which the medium is optically thick. As was pointed out earlier this approximation is not valid in regions optically close to a radiation boundary or in regions in which the optical and thermodynamic properties vary significantly within an optical path length. Some investigators have attempted to correct the former deficiency through the use of temperature jump boundary conditions and have achieved considerable success in problems of pure radiant or combined radiant and conductive energy transport.

In this section, an attempt will be made to use the Rosseland approximation and temperature jump boundary conditions to analyze the optically thick shock layer. It is hoped that this exercise will provide some insight into the attributes and limitations of this approximation in problems of combined radiant and convective energy transport.

With the Rosseland approximation for the divergence of the radiant flux, the energy equation becomes

$$B''(\tau) + \frac{3}{2}\,\frac{k_P^2}{\epsilon}\,f(\tau)h'(\tau) = 0 \qquad (5.36)$$

This equation is the same as equation (5.6) except for the omission of the third-order differential term $\left[f(\tau)h'(\tau)\right]''$.

In the interior of the optically thick shock layer, equation (5.36) reduces to

$$f(\tau)h'(\tau) = 0$$

provided $k_P \gg \frac{\epsilon}{k_P}$. This result is identical to the result obtained by means of the substitute kernal approximation. This agreement is not surprising because the diffusion approximation is known to be valid in this region. Of course, the value of the constant enthalpy in the interior of the shock layer cannot be determined until something is known about the shock boundary layer.

If the usual type of boundary layer analysis is applied to the energy equation in the Rosseland approximation (5.36) for the neighborhood of the wall the result is

$$B''(\zeta) + \frac{3}{2}\left(\frac{k_P}{\epsilon}\right) b\zeta\, h'(\zeta) = 0$$

This equation is identical to the wall boundary layer equation in the substitute kernal analysis. Two boundary conditions are required to completely determine the solution to this equation. One of these conditions is

$$\lim_{\zeta \to \infty} B(\zeta) = B_2$$

Here B_2 is the black-body emissive power of the gas in the interior of the shock layer. The second is the jump boundary condition, written in terms of the black-body emissive power B rather than the temperature.

$$B_w = CB'(0) = \frac{3}{2}\left(\frac{k_P^2}{\epsilon}\right)Cq_w^R \tag{5.37}$$

The second equality follows from the expression for the radiant flux in the Rosseland approximation. The constant C is usually evaluated by requiring the flux to be correct in the black-body limit (see, for example, ref. 29). However, it is noted that condition (5.37) is identical to the condition used in the substitute kernal approximation (i.e. (5.33)) if C is chosen to be

$$C = \frac{2}{3k_P}\left(\frac{1 + r_w}{1 - r_w}\right) \tag{5.38}$$

Thus, the results obtained in the wall boundary layer by the two methods are identical if C is chosen to satisfy (5.38). It has been shown that the two methods also give identical results when applied to the problem of combined radiative and conductive energy transport between two infinite parallel plates separated by a radiating and conducting gas (ref. 29).

If the usual boundary layer analysis is used to obtain the boundary layer form of the energy equation in the Rosseland approximation for the neighborhood of the shock the result is

$$B'(\xi) - \frac{3}{2}\left(\frac{k_P}{\epsilon}\right)h(\xi) = \text{Const} \tag{5.39}$$

This equation is not identical with the shock boundary layer equation in the substitute kernal approximation because of the omission of the third-order differential term. Inspection of equation (5.39) indicates that any solution other than the trivial solution $h(\xi) \equiv h_2$ will not tend to a constant h_2 as ξ becomes very large. Thus equation (5.39) cannot be forced to simultaneously satisfy the conditions $h(o) = 1$ and $\lim_{\xi \to \infty} h(\xi) = h_2$. Apparently then the jump boundary condition at the shock must be $h(o) = h_2$, but this result leads nowhere as there is insufficient information to accurately determine h_2.

It must be concluded then that the Rosseland approximation with slip boundary conditions is not sufficient by itself to be used in the analysis of the complete shock layer. It can be used in the combined radiation and conduction problem because the two separate energy fluxes are represented by similar mathematical models and may be treated as an equivalent radiation alone or conduction alone problem. Even in this case, it is not possible to obtain a temperature distribution nor to separately determine the radiant and conductive fluxes optically close to a boundary. In the combined radiation and convection problem, this inability to determine a temperature distribution or to separate the radiant and convective fluxes optically close to a boundary (such as a transparent shock) where convection is important presents a serious obstacle to solution because the convective flux depends on the unknown temperature (or enthalpy) distribution.

E. Results and Discussion

The analysis presented in this chapter applies only when the two enthalpy boundary layers are thin compared to the shock standoff distance with these distances expressed in terms of the Dorodnitsyn variable η. When ϵ/k_P, the ratio of the radiation cooling parameter and the Bouguer number, is much less than one, the thickness of the shock boundary layer is characterized by the inverse of the Bouguer number, k_P^{-1}, while when ϵ/k_P is large the shock boundary layer thickness is characterized by the inverse of the radiation cooling parameter, ϵ^{-1}. The thickness of the wall boundary layer is characterized by the parameter $\left(\epsilon/k_P^2\right)^{1/2}$. Thus, the most restrictive conditions on the applicability of the optically thick analysis are that $k_P \gg 1$ for ϵ small and $k_P \gg \epsilon^{1/2}$ for ϵ large.

Several enthalpy distributions were calculated with the formulas developed in the preceding section. The results are presented in figures 5.5a and 5.5b. The previous discussion of the effects of the parameters on the thicknesses of the boundary layers is substantiated by these results. The effect of the Bouguer number, k_P, and the radiation cooling parameter to Bouguer number ratio, ϵ/k_P on the shock layer optical thickness $k_P\tau_\Delta$ is also shown. The effect of ϵ/k_P depends on the enthalpy variation of the absorption coefficient. In the cases shown the absorption coefficient is proportional to the fourth power of the enthalpy and an increase in ϵ/k_P brings about a

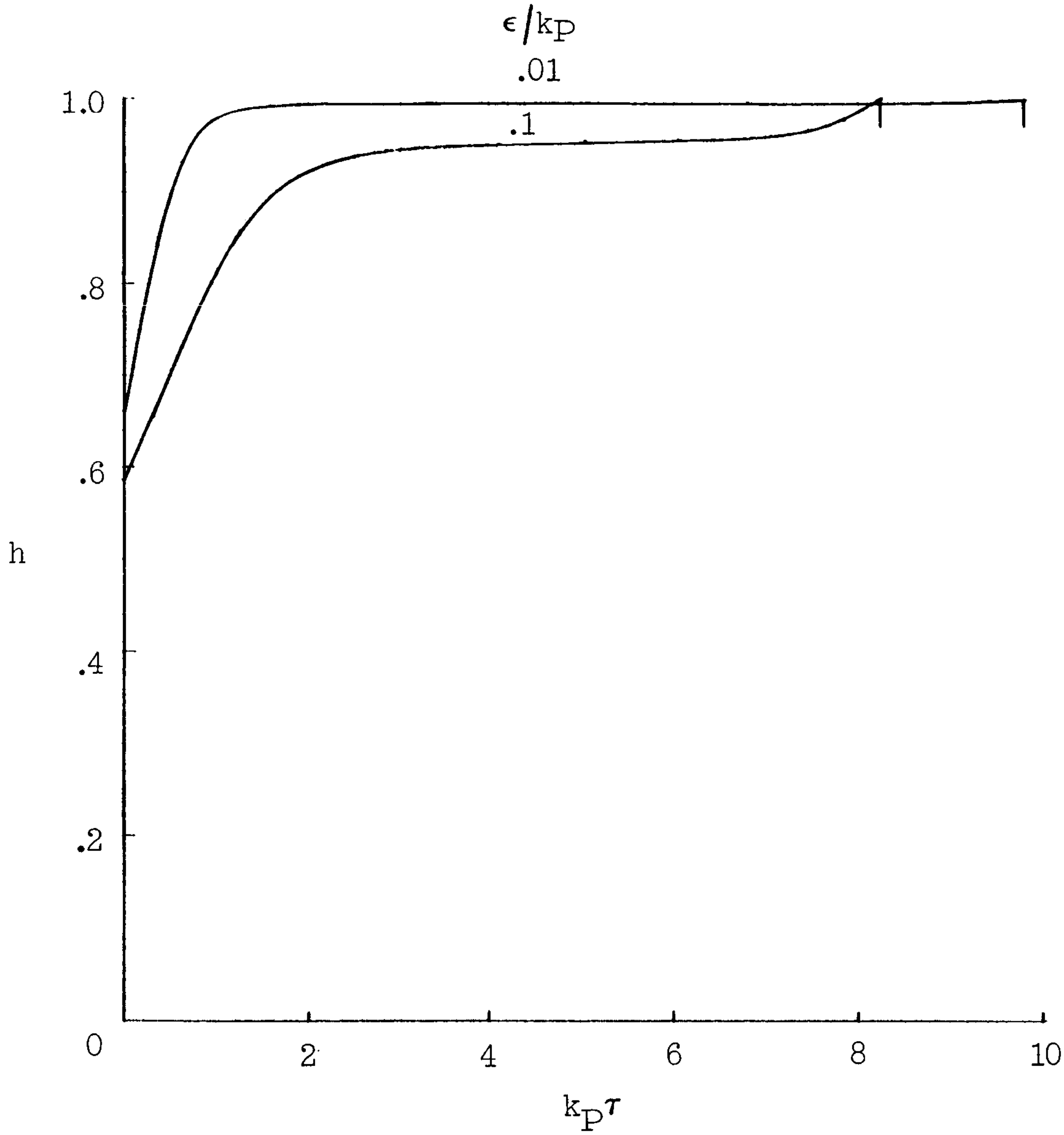

(a) $k_P = 10$.

Figure 5.5.- Effect of the parameters ϵ/k_P and k_P on the enthalpy distribution in an optically thick shock layer.

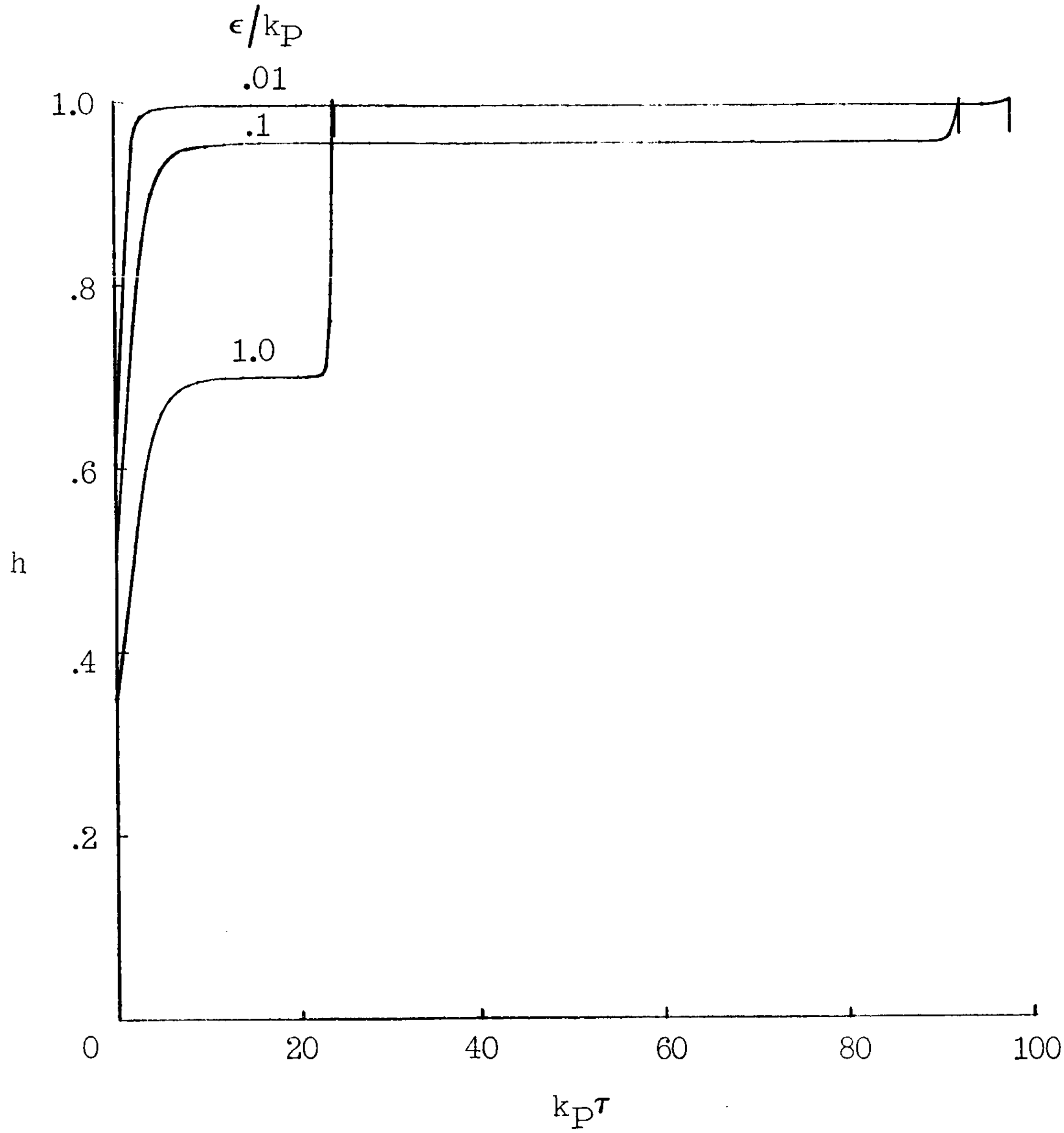

(b) $k_P = 100$

Figure 5.5.- Concluded.

reduction in the shock layer optical depth. The value of the enthalpy of the gas adjacent to the wall (which is related to the ratio of radiant heat transfer to the wall through equation (5.5) and the correlation formula $B = h^2$) decreases with increasing ϵ/k_P and/or k_P.

The effect of γ (where γ is the exponent in the correlation formula $\kappa = h^\gamma$) and the surface reflectivity r_w on the character of the wall boundary layer has not been shown but can be readily deduced from the curves of figures 5.3 and 5.4. Increasing γ tends to reduce the optical thickness of the wall boundary layer and increase the value of the enthalpy of the gas adjacent to the wall. It can be shown that the wall boundary layer thickness expressed in terms of the Dorodnitsyn coordinate η is only slightly effected by a change in γ. Increasing the surface reflectivity r_w tends to increase the optical thickness of the wall boundary layer and increase the value of the enthalpy of the gas adjacent to the wall. When expressed in terms of the Dorodnitsyn coordinate η the boundary layer thickness decreases with increasing r_w. These results are consistent with the results of Chapter 3.

The manner in which the rate of radiant heat transfer to the wall, q_w^R, depends on the radiation cooling parameter to Bouguer number ratio, ϵ/k_P, the Bouguer number, k_P, the variation with enthalpy of the absorption coefficient (through the exponent γ of the correlation formula $\kappa = h^\gamma$), and the surface reflectivity, r_w, is indicated in figures 5.3a to 5.3b. For fixed values of k_P, γ, and r_w the rate of radiant heat transfer to the wall, q_w^R, increases with increasing ϵ/k_P. It appears that q_w^R would become asymptotic to the available energy limit of 1/2 as ϵ/k_P increased without limit. As the Bouguer number, k_P, increases (hence increasing the shock layer optical thickness), all other parameters remaining fixed, the value of q_w^R decreases and becomes asymptotic to zero. This is the same trend exhibited in the problem of radiant energy transfer between two plane parallel walls separated by an absorbing and emitting, but motionless and nonheat conducting gas (see, for example, ref. 11). Increasing γ while holding the other parameters fixed results in an increase in q_w^R. This trend is the reverse of that for a transparent shock layer (see fig. 4.6). The results of Chapter 3 (see fig. 3.6) show that this reversal occurs at intermediate values of the Bouguer number k_P. Finally, it is apparent from figure 5.3 that an increase in surface reflectivity r_w for fixed values of the other parameters results in a decrease in q_w^R. The change in q_w^R with r_w satisfies the inequality

$$q_w^R \geq \left(1 - r_w\right) \left(q_w^R\right)_{r_w = 0}$$

which agrees with the physical argument presented in section 4 of chapter III.

CHAPTER VI

THE RADIATION DEPLETED SHOCK LAYER

A. The Strong Radiation Approximation

When the radiation cooling parameter ϵ is very much greater than both one and k_P^2, the Bouguer number squared, a particle leaving the shock with an initial enthalpy of $\frac{1}{2} W_\infty^2$ will emit radiation at such a rapid rate that it will lose a significant amount of its energy before traveling the distance of a photon mean free path. Because this energy is emitted in a region of small optical thickness adjacent to the transparent shock most of it will escape from the shock layer, and the enthalpy level within the shock layer will be quite small in comparison to the value at the shock. In fact, as will be shown subsequently, the zero-order solution for the enthalpy in the interior of the shock layer is identically zero. It is for this reason that the term "radiation depleted shock layer" has been coined. Of course, the narrow region adjacent to the shock in which the large change in enthalpy occurs can be described as a boundary layer and boundary layer techniques can be applied to obtain solutions in it.

The conditions which must hold in order that there be a radiation depleted shock layer, that is ϵ very large and k_P^2 not too large, occur at high altitudes for rather large objects (shock radius greater than 1 meter) entering at extremely high speeds (entry speeds close to 70 km sec). It is not at all clear that the requirement for chemical equilibrium can be satisfied under these condition, particularly in view of the existance of a shock boundary layer in which large changes occur over a short distance, and hence, a short time. Dispite this objection, the solutions for the radiation depleted shock layer represent an interesting limiting case which should lead to an increased understanding of the radiating shock layer and provide a firm base for extension into areas of more practical concern.

B. Analysis

Once again, as was the case for the optically thin and optically thick shock layers, analysis can be facilitated through the use of the substitute kernal approximation. In this case, the energy equation, written in terms of the optical path length, is

$$\left[f(\tau)h'(\tau)\right]'' - \frac{3}{2}\,\epsilon\, B''(\tau) - \frac{9}{4}\,k_P^2\, f(\tau)h'(\tau) = 0 \qquad (6.1)$$

Here f is the nondimensional stream function, h the nondimensional enthalpy, B the nondimensional black-body emissive power, ϵ the radiation cooling parameter, k_P the Bouguer number, and τ the optical path length. It should be remembered that use of this equation restricts the analysis to gray gases only. The boundary conditions on the enthalpy are, as before

$$h\left(\tau_\Delta\right) = 1 \qquad (6.2)$$

and the integral condition

$$f(\tau)h'(\tau) - \frac{3}{2}\epsilon\Bigg[B(\tau) - \frac{3}{4}k_P\int_0^{\tau_\Delta} B(t)e^{-\frac{3}{2}k_P|t-\tau|}\,dt$$
$$- \frac{3}{4}k_P\, r_w\, e^{-\frac{3}{2}k_P\tau}\int_0^{\tau_\Delta} B(t)e^{-\frac{3}{2}k_P t}\,dt\Bigg] = 0 \qquad (6.3)$$

The particular form of the substitute kernal employed here, that is, $E_2(\tau) \approx \frac{3}{4}e^{-\frac{3}{2}k_P\tau}$, was chosen for simplicity. Somewhat greater accuracy might be achieved by letting the constants depend on the optical depth $k_P\tau_\Delta$. However, it was not felt that this procedure would lead to a better understanding of the radiation depleted shock layer.

The momentum equation, in terms of the Dorodnitsyn coordinate, and the boundary conditions on the nondimensional stream function are

$$2f(\eta)f''(\eta) - \left[f'(\eta)\right]^2 + a^2 h = 0 \qquad (6.4)$$

$$f(0) = 0 \qquad (6.5)$$

$$f\left(\eta_\Delta\right) = 1 \qquad (6.6)$$

$$f'\left(\eta_\Delta\right) = \frac{2}{X}\left(\frac{\Delta}{R_s}\right) = \frac{a}{\sqrt{2X(1 - X)}} \qquad (6.7)$$

When the radiation cooling parameter ϵ is very much greater than one and κ_P^2 the energy equation (6.1) admits the asymptotic solution

$$B(\tau) = C_1 + C_2 \tau \qquad (6.8)$$

Substitution into the asymptotic form of the integral condition (6.3) reveals that each of the two constants must be identically zero. Thus, in the interior of the shock layer $B(\tau)$ and $h(\tau)$ are zero. In this case, the density is infinite and the momentum equation can be readily solved for $f(\eta)$ with the result

$$f(\eta) = \left(\frac{\eta}{\eta_\Delta}\right)^2 \qquad (6.9)$$

and, of course, the shock standoff distance tends to zero.

In order to investigate the shock boundary layer, it is convenient to introduce the "stretched" coordinates

$$\xi = \left(\tau_\Delta - \tau\right)\epsilon^n \qquad (6.10)$$

and

$$\zeta = \left(\eta_\Delta - \eta\right)\epsilon^n \qquad (6.11)$$

into the energy and momentum equations, respectively. Performing the usual manipulations (details are presented in appendix D) shows that the boundary layer is characterized by the parameter ϵ^{-1} and it would seem proper to expand both the boundary layer and asymptotic solutions in power series of this small parameter. However, $f_a(\eta)$

(where the subscript a indicates the asymptotic solution valid far from the shock) is not analytic in ϵ^{-1} near $\epsilon^{-1} = 0$, but is analytic in $\epsilon^{-1/2}$. Consequently, the solutions must be expanded as power series in $\epsilon^{-1/2}$.

The lowest-order form of the energy equation in the boundary layer is

$$\left(\frac{dh}{dB_{b_o}}\right) B'_{b_o}(\xi) + \frac{3}{2} B_{b_o}(\xi) = C_1 + C_2 \xi \tag{6.12}$$

The subscript b_o has been used to denote the zero-order boundary layer solutions. This equation must satisfy the boundary conditions that both $B_{b_o}(\xi)$ and $B'_{b_o}(\xi)$ vanishes as ξ increases without limit. Thus, the constants C_1 and C_2 are both identically zero. The third condition to be satisfied is

$$B_{b_o}(0) = 1 \tag{6.13}$$

The solution to equation (6.12) subject to the boundary conditions is

$$\xi = \frac{2}{3} \int_{B_{b_o}}^{1} \left(\frac{dh}{dB}\right) \frac{dB}{B} \tag{6.14}$$

Solution of the momentum equation in the boundary layer gives the zero-order form of the nondimensional stream function

$$f_{b_o}(\zeta) = 1 \tag{6.15}$$

These zero-order solutions can be used to generate solutions of higher order. Mathematical details are presented in appendix D. In general, the analysis follows the procedure outlined by Van Dyke (ref. 56).

A complete listing of these solutions up to second-order in the parameter $\epsilon^{-1/2}$ is presented below.

Zero-order solutions.-

$$B_{a_o}(\tau) = 0 \tag{6.16}$$

$$f_{a_o}(\eta) = \left(\frac{\eta}{\eta_\Delta}\right)^2 \tag{6.17}$$

$$\xi = \frac{2}{3}\int_{B_{b_o}}^{1}\left(\frac{dh}{dB}\right)\frac{dB}{B} \tag{6.18}$$

$$f_{b_o}(\zeta) = 1 \tag{6.19}$$

$$\eta_{\Delta_o} = \frac{2\sqrt{2X(1 - X)}}{a} = 1 + \sqrt{2X(1 - X)} \tag{6.20}$$

$$\tau_{\Delta_o} = \frac{\eta_{\Delta_o}}{\kappa_p^{-1}(0)} \tag{6.21}$$

First-order solutions.-

$$B_{a_1}(\tau) = 0 \tag{6.22}$$

$$f_{a_1}(\eta) = a\eta_{\Delta_o}\sqrt{\dot{h}(0)B_{a_2}(0)}\left(\frac{\eta}{\eta_{\Delta_o}}\right)\left[1 - \left(\frac{\eta}{\eta_{\Delta_o}}\right)\right] \tag{6.23}$$

$$B_{b_1}(\xi) = 0 \tag{6.24}$$

$$f_{b_1}(\zeta) = 0 \tag{6.25}$$

$$\eta_{\Delta_1} = \frac{1}{2}a\eta^2_{\Delta_o}\sqrt{\dot{h}(0)B_{a_2}(0)} \tag{6.26}$$

$$\tau_{\Delta_1} = \frac{\eta_{\Delta_1}}{\kappa_P^{-1}(0)} \tag{6.27}$$

<u>Second-order solutions.-</u>

$$B_{a_2}(\tau) = \frac{k_P\left(1 + r_w\right)\left[1 + \frac{3}{2}k_P\tau\right]}{2\left[1 + \frac{3}{4}\left(1 - r_w\right)k_P\tau_{\Delta_o}\right]} \tag{6.28}$$

$$\begin{aligned} f_{a_2}(\eta) = &\left[\left(\frac{\eta_{\Delta_1}}{\eta_{\Delta_o}}\right)^2 - 2\left(\frac{\eta_{\Delta_2}}{\eta_{\Delta_o}}\right) - A\ln\eta_{\Delta_o}\right]\left(\frac{\eta}{\eta_{\Delta_o}}\right)^2 \\ &+ \left[A\ln\eta_{\Delta_o}\right]\left(\frac{\eta}{\eta_{\Delta_o}}\right) + A\left(\frac{\eta}{\eta_{\Delta_o}}\right)\ln\left(\frac{\eta}{\eta_{\Delta_o}}\right) \end{aligned} \tag{6.29}$$

where

$$A = 3\left(\frac{\eta_{\Delta_1}}{\eta_{\Delta_o}}\right)^2 k_P \tau_{\Delta_o}$$

$$\eta_{\Delta_2} = -\eta_{\Delta_o}\left(\frac{\eta_{\Delta_1}}{\eta_{\Delta_o}}\right)^2\left[1 + \frac{3}{2} k_P \tau_{\Delta_o}\left(1 - \ln\eta_{\Delta_o}\right)\right] \tag{6.30}$$

$$\tau_{\Delta_2} = \frac{\eta_{\Delta_2}}{\kappa_P^{-1}(0)} + \eta_{\Delta_o}\frac{\left[\dot{\kappa}_P^{-1}(0)\right]}{\left[\kappa_P^{-1}(0)\right]^2} B_{a_2}(0)\left[1 + \frac{3}{4} k_P \tau_{\Delta_o}\right]$$
$$+ \int_0^{\epsilon\tau_{\Delta_o}+\epsilon^{1\ 2}\tau_{\Delta_1}+\tau_{\Delta_2}}\left[\frac{\kappa_P^{-1}\left(B_{b_o}(\xi)\right)}{\kappa_P^{-1}(0)} - 1\right]d\xi \tag{6.31}$$

Radiant heat-flux and standoff distance.- The total radiant heat flux to the wall q_w^R and the ratio of the shock standoff distance to the shock standoff distance for radiationless flow $\bar{\Delta}$ are given by the following expressions.

$$\frac{q_w^R}{1 - r_w} = \frac{1}{2\left[1 + \frac{3}{4}\left(1 - r_w\right) k_P \tau_{\Delta_o}\right]} \tag{6.32}$$

$$\bar{\Delta} = \epsilon^{-1}\left\{\eta_{\Delta_o}\left[\dot{h}(0) + h(0)\,\frac{\left(\dot{\kappa_P^{-1}(0)}\right)}{\kappa_P^{-1}(0)}\right]B_{a_2}(0)\left[1 + \frac{3}{4}\,k_P\,\tau_{\Delta_o}\right]\right.$$

$$\left. + \int_0^{\epsilon\tau_{\Delta_o}+\epsilon^{1/2}\tau_{\Delta_1}+\tau_{\Delta_2}} h\left(B_{b_o}(\xi)\right)\kappa_P^{-1}\left(B_{b_o}(\xi)\right)d\xi\right\} \tag{6.33}$$

C. Results and Discussion

In the analysis of the preceeding section, it was convenient to use the black-body emissive power B rather than the enthalpy h as the dependent variable. This choice necessitated the assumption that the thermodynamic and optical properties (in particular h and κ_P^{-1}) be analytic functions of B in the interval $(0,1)$. Unfortunately, this condition does not hold for the correlations of chapter II written in terms of B in the limit as B approaches zero. This difficulty can be circumvented through the use of analytic approximations to the correlating functions. For example, the enthalpy might be approximated by the function

$$h = (B + B^*)^{1/2} \tag{6.34}$$

where B^* is a very small positive number. Use of formula (6.34) in expression (6.18) results in the following solution for $B_{b_o}(\xi)$

$$B_{b_o}(\xi) = B^*\left[\left(\frac{1 + Ce^{-3\sqrt{B^*}\,\xi}}{1 - Ce^{-3\sqrt{B^*}\,\xi}}\right)^2 - 1\right] \tag{6.35}$$

where

$$C = \frac{\sqrt{1 + B^*} - \sqrt{B^*}}{\sqrt{1 + B^*} + \sqrt{B^*}} \tag{6.36}$$

For large values of ξ, that is

$$\xi \gg 1/3\sqrt{B^*}$$

the value of $B_{b_o}(\xi)$ is directly proportional to B^*. It is clear then that B^* should be chosen sufficiently small to insure that $B_{b_o}(\xi)$ is nearly independent of B^* for values of B_{b_o} as small as $\epsilon^{-1}B_{a_2}(0)$.

Because of the unlikelihood of establishing local thermodynamic and chemical equilibrium in a physical shock layer under those conditions for which this model analysis is supposed to apply, it would be somewhat superfluous to present the results of detailed calculations for the enthalpy distribution and shock standoff distance. Suffice it to say that the shock layer is characterized by an enthalpy boundary layer immediately behind the shock the thickness of which (in terms of the Dorodnitsyn variable η) is characterized by the inverse of the radiation cooling parameter ϵ^{-1}. It should also be pointed out that the shock boundary layer is always very much less than a photon mean free path and hence is always optically thin. The enthalpy level in the interior of the shock layer is order of magnitude k_p/ϵ. The ratio of the shock standoff distance to the shock standoff distance for radiationless flow is order of magnitude ϵ^{-1}.

Curves representing the magnitude of the radiant heat flux which is absorbed by the wall q_w^R are presented in figure 6.1. In the optically thin limit $\left(k_P \tau_{\Delta_o} \ll 1\right)$ the radiant heat flux approaches the "available energy limit" of $\left(1 - r_w\right)/2$. As the optical thickness of the wall increases and absorption becomes more important, less of the energy emitted from the gas in the shock boundary layer in the direction of the wall is able to penetrate the shock layer and reach the wall before being absorbed. Part of what is absorbed is then reradiated in the forward direction and escapes from the shock layer through the transparent shock. Finally, as $k_P \tau_{\Delta_o}$ tends to infinity none of the energy emitted in the shock boundary layer reaches the wall and the radiant flux incident on the wall vanishes.

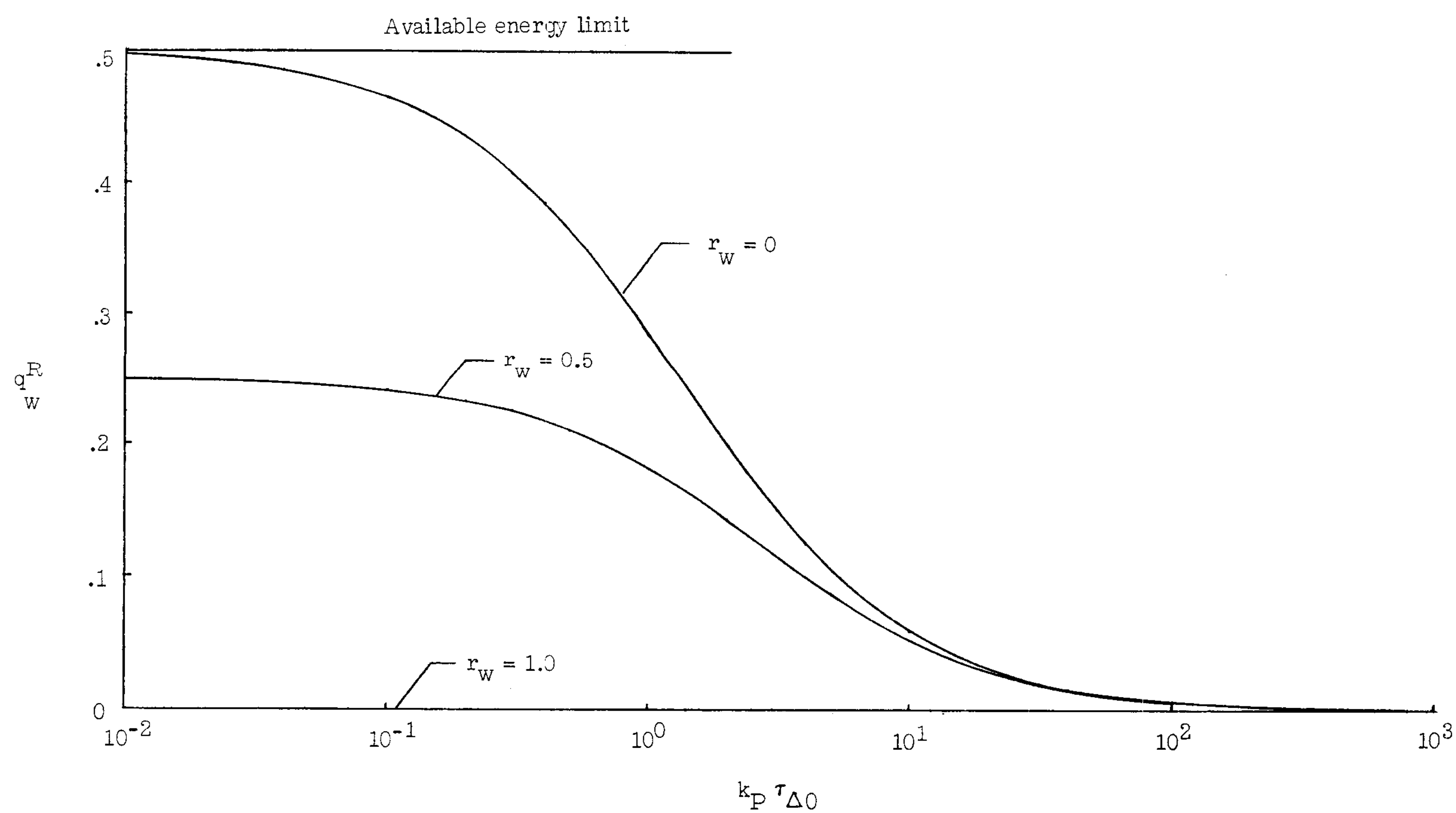

Figure 6.1.- Radiant heat flux from radiation depleted shock layer.

CHAPTER VII

RADIATING SHOCK LAYERS

A. Discussion of the Approximate Solutions

Four different approximate stagnation point solutions for an inviscid, radiating shock layer were obtained in preceding chapters. Each one represents a limiting case for some combination of the radiation cooling parameter ϵ and the Bouguer number k_P. The regions of validity of the approximate solutions are depicted in figure 7.1. The boundaries as drawn pertain only to a gray gas with constant absorption coefficient. It would be necessary to redraw the boundaries for each nongray gas and for every change in the enthalpy dependence of the absorption coefficient. As was pointed out in chapter IV, the criterion for validity of the optically thin solution is that the gas layer be optically thin in all wavelength intervals in which a significant amount of energy is transported by radiation. For a gray gas, this means $k_P\tau_\Delta \ll 1$. Thus, the boundary is not specified completely by k_P but varies with ϵ as well (since $k_P\tau_\Delta$, the shock layer optical thickness depends on ϵ as well as k_P when the absorption coefficient is a function of the enthalpy). When applied to a nongray gas, the criterion for validity of the optically thin solution is always more restrictive than the condition that the Planck mean optical depth be small. Thus, the boundaries for all nongray gases will be displaced to the left of the boundary for the "Planck-equivalent" gray gas. A "Planck-equivalent" gray gas is one in which the wavelength independent

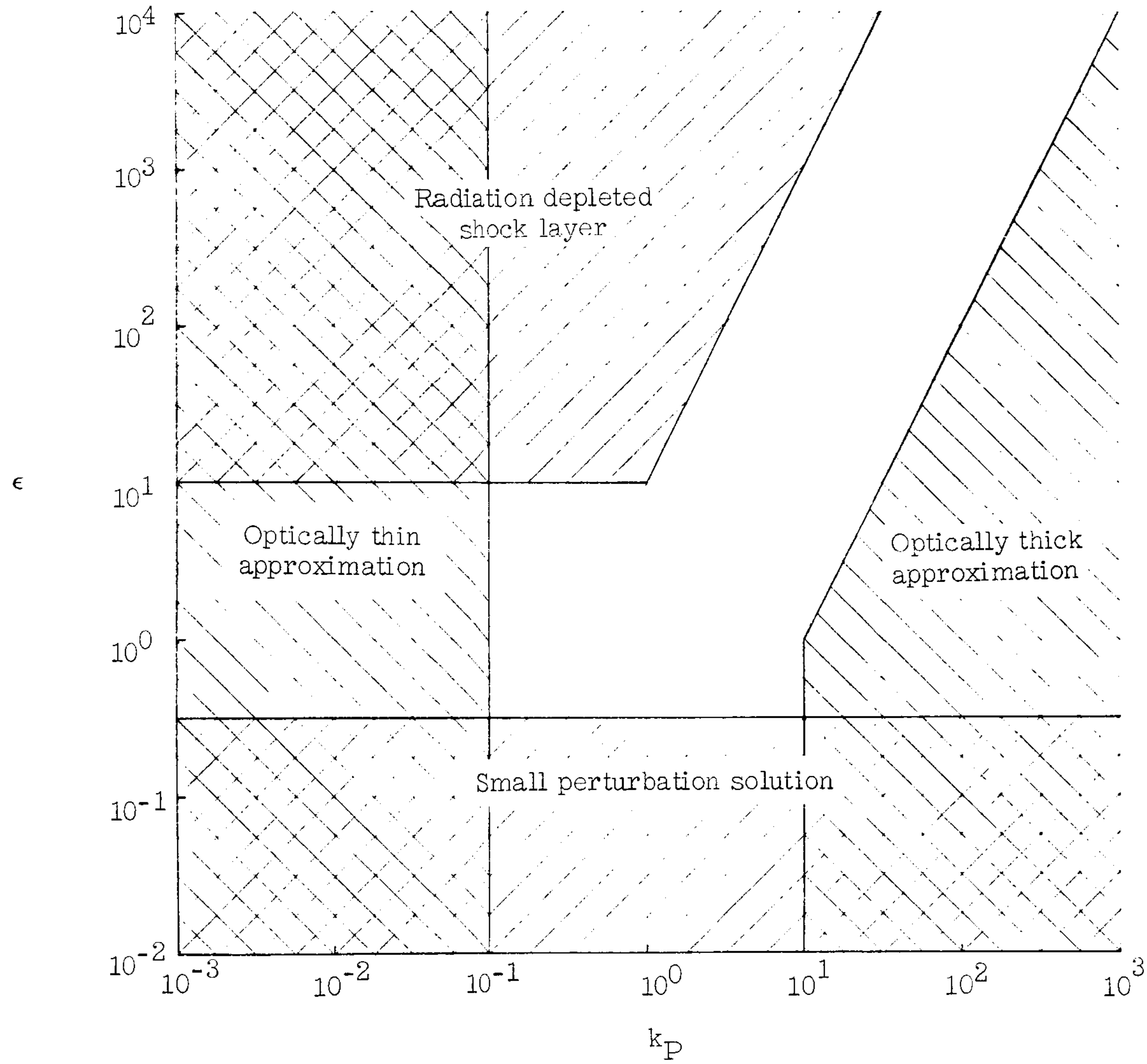

Figure 7.1.- Radiating shock layer regimes.

absorption coefficient is equal to the Planck mean absorption coefficient in the nongray gas.

The location of the boundary for the small perturbation approximation depends on the radiation cooling parameter ϵ and the enthalpy variation of the absorption coefficient. The value of ϵ for which the solution will yield results of a given accuracy is reduced with an increase in γ (where γ is the exponent in the correlation formula $\kappa_P = h^\gamma$), because of the reduced accuracy of the truncated expansion for κ_P (equation (B-43) of appendix B). Since the small perturbation solution was shown to be correct to second-order throughout most of the domain of the problem the condition for establishing the boundary is $\epsilon^2 \ll 1$.* The location of the boundary does not depend on the wavelength dependence of the absorption coefficient.

The most restrictive condition limiting the validity of the optically thick analysis for moderate values of the radiation cooling parameter ϵ is the thickness of the enthalpy layer adjacent to the shock. This thickness is characterized by the inverse of the Bouguer number $1/k_P$. Thus, the criterion for validity is $k_P \gg 1$. For larger values of ϵ the condition $\left(\epsilon/k_P^2\right)^{1/2} \ll 1$ becomes more restrictive and must be used to establish the boundary. This latter condition insures that the enthalpy boundary layer adjacent to the wall is thin compared to

*This condition holds when $\gamma = 0$. When $\gamma = 4$ the proper condition becomes $10\ \epsilon^2 \ll 1$.

the shock standoff distance. The analysis presented in chapter V is restricted to the case of a gray gas but could be extended rather simply to the case of an absorption coefficient with a step function dependence on wavelength for which the step heights are either $\alpha(h)\ \kappa_P(h)$ or zero. There is no restriction to the number of width of the steps. The only changes that would appear in the formulas would be the substitution of $\alpha(h)\ \kappa_P(h)$ for $\kappa_P(h)$ and $B(h)/\alpha(h)$ for $B(h)$. The boundary to the region of validity of the optically thick shock layer analysis would be displaced to the left for this particular class of nongray gases.

The region of validity of the radiation depleted shock layer analysis is restricted by the conditions $\epsilon \gg 1$ and $\epsilon \gg k_P^2$. The first condition insures that the thickness of the enthalpy boundary layer adjacent to the shock is small compared to the shock standoff distance, while the second condition insures that radiation is the preponderant mode of energy transport within the shock layer. Like the analysis of chapter V, the radiation depleted shock layer analysis is restricted to gray gases but can be extended to the nongray model absorption coefficient with multiple steps of uniform height. Use of such a nongray model would cause a leftward shift in the boundaries to the region of validity. Of course, the regions of validity of both the optically thick and radiation depleted shock layer analyses must vanish for all other classes of nongray gases.

In order to relate the radiation shock-layer regimes to the problem of entry into the atmosphere of the earth, several trajectories are indicated on the $\epsilon - k_p$ map presented in figure 7.2. The arrows indicate the direction of increasing time. Trajectories 1 and 2 represent iron spheres of radius 1 meter and 1 centimeter, respectively, entering vertically with an initial velocity of 70 km/sec.* Trajectories for all other objects of the same size and lesser or equal initial velocities must lie below them in the $\epsilon - k_p$ space. The third trajectory corresponds to the entry of a round-trip Martian probe which would encounter some of the more severe heating conditions of the currently envisioned class of manmade objects. It is apparent that the small perturbation approximation has considerable utility for the analysis of radiation effects on the entry of manmade objects. It also appears that the optically thin shock layer analysis might enjoy wide applicability. However, in the more realistic case of a nongray gas the boundary would be shifted to the left one or two orders of magnitude in the Bouguer number k_p, considerably reducing the practical usefulness of the optically thin approximation. The optically thick and radiation depleted shock layer analysis would seem to be nearly devoid of direct practical usefulness, both because of the inacessibility of the proper magnitudes of the parameters ϵ and k_p to objects of interest and because of the restriction of these analyses to the gray case (and the simple

*No account has been taken of mass loss of these spheres due to ablation.

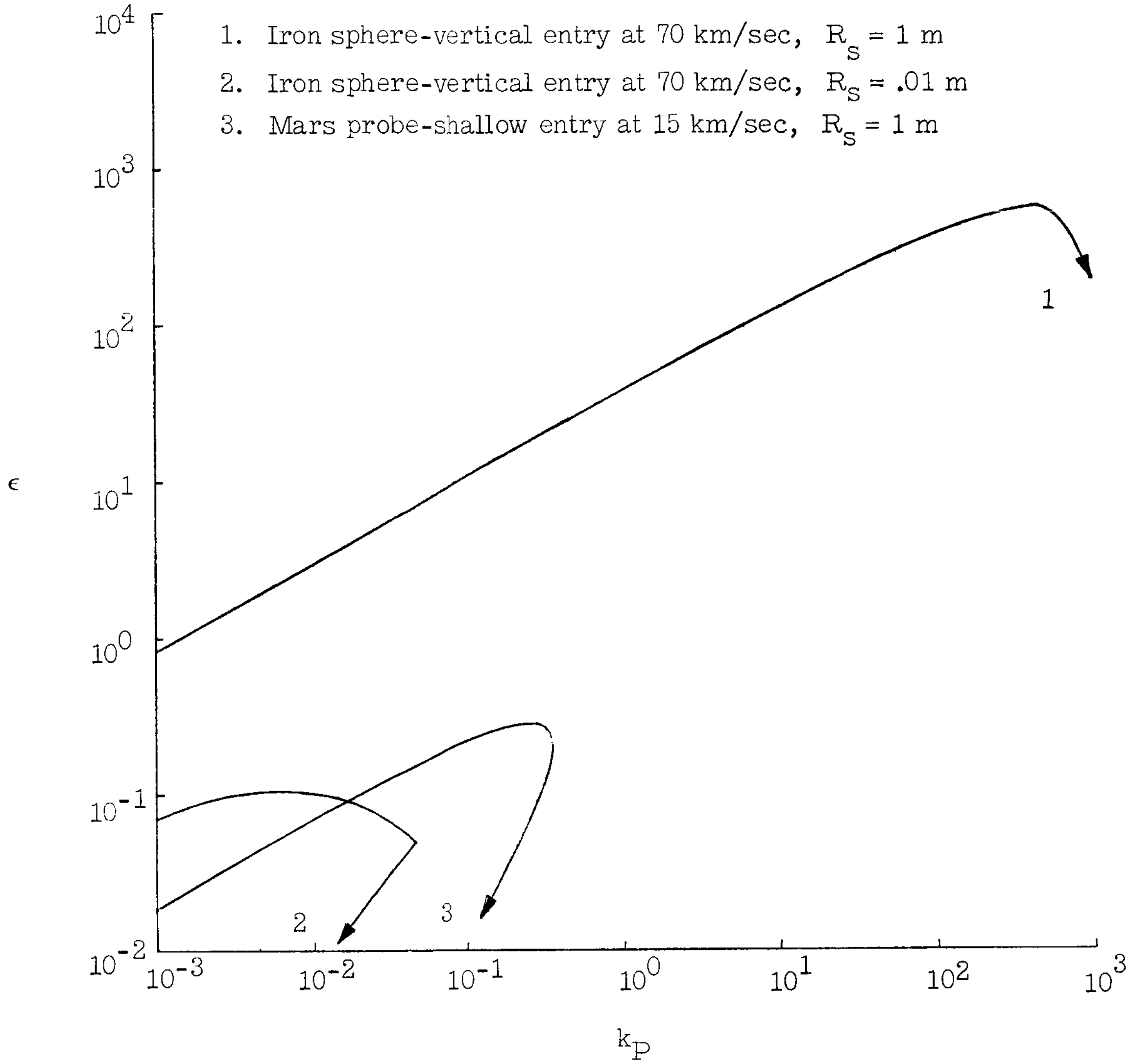

Figure 7.2.- Entry trajectories in the ϵ-k_P space.

nongray model absorption coefficient with multiple steps of uniform height).

B. A Model Earth Entry Environment

The four approximate solutions can be used to compute the radiant heat transfer to the stagnation point over a wide range of the radiation cooling parameter ϵ and the Bouguer number k_P. The results depend on the particular gas, the surface reflectivity, and the size of the object and must be recomputed for every change in these variables. Actually, the size of the object is important only if the exponent γ (which appears in the correlation formula $\kappa_P = h^\gamma$) varies throughout the $\epsilon - k_P$ space. In this event, the value of h at which a change in γ occurs depends on the parameter $k_P = \rho_s \kappa_{P_s} \Delta_A$ which is influenced by the body size through the radiationless shock standoff distance Δ_A.

Contours of constant values of T_s (the temperature immediately behind the shock), $\rho_s \kappa_{P_s}$ (The Planck mean volume absorption coefficient immediately behind the shock), ϵ/k_P, and X (the ratio of free-stream density to the density immediately behind the shock) on plots of ambient density ratio ρ_∞/ρ_{SL} versus free-stream velocity W_∞ up to 70 km/sec are presented in figures 7.3a through 7.3d, for a model earth entry environment. This entry environment was obtained by combining the thermodynamic and optical property correlations presented in chapter II, section E with the strong normal shock relations. The resulting formulas are:

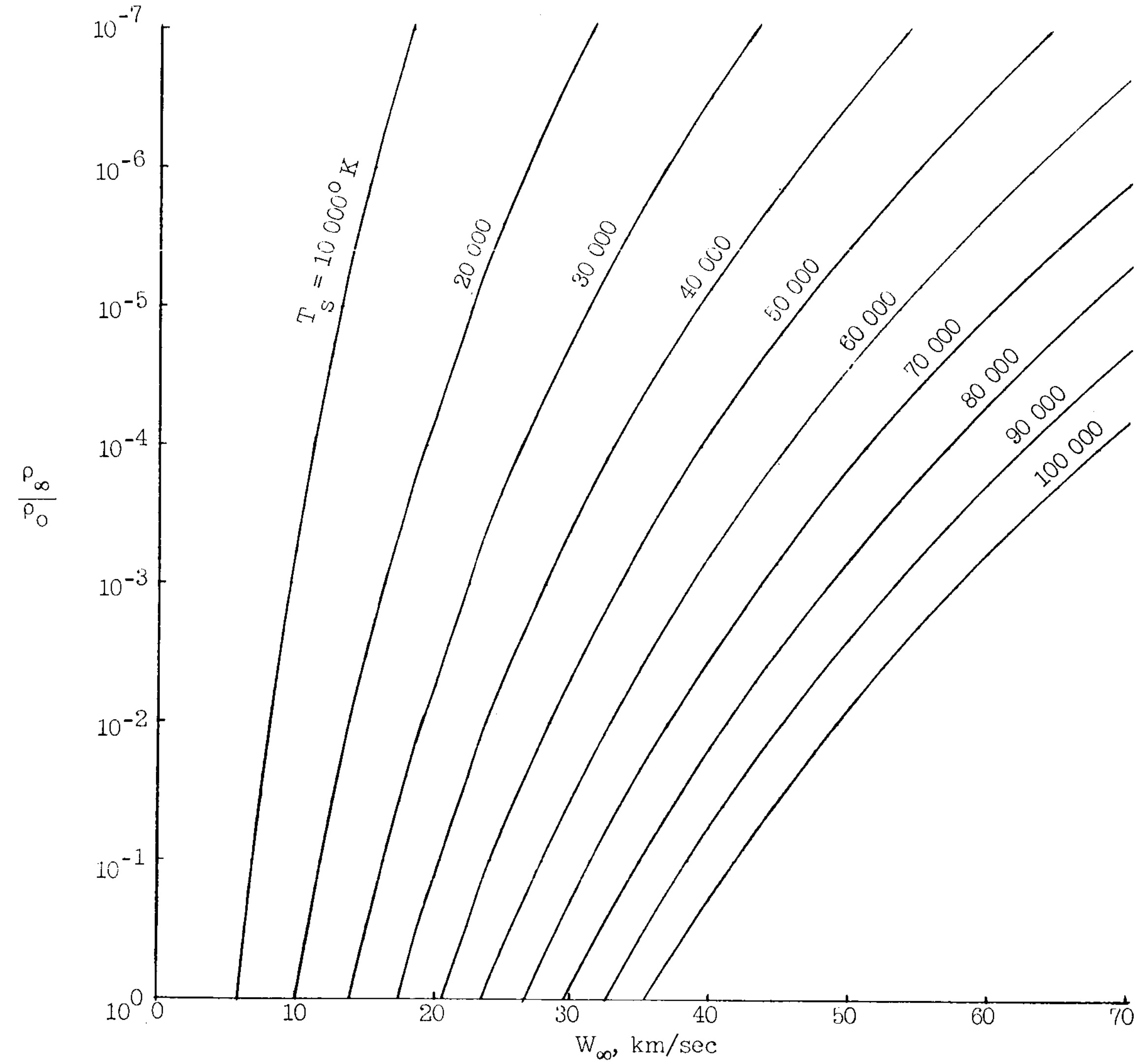

(a) Contours of constant normal shock equilibrium temperatures.

Figure 7.3.- The earth entry environment.

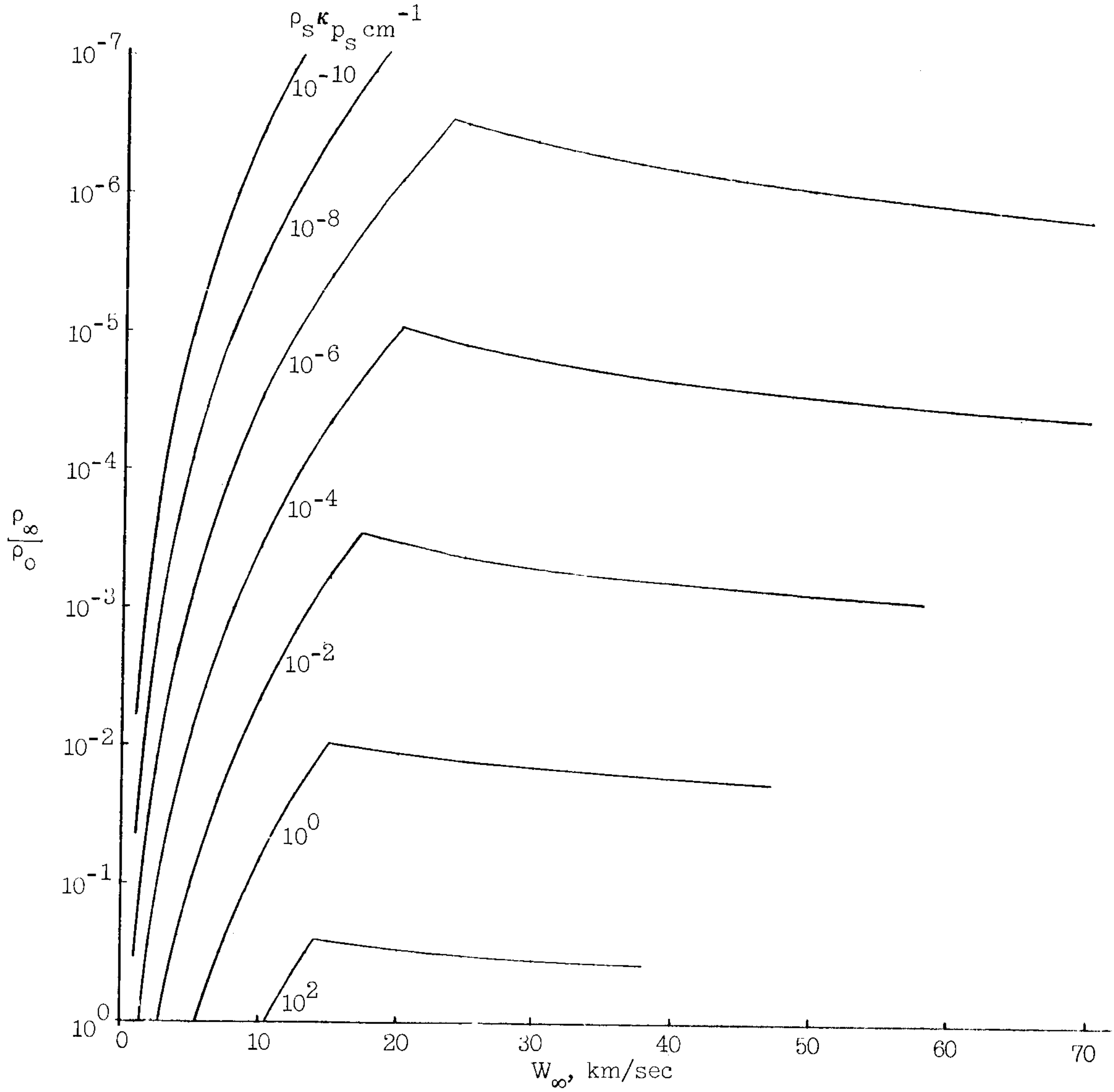

(b) Contours of constant normal shock equilibrium values of the Planck mean volume absorption coefficient, $\rho_s \ \kappa_{P_s}$.

Figure 7.3.- Continued.

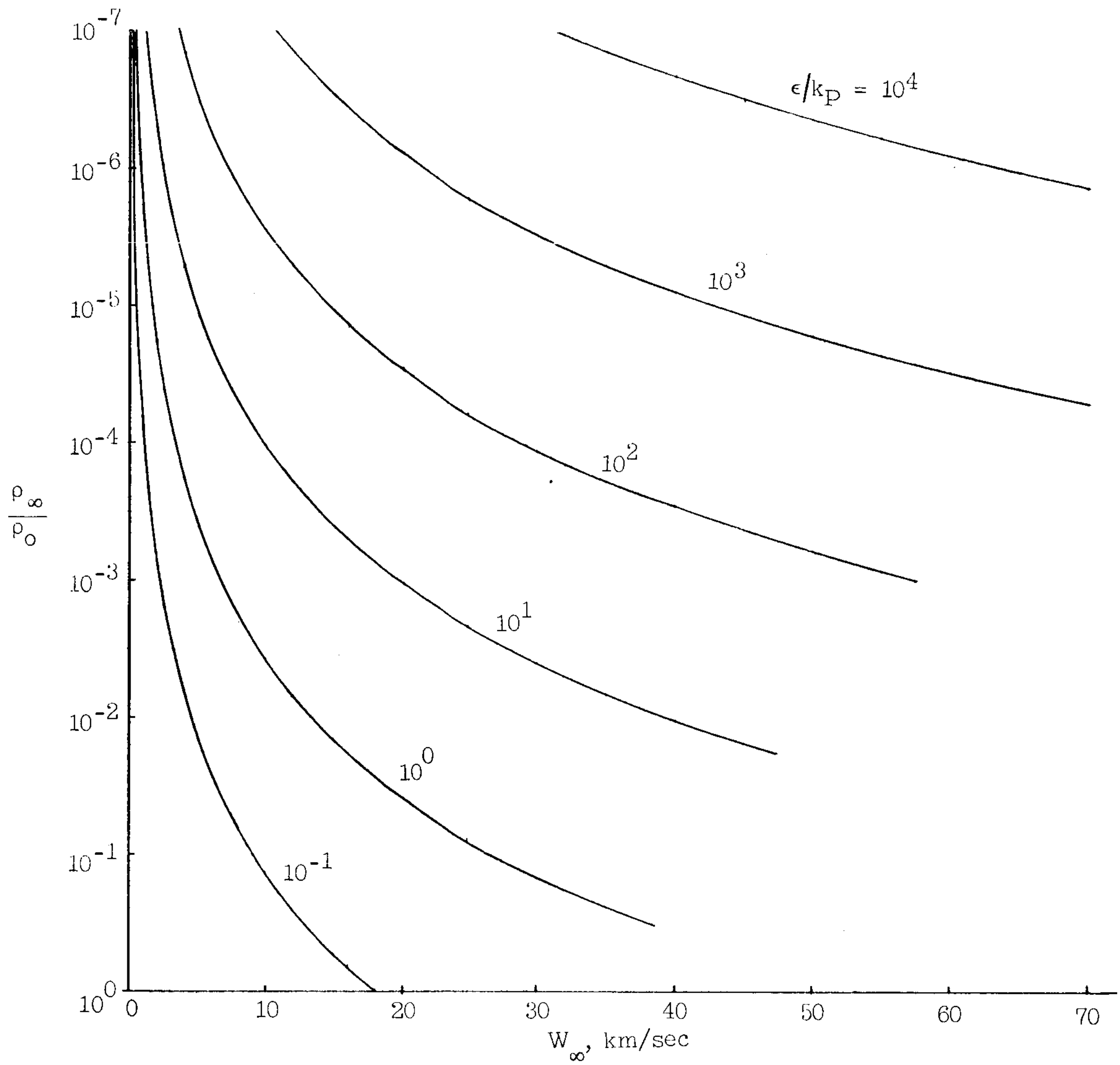

(c) Contours of constant values of $\epsilon/k_P = 4\sigma T_s^4/\rho_\infty W_\infty^2$.

Figure 7.3.- Continued.

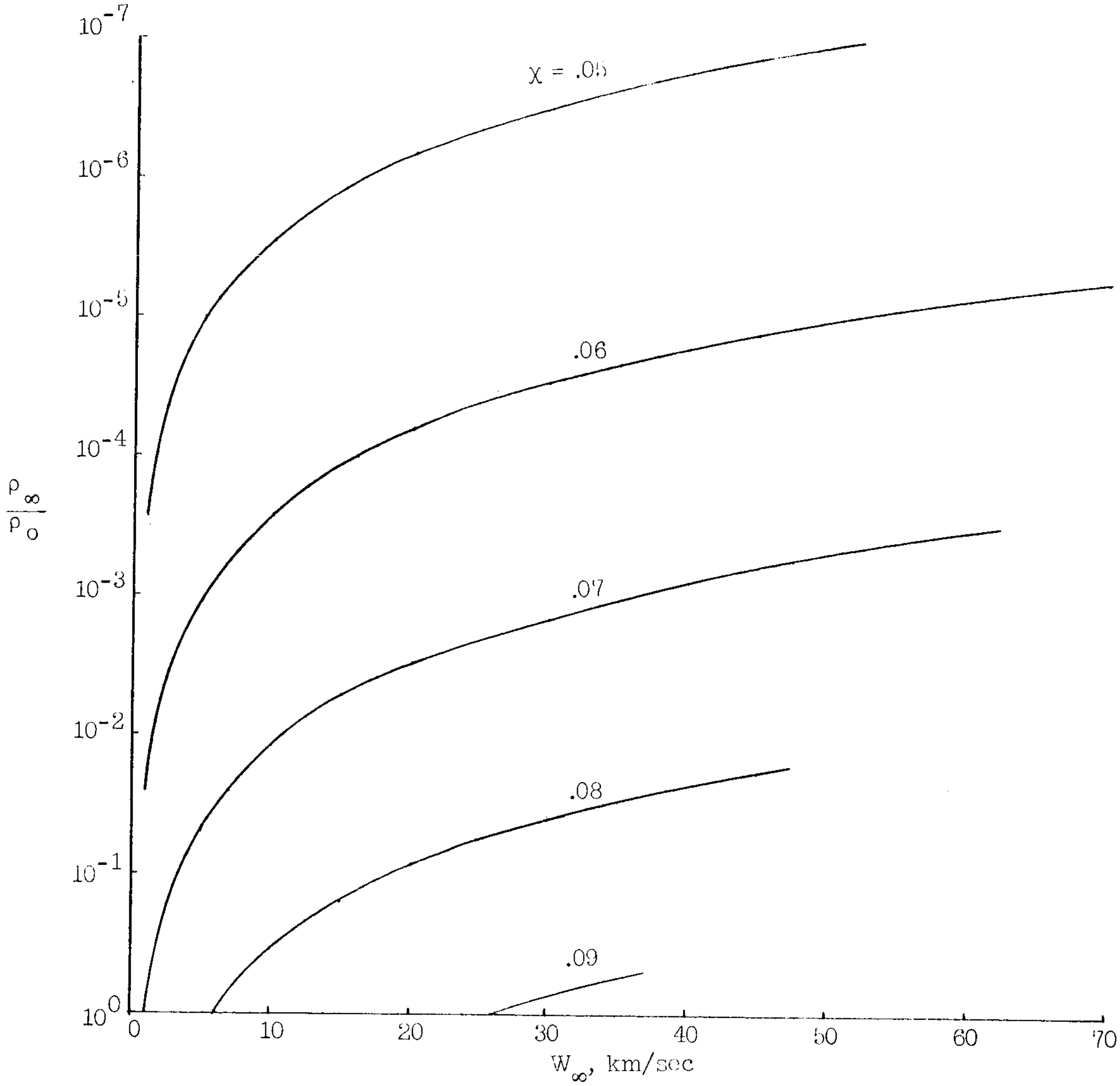

(d) Contours of constant normal shock equilibrium density ratios.

Figure 7.3.- Concluded.

$$T_s = 1.038 \times 10^3 \left(\frac{\rho_\infty}{\rho_{SL}}\right)^{.09} W_\infty^{1.28}, \ ^oK \qquad (7.1)$$

$$X = \left(\frac{\rho_s}{\rho_\infty}\right)^{-1} = 6.95 \times 10^{-2} \left(\frac{\rho_\infty}{\rho_{SL}}\right)^{.04} W_\infty^{.08} \qquad (7.2)$$

$$\frac{\epsilon}{k_P} = 1.852 \times 10^{-16} \, T_s^{\,4} \left(\frac{\rho_\infty}{\rho_{SL}}\right)^{-1} W_\infty^{-3} \qquad (7.3)$$

$$\rho_s \kappa_{P_s} = 7.94 \times 10^{-26} \left(X^{-1} \frac{\rho_\infty}{\rho_{SL}}\right)^{3.25} T_s^{\,6.0 - 0.5 \, \mathrm{Log}_{10} \left(X^{-1} \frac{\rho_\infty}{\rho_{SL}}\right)}, \ \mathrm{cm}^{-1} \qquad (7.4a)$$

for the lower temperatures (less than about $20{,}000^o$ K) and

$$\rho_s \kappa_{P_s} = 9.33 \times 10^2 \left(X^{-1} \frac{\rho_\infty}{\rho_{SL}}\right)^{0.507} T_s^{\,-0.39 + 0.21 \, \mathrm{Log}_{10} \left(X^{-1} \frac{\rho_\infty}{\rho_{SL}}\right)}, \ \mathrm{cm}^{-1} \qquad (7.4b)$$

for the higher temperatures.

The values of X and γ (the exponent in the correlation formula $\kappa_P = h^\gamma$) do not vary greatly over a rather extensive range of ambient densities and velocities. Consequently, it was decided to fix these quantities at the constant values, $X = 0.06$ and $\gamma = 4.0$, for the discussions which follow.

C. Radiant Heat Transfer

The rate of radiant heat transfer to the stagnation point of a blunt object, q_w^R, was calculated by the four approximate methods for a wide range of the radiation cooling parameter ϵ and the Bouguer number k_P. The results are presented in figure 7.4 as a plot of q_w^R against k_P for various values of the ratio ϵ/k_P. This ratio, sometimes known as the inverse of the Boltzmann number, was used because it is what might be termed an "environmental parameter," that is a parameter dependent only on free-stream conditions (ambient density and velocity) and not on body geometry. The Bouguer number k_P, on the other hand, is directly proportional to the body nose radius for a given set of free-stream conditions. Thus, each curve in figure 7.4 can be thought of as representing the effect of body nose radius on radiant heat transfer at a given trajectory point.

For the purpose of calculating the results presented in figure 7.4, the shock layer gas was assumed to have a gray mass absorption coefficient which varies as the fourth power of the enthalpy. The surface of the object was considered to be nonreflecting. The dashed portions of the curves do not represent computed data, but rather represent arbitrary connections across regions in which the various approximate solutions are invalid.

The radiation cooling parameter ϵ is equal to the radiant flux leaving each side of a transparent, isenthalpic gas slab in which the nondimensional enthalpy takes the value one. Hence, this product

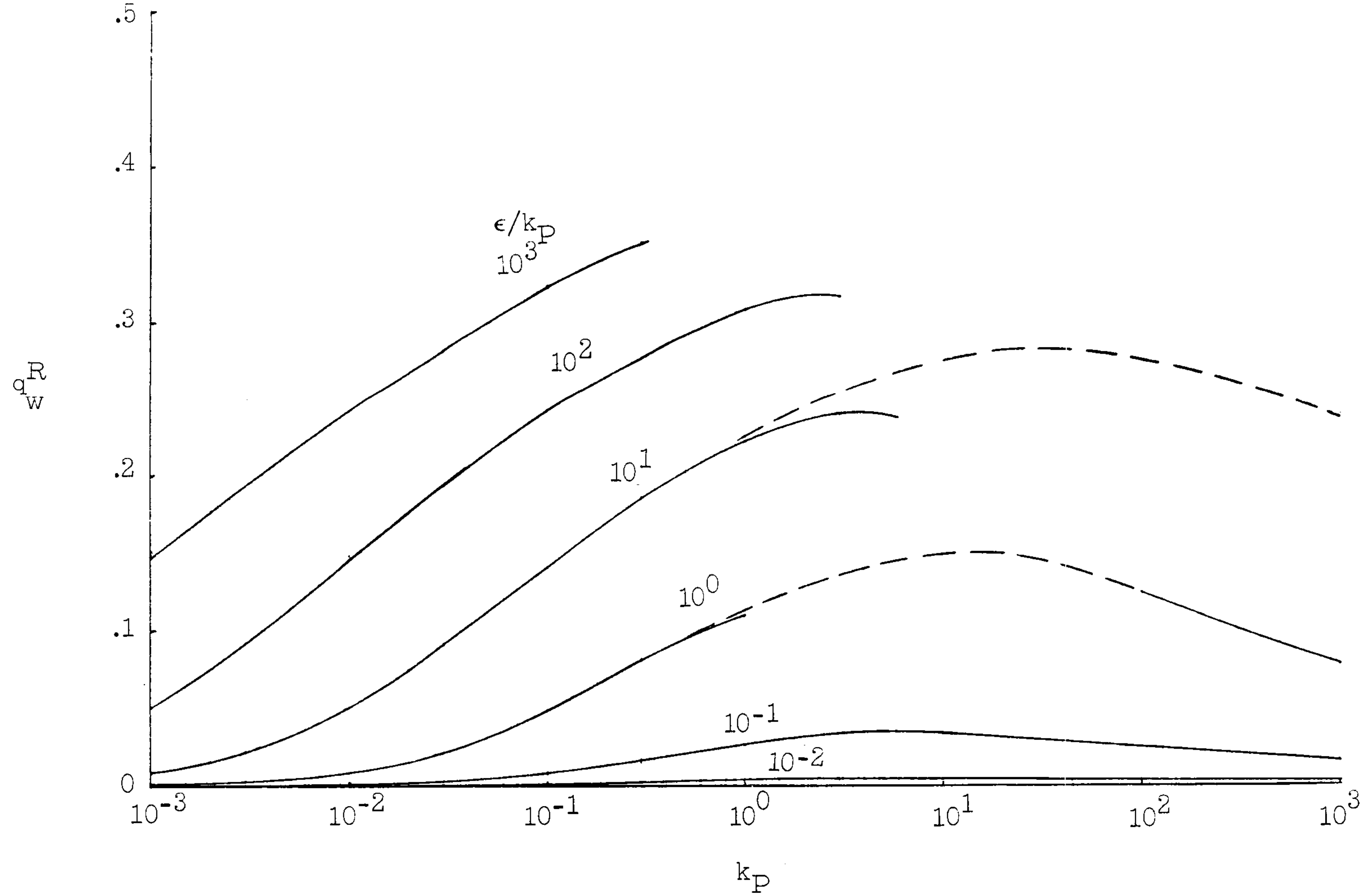

Figure 7.4.- Stagnation point radiant heating rate in a model entry environment with a gray absorption coefficient. $\dot{k}_P = 4$, $r_w = 0$.

represents an upperbound to the rate of radiant heat transfer to the stagnation point (or wall), q_w^R. When this product is small, the rate of energy loss through radiation is small, and the average intensity is only slightly perturbed from the isenthalpic value. However, as ϵ increases (the Bouguer number k_P remaining very much less than one) the increased energy lost by radiation is reflected in decreased levels of enthalpy and average intensity. Hence, q_w^R becomes a decreasing fraction of ϵ. Finally, as ϵ becomes very large, (k_P still small) nearly all of the energy is removed from the shock layer by radiation and q_w^R which represents the rate at which radiant energy leaves one side of the transparent layer, approaches the physical maximum of 1/2.

As k_P increases toward and beyond unity, absorption becomes important and this mechanism, which tends to inhibit radiant energy transfer, halts the increasing trend of q_w^R with k_P. As k_P continues to increase, the trend is reversed and q_w^R decreases and becomes asymptotic to zero. Consequently, the curves of rate of radiant heat transfer to the stagnation point q_w^R against Bouguer number k_P for constant values of the ratio ϵ/k_P have maximums the locations and heights of which depend on ϵ/k_P. It can be inferred from this that for every altitude and velocity in this simple model atmosphere, there is a finite value of nose radius for which the rate of radiant heat transfer to the stagnation point will be a maximum.

In order to obtain some understanding of the effects of radiation cooling, gray absorption, and spectral absorption of the rate of radiant heat transfer to the stagnation point a series of calculations utilizing various approximations were performed. The results of these calculations corresponding to a free-stream velocity of 14.2 km/sec and an altitude of 32.4 km are plotted against body nose radius R_N in meters in figure 7.5. The curve labeled 1 was computed by assuming that the shock layer was both isenthalpic and nonabsorbing. In this case the rate of radiant heat transfer to the stagnation point is given by the simple expression, $q_w^R = \epsilon$. This approximation was used in the early estimates of radiant heating (refs. 1 and 2). Curve number 2 was computed by assuming that the shock layer was isenthalpic and contained a gray, absorbing gas. The effect of gray absorption is seen to be small (under the conditions of this example) for a nose radius as large as 0.1 m. The third curve was obtained using the transparent approximation discussed in chapter IV. This assumption of a nonabsorbing but radiation cooled shock layer is frequently employed in the literature (see, for example, refs. 3-7). For this example, at least, the effect of radiation cooling is more important then the effect of gray absorption for nose radii of 0.1 m or less. Curve number 4 contains the effects of both radiation cooling and gray absorption. These combined effects are included in the numerical solutions of Howe and Veigas (ref. 9). It can be seen that for small nose radii (less than about 0.1 m) gray absorption has little effect. However, gray absorption plays an

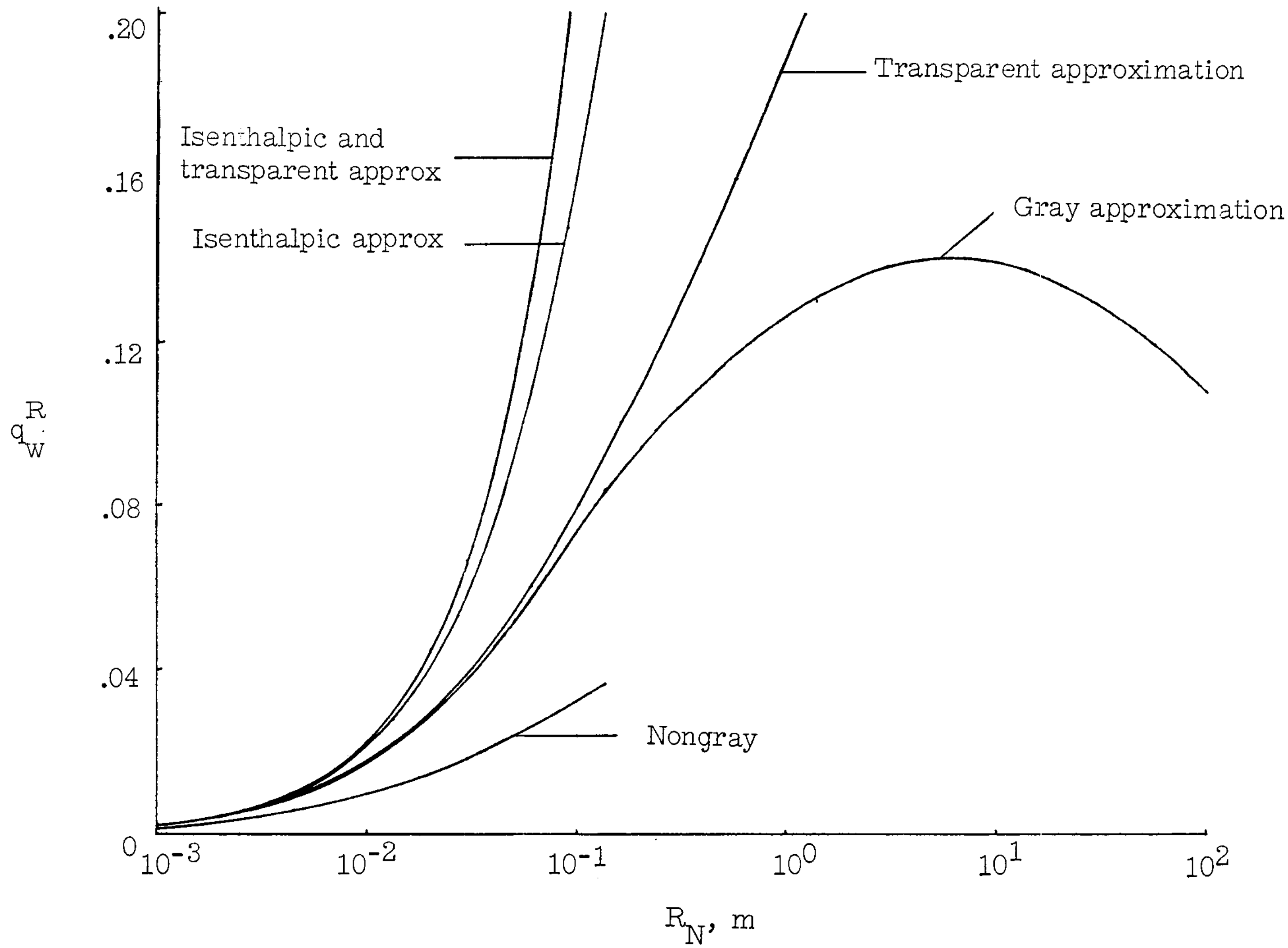

Figure 7.5.- The effect of body nose radius on the stagnation-point radiant heating rate. W_∞ = 14.2 km/sec, alt. = 32.4 km.

increasingly important role as the radius increases. The final curve, numbered 5, includes the combined effects of radiation cooling and nongray absorption. The absorption coefficient used in these calculations was the step function model introduced in chapter III (see fig. 3.10). The curve is limited to small values of nose radius because of the restricted region of validity of the small perturbation method with which this curve was computed. It is very apparent from these results that nongray effects cannot be ignored if one wishes to obtain a realistic evaluation of the radiant heating of objects during entry at hyperbolic velocities.

The analysis of this paper has been restricted to a shock layer with plane-parallel geometry. The largest effect of this assumption is felt in the calculation of the rate of radiant heat transfer. Koh (ref. 19) has shown that the plane-parallel geometry assumption can lead to an overestimation of q_w^R by no more than 15-percent when the gas is transparent to its own radiation and when the shock standoff distance to shock radius ratio is no greater than 0.05. As the Bouguer number k_P increases, the size of the error decreases and vanishes when the shock layer becomes optically thick. Because the effective optical thickness of a nongray shock layer is greater than that for a Planck equivalent gray gas, the error due to geometry will be smaller for a given Bouguer number in the more realistic nongray case.

D. Convective Heat Transfer

Even though the analysis of this investigation is based on the assumption that the gas in the shock layer is inviscid and nonheat conducting, it is possible to draw some conclusions regarding the coupling between radiant heat transfer and convection heating. The convective heating rate (sometimes referred to as the aerodynamic heating rate) is, in the case of a laminar boundary layer, the rate at which heat energy is transferred to the body surface by means of conduction.

To first order in the boundary layer parameter $Pe^{-1/2}$* (see section D of chapter II) the convective heating rate is proportional to the enthalpy difference across the conduction boundary layer. If the wall is cold (as has been assumed throughout this investigation the enthalpy of the wall can be neglected and the convective heating rate becomes proportional to the enthalpy at the outer edge of the boundary layer. The location of the outer edge depends upon the Peclét number. Since it has been assumed throughout this investigation that the viscous boundary layer is thin (in terms of both the Dorodnitsyn coordinate and the optical path length) the location of the edge of the viscous boundary layer will be arbitratily specified as $\eta/\eta_\Delta = 0.05$ for both the small perturbation and the transparent solutions. The rapid change in enthalpy near the wall, particularly for the transparent approximation which

---

*The inverse square root of the Peclét number.

gives a value of zero for the enthalpy of the gas adjacent to the wall, necessitates choosing an edge location other than zero. For the optically thick and radiation depleted shock layers, it is more convenient to specify the edge of the viscous boundary layer in terms of the normalized optical path length τ. The variation of enthalpy near the wall is quite small in the case of the radiation depleted shock layer. Consequently, the edge of the viscous boundary layer can be considered to be located at $\tau = 0$ for this case. A wall boundary layer due to radiation has been shown to exist in the optically thick shock layer. This wall boundary layer is always thicker than a photo mean free path, and, of course, is very much thicker than the optically thin viscous boundary layer. Therefore, $\tau = 0$ can be considered as the edge of the viscous boundary layer for this case also. Values of the enthalpy h_e at the edge of the viscous boundary layer have been determined from the four approximate solutions for a wide range of the ratio of the radiation cooling parameter to the Bouguer number ϵ/k_P and the Bouguer number k_P. The results are shown in figure 7.6. The dashed portions of the curves represent arbitrary connections across regions of nonvalidity.

The quantity h_e is a rough approximation to the ratio of the convective heating rate for a radiating shock layer to that for a nonradiating shock layer. When radiant energy transport is important, the convective heating is reduced from the radiationless value $(h_e = 1)$. The effect becomes larger as both ϵ/k_P increase. It is

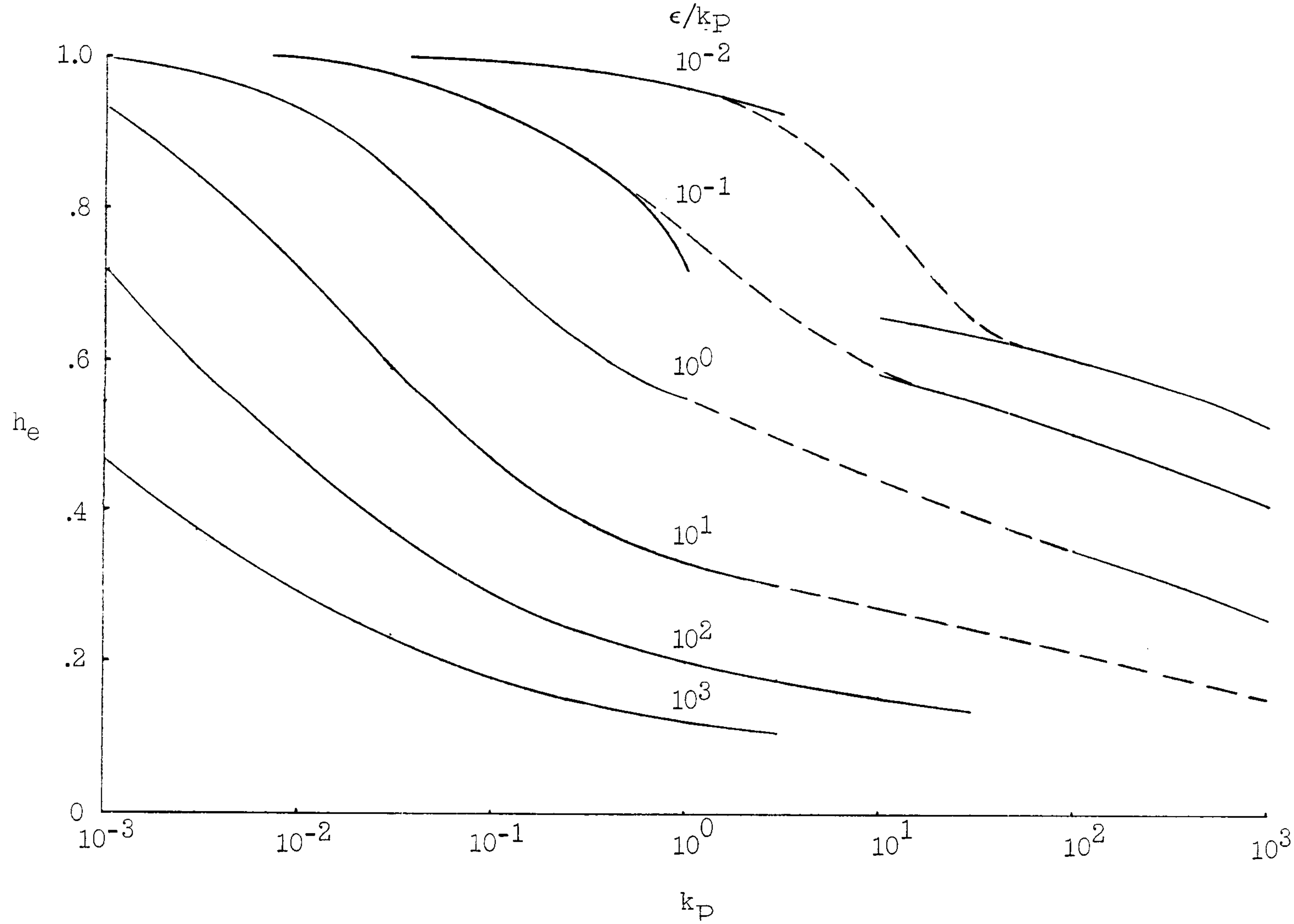

Figure 7.6.- The effect of radiant energy transport on convective heating.

interesting to note than the convective heating continues to decrease for increasing k_p even when the shock layer is optically thick and the rate of radiant heat transfer is decreasing as a result of absorption. Even though the total heating rate (radiant plus convective) cannot be deduced from an inviscid analysis, it is apparent that the total heating rate decreases with increasing shock layer optical thickness for all values of k_p at least as large as the value for maximum rate of radiant heat transfer to the stagnation point q_w^R.

Of course, the results of figure 7.6 only give an order-of-magnitude estimate of the radiation-convection heating coupling. Not included are the effects of variable transport properties, enthalpy gradient at the edge of the boundary layer, and differences in the characteristic Reynolds and Prandtl numbers between the radiating and nonradiating cases. Also no account has been taken of the effect of radiation in the boundary layer. In the cooled region of the boundary layer adjacent to the wall the gas will absorb more radiant energy than it will emit. This will tend to increase the slope of the enthalpy distribution adjacent to the wall thereby increasing the convective heat transfer somewhat.

The effects of radiation cooling, gray absorption, and spectral absorption on the ratio of convective heating rate for a radiating shock layer to that for a nonradiating shock layer, h_e, is shown in figure 7.7. It is apparent that radiation cooling plays the major role while absorption (both gray and nongray) tends to reduce the

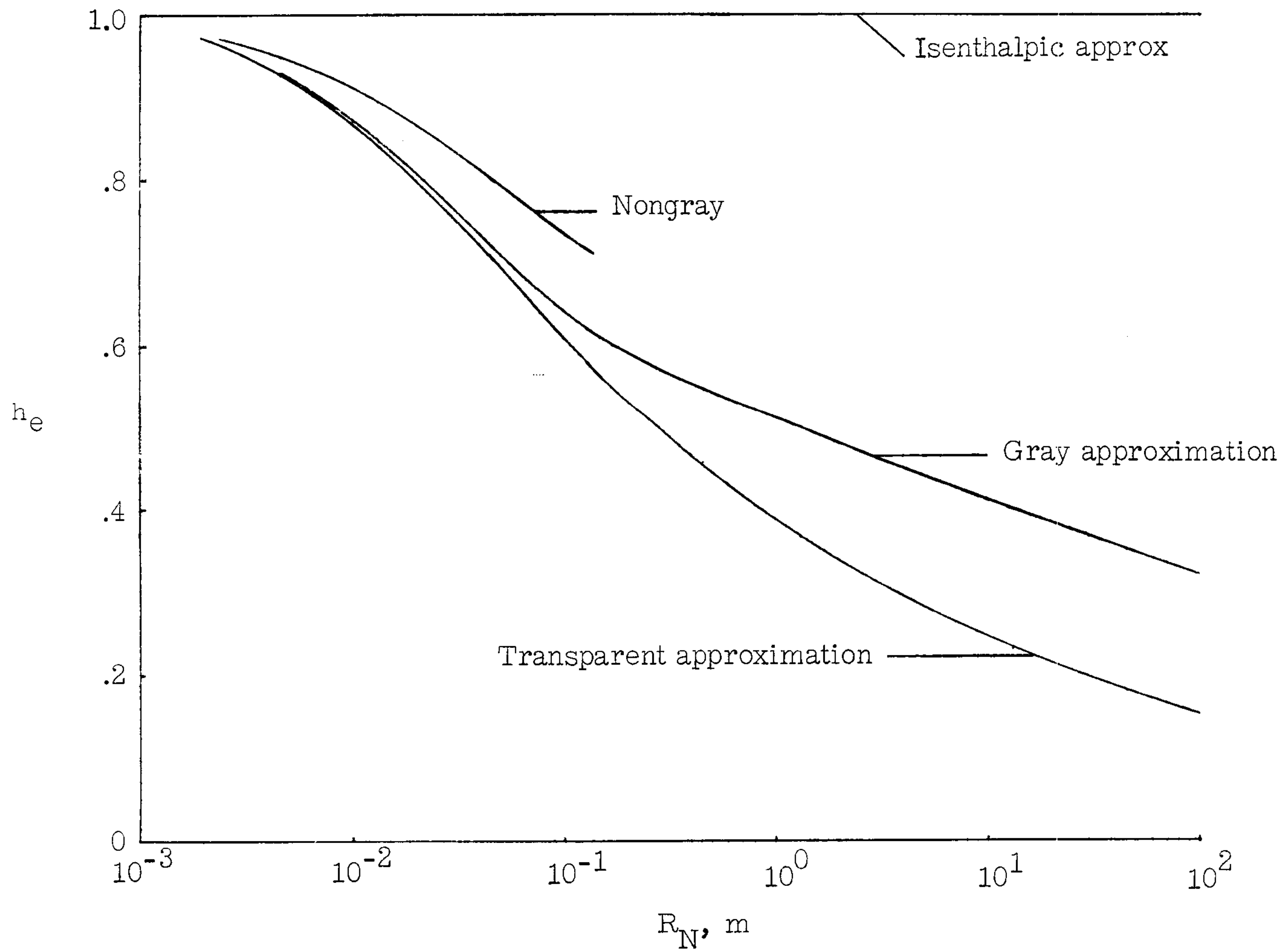

Figure 7.7.- The effect of body nose radius on the stagnation-point convective heating rate. W_∞ = 14.2 km/sec, alt. = 32.4 km.

effectiveness of radiation cooling. The calculations for curves 1 and 2 ignored cooling. Consequently, no reduction in the calculated value of the convective heating rate was obtained. Curve 3 includes radiation cooling and ignores absorption. Thus the reduction in the calculated value of the convective heating rate is maximized in this approximation. Finally curves 4 and 5 indicate that absorption inhibits the effectiveness of radiation cooling, and since absorption is more important in a nongray gas than it is in a Planck equivalent gray gas the rate of convective heating will be greater in the nongray case.

E. The Role of the Radiation Cooling Parameter and the Bouguer Number

The radiation cooling parameter ϵ admits of several physical interpretations which are useful in the understanding of the radiating shock layer. Of these, one of the most useful is the following:

$$\epsilon = \frac{\begin{pmatrix}\text{rate of emission from}\\ \text{element of volume of gas}\\ \text{emerging from shock}\end{pmatrix}\begin{pmatrix}\text{time required by element of}\\ \text{volume to traverse distance}\\ \Delta_A \text{ at rate of emergence from}\\ \text{shock}\end{pmatrix}}{2\ (\text{energy of element of volume upon emergence from shock})}$$

Here Δ_A is the shock standoff distance in a nonradiating (or adiabatic) flow.

It can be seen from this interpretation that the radiation cooling parameter is indicative of the slope of the enthalpy distribution immediately behind the shock. In fact, in the transparent limit there is a direct relation between ϵ and the initial slope. That is,

$$dh/d\left(\eta/\eta_{\Delta}\right) = 2\epsilon$$

(see, for example, chapter IV, figure 4.2)

In the case of an optically thick shock layer, the initial enthalpy gradient is reduced by absorption. However, a lower bound to the gradient is the value ϵ (one-half the transparent value) because the emergent elemetary volume will emit at least twice as much energy as it absorbs; it emits energy at a rate proportional to the Planck function at the equilibrium shock temperature, T_s, in both the upstream and downstream directions while it absorbs energy at a rate at most proportional (by the same factor; the monochromatic volume absorption coefficient) to the Planck function at temperature T_s from only the downstream side.

A physical interpretation of the Bouguer number is given below:

$$k_P = \frac{\left(\text{radiationless shock standoff distance, } \Delta_A\right)}{\left(\begin{array}{l}\text{Planck average photon mean free path in gas emerging} \\ \quad\text{from shock}\end{array}\right)}$$

Only when conditions do not vary greatly across the shock layer will the Bouguer number be indicative of the Planck mean optical thickness and only when the gas is nearly gray will the Planck mean optical thickness be indicative of the various important monochromatic optical thicknesses. Consequently, critical values of the Bouguer number are subject to a number of influences; among them, the enthalpy and spectral variation of the absorption coefficient and the value of the radiation cooling parameter. For example, the value of k_p for which absorption first becomes important is about 0.1, when the radiation cooling parameter is very much less than one and the absorption coefficient is independent of wavelength. When the absorption coefficient varies spectrally as shown in figure 3.10, chapter III, and when ϵ is very small, absorption begins to become important for Bouguer numbers as small as 0.001. With ϵ about 10 for a gray gas absorption is important for values of the Bouguer number greater than about three. Dispite these drawbacks, the Bouguer number as defined in this investigation is about the best a priori indicator of the importance of absorption that can be obtained.

When the radiation cooling parameter ϵ is very much less than one, an elementary volume of gas will lose very little of its energy by radiant emission in the time required to traverse most of the shock layer (of course, it takes an elementary volume of gas travelling along the stagnation streamline an infinite time to reach the wall). Hence, radiation cooling of the shock layer will be slight. When the radiation cooling parameter is very much greater than one, an elementary volume of gas will emit energy at such a rapid rate that the energy of the volume will be reduced a significant amount before it leaves the vicinity of the shock.

This is true whether the shock layer is optically thick or optically thin (that is, regardless of the size of the Bouguer number). This physical argument is used to establish the existance of the thermal boundary layer behind the shock in the radiation depleted shock layer (chapter VI). If the shock layer is optically thick, the reduction in enthalpy will continue only so long as the elementary volume is within about a photon mean free path of the shock. Beyond this point, the elementary gas volume receives radiation from all sides and begins to establish a condition of radiative equilibrium with its surroundings. The energy lost during the time required by the elementary volume to travel a single photon mean free path is characterized by the ratio of the radiation cooling parameter to the Bouguer number, ϵ/k_P (it was shown in chapter V that the enthalpy level in the interior of an optically thick shock layer was characterized solely by the parameter, ϵ/k_P).

Within the interior of an optically thick shock layer, radiation heat transfer can be treated in a manner analogous to conductive heat transfer. Thus, one would expect that a parameter analogous to the Peclét number could be constructed which would suggest the nature of the enthalpy boundary layer adjacent to the wall. Such a parameter, which is a ratio of the importance of convective to radiative heat transfer is given by the grouping k_P^2/ϵ.* Since the thickness of the enthalpy boundary layer is characterized by $Pe^{-1/2}$ in the conduction problem, one expects, by analogy, the thickness of the enthalpy boundary layer adjacent to the wall in an optically thick radiating shock layer to be characterized by $\epsilon^{1/2}/k_P$. The importance of this parameter (in a somewhat different form) and its analogy with the Peclét number was pointed out previously by Goulard (ref. 21).

The importance of the surface reflectivity, r_w, depends on the importance of absorption in the shock layer. When absorption is negligible, the effects of surface reflectivity are negligible because all photons originating within the shock layer will escape the layer and it matters not whether some of these photons are absorbed by the cold wall or reflected by the wall into the free stream. However, when absorption is important, the reflected photons have a large probability of being recaptured in the shock layer. Thus, an increase in surface reflectivity tends to raise the enthalpy level of an absorbing gas in the vicinity of the wall.

In this section it was shown that both the radiation cooling parameter ϵ and the Bouguer number k_P play prominent and inter-related roles in determining the character of the radiating shock

---

*In the optically thick shock layer analysis of chapter V the gas was assumed to be gray. Thus the fact that the Bouguer number was based on a Planck mean absorption ceofficient was of no consequence. However, in the case of a nongray gas, it would probably be more correct to use a Bouguer number based on a Rosseland mean absorption coefficient.

layer. Further, it was shown that the spectral variation of the absorption coefficient greatly influences the role of the Bouguer number. In general, then, one cannot ignore either of the processes of radiation cooling and nongray absorption.

CHAPTER VIII

SUMMARY AND CONCLUSIONS

A mathematical model for the stagnation region of a radiating shock layer was derived in this investigation subject to the following conditions: (1) the gas in the shock layer is in local thermodynamic and chemical equilibrium, (2) the body geometry is axisymmetric, (3) there is no mass addition to the flow from the body surface, (4) the thicknesses of the shock and the viscous boundary layer are small in comparison to the shock standoff distance, and (5) absorption in the free stream ahead of the body is negligible. The divergence of the radiant flux vector, which appears in the energy equation, was formulated to include a wavelength varying absorption coefficient. The body surface was considered to be cold and to reflect diffusely and independently of wavelength a fraction r_w of the incident radiation. The results of a boundary layer analysis indicate that the equations for the flow in the inviscid region are independent of the boundary layer equations only when the boundary layer is optically thin or optically thick. It has been assumed throughout this study that the boundary layer is optically thin. Simple correlation formulas for the thermodynamic and optical properties of high temperature equilibrium air were developed and used herein.

The general form of the governing system of equations was found to be integrodifferential in character. The solution of this system is extremely difficult to find even with numerical techniques and high speed electronic computing machines. The approach of this investigation was to take advantage of the simplified form to which the governing equations were reduced when the radiation cooling parameter ϵ and the Bouguer number k_P took on limiting values and obtain approximate analytic solutions if available. It was found that the general problem reduced to a singular perturbation problem in each of the four cases studied. A small perturbation solution valid when the energy lost to the shock layer by radiation is small (i.e., when the radiation cooling parameter is small) is described in chapter III. The Poincare-Lighthill-Kuo perturbation of coordinate method was used to obtain a uniformly valid solution. This solution was used to study radiation cooling, absorption, effects of surface reflectivity, and effects of nongray optical properties.

An optically thin shock layer method of solution, discussed in chapter IV, utilizes an expansion in terms of the Bouguer number k_P to reduce the governing system to purely differential form. Again it was necessary to resort to the P-L-K method to obtain a uniformly valid solution. This solution was used to study radiation cooling, absorption, and the effects of surface reflectivity.

The optically thick approximation, valid when the optical thickness of the shock layer is very large (i.e., the Bouguer number very much greater than 1) was used to obtain the solutions of chapter V. The governing equations were reduced to differential form through the use of a substitute kernal approximation. Two thermal boundary layers were seen to exist; one adjacent to the shock and the other adjacent to the wall. It was noted that the Rosseland approximation together with a properly specified temperature jump or slip condition at the wall reduces the governing equations to the same form as the substitute kernal approximation in the interior or isenthalpic portion of the shock layer and in the wall boundary layer. However, the Rosseland approximation with slip conditions was found to be inadequate for analyzing the shock boundary layer. The optically thick solutions were restricted to gray gases but were used to study radiation cooling, absorption, and the effects of surface reflectivity.

The radiation depleted shock layer was analyzed in chapter VI. This approximation is valid when the rate at which energy is radiated away from the shock layer is nearly equal to the rate at which energy enters the shock layer (i.e., the radiation cooling parameter is very large) so that the enthalpy level is very much less than the radiationless value. The substitute kernal approximation was used to reduce the governing system of equations to differential form. The method of matching of inner and outer expansions was used to obtain solutions valid in the thermal boundary layer adjacent to the shock and in the interior of the shock layer. These solutions were restricted to gray gases but were used to study radiation cooling, absorption and the effects of surface reflectivity.

It is apparent from the results presented in chapters III through VI, that radiation cooling first becomes important when the rate of energy lost by radiation from the shock layer is only about 1 percent of the rate with which energy enters the shock layer. Absorption in a gray gas begins to become important for shock layer optical thicknesses greater than about one-tenth. An increase in the surface reflectivity r_w from zero reduces the radiant heat transfer by a factor of roughly $1 - r_w$, and increases the heat transfer rate to the wall by conduction because of an increase in enthalpy level near the wall.

The results of some nongray calculations are presented in chapter III. The Planck mean absorption coefficient can be used to compute the enthalpy distribution and the radiation heat transfer rate to the wall as long as the optical depth of the shock layer is very much less than 1 in all wavelength regions in which a significant amount of radiant energy is emitted. For larger optical thicknesses nongray effects are very important.

The various approximate solutions were used to compute the rate of radiant heat transfer to the stagnation point of blunt objects traversing an optically gray model earth atmosphere. The results of this computation indicate that at every altitude and velocity there is a finite value of body nose radius for which the rate of radiant heat transfer to the stagnation point is a maximum (this result is contrary to the earlier results, based on the assumptions of an isenthalpic and transparent shock layer, which indicated that the heating rate was directly proportional to nose radius). A significant reduction in the computed value of the radiant heating resulted upon taking the nongray character of air into account. This served to emphasize that the nongray character of gases plays a very real and important part in problems of radiation gas dynamics.

In general, the coupling between radiant and convective heat transfer is such that increases in the rate of radiant heat transfer result in decreases in the rate of convective heat transfer to the body surface. Of course, the amount by which the total heating rate is affected cannot be determined from this inviscid analysis.

It is hoped that the methods used in this investigation will point the way to simplified methods for treating the general problem. For example, the study of nongray absorption coefficients by means of the small perturbation method may lead to the difinition of an approximate mean absorption coefficient through which the general nongray problem can be reduced to an equivalent gray problem. As was pointed out previously (chapters V and VI) the integrodifferential system of governing equations for gray gases can then be reduced to purely differential form through the use of the substitute kernal method or other available methods (see for example, refs. 34 and 53).

Obviously such simplifications are urgently needed if current analyses are to be extended to include the important effects of chemical nonequilibrium, absorption in the free stream ahead of the shock, and the injection of foreign species into the shock layer due to ablation of the body surface.

REFERENCES

1. Kivel, B.: Radiation From Hot Air and Stagnation Heating, Avco-Everett Research Report 79, 1959.

2. Yoshikawa, K. K.; and Wick, B. H.: Radiative Heat Transfer During Atmospheric Entry at Parabolic Velocity, NASA Technical Note D-1074, 1961.

3. Goulard, R.: The Coupling of Radiation and Convection in Detached Shock Layers, Jour. of Quant. Mol. Spectros. Rad. Transfer, Vol. 1, 1961, pp. 249-257.

4. Lunev, V. V.; and Murzinov, I. N.: The Effect of Radiation on the Flow in the Neighborhood of the Stagnation Point of a Blunt Body. Zhurnal Prikladnoi Mekhaniki i Technicheskoi Fiziki, Vol. 1, No. 2, Mar.-Apr., 1961, pp. 26-30.

5. Goulard, R.: Preliminary Estimates of Radiative Transfer Effects on Detached Shock Layers. AIAA Jour., Vol. 2, No. 3, Mar. 1964. pp. 494-502.

6. Hanley, G. M.; and Korkan, K. D.: Approximate Inviscid, Nonadiabatic Stagnation Region Flow Field Solution, AIAA Jour., Vol. 3, No. 8, August 1965.

7. Wilson, K. H.; and Hoshizaki, H.: Inviscid Nonadiabatic Flow About Blunt Bodies, AIAA Aerospace Sciences Meeting, New York, N.Y., Jan. 20-22, 1964. Reprint No. 64-70.

8. Yoshikawa, K. K.; and Chapman, D. R.: Radiative Heat Transfer and Absorption Behind a Hypersonic Normal Shock Wave. NASA TN D-1424, 1962.

9. Howe, John T.; and Viegas, John R.: Solutions of the Ionized Radiating Shock Layer, Including Reabsorption and Foreign Species Effects and Stagnation Region Heat Transfer. NASA TR R-159, 1963.

10. Fay, J. A.; Moffatt, W. C.; and Probstein, R. F.: An Analytical Study of Meteor Entry, AIAA Jour., Vol. 2, No. 5, May 1964, pp. 845-854.

11. Lick, W. J.: Energy Transfer by Radiation and Conduction. Proceedings of the 1963 Heat Transfer and Fluid Mechanics Institute, Stanford University Press, pp. 14-26.

12. Greif, R.: Energy Transfer by Radiation and Conduction With Variable Properties. International Jour. of Heat and Mass Transfer, Vol. 7, No. 8, Aug. 1964, p. 891.

13. Goulard, R.: Fundamental Equations of Radiation Gas Dynamics, The High Temperature Aspects of Hypersonic Flow. Pergamon Press. pp. 529-554.

14. Cohen, N. B.: Correlation Formulas and Tables of Density and Some Transport Properties of Equilibrium Dissociating Air for Use in Solutions of the Boundary Layer Equations. NASA TN D-194, 1960.

15. Kivel, B.; and Mayer, H.: Opacity of Highly Ionized Air, Jour. Quant. Spectrosc. Radiat. Transfer., Vol. 5, (1965), pp. 13-38.

16. Vaglio-Laurin, R.; and Ferri, A.: Theoretical Investigation of the Flow Field About Blunt Nosed Bodies in Supersonic Flight, Jour. Aerospace Sciences. 25, 1958, 761.

17. Gravalos, F. G.; Edelfelt, I. H.; and Emmons, H. W.: The Supersonic Flow About a Blunt Body of Revolution for Gases at Chemical Equilibrium, Ninth International Astronautical Congress, Springer Verlag, Vienna, Vol. 1, 1959, pp. 312-332.

18. Hayes, W. D.; and Probstein, R. F.: Hypersonic Flow Theory, Academic Press, Inc., New York, 1959.

19. Koh, J. C. Y.: Radiation From Nonisothermal Gases to the Stagnation Point of a Hypersonic Blunt Body, ARS Jour., Vol. 32, Sept. 1962, pp. 1374-1377.

20. Goulard, R.: One-Dimensional Energy Transfer in Radiant Media. Inst. J. Heat Mass Transfer, Vol. 1, Pergamon Press, 1960. pp. 81-91.

21. Goulard, R.: Similarity Parameters in Radiation Gas Dynamics, Proceedings of the International Symposium on High Temperature in Aeronautics, edited by C. Ferrari (Pergamon Press, New York, 1963).

22. Penner, S. S.; Thomas, M.; and Adomeit, G.: Similarity Para-Meters for Radiative Energy Transfer in Isothermal and Non-Isothermal Gas Mixtures, California Institute of Technology Technical Report No. 1, 1962.

23. Krook, M.: Structure of Stellar Atmospheres II. Astrophysical Jour., Vol. 129, 1959, pp. 724-733.

24. Stone, P. H.: Approximate Integral Equations for the Temperature in Non-Gray Model Atmospheres. The Astrophysical Jour., 137, No. 2, Feb. 1963.

25. Carrier and Avrett: A Non-Grey Radiative Transfer Problem. The Astrophysical Jour., Vol. 134, No. 2, Sept. 1961.

26. Krook, Max : A Perturbation Method for Non-Gray Stellar Atmospheres, The Astrophysical Jour., Vol. 137, No. 3, Apr. 1963.

27. Rhyming, I. L.: Effects of Non-Grey Radiation on Wave Propagation in a Simple Dissociating Flow. Aerospace Corp. SSD-TDR-63-355.

28. Kourganoff, V.: Basic Methods in Transfer Problems. Dover Publications, Inc.

29. Krook, M.: On the Solution of Equations of Transfer I. The Astrophysical Journal, 1955, 122, 488.

30. Clarke, J. F.: Radiation-Resisted Shock Waves. Stanford University Dept. Aeronaut. and Astronaut., Rpt. SUDAER (2) Feb. 1962.

31. Heaslet, M. A.; and Baldwin, B. S.: Predictions of the Structures of Radiation-Resisted Shock Waves. (To be submitted to the "Physics of Fluids.")

32. Traugott, S. C.: A Differential Approximation for Radiative Transfer with Application to Normal Shock Structure. Proceedings of the 1963 Heat Transfer and Fluid Mechanics Institute, Stanford University Press. pp. 1-13.

33. Thomas, P. D.: Transparency Assumption in Hypersonic Radiative Gas Dynamics, AIAA Jour., Vol. 3, No. 8, August 1965.

34. Viskanta, R.: Interaction of Heat Transfer by Conduction, Convection, and Radiation in a Radiating Fluid. Jour. of Heat Transfer, Transactions of the ASME, Nov. 1963.

35. Probstein, R. F.: Radiation Slip. Fluid Mechanics Laboratory, Dept. of Mech. Eng'g., M.I.T., Feb. 1963.

36. Van Dyke, M.: Perturbation Methods in Fluid Mechanics, Academic Press, New York, 1964.

37. Hayes, W. D.: Some Aspects of Hypersonic Flow. The Ramo-Wooldridge Corp., Jan. 4, 1955.

38. Li, T. Y.; and Geiger, R. E.: Stagnation Point of a Blunt Body in Hypersonic Flow. Jour. Aero. Sci. 24, 1957. pp. 25-32.

39. Kaatari, G. E.: Predicted Shock Envelopes About Two Types of Vehicles at Large Angles of Attack. NASA Technical Note D-860, 1961.

40. Staff of the Chance Vought Research Center: The Thermodynamic Properties of High Temperature Air. Chance Vought Research Center, Dallas, Texas, Report No. RE-1R-14.

41. Kivel, B.; and Bailey, K.: Tables of Radiation From High Temperature Air, Avco Res. Lab. Res. Report 21, 1957.

42. Gilmore, F. R.: Approximate Radiation Properties of Air Between 2,000 and 8,000° K, Rand Corp, Memorandum (RM-3997-ARPA), Mar. 1964.

43. Armstrong, B. H.; Sokoloff, J.; Nichols, R. W.; Holland, D. H.; and Meyrott, R. E.: Radiative Properites of High Temperature Air, J. Quant. Spectry. Radiative Transfer 1, 143-162 (1961).

44. Sewell, K. G.: The Radiative Properties of Air in Thermodynamic Equilibrium. LTV Research Center, Report No. 0-7100/2R-26, July 1962.

45. Nardone, M. C.; Breene, R. G.; Zeldin, S. S.; and Reithof, T. R.: Radiance of Species in High Temperature Air, G. E. Space Sciences Lab. R63SD3, June 1963.

46. Hahne, G. E.: The Vacuum Ultraviolet Radiation from N^+-O^+-Electron Recombination in High Temperature Air. NASA TND-2794, 1965.

47. Tsein, H. S.: "The Poincare-Lighthill-Kuo Method", Advances in Applied Mechanics, Vol. 4, 1954.

48. Pritulo, M. F.: On the Determination of the Uniformly Accurate Solutions to Differential Equations by Means of the Method of the Perturbation Coordinates, Prikladnoya Matematika i Mekhanika OTN, Vol. 26, No. 3. Honeywell Military Products Group translation. May-June, 1962, p. 444-448.

49. Viskanta, R.: Concerning the Definition of the Mean Absorption Coefficient, Int. J. Heat Mass transfer, Vol. 7, pp. 1047-1049, 1964.

50. Pearson, W. E.: On the Direct Solution of the Governing Equations for Radiation-Resisted Shock Waves, NASA TN D-2128, 1964.

51. Deissler, R. G.: Diffusion Approximation for Thermal Radiation in Gases with Jump Boundary Condition, (Prepared for Journal of Heat Transfer) (X63-11216).

52. Adrianov, V. N.; and Polyak, G. L.: Differential Methods for Studying Radiant Heat transfer, Int. J. Heat Mass Transfer, Vol. 6, pp. 355-362, 1963.

53. Thomas, M.; and Rigdon, W. S.: A Simplified Formulation for Radiative transfer, AIAA Journal, Vol. 2, No. 11, pp. 2052-2054, 1964.

54. Carrier, G. F.: Boundary Layer Problems in Applied Mechanics, Advances in Appl. Mech., Vol. III, Academic Press, N.Y., 1953.

55. Ince, E. L.: Ordinary Differential Equations, Dover Publication, Inc., 1956.

APPENDIX A

THE VISCOUS BOUNDARY LAYER

In this appendix, a boundary layer analysis will be performed on the integro-differential system (2.51) to (2.58) to determine the form of the equations in the inviscid region and the viscous boundary layer and to determine under what conditions such a separation can be achieved. For convenience, the system will be rewritten here

$$f(\eta)\, h'(\eta) + \lambda^2 \left[\mathcal{F}_1(h)\, h'(\eta)\right]' + \epsilon I\left[\eta\right] = 0 \qquad \text{(A-1)}$$

$$2\lambda^2 \left[\mathcal{F}_2^*(h)\, f''(\eta)\right]' + 2f(\eta)\, f''(\eta) - \left[f(\eta)\right]^2 + a^2 h(\eta) = 0 \qquad \text{(A-2)}$$

$$f(0) = 0 \qquad \text{(A-3)}$$

$$f'(0) = 0 \qquad \text{(A-4)}$$

$$f\left(\eta_\Delta\right) = 1 \qquad \text{(A-5)}$$

$$f'\left(\eta_\Delta\right) = \frac{a}{\sqrt{2X(1 - X)}} \qquad \text{(A-6)}$$

$$h(0) = h_w \qquad \text{(A-7)}$$

$$h\left(\eta_\Delta\right) = 1 \qquad \text{(A-8)}$$

where

$$\epsilon = \Gamma\rho_s \, \kappa_{P_s} \, \Delta_A \tag{A-9}$$

$$\mathcal{F}_2^*(h) = Pr_s \, \mathcal{F}_2(h) \tag{A-10}$$

and λ, introduced here for convenience of notation, is the inverse square root of the Peclet number.

When the parameter λ is very much less than one, a perturbation type solution can be attempted. However, the energy and momentum equations each lose the most highly differentiated term as λ vanishes. As a result, neither the zero-order (in the small parameter λ) solution for $f(\eta)$ nor that for $h(\eta)$ can satisfy all the boundary conditions. In particular, the conditions $f'(0) = 0$ and $h(0) = 0$ must be relaxed, and the perturbation solution will not be valid as η approaches zero. Thus, this problem is a singular perturbation problem of the "boundary layer" type (refs. 36 and 54).

In order to obtain the boundary layer form of the equations, the "stretched" coordinate $\xi = \lambda^{-\alpha}\eta$ is introduced where α is an as yet undetermined constant. It is also convenient, to avoid confusion, to introduce the change in notation

$$i(\xi) = h(\eta) \tag{A-11}$$

$$g'(\xi) = f'(\eta) \tag{A-12}$$

$$J[\xi] = I[\eta] \tag{A-13}$$

(A-12) is written in this particular form because it is $f'(\eta)$ and not $f(\eta)$ which fails to satisfy the boundary condition at $\eta = 0$.

When the stretched coordinate ξ and the definitions (A-11) to (A-13) are introduced into system (A-1) through (A-8), the only choice for α which will retain the most highly differentiated terms without loss of the most significant terms in the "unstretched" problem is $\alpha = 1$. Thus, λ and not λ^2 is the significant small parameter and the stretched coordinate is

$$\xi = \lambda^{-1}\eta \tag{A-14}$$

Perturbation solutions are now sought in the forms

$$i(\xi,\lambda) = \sum_{n=0}^{\infty} \lambda^n \, i_n(\xi) \tag{A-15}$$

$$g(\xi,\lambda) = \sum_{n=0}^{\infty} \lambda^n \, g_n(\xi) \tag{A-16}$$

in the boundary layer, and

$$h(\eta,\lambda) = \sum_{n=0}^{\infty} \lambda^n \, h_n(\eta) \tag{A-17}$$

$$f(\eta,\lambda) = \sum_{n=0}^{\infty} \lambda^n \, f_n(\eta) \tag{A-18}$$

in the inviscid region.

It shall be assumed that all functions of h (and i) are analytic about the value h_o (and i_o) so that they may be expanded in Taylor series about $h = h_o$ and $i = i_o$ in the following manner:

$$F(h) \equiv F\left[h_o + \lambda h_1 + \lambda^2 h_2 + \cdots\right] = F(h_o) + \lambda\dot{F}(h_o)h_1 + \lambda^2\left[\dot{F}(h_o)h_2 + \frac{1}{2}\ddot{F}(h_o)h_1^2 + \cdots\right] \tag{A-19}$$

The existance of the expansions

$$I[\eta,\lambda] = \sum_{n=o}^{\infty} \lambda^n I_n[\eta] \tag{A-20}$$

$$J[\xi,\lambda] = \sum_{n=o}^{\infty} \lambda_n J_n[\xi] \tag{A-21}$$

$$a = \sum_{n=o}^{\infty} \lambda^n a_n \tag{A-22}$$

$$\eta_\Delta = \sum_{n=0}^{\infty} \lambda^n \eta_{\Delta_n} \tag{A-23}$$

is also assumed without, for the present, specifying details of the terms $I_n[\eta]$ and $J_n[\xi]$.

Furthermore, to insure compatibility of the boundary layer and inviscid solutions, it is necessary that the inner boundary condition on the outer solution be written in the form

$$f(\delta) = 0 \tag{A-24}$$

where δ (the displacement distance) is specified by the matching condition

$$\lim_{\xi \to \infty} g(\xi) = \lambda^{-1} f(\eta) \tag{A-25}$$

The quantity δ depends on λ and must be written in expanded form

$$\delta = \sum_{n=1}^{\infty} \lambda^n \delta_n \tag{A-26}$$

The term δ_o was chosen to be zero because δ is order λ.

The system which describes the solutions valid in the inviscid region can be obtained by substituting expansions (A-17) - (A-23), and (A-26) into system (A-1) - (A-8). The result is an infinite power series in λ the sum of which is zero for all values of λ. The only such series is one for which the coefficient of each of the λ^n terms is identically zero. These coefficients yield a set of recursive integro-differential systems. The system of zero order is

$$f_o(\eta)\ h_o'(\eta) + \epsilon I_o[\eta] = 0 \tag{A-27}$$

$$2f_o(\eta)\ f_o''(\eta) - \left[f_o'(\eta)\right]^2 + a_o^2\ h_o(\eta) = 0 \tag{A-28}$$

$$f_o(0) = 0 \tag{A-29}$$

$$f_o\left(\eta_{\Delta_o}\right) = 1 \tag{A-30}$$

$$f_o'\left(\eta_{\Delta_o}\right) = \frac{a_o}{\sqrt{2X(1 - X)}} \tag{A-31}$$

$$h_o\left(\eta_{\Delta_o}\right) = 1 \tag{A-32}$$

The system which describes the solutions valid in the boundary layer can be obtained by substituting expansions (A-15), (A-16), and (A-19) - (A-23) into system (A-1) - (A-8). As for the inviscid case, this procedure results in a set of differential systems. The zero-order system is

$$\left[\mathcal{F}_1\left(i_o\right)\ i_o'(\xi)\right]' + g_o(\xi)\ i_o'(\xi) + \epsilon J_o[\xi] = 0 \tag{A-33}$$

$$2\left[\mathcal{F}_2^*\left(i_o\right) g_o''(\xi)\right]' + 2g_o(\xi)\, g_o''(\xi) - \left[g_o'(\xi)\right]^2 + a_o^2\, i_o(\xi) = 0$$

(A-34)

$$g_o(0) = 0 \qquad \text{(A-35)}$$

$$g_o'(0) = 0 \qquad \text{(A-36)}$$

$$\lim_{\xi \to \infty} g_o'(\xi) = f_o'(0) \qquad \text{(A-37)}$$

$$i_o(0) = h_w \qquad \text{(A-38)}$$

$$\lim_{\xi \to \infty} i_o(\xi) = h_o(0) \qquad \text{(A-39)}$$

The first-order term of the displacement distance δ_1, is found from the matching condition

$$\lim_{\xi \to \infty} g_o(\xi) = \left(\xi - \delta_1\right) f_o'(0) \qquad \text{(A-40)}$$

It is apparent that the zero-order solution for the boundary layer equations depends only on the inviscid enthalpy level in the vicinity of the wall and not the enthalpy gradient. The enthalpy gradient will, of course, have an effect on the first order boundary layer solution. Thus, if the enthalpy gradient is very large, as it can be for a radiating shock layer, the boundary layer solutions must be carried out to first order in λ.

The divergence of the radiation flux (see eq. (2.63)) includes integrals which extend over the whole domain of the problem. It is convenient to separate each of these integrals into two integrals as follows:

$$\int_0^{\tau_{\lambda_\Delta}} B_\lambda\left(t_\lambda\right) E_1\left(k_P\left|\tau_\lambda - t_\lambda\right|\right) dt_\lambda = \int_{\tau_\lambda^*}^{\tau_{\lambda_\Delta}} B_\lambda\left[h\left(t_\lambda\right)\right] E_1\left(k_P\left|\tau_\lambda - t_\lambda\right|\right) dt_\lambda$$
$$+ \int_0^{\sigma_\lambda^*} B_\lambda\left[i\left(s_\lambda\right)\right] E_1\left(k_P\left|\tau_\lambda - \lambda s_\lambda\right|\right) ds_\lambda \tag{A-41}$$

and

$$\int_0^{\tau_{\lambda_\Delta}} B_\lambda\left(t_\lambda\right) E_2\left(k_P\, t_\lambda\right) dt_\lambda = \int_{\tau_\lambda^*}^{\tau_{\lambda_\Delta}} B_\lambda\left[h\left(t_\lambda\right)\right] E_2\left(k_P\, t_\lambda\right) dt_\lambda$$
$$+ \lambda \int_0^{\sigma^*} B_\lambda\left[i\left(s_\lambda\right)\right] E_2\left(k_P\, \lambda s_\lambda\right) ds_\lambda \tag{A-42}$$

where

$$\tau_\lambda^* = \lambda\sigma_\lambda^* = \lambda \int_0^{\xi^*} k_\lambda(i)\, d\xi \tag{A-43}$$

is the monochromatic optical thickness of the boundary layer. ξ^* is the thickness of the boundary layer in terms of the stretched Dorodnitsyn variable ξ.

It is convenient to redefine the monochromatic optical path length as

$$\tau_\lambda = \begin{cases} \lambda \displaystyle\int_0^{\xi} \kappa_\lambda(i)d\xi; \quad \text{for} \quad \tau_\lambda \leq \tau_\lambda^* & \text{(A-44)} \\ \\ \displaystyle\int_{\lambda\xi^*}^{\eta} \kappa_\lambda(h)d\eta + \tau_\lambda^*; \quad \text{for} \quad \tau_\lambda > \tau_\lambda^* & \text{(A-45)} \end{cases}$$

In order to expand equation (2.63) as a power series in λ, it is necessary to expand the exponential integral functions and all functions of h (and i) as well. Expanding the optical thickness yields, for $\tau_\lambda \leq \tau_\lambda^*$

$$\tau_\lambda = \lambda\sigma_\lambda = \lambda \int_0^{\xi} \kappa_\lambda\left(i_o\right)d\xi + \lambda^2 \int_0^{\xi} i_1(\xi)\dot{\kappa}_\lambda\left(i_o\right)d\xi + \ldots \tag{A-46}$$

and for $\tau_\lambda > \tau_\lambda^*$

$$\tau_\lambda = \int_0^{\eta} \kappa_\lambda\left(h_o\right)d\eta + \lambda\left\{\int_0^{\eta} h_1(\eta)\dot{\kappa}_\lambda\left(h_o\right)d\eta - \int_0^{\infty}\left[\kappa_\lambda\left(h_o(0)\right) - \kappa_\lambda\left(i_o\right)\right]d\xi\right\} + \ldots \tag{A-47}$$

The exponential integral functions can be expanded in the Taylor series

$$\begin{aligned} E_n(x - y) &\equiv E_n\left[\left(x_o - y_o\right) + \lambda\left(x_1 - y_1\right) + \cdots\right] \\ &\equiv E_n\left(x_o - y_o\right) - \lambda\left(x_1 - y_1\right)E_{n-1}\left(x_o - y_o\right) + \cdots \end{aligned} \tag{A-48}$$

If the argument is order λ

$$\begin{aligned} E_n(\lambda x) = E_n(0) &- \lambda_1\, xE_{n-1}(0) + \cdots \\ &+ (-1)^{n-2}\,\lambda^{n-2}\,\frac{x^{n-2}}{(n-2)!}\,E_2(0) \\ &- (-1)^{n-1}\left(\lambda^{n-1}\,ln\lambda\right)\frac{x^{n-1}}{(n-1)!} \\ &- (-1)^{n-1}\,\lambda^{n-1}\,\frac{x^{n-1}}{(n-1)!}\left[\gamma + lnx\right] + \cdots \end{aligned} \tag{A-49}$$

where γ is Euler's constant ($\gamma = 0.577216$). Use of this expansion, while it avoids any dependence of the terms $I_n[\xi]$ on λ, introduces terms of order $\lambda\, ln\, \lambda$ into the boundary layer solutions.

Incorporating the various expansions into equation (2.63) and separating the result into powers of λ and $\lambda\, ln\, \lambda$ yields the zero-order expressions

$$
\begin{aligned}
I_o[\eta] = &- 2\kappa_P[h_o(\eta)]B[h_o(\eta)] \\
&+ k_P \int_o^{\infty} \kappa_\lambda[h_o(\eta)] \Bigg\{ \int_o^{\eta_\Delta} \kappa_\lambda[h_o(\eta')]B_\lambda[h_o(\eta')]E_1\Big(k_P \left|\tau_\lambda(\eta) - \tau_\lambda(\eta')\right|\Big)d\eta' \\
&+ 2r_w E_2\big(k_P\tau_\lambda(\eta)\big) \int_o^{\eta_\Delta} \kappa_\lambda[h_o(\eta')]B_\lambda[h_o(\eta')]E_2\big(k_P\tau_\lambda(\eta')\big)d\eta' \Bigg\} d\lambda
\end{aligned}
\tag{A-50}
$$

and

$$
\begin{aligned}
J_o[\xi] = &- 2\kappa_P[i_o(\xi)]B[i_o(\xi)] \\
&+ k_P \int_o^{\infty} \kappa_\lambda[i_o(\xi)] \Bigg\{ \int_o^{\eta_\Delta} \kappa_\lambda[h_o(\eta')]B_\lambda[h_o(\eta')]E_1\big(k_P\tau_\lambda(\eta')\big)d\eta' \\
&+ 2r_w \int_o^{\eta_\Delta} \kappa_\lambda[h_o(\eta')]B_\lambda[h_o(\eta')]E_2\big(k_P\tau_\lambda(\eta')\big)d\eta' \Bigg\} d\lambda
\end{aligned}
\tag{A-51}
$$

The second of these expressions, which contains only definite integrals, is valid only when expansion (A-48) holds. But equation (A-48) converges in the first few terms only if the arguement λx (or in the terms of this problem $\lambda k_p \sigma$) is small compared to 1. Thus, expressions (A-49) and (A-50) can be used only when the boundary layer is optically thin, that is,

$$\lambda k_p \sigma^* = k_p \tau^* \ll 1.0$$

APPENDIX B

THE METHOD OF SMALL PERTURBATIONS - MATHEMATICAL DEVELOPMENT

In this appendix, the method of small perturbations is used to obtain a solution to the integro-differential system of equations governing the flow in the inviscid region of a radiating shock layer. Mathematical details which are not considered to be appropriate to the main test (chapter III) are included herein.

The system of equations to be treated are presented below.

$$f(\eta)\ h'(\eta) + \epsilon I[\eta] = 0 \tag{B-1}$$

$$2f(\eta)\ f''(\eta) - \left[f'(\eta)\right]^2 + a^2\ h(\eta) = 0 \tag{B-2}$$

$$h(\eta_\Delta) = 1 \tag{B-3}$$

$$f(0) = 0 \tag{B-4}$$

$$f(\eta_\Delta) = 1 \tag{B-5}$$

$$f'(\eta_\Delta) = \frac{a}{\sqrt{2X(1 - X)}} \tag{B-6}$$

The conventional perturbation procedure.- If it is assumed that the functions $h(\eta;\epsilon)$ and $f(\eta;\epsilon)$ are analytic in the vicinity of $\epsilon = 0$ they may be written in the expanded form

$$h(\eta;\epsilon) = \sum_{n=0}^{\infty} \epsilon^n h_n(\eta) \tag{B-7}$$

$$f(\eta;\epsilon) = \sum_{n=0}^{\infty} \epsilon^n f_n(\eta) \tag{B-8}$$

It is anticipated that the first few terms of these expansions will provide an accurate estimate to the solution of system (B-1) - (B-6) when the parameter ϵ is small compared to unity.

The integral term $I[\eta]$ and the constant η_Δ also depend on the parameter ϵ through their dependence on the functions $h(\eta;\epsilon)$ and $f(\eta;\epsilon)$. These quantities will also be assumed to be analytic functions of ϵ near $\epsilon = 0$, so that

$$I[\eta;\epsilon] = \sum_{n=0}^{\infty} \epsilon^n I_n[\eta] \tag{B-9}$$

$$\eta_\Delta = \sum_{n=1}^{\infty} \epsilon^n \eta_{\Delta_n} \tag{B-10}$$

Substituting the expansions (B-7) - (B-10) into system (B-1) - (B-6) yields

$$\left\{f_o h_o'\right\} + \epsilon\left\{f_1 h_o' + f_o h_1' + I_o[\eta]\right\} + \epsilon^2\left\{f_2 h_o' + f_1 h_1' + f_o h_2' + I_1[\eta]\right\} + \cdots = 0 \tag{B-11}$$

$$\left\{2f_o f_o'' - \left[f_o'\right]^2 + a^2 h_o\right\} + \epsilon\left\{2f_o f_1'' - 2f_o' f_1' + 2f_o'' f_1 + a^2 h_1\right\} + \epsilon^2\left\{2f_o f_2'' - 2f_o' f_2'' + 2f_o'' f_2 + 2f_1 f''_1 - \left[f_1'\right]^2 + a^2 h_2\right\} + \cdots = 0 \tag{B-12}$$

$$\left\{h_o\left(\eta_{\Delta_o}\right) - 1\right\} + \epsilon\left\{h_1\left(\eta_{\Delta_o}\right) + \eta_{\Delta_1}\ h_o'\left(\eta_{\Delta_o}\right)\right\} + \epsilon^2\left\{h_2\left(\eta_{\Delta_o}\right) + \eta_{\Delta_1}\ h_1'\left(\eta_{\Delta_o}\right) + \eta_{\Delta_2}\ h_o'\left(\eta_{\Delta_o}\right) + \frac{1}{2}\,\eta_{\Delta_1}^2 h_o''\left(\eta_{\Delta_o}\right)\right\} + \cdots = 0 \tag{B-13}$$

$$\left\{f_o(0)\right\} + \epsilon\left\{f_1(0)\right\} + \epsilon^2\left\{f_2(0)\right\} + \cdots = 0 \tag{B-14}$$

$$\left\{f_o\left(\eta_{\Delta_o}\right) - 1\right\} + \epsilon\left\{f_1\left(\eta_{\Delta_o}\right) + \eta_{\Delta_1} f'_o\left(\eta_{\Delta_o}\right)\right\}$$

$$+ \epsilon^2\left\{f_2\left(\eta_{\Delta_o}\right) + \eta_{\Delta_1} f'_1\left(\eta_{\Delta_o}\right) + \eta_{\Delta_2} f'_o\left(\eta_{\Delta_o}\right)\right.$$

$$\left. + \frac{1}{2} \eta^2_{\Delta_1} f''_o\left(\eta_{\Delta_o}\right)\right\} + \cdots = 0 \qquad \text{(B-15)}$$

$$\left\{f'_o\left(\eta_{\Delta_o}\right) - \frac{a}{\sqrt{2X(1-X)}}\right\} + \epsilon\left\{f'_1\left(\eta_{\Delta_o}\right) + \eta_{\Delta_1} f''_o\left(\eta_{\Delta_o}\right)\right\}$$

$$+ \epsilon^2\left\{f'_2\left(\eta_{\Delta_o}\right) + \eta_{\Delta_1} f''_1\left(\eta_{\Delta_o}\right) + \eta_{\Delta_2} f''_o\left(\eta_{\Delta_o}\right)\right.$$

$$\left. + \frac{1}{2} \eta^2_{\Delta_1} f'''_o\left(\eta_{\Delta_o}\right)\right\} + \cdots = 0 \qquad \text{(B-16)}$$

Since the small parameter ϵ is arbitrary system (B-11) - (B-16) can be satisfied only if each coefficient of each expansion in ϵ is identically zero. This leads to a recursive set of purely differential systems.

The zero-order system is

$$h'_o = 0 \qquad \text{(B-17)}$$

$$2f_o f''_o - \left[f'_o\right]^2 + a^2 h_o = 0 \qquad \text{(B-18)}$$

$$h_o\left(\eta_{\Delta_o}\right) = 1 \tag{B-19}$$

$$f_o(0) = 0 \tag{B-20}$$

$$f_o\left(\eta_{\Delta_o}\right) = 1 \tag{B-21}$$

$$f'_o\left(\eta_{\Delta_o}\right) = \frac{a}{\sqrt{2X(1 - X)}} \tag{B-22}$$

The solutions to this system are easily found with the result

$$h_o = 1 \tag{B-23}$$

$$f_o = (1 - a)\ \eta^2 + a\ \eta \tag{B-24}$$

$$\eta_{\Delta_o} = 1 \tag{B-25}$$

The systems of first and second-order may be written in the general form

$$f_o h'_n + f_1 h'_{n-1} + I_{n-1} = 0 \tag{B-26}$$

$$f_o f''_n - f'_o f'_n + f''_o f_n = \Phi_n(\eta) \tag{B-27}$$

$$h_n(1) = \phi_n \tag{B-28}$$

$$f_n(0) = 0 \tag{B-29}$$

$$f_n\left({}^{\eta}\Delta_o\right) = \theta_n \tag{B-30}$$

$$f'_n\left({}^{\eta}\Delta_o\right) = \psi_n \tag{B-31}$$

Equation (B-26) can be integrated directly to obtain

$$h_n(\eta) = \phi_n + \int_{\eta}^{1} \frac{I_{n-1}[x] + f_1(x)\ h'_{n-1}(x)}{f_o(x)}\ dx \tag{B-32}$$

The abriged version of equation (B-7b) admits the pair of linearly independent solutions $\eta + a/2(1 - a)$ and η^2. Following Ince (ref. 55) the complete solution is found to be

$$\begin{aligned} f_n(\eta) = {} & \theta_n\ \eta^2 - \frac{1}{2}\left[2(1 - a)\ \eta + a\right] \int_o^{\eta} \frac{\Phi_n(x)\ dx}{\left[(1 - a)\ x + a\right]^2} \\ & - \frac{1}{2}\ \eta^2 \int_{\eta}^{1} \frac{2(1 - a)\ x - a}{x^2\left[(1 - a)\ x + a\right]^2}\ \Phi_n(x)\ dx \\ & + \frac{1}{2}\ (2 - a)\ \eta^2 \int_o^{1} \frac{\Phi_n(x)\ dx}{\left[(1 - a)\ x + a\right]^2} \end{aligned} \tag{B-33}$$

Substituting this expression into condition (B-31) provides a relation for the determination of η_{Δ_n}, that is

$$2\theta_n + \int_0^1 \frac{\Phi_n(x)\, dx}{\left[(1 - a)\, x + a\right]^2} = \Psi_n \tag{B-34}$$

The quantities $\Phi_n(\eta)$, ϕ_n, θ_n, and Ψ_n are

$$\Phi_1(\eta) = -\frac{1}{2}\, a^2 h_1(\eta) \tag{B-35}$$

$$\Phi_2(\eta) = -2\, f_1 f_1'' + \left[f_1'\right]^2 - \frac{1}{2}\, a^2 h_2(\eta) \tag{B-36}$$

$$\phi_1 = 0 \tag{B-37}$$

$$\phi_2 = \eta_{\Delta_1}\, I_o[1] \tag{B-38}$$

$$\theta_1 = -(2 - a)\eta_{\Delta_1} \tag{B-39}$$

$$\theta_2 = -\left[2\theta_1 + \int_0^1 \frac{\Phi_1(x)\, dx}{\left[(1 - a)\, x + a\right]^2}\right]\eta_{\Delta_1} - (2 - a)\eta_{\Delta_2} - (1 - a)\eta_{\Delta_1}^2 \tag{B-40}$$

$$\Psi_1 = -2\,(1 - a)\eta_{\Delta_1} \tag{B-41}$$

$$\psi_2 = -\left\{2(2 - a)\eta_{\Delta_1} + (2 - a)\int_0^1 \frac{\Phi_1(x)\ dx}{\left[(1 - a)\ x + a\right]^2}\right\}\eta_{\Delta_1} - 2(1 - a)\eta_{\Delta_2}$$

(B-42)

The divergence of the radiant flux $I[\eta]$ may be written in expanded form by substitution of (B-7) and the expansions of the quantities $\kappa_\lambda(h)$, $B_\lambda(h)$, $\tau_\lambda(\eta;\epsilon)$, and $E_n\left[\tau_\lambda(\eta;\epsilon)\right]$ into expression (2.86) of the text. For completeness the expanded forms of κ_λ, B_λ, τ_λ, and $E_n\left(\tau_\lambda\right)$ are written down here.

$$\kappa_\lambda(h) = \kappa_\lambda(1) + \epsilon\ \dot{\kappa}_\lambda(1)\ h_1(\eta) + \epsilon^2\left[\dot{\kappa}_\lambda(1)\ h_2(\eta) + \frac{1}{2}\ \ddot{\kappa}_\lambda(1)\ h_1^2(\eta)\right] + \cdots \qquad \text{(B-43)}$$

$$B_\lambda(h) = B_\lambda(1) + \epsilon\ \dot{B}_\lambda(1)\ h_1(\eta) + \epsilon^2\left[\dot{B}_\lambda(1)\ h_2(\eta) + \frac{1}{2}\ \ddot{B}_\lambda(1)\ h_1^2(\eta)\right] + \cdots \qquad \text{(B-44)}$$

$$\tau_\lambda(\eta;\epsilon) = k_P\int_0^\eta \kappa_\lambda(\eta)\ d\eta$$

$$= k_P\left[\kappa_\lambda(1)\eta + \epsilon\ \dot{\kappa}_\lambda(1)\int_0^\eta h_1(\eta)\ d\eta + \cdots\right]$$

(B-45)

$$E_n\left[\tau_\lambda(\eta) - \tau_\lambda(\xi)\right] \equiv E_n\left(k_P\left[\kappa_\lambda(1)\,(\eta - \xi) + \epsilon\dot{\kappa}_\lambda(1)\int_o^\eta h_1(x)dx + \cdots\right]\right)$$

$$= E_n\left[k_P\,\kappa_\lambda(1)\,(\eta - \xi)\right]$$

$$- \epsilon k_P\,\dot{\kappa}_\lambda(1)\left[\int_\xi^\eta h_1(x)dx\right]E_{n-1}\left[k_P\,\kappa_\lambda(1)(\eta - \xi)\right] + \cdots$$

(B-46)

The following property of the exponential integral functions was used to obtain (B-46)

$$E_{n-1}(x) = -\frac{d}{dx}E_n(x)$$

With these expansions in hand, expressions for the terms $I_o[\eta]$ and $I_1[\eta]$ can be obtained. The results are

$$I_o[\eta] = -\int_o^\infty \kappa_\lambda\,B_\lambda\left\{E_2\left[k_\lambda(1 - \eta)\right] + \left(1 - r_{o_\lambda}\right)E_2\left[k_\lambda\eta\right]\right\}d\lambda$$

(B-47)

$$I_1[\eta] = -h_1(\eta)\int_o^\infty\left\{\left[\dot{\kappa}_\lambda\,B_\lambda\left\{E_2\left[k_\lambda(1 - \eta)\right] + \left(1 - r_{o_\lambda}\right)E_2\left[k_\lambda\eta\right]\right\} - 2\kappa_\lambda\,\dot{B}_\lambda\right]\right\}d\lambda$$

$$+\int_o^\infty k_\lambda\left\{\left[\kappa_\lambda\,\dot{B}_\lambda\int_o^1 h_1(\xi)\,E_1\left[k_\lambda|\eta - \xi|\right]d\xi\right.\right.$$

$$+ \dot{\kappa}_\lambda B_\lambda \left\{ E_1\left[k_\lambda(1 - \eta)\right] \int_\eta^1 h_1(\xi)\, d\xi \right.$$

$$\left. + \left(1 - r_{o_\lambda}\right) E_1\left[k_\lambda \eta\right] \int_o^\eta h_1(\xi)\, d\xi \right\} + r_{1_\lambda} E_2\left[k_\lambda \eta\right] \Bigg] d\lambda \tag{B-48}$$

In these expressions, the notation has been simplified somewhat by omitting the argument 1 in the terms κ_λ, $\dot{\kappa}_\lambda$, B_λ, and $\dot{B}_\lambda$ and by introducing the quantities

$$k_\lambda = k_P \kappa_\lambda \tag{B-49}$$

$$r_{o_\lambda} = r_w \left[1 - 2 E_3\left(k_\lambda\right)\right] \tag{B-50}$$

$$r_{1_\lambda} = 2r_w \left\{ \kappa_\lambda \dot{B}_\lambda \int_o^1 h_1(\xi)\, E_2\left(k_\lambda \xi\right) d\xi \right.$$

$$\left. + \dot{\kappa}_\lambda B_\lambda E_2\left(k_\lambda\right) \int_o^1 h_1(\xi)\, d\xi + \eta_{\Delta_1} \kappa_\lambda B_\lambda E_2\left(k_\lambda\right) \right\} \tag{B-51}$$

<u>The P - L - K solution</u>.- It has been pointed out in the text that the first order solution for the enthalpy distribution has a logarithmic singularity at the point $\eta = 0$ and the second order solution behaves like the logarithm squared. As a consequence the assumed expansion diverges as the origin is approached and the small perturbation solution is not uniformly valid. In order to obtain a solution which is uniformly valid throughout the domain of

the problem, the Poincare - Lighthill - Kuo method (see ref. 47) will be used. In this method the independent variable as well as the dependent variables is expanded in a McLauren series of ϵ. For this problem

$$\eta = x + \epsilon\, \eta_1^*(x) + \epsilon^2\, \eta_2^*(x) + \cdots \tag{B-52}$$

$$h(\eta;\epsilon) = h_o^*(x) + \epsilon\, h_1^*(x) + \epsilon^2\, h_2^*(x) + \cdots \tag{B-53}$$

The superscript $*$ has been used here to distinguish between the coefficients in the P-L-K expansion and the coefficients in the conventional expansion (equation (B-7)). The quantities $f(\eta)$ and $I[\eta]$ may also be expanded in terms of x as follows:

$$\begin{aligned} f(\eta) &= \sum_{n=o}^{\infty} \epsilon^n f_n(\eta) \equiv \sum_{n=o}^{\infty} \epsilon^n f_n\left[x + \epsilon\eta_1^*(x) + \cdots\right] \\ &= f_o(x) + \epsilon\left[f_1(x) + \eta_1^*(x)\, f_o'(x)\right] + \epsilon^2\left[f_2(x) + \eta_1^*(x)\, f_1'(\eta)\right. \\ &\quad \left. + \eta_2^*(x)\, f_o'(x) + \frac{1}{2}\, \eta_1^{*2}(x)\, f_o''(x)\right] + \cdots \end{aligned} \tag{B-54}$$

Similarly,

$$I[\eta] = I_o[x] + \epsilon\left\{I_1[x] + \eta_1^*(x)\, I_o'[x]\right\} + \cdots \tag{B-55}$$

When expansions (B-52) - (B-55) are substituted into equation (B-1), a set of equations for $h_o^*(x)$, $h_1^*(x)$, $h_2^*(x)$, and so forth result.

The quantities $\eta_1^*(x)$, $\eta_2^*(x)$, and so forth and their first derivatives also appear. These quantities are arbitrary and should be chosen in such a manner as to reduce the strength of the singularities in the higher order terms, $h_n^*(x)$, so that these singularities are never stronger than that of the lowest order singular term (in our case the first order term). Pritulo (ref. 48) has shown that the coefficients in the expansion of $h(\eta;\epsilon)$ in the P-L-K method are related to the coefficients of the conventional expansion in the following manner:

$$h_o^*(x) = h_o(x) \tag{B-56}$$

$$h_1^*(x) = h_1(x) + \eta_1^*(x)\ h_o'(x) = h_1(x) \tag{B-57}$$

$$\begin{aligned} h_2^*(x) &= h_2(x) + \eta_1^*(x)\ h_1'(x) + \eta_2^*(x)\ h_o'(x) + \frac{1}{2}\ \eta_1^*(x)\ h_o''(x) \\ &= h_2(x) + \eta_1^*\ h_1'(x) \end{aligned} \tag{B-58}$$

Now, instead of choosing differential equations for the $\eta_n^*(x)$ in order to satisfy the criterion previously states, one can choose the values of the $\eta_n^*(x)$ directly. In this case, an obvious choice is simply*

*This choice satisfies the condition $\eta_1^*(1) = \eta_{\Delta_1}$.

$$\eta_1^*(x) = -h_2(x) \Big/ h_1'(x) \tag{B-59}$$

which gives $h_2^*(x) \equiv 0$.

The result of transforming the independent variable by means of formula (B-52) is to remove the singularity from the domain of the problem. That this is true can be seen by noting that the condition $\eta = 0$ does not imply $x = 0$ but rather (for this problem) implies that x is some small positive number x_o. Hence, to first order $h(\eta;\ \epsilon) = 1 + \epsilon h_1^*(\eta)$ is nonsingular in the domain $0 \leq \eta \leq 1$.

APPENDIX C

OPTICALLY THIN SHOCK LAYERS - MATHEMATICAL DEVELOPMENT

With the substitute kernal approximation the divergence of the radiant flux vector can be written

$$I\left[\eta\right] = 2\kappa_P(\eta)B(\eta) - 2k_P \int_0^{\infty} \kappa_\lambda(\eta) \left\langle \int_0^{\eta_\Delta} \kappa_\lambda(\xi)B_\lambda(\xi)e^{-2k_P\left|\tau_\lambda(\eta)-\tau_\lambda(\xi)\right|} d\xi \right.$$

$$\left. + r_w\, e^{-2k_P\tau_\lambda(\eta)} \int_0^{\eta_\Delta} \kappa_\lambda(\xi)B_\lambda(\xi)e^{-2k_P\tau_\lambda(\xi)}\, d\xi \right\rangle d\lambda \tag{C-1}$$

The monochromatic optical path length $k_P\tau_\lambda(\eta)$ is given by the expression

$$k_P\tau_\lambda(\eta) = k_P \int_0^{\eta} \kappa_\lambda(\xi)d\xi \tag{C-2}$$

where k_P is the Bouguer number

$$k_P = \rho_s\, \kappa_{P_s}\, \Delta_A \tag{C-3}$$

The approximate governing system presented in chapter IV is

$$f(\eta)h'(\eta) + \epsilon I\left[\eta\right] = 0 \tag{C-4}$$

$$2f(\eta)f''(\eta) - \left[f'(\eta)\right]^2 + a^2\bar{h} = 0 \tag{C-5}$$

$$f(0) = 0 \tag{C-6}$$

$$f\left(\eta_\Delta\right) = 1 \tag{C-7}$$

$$f'\left(\eta_\Delta\right) = \frac{2}{1 + \sqrt{2X(1 - X)}} \tag{C-8}$$

$$h\left(\eta_\Delta\right) = 1 \tag{C-9}$$

The quantity $\bar{h}$ is defined by the expression

$$\bar{h} = \frac{1}{\eta_\Delta} \int_0^{\eta_\Delta} h(\xi)d\xi \tag{C-10}$$

<u>The conventional perturbation procedure</u>.- If the functions $h(\eta;\, k_p)$ and $f(\eta;\, k_p)$ are analytic in the vicinity of $k_p = 0$*, they may be written in the expanded form

$$h(\eta;\, k_p) = \sum_{n=0}^{\infty} k_p^n\, h_n(\eta) \tag{C-11}$$

$$f(\eta;\, k_p) = \sum_{n=0}^{\infty} k_p^n\, h_n(\eta) \tag{C-12}$$

It is anticipated that the first few terms of these expansions will

*It is assumed herein that such is the case.

provide an accurate estimate of the solution to the system (C-4) to (C-10) when k_P is small compared to unity.

In addition, all quantities which depend on the parameter k_P either directly or indirectly must be expanded in terms of k_P. For example, a function $\mathcal{F}[h(\eta)]$ becomes

$$\mathcal{F}\left[h(\eta)\right] \equiv \mathcal{F}\left[h_o(\eta) + k_P\, h_1(\eta) + \ldots\right]$$

$$= \mathcal{F}\left[h_o(\eta)\right] + k_P\, \dot{\mathcal{F}}\left[h_o(\eta)\right] h_1(\eta) + \ldots \tag{C-13}$$

$$= \mathcal{F}_o(\eta) + k_P\, \dot{\mathcal{F}}_o(\eta) h_1(\eta) + \ldots \tag{C-14}$$

The quantities $\mathcal{F}_o(\eta)$ and $\dot{\mathcal{F}}_o(\eta)$ have been introduced to simplify the notation. The constant η_Δ is given by the expansion

$$\eta_\Delta = \eta_{\Delta_o} + k_P\, \eta_{\Delta_1} + \ldots \tag{C-15}$$

Substituting the expansions (C-11) to (C-15) into system (C-4) to (C-10) yields

$$\begin{aligned}
&\left\{f_o(\eta)h_o'(\eta) - 2\epsilon\kappa_{P_o}(\eta)B_o(\eta)\right\} \\
&\quad + k_P\left\{f_o(\eta)h_1'(\eta) + f_1(\eta)h_o'(\eta) - 2\epsilon\left[\dot{\kappa}_{P_o}(\eta)B_o(\eta)\right.\right. \\
&\quad \left. + \kappa_{P_o}(\eta)\dot{B}_o(\eta)\right]h_1(\eta) \\
&\quad \left. + 2\epsilon\left(1 + r_W\right)\int_0^\infty \left[\kappa_{\lambda_o}(\eta)\int_0^{\eta_{\Delta_o}} \kappa_{\lambda_o}(\xi)B_{\lambda_o}(\xi)d\xi\right]d\lambda\right\} + \ldots = 0
\end{aligned} \tag{C-16}$$

$$\left\{2f_o(\eta)f_o''(\eta) - \left[f_o'(\eta)\right]^2 + a^2\,\bar{h}_o\right\} + k_P\left\{2f_o(\eta)f_1''(\eta) - 2f_o'(\eta)f_1'(\eta) + 2f_o''(\eta)f_1(\eta) + a^2\,\bar{h}_1\right\} + \ldots = 0 \tag{C-17}$$

$$f_o(0) + k_P f_1(0) + \ldots = 0 \tag{C-18}$$

$$f_o\left(\eta_{\Delta_o}\right) + k_P\left[f_1\left(\eta_{\Delta_o}\right) + \eta_{\Delta_1} f_o'\left(\eta_{\Delta_o}\right)\right] + \ldots = 0 \tag{C-19}$$

$$f_o'\left(\eta_{\Delta_o}\right) + k_P\left[f_1'\left(\eta_{\Delta_o}\right) + \eta_{\Delta_1} f_o''\left(\eta_{\Delta_o}\right)\right] + \ldots = \frac{2}{1 + \sqrt{2X(1 - X)}} \tag{C-20}$$

$$h_o\left(\eta_{\Delta_o}\right) + k_P\left[h_1\left(\eta_{\Delta_o}\right) + \eta_{\Delta_1} h_o'\left(\eta_{\Delta_o}\right)\right] + \ldots = 1 \tag{C-21}$$

where

$$\bar{h}_o + k_P\bar{h}_1 + \ldots = \frac{1}{\eta_{\Delta_o}} \int_0^{\eta_{\Delta_o}} h_o(\xi)d\xi + k_P\left\{\frac{1}{\eta_{\Delta_o}} \int_0^{\eta_{\Delta_o}} h_1(\xi)d\xi - \frac{\eta_{\Delta_1}}{\eta_{\Delta_o}^2} \int_0^{\eta_{\Delta_o}} h_o(\xi)d\xi + \frac{\eta_{\Delta_1}}{\eta_{\Delta_o}}\right\} + \ldots \tag{C-22}$$

Since the small parameter is arbitrary system (C-16) to (C-21) can be satisfied only if each coefficient of each term is identically zero. This leads to a recursive set of purely differential systems.

The zero-order system is

$$f_o(\eta)h_o'(\eta) - 2\epsilon\kappa_{p_o}(\eta)B_o(\eta) = 0 \tag{C-23}$$

$$2f_o(\eta)f_o''(\eta) - \left[f_o'(\eta)\right]^2 + a^2\,\bar{h}_o = 0 \tag{C-24}$$

$$f_o(0) = 0 \tag{C-25}$$

$$f_o\left(\eta_{\Delta_o}\right) = 1 \tag{C-26}$$

$$f_o'\left(\eta_{\Delta_o}\right) = \frac{2}{1 + \sqrt{2X(1 - X)}} \tag{C-27}$$

$$h_o\left(\eta_{\Delta_o}\right) = 1 \tag{C-28}$$

$$\bar{h}_o = \frac{1}{\eta_{\Delta_o}} \int_o^{\eta_{\Delta_o}} h_o(\xi)d\xi \tag{C-29}$$

The solutions to this system are

$$\int_{h_o}^{1} \frac{dh}{\kappa_p(h)B(h)} = \frac{2\epsilon\eta_{\Delta_o}}{a^*}\, \ln \frac{(1 - a^*)x + a^*}{x} \tag{C-30}$$

$$f_o(\eta) = \left(1 - a\sqrt{\bar{h}_o}\;\eta_{\Delta_o}\right)\left(\frac{\eta}{\eta_{\Delta_o}}\right)^2 + a\sqrt{\bar{h}_o}\;\eta_{\Delta_o}\left(\frac{\eta}{\eta_{\Delta_o}}\right) \tag{C-31a}$$

$$= (1 - a^*)x^2 + a^*\,x \tag{C-31b}$$

$$\eta_{\Delta_o} = \frac{1 + \sqrt{2X(1 - X)}}{1 + \sqrt{2\bar{h}_o\ X(1 - X)}} \tag{C-32}$$

$$\bar{h}_o = \int_0^1 h_o(x)dx \tag{C-33}$$

where the definitions

$$a^* = a\sqrt{\bar{h}_o}\ \eta_{\Delta_o} \tag{C-34}$$

$$x = \eta/\eta_{\Delta_o} \tag{C-35}$$

have been added to help simplify the notation.

The first-order system is

$$f_o(\eta)h_1'(\eta) - 2\epsilon\left[\dot{\kappa}_{P_o}(\eta)B_o(\eta) + \kappa_{P_o}(\eta)\dot{B}_o(\eta)\right]h_1(\eta)$$

$$= -f_1(\eta)h_o'(\eta) - 2\epsilon\left(1 + r_w\right)\int_0^\infty\left[\kappa_{\lambda_o}(\eta)\int_0^{\eta_{\Delta_o}}\kappa_{\lambda_o}(\xi)B_{\lambda_o}(\xi)d\xi\right]d\lambda \tag{C-36}$$

$$f_o(\eta)f_1''(\eta) - f_o'(\eta)f_1'(\eta) + f_o''(\eta)f_1(\eta) + \frac{1}{2}a^2\bar{h}_1 = 0 \tag{C-37}$$

$$f_1(0) = 0 \tag{C-38}$$

$$f_1\left(\eta_{\Delta_o}\right) = -\eta_{\Delta_1}f_o'\left(\eta_{\Delta_o}\right) = -\frac{2\eta_{\Delta_1}}{1 + \sqrt{2X(1 - X)}} \tag{C-39}$$

$$f_1'\left(\eta_{\Delta_o}\right) = -\eta_{\Delta_1} f_o''\left(\eta_{\Delta_o}\right) = -\frac{2(1 - a^*)\eta_{\Delta_1}}{\eta_{\Delta_o}^2} \tag{C-40}$$

$$h_1\left(\eta_{\Delta_o}\right) = -\eta_{\Delta_1} h_o'\left(\eta_{\Delta_o}\right) = -2\epsilon\eta_{\Delta_1} \tag{C-41}$$

The solutions to this system are

$$h_1(\eta) = -2\epsilon\kappa_{P_o}(x)B_o(x)\left\{\eta_{\Delta_1} + \left(\frac{\eta_{\Delta_o}\bar{h}_1}{2\bar{h}_o}\right)\left[\left(1 - \frac{a^*\eta_{\Delta_o}}{1 + \sqrt{2x(1 - x)}}\right)\frac{(1 - x)}{(1 - a^*)x + a^*} - \frac{1}{a^*} \ln \frac{(1 - a^*)x + a^*}{x}\right]\right\}$$

$$+2\epsilon\left(1 + r_w\right) \quad \kappa_{P_o}(x)B_o(x)\eta_{\Delta_o}^2 \int_x^1 \frac{\int_o^\infty\left[\kappa_{\lambda_o}(\xi)\int_o^1 \kappa_{\lambda_o}(\xi')B_{\lambda_o}(\xi')d\xi'\right]d\lambda}{f_o(\xi)\kappa_{P_o}(\xi)B_o(\xi)}\, d\xi \tag{C-42}$$

$$f_1(x) = 2\,\frac{\eta_{\Delta_1}}{\eta_{\Delta_o}}\, x\left[1 - \left(\frac{2 + \sqrt{2\bar{h}_o X(1 - X)}}{1 + \sqrt{2\bar{h}_o X(1 - X)}}\right)x\right] \tag{C-43}$$

$$\eta_{\Delta_1} = -\frac{a^*\bar{h}_1}{4\bar{h}_o}\,\eta_{\Delta_o} \tag{C-44}$$

$$\bar{h}_1 = \frac{\bar{h}_o \int_o^1 h_1(x)dx}{\left[\bar{h}_o + \frac{a^*}{4}\left(1 - \bar{h}_o\right)\right]} \tag{C-45}$$

The expression for $h_1(\eta)$ (eq. (C-42)) can be simplified somewhat by transforming the integral over ξ into an integral over h_o through the use of equation (C-23). The result of this transformation is

$$h_1(x) = -2\epsilon\kappa_{P_o}(x)B_o(x)\Bigg\{\eta_{\Delta_1} + \left(\frac{\eta_{\Delta_o}\bar{h}_1}{2\bar{h}_o}\right)\Bigg[\Bigg(1 - \frac{a^*\eta_{\Delta_o}}{1 + \sqrt{2X(1 - X)}}\Bigg)\frac{(1 - x)}{(1 - a^*)x + a^*} - \frac{1}{a^*}\ln\frac{(1 - a^*)x + a^*}{x}\Bigg]\Bigg\}$$

$$+ \left(1 + r_w\right)\kappa_{P_o}(x)B_o(x)\eta_{\Delta_o}\int_o^\infty\left\{\left[\int_o^1 \kappa_{\lambda_o}(\xi')B_{\lambda_o}(\xi')d\xi'\right]\int_{h_o}^1 \frac{\kappa_\lambda(h)dh}{\left[\kappa_P(h)B(h)\right]^2}\right\}d\lambda \tag{C-46}$$

The P-L-K solution.- It can be seen on careful inspection of equation (C-46) that the first-order term $h_1(x)$ displays a singular behavior in the vicinity of the wall $(x = 0)$.* Consequently, the assumed expansion for $h(x; k_p)$ diverges as the origin is approached and the perturbation solution is not uniformly valid. However, if the coordinate x is perturbed, the solution can be made uniformly valid. Thus, according to the P-L-K method,

$$x = y + k_p\, x_1^*(y) + \ldots \tag{C-48}$$

where y is the transformed variable. The enthalpy when expanded in terms of k_p with coefficients as functions of y, not x, becomes

$$h(x; k_p) = h_o^*(y) + k_p\, h_1^*(y) + \ldots \tag{C-49}$$

and the nondimensional stream function

$$f(x; k_p) = f_o^*(y) + k_p\, f_1^*(y) + \ldots \tag{C-50}$$

According to Pritulo (ref. 48), the coefficients in the P-L-K-expansions can be related to the coefficients in regular expansions in the following manner

$$h_o^*(y) = h_o(y) \tag{C-51}$$

$$h_1^*(y) = h_1(y) + x_1^*(y)h_o'(y) \tag{C-52}$$

---

*See chapter IV for a more complete discussion of this singularity.

$$f_o^*(y) = f_o(y) \tag{C-53}$$

$$f_1^*(y) = f_1(y) + x_1^*(y)f_o'(y) \tag{C-54}$$

The arbitrary quantity $x_1^*(y)$ should be chosen so as to eliminate the singularity in $h_1^*(y)$. An obvious choice is

$$x_1(y) = -h_1(y)/h_o'(y) \tag{C-55}$$

The transformation of the independent variable by means of formula (C-48) removes the singularity from the domain of the problem, because y takes on some small positive value when x is zero. Hence, the first-order term $h_1^*(y)$ is nonsingular throughout the domain of the problem $0 \leq x \leq x_\Delta$.

APPENDIX D

THE RADIATION DEPLETED SHOCK LAYER - MATHEMATICAL DEVELOPMENT

The system of equations governing the flow in the stagnation region of a radiating shock layer is derived in the text using the substitute kernal approximation (see chapter VI). This system is

$$\left[f(\tau)h'(\tau)\right]'' - \frac{3}{2}\,\epsilon B''(\tau) - \frac{9}{4}\,k_P^2\,f(\tau)h'(\tau) = 0 \tag{D-1}$$

$$2f(\eta)f''(\eta) - \left[f'(\eta)\right]^2 + a^2h(\eta) = 0 \tag{D-2}$$

$$f(0) = 0 \tag{D-3}$$

$$f\left(\eta_\Delta\right) = 1 \tag{D-4}$$

$$f'\left(\eta_\Delta\right) = \frac{a}{\sqrt{2X(1 - X)}} = \frac{2}{X}\left(\frac{\Delta}{R_s}\right) \tag{D-5}$$

$$h\left(\tau_\Delta\right) = 1 \tag{D-6}$$

This set of equations is subject to the additional condition

$$f(\tau)h'(\tau) + \epsilon\left\{\frac{9}{8}\,k_P \int_0^{\tau_\Delta} B(t)e^{-\frac{3}{2}k_P|t-\tau|}\,dt - \frac{3}{2}\,B(\tau) + \frac{9}{8}\,re^{-\frac{3}{2}k_P\tau}\right\} \tag{D-7}$$

where

$$r = r_w k_P \int_0^{\tau_\Delta} B(t) e^{-\frac{3}{2} k_P \tau} \, dt$$

When the parameter ϵ is very much larger than unity and k_P^2 the asymptotic solution to the energy equation (D-1) is simply $B(\tau) = C_1 + C_2 \tau$. Substitution of this solution into the asymptotic form of the integral condition (D-7) gives $C_1 = C_2 = 0$. This solution obviously does not satisfy the boundary condition $h\left(\tau_\Delta\right) = 1$, which indicates that the asymptotic solution is not valid in the vicinity of the boundary (shock) at $\tau = \tau_\Delta$. This is not surprizing when it is recalled that the existance of a thermal boundary layer has been established on physical grounds in the text (chapter VI).

In order to determine the form of the "boundary layer" equation valid near the shock, the stretched coordinate

$$\xi = \left(\tau_\Delta - \tau\right)\epsilon^n \tag{D-9}$$

and the functions

$$B_b(\xi) = B(\tau) \tag{D-10}$$

$$f_b(\xi) = f(\tau) \tag{D-11}$$

are introduced. The subscript b indicates that these functions are valid only in the boundary layer.

Rewritten in terms of the boundary layer variables, equation (D-1) becomes

$$-\epsilon^{3n-1}\left[f_b(\xi)h_b'(\xi)\right]'' + \epsilon^{n-1}\,\frac{9}{4}\,k_P^2\,f_b(\xi)h_b'(\xi)$$

$$-\ \epsilon^{2n}\,\frac{3}{2}\,B_b''(\xi) = 0$$

If n is set equal to 1 and ϵ is allowed to grow without limit, the most highly differentiated term will be retained without losing the significant term of the unstretched problem. The resulting differential equation is

$$\left[f_b(\xi)h_b'(\xi)\right]'' + \frac{3}{2}\,B_b''(\xi) = \epsilon^{-2}\,\frac{9}{4}\,k_P^2\,f_b(\xi)h_b'(\xi) \qquad \text{(D-12)}$$

The momentum equation, when written in terms of the stretched coordinate $\zeta = \left(\eta_\Delta - \eta\right)\epsilon$ becomes

$$2f_b(\zeta)f_b''(\zeta) - \left[f_b'(\zeta)\right]^2 = -\epsilon^{-2}\,a^2h_b(\zeta) \qquad \text{(D-13)}$$

It has been shown that the boundary layer is characterized by the parameter ϵ^{-1} and it would seem proper to expand both the boundary layer and asymptotic solutions as power series in ϵ^{-1}. However, $f_a(\eta)$ (where the subscript a indicates the asymptotic solution valid far from the shock) is not analytic in ϵ^{-1} near $\epsilon^{-1} = 0$, but is analytic in $\epsilon^{-1/2}$. Consequently, the solutions will be expanded as power series in $\epsilon^{-1/2}$, that is

$$B_a(\tau) = \sum_{n=0}^{\infty} \epsilon^{-n/2} B_{a_n}(\tau) \tag{D-14}$$

$$f_a(\eta) = \sum_{n=0}^{\infty} \epsilon^{-n/2} f_{a_n}(\eta) \tag{D-15}$$

$$B_b(\xi) = \sum_{n=0}^{\infty} \epsilon^{-n/2} B_{b_n}(\xi) \tag{D-16}$$

$$f_b(\zeta) = \sum_{n=0}^{\infty} \epsilon^{-n/2} f_{b_n}(\zeta) \tag{D-17}$$

In addition, it will be assumed that the enthalpy h is an analytic function of B throughout the interval $0 \leq B \leq 1$, and from physical considerations it will be assumed that $h = 0$ when $B = 0$. Then

$$h(B) = h\left(B_o\right) + \epsilon^{-1/2} B_1 \dot{h}\left(B_o\right) + \epsilon^{-1}\left[B_2 \dot{h}\left(B_o\right) + - B_1^2 \ddot{h}\left(B_o\right)\right] + \ldots \tag{D-18}$$

where the dot $(\dot{\ })$ indicates differentiation with respect to the variable B_o. Substitution of expansion (D-14), (D-15), and (D-18) into system (D-1) to (D-7) gives

$$\frac{3}{2} B''_{a_o}(\tau) + \epsilon^{-1/2} \frac{3}{2} B''_{a_1}(\tau)$$

$$+ \epsilon^{-1}\left\{\frac{3}{2} B''_{a_2}(\tau) - \left[f_{a_o}(\tau)\dot{h}\left(B_{a_o}\right)B'_{a_o}(\tau)\right]''\right.$$

$$\left. + \frac{9}{4} k_P^2 f_{a_o}(\tau)\dot{h}\left(B_{a_o}\right)B'_{a_o}(\tau)\right\} + \dots = 0 \tag{D-19}$$

$$\left\{2f_{a_o}(\eta)f''_{a_o}(\eta) - \left[f'_{a_o}(\eta)\right]^2 + a^2\, h\left(B_{a_o}\right)\right\} + \epsilon^{-1/2}\left\{2f_{a_o}(\eta)f''_{a_1}(\eta)\right.$$

$$- 2f'_{a_o}(\eta)f'_{a_1}(\eta) + 2f''_{a_o}(\eta)f_{a_1}(\eta)$$

$$\left. + a^2\, \dot{h}\left(B_{a_o}\right)B_{a_1}(\eta)\right\} + \dots = 0 \tag{D-20}$$

$$f_{a_o}(0) + \epsilon^{-1/2}\, f_{a_1}(0) + \epsilon^{-1}\, f_{a_2}(0) + \dots = 0 \tag{D-21}$$

$$\left\{f_{a_o}\left(\eta_{\Delta_o}\right) - 1\right\} + \epsilon^{-1/2}\left\{f_{a_1}\left(\eta_{\Delta_o}\right) + \eta_{\Delta_1}\, f'_{a_o}\left(\eta_{\Delta_o}\right)\right\}$$

$$+ \epsilon^{-1}\left\{f_{a_2}\left(\eta_{\Delta_o}\right) + \eta_{\Delta_1}\, f'_{a_1}\left(\eta_{\Delta_o}\right) + \eta_{\Delta_2}\, f'_{a_o}\left(\eta_{\Delta_o}\right)\right.$$

$$\left. + \frac{1}{2}\, \eta_{\Delta_1}^2\, f''_{a_o}\left(\eta_{\Delta_o}\right)\right\} + \dots = 0 \tag{D-22}$$

$$\left\{f'_{a_o}\left(\eta_{\Delta_o}\right) - \frac{a}{\sqrt{2X(1 - X)}}\right\} + \epsilon^{-1/2}\left\{f'_{a_1}\left(\eta_{\Delta_o}\right) + \eta_{\Delta_1} f''_{a_o}\left(\eta_{\Delta_o}\right)\right\}$$

$$\epsilon^{-1}\left\{f'_{a_2}\left(\eta_{\Delta_o}\right) + \eta_{\Delta_1} f''_{a_1}\left(\eta_{\Delta_o}\right) + \eta_{\Delta_2} f''_{a_o}\left(\eta_{\Delta_o}\right) + \frac{1}{2}\eta^2_{\Delta_1} f'''_{a_o}\left(\eta_{\Delta_o}\right)\right\} + \ldots = 0 \tag{D-23}$$

$$\left\{\frac{9}{8} k_P \int_0^{\tau_{\Delta_o}} B_{a_o}(t) e^{-\frac{3}{2} k_P |\tau - t|} dt - \frac{3}{2} B_{a_o}(\tau) + \frac{9}{8} r_o e^{-\frac{3}{2} k_P \tau}\right\}$$

$$+ \epsilon^{-1/2}\left\{\frac{9}{8} k_P \int_0^{\tau_{\Delta_o}} B_{a_1}(t) e^{-\frac{3}{2} k_P |\tau - t|} dt + \frac{9}{8} k_P \tau_{\Delta_1} B_{a_o}\left(\tau_{\Delta_o}\right)\right.$$

$$\left. - \frac{3}{2} B_{a_1}(\tau) + \frac{9}{8} r_1 e^{-\frac{3}{2} k_P \tau}\right\} + \epsilon^{-1}\left\{\frac{9}{8} k_P \int_0^{\tau_{\Delta_o}} B_{a_2}(t) e^{-\frac{3}{2} k_P |\tau - t|} dt\right.$$

$$+ \frac{9}{8} k_P \tau_{\Delta_1} B_{a_1}\left(\tau_{\Delta_o}\right) + \frac{9}{8} k_P \tau_{\Delta_2} B_{a_o}\left(\tau_{\Delta_o}\right) - \frac{3}{2} B_{a_2}(\tau)$$

$$+ \frac{9}{8} r_2 e^{-\frac{3}{2} k_P \tau} + f_{a_o}(\tau)\dot{h}\left(B_{a_o}\right) B'_{a_o}(\tau)$$

$$\left. + \frac{9}{8} k_P e^{-\frac{3}{2} k_P \left(\tau_{\Delta_o} - \tau\right)} \int_0^{\epsilon \tau_\Delta} \left[B_{b_o}(\xi) - B_{a_o}\left(\tau_{\Delta_o}\right)\right] d\xi\right\} + \ldots = 0 \tag{D-24}$$

where

$$r_o = r_w k_P \int_0^{\tau_{\Delta_o}} B_{a_o}(t) e^{-\frac{3}{2} k_P t} dt \tag{D-25}$$

$$r_1 = r_w k_P \int_0^{\tau_{\Delta_o}} B_{a_1}(t) e^{-\frac{3}{2} k_P t} \, dt + r_w k_P \tau_{\Delta_1} B_{a_o}\left(\tau_{\Delta_o}\right) \tag{D-26}$$

$$r_2 = r_w k_P \int_0^{\tau_{\Delta_o}} B_{a_2}(t) e^{-\frac{3}{2} k_P t} \, dt + r_w k_P \tau_{\Delta_2} B_{a_2}\left(\tau_{\Delta_o}\right)$$
$$+ r_w k_P \tau_{\Delta_1} B_{a_1}\left(\tau_{\Delta_o}\right) + r_w k_P e^{-\frac{3}{2} k_P \tau_{\Delta_o}} \int_0^{\epsilon \tau_\Delta} \left[B_{b_o}(\xi) - B_{a_o}\left(\tau_{\Delta_o}\right)\right] d\xi \tag{D-27}$$

The shock layer optical thickness is determined from the condition

$$\left\{\eta_{\Delta_o} - \int_0^{\tau_{\Delta_o}} \kappa_P^{-1}\left(B_{a_o}\right) dt\right\} + \epsilon^{-1\,2} \left\{\eta_{\Delta_1}\right.$$
$$\left. - \tau_{\Delta_1} \kappa_P^{-1}\left[B_{a_o}\left(\tau_{\Delta_o}\right)\right] - \int_0^{\tau_{\Delta_o}} \left(\dot{\kappa}_P^{-1}\left(B_{a_o}\right)\right) B_{a_1}(t) dt\right\}$$
$$+ \epsilon^{-1} \left\{\eta_{\Delta_2} - \tau_{\Delta_2} \kappa_P^{-1}\left[B_{a_o}\left(\tau_{\Delta_o}\right)\right]\right.$$
$$- \tau_{\Delta_1}\left(\dot{\kappa}_P^{-1}\left[B_{a_o}\left(\tau_{\Delta_o}\right)\right]\right) B_{a_1}\left(\tau_{\Delta_o}\right) - \int_0^{\tau_{\Delta_o}} \left(\dot{\kappa}_P^{-1}\left(B_{a_o}\right)\right) B_{a_2}(t) dt$$
$$- \frac{1}{2} \int_0^{\tau_{\Delta_o}} \left(\ddot{\kappa}_P^{-1}\left(B_{a_o}\right)\right) B_{a_1}^2(t) dt$$
$$\left. - \int_0^{\epsilon \tau_\Delta} \left[\kappa_P^{-1}\left(B_{b_o}(\xi)\right) - \kappa_P^{-1}\left(B_{a_o}\left(\tau_{\Delta_o}\right)\right)\right] d\xi\right\} + \dots = 0 \tag{D-28}$$

The corresponding boundary layer equations are obtained by substituting the expansions for B_b and f_b into equations (D-12) and (D-13) with the result

$$\left[f_{b_o}(\zeta)\dot{h}\left(B_{b_o}\right)B'_{b_o}(\xi) + \frac{3}{2}B_{b_o}(\xi)\right]''$$

$$+ \epsilon^{-1/2}\left[f_{b_o}(\xi)\dot{h}\left(B_{b_o}\right)B'_{b_1}(\xi) + f_{b_o}(\xi)\ddot{h}\left(B_{b_o}\right)B'_{b_o}(\xi)B_{b_1}(\xi)\right.$$

$$\left. + f_{b_1}(\xi)\dot{h}\left(B_{b_o}\right)B'_{b_o}(\xi) + \frac{3}{2}B_{b_1}(\xi)\right]''$$

$$+ \epsilon^{-1}\left[f_{b_o}(\xi)\dot{h}\left(B_{b_o}\right)B'_{b_2}(\xi) + \ldots\right]'' + \ldots = 0 \qquad \text{(D-29)}$$

$$\left\{2f_{b_o}(\zeta)f''_{b_o}(\zeta) - \left[f'_{b_o}(\zeta)\right]^2\right\} + \epsilon^{-1/2}\left\{2f_{b_o}(\zeta)f''_{b_1}(\zeta)\right.$$

$$\left. - 2f'_{b_o}(\zeta)f'_{b_1}(\zeta) + 2f''_{b_o}(\zeta)f_{b_1}(\zeta)\right\}$$

$$+ \epsilon^{-1}\left\{2f_{b_o}(\zeta)f''_{b_2}(\zeta) + \ldots\right\} + \ldots = 0 \qquad \text{(D-30)}$$

$$f_b(0) + \epsilon^{-1\ 2}\, f_{b_1}(0) + \epsilon^{-1}\, f_{b_2}(0) + \ldots = 0 \qquad \text{(D-31)}$$

$$\left\{\lim_{\zeta \to \infty} f_{b_o}(\zeta) - 1\right\} + \epsilon^{-1/2}\left\{\lim_{\zeta \to \infty} f_{b_1}(\zeta)\right\}$$

$$+ \epsilon^{-1}\left\{\lim_{\zeta \to \infty} f_{b_2}(\zeta) + \frac{a\zeta}{\sqrt{2X(1 - X)}}\right\} + \dots = 0 \tag{D-32}$$

$$B_{b_o}(0) + \epsilon^{-1/2} B_{b_1}(0) + \epsilon^{-1} B_{b_2}(0) + \dots = 1 \tag{D-33}$$

$$\left\{\lim_{\zeta \to \infty} B_{b_o}(\xi) - B_{a_o}\left(\tau_{\Delta_o}\right)\right\} + \epsilon^{-1/2}\left\{\lim_{\zeta \to \infty} B_{b_1}(\xi)\right.$$

$$\left. - B_{a_1}\left(\tau_{\Delta_o}\right) - \tau_{\Delta_1} B'_{a_o}\left(\tau_{\Delta_o}\right)\right\} + \epsilon^{-1}\left\{\lim_{\zeta \to \infty} B_{b_2}(\xi)\right.$$

$$- B_{a_2}\left(\tau_{\Delta_o}\right) - \tau_{\Delta_1} B'_{a_1}\left(\tau_{\Delta_o}\right) - \tau_{\Delta_2} B'_{a_o}\left(\tau_{\Delta_o}\right) - \xi B'_{a_o}\left(\tau_{\Delta_o}\right)$$

$$\left. - \frac{1}{2} \tau_{\Delta_1}^{2} B''_{a_o}\left(\tau_{\Delta_o}\right)\right\} + \dots = 0 \tag{D-34}$$

$$\left\{\lim_{\xi \to \infty} B'_{b_o}(\xi)\right\} + \epsilon^{-1/2}\left\{\lim_{\xi \to \infty} B'_{b_1}(\xi)\right\}$$

$$+ \epsilon^{-1}\left\{\lim_{\xi \to \infty} B'_{b_2}(\xi) - B'_{a_o}\left(\tau_{\Delta_o}\right)\right\} + \dots = 0 \tag{D-35}$$

Systems (D-19) to (D-24) and (D-29) to (D-35) lead to a set of recursive systems for the solution of B_{a_i}, f_{a_i}, B_{b_i}, and f_{b_i}.

<u>Zero-order solutions</u>.- The differential system which describes the asymptotic solutions to zero-order in the small parameter $\epsilon^{-1\,2}$ is

$$B''_{a_o}(\tau) = 0 \tag{D-36}$$

$$2f_{a_o}(\eta)f''_{a_o}(\eta) - \left[f'_{a_o}(\eta)\right]^2 + a^2\, h\left(B_{a_o}\right) = 0 \tag{D-37}$$

$$f_{a_o}(0) = 0 \tag{D-38}$$

$$f_{a_o}\left(\eta_{\Delta_o}\right) = 1 \tag{D-39}$$

$$f'_{a_o}\left(\eta_{\Delta_o}\right) = \frac{a}{\sqrt{2X(1 - X)}} \tag{D-40}$$

$$\frac{3}{2} k_P \int_0^{\tau_\Delta} B_{a_o}(t)e^{-\frac{3}{2} k_P|t-\tau|}\, dt - 2B_{a_o}(\tau) - \frac{3}{2} r_o e^{-\frac{3}{2} k_P\tau} = 0 \tag{D-41}$$

The solution is

$$B_{a_o}(\tau) = 0 \tag{D-42}$$

$$f_{a_o}(\eta) = \left(\frac{\eta}{\eta_{\Delta_o}}\right)^2 \tag{D-43}$$

$$\eta_{\Delta_o} = \frac{2\sqrt{2X(1 - X)}}{a} = 1 + \sqrt{2X(1 - X)} \tag{D-44}$$

$$\tau_{\Delta_o} = \frac{\eta_{\Delta_o}}{\kappa^{-1}(0)} \tag{D-45}$$

The zero-order boundary layer system is

$$f_{b_o}(\xi)\dot{h}\left(B_{b_o}\right)B'_{b_o}(\xi) + \frac{3}{2}B_{b_o}(\xi) = C_1^{(o)} + C_2^{(o)}\,\xi \tag{D-46}$$

$$2f_{b_o}(\zeta)f''_{b_o}(\zeta) - \left[f'_{b_o}(\zeta)\right]^2 = 0 \tag{D-47}$$

$$f_{b_o}(0) = 1 \tag{D-48}$$

$$\lim_{\xi \to \infty} f_{b_o}(\xi) = 1 \tag{D-49}$$

$$B_{b_o}(0) = 1 \tag{D-50}$$

$$\lim_{\xi \to \infty} B_{b_o}(\xi) = 0 \tag{D-51}$$

$$\lim_{\xi \to \infty} B'_{b_o}(\xi) = 0 \tag{D-52}$$

The solution to this system is

$$\xi = \frac{2}{3} \int_{B_{b_o}}^{1} \dot{h}(B) \frac{dB}{B} \tag{D-53}$$

$$f_{b_o}(\zeta) = 1 \tag{D-54}$$

<u>First-order solutions</u>.- The differential system which describes the asymptotic solutions to first order in $\epsilon^{-1\ 2}$ is

$$B''_{a_1}(\tau) = 0 \tag{D-55}$$

$$2\eta^2 f''_{a_1}(\eta) - 4\eta f'_{a_1}(\eta) + 4f_{a_1}(\eta) + 8X(1 - X)\dot{h}(0)B_{a_1}(\eta) = 0 \tag{D-56}$$

$$f_{a_1}(0) = 0 \tag{D-57}$$

$$f_{a_1}\left(\eta_{\Delta_o}\right) = -2\left(\frac{\eta_{\Delta_1}}{\eta_{\Delta_o}}\right) \tag{D-58}$$

$$f'_{a_1}\left(\eta_{\Delta_o}\right) = -2\left(\frac{\eta_{\Delta_1}}{\eta^2_{\Delta_o}}\right) \tag{D-59}$$

$$\frac{3}{2} k_P \int_0^{\tau_{\Delta_0}} B_{a_1}(t) e^{-\frac{3}{2}|t-\tau| k_P} dt - 2B_{a_1}(\tau) + \frac{3}{2} r_1 e^{-\frac{3}{2} k_P \tau}$$

$$+ \frac{3}{2} k_P \, \tau_{\Delta_1} B_{a_0}\left(\tau_{\Delta_0}\right) = 0 \qquad \text{(D-60)}$$

The system for determining $B_{a_1}(\tau)$ is identical to the system for obtaining $B_{a_0}(\tau)$. Therefore,

$$B_{a_1}(\tau) = 0 \qquad \text{(D-61)}$$

and equation (D-56) becomes

$$2\eta^2 f''_{a_1}(\eta) - 4\eta f'_{a_1}(\eta) + 4f_{a_1}(\eta) = 0$$

subject to the boundary conditions (D-57) and (D-58). Inspection of the preceeding equation indicates that condition (D-57) is satisfied automatically, so that another independent condition or equation must be specified in order to obtain a nonarbitrary solution for $f_{a_1}(\eta)$. This condition can be obtained from the differential system for terms of second order.

The system which determines the first-order boundary layer solutions is

$$\dot{h}\left(B_{b_0}\right) B'_{b_1}(\xi) + \ddot{h}\left(B_{b_0}\right) B'_{b_0}(\xi) B_{b_1}(\xi)$$

$$+ \frac{3}{2} B_{b_1}(\xi) = C_1^{(1)} + C_2^{(2)} \xi \qquad \text{(D-62)}$$

$$f''_{b_1}(\xi) = 0 \tag{D-63}$$

$$f_{b_1}(0) = 0 \tag{D-64}$$

$$\lim_{\zeta \to \infty} f_{b_1}(\zeta) = 0 \tag{D-65}$$

$$B_{b_1}(0) = 0 \tag{D-66}$$

$$\lim_{\xi \to \infty} B_{b_1}(\xi) = 0 \tag{D-67}$$

$$\lim_{\xi \to \infty} B'_{b_1}(\xi) = 0 \tag{D-68}$$

The solution to this trivial system is, of course,

$$B_{b_1}(\xi) = 0 \tag{D-69}$$

$$f_{b_1}(\xi) = 0 \tag{D-70}$$

Second-order solutions.- The differential system which determines the second-order asymptotic solution is

$$B''_{a_2}(\tau) = 0 \tag{D-71}$$

$$2\eta^2 f''_{a_2}(\eta) - 4\eta f'_{a_2}(\eta) + 4f_{a_2}(\eta) = -\eta^2_{\Delta_o}\left[2f_{a_1}(\eta)f''_{a_1}(\eta) - \left[f'_{a_1}(\eta)\right]^2 + a^2\dot{h}(0)B_{a_2}(\eta)\right] \tag{D-72}$$

$$f_{a_2}(0) = 0 \tag{D-73}$$

$$f_{a_2}\left(\eta_{\Delta_o}\right) = -\eta_{\Delta_1} f'_{a_1}\left(\eta_{\Delta_o}\right) - 2\left(\frac{\eta_{\Delta_2}}{\eta_{\Delta_o}}\right) - \left(\frac{\eta_{\Delta_1}}{\eta_{\Delta_o}}\right)^2 \tag{D-74}$$

$$f'_{a_2}\left(\eta_{\Delta_o}\right) = -\eta_{\Delta_1} f''_{a_1}\left(\eta_{\Delta_o}\right) - 2\,\frac{\eta_{\Delta_2}}{\eta^2_{\Delta_o}} \tag{D-75}$$

$$\frac{3}{2}k_P \int_0^{\tau_{\Delta_o}} B_{a_2}(t)e^{-\frac{3}{2}k_P|t-\tau|}\,dt - 2B_{a_2}(\tau) + \frac{3}{2}r_2 e^{-\frac{3}{2}k_P\tau}$$

$$+ \frac{3}{2}k_P\tau_{\Delta_1}B_{a_1}\left(\tau_{\Delta_o}\right) + \frac{3}{2}k_P\tau_{\Delta_2}B_{a_o}\left(\tau_{\Delta_o}\right)$$

$$+ \frac{3}{2}k_P e^{-\frac{3}{2}k_P\left(\tau_{\Delta_o}-\tau\right)}\int_0^{\epsilon\tau_\Delta}\left[B_{b_o}(\xi) - B_{a_o}\left(\tau_{\Delta_o}\right)\right]d\xi = 0 \tag{D-76}$$

The solution to this system is

$$B_{a_2}(\tau) = \frac{k_P\left(1 + r_w\right)\left[1 + \frac{3}{2}k_P\tau\right]}{2\left[1 + \frac{3}{4}\left(1 - r_w\right)k_P\tau_{\Delta_o}\right]} \tag{D-77}$$

The second condition for the quantity $f_{a_1}(\eta)$ can be obtained by evaluating equation (D-72) at $\eta = 0$, which gives

$$f'_{a_1}(0) = a\sqrt{\dot{h}(0)B_{a_2}(0)} \tag{D-78}$$

With this condition, the solution for $f_{a_1}(\eta)$ can be completely specified with the result

$$f_{a_1}(\eta) = a\sqrt{\dot{h}(0)B_{a_2}(0)}\left(\frac{\eta}{\eta_{\Delta_o}}\right)\left[1 - \left(\frac{\eta}{\eta_{\Delta_o}}\right)\right]\eta_{\Delta_o} \tag{D-79}$$

In addition

$$\eta_{\Delta_1} = - a\eta_{\Delta_o}^2 \sqrt{\dot{h}(0)B_{a_2}(0)} \tag{D-80}$$

and

$$\tau_{\Delta_1} = \frac{\eta_{\Delta_1}}{\kappa_p^{-1}(0)} \tag{D-81}$$

As before, it is necessary to look to the next higher order system in order to obtain a second independent condition or equation for $f_{a_2}(\eta)$. This condition is

$$f'_{a_2}(0) = 0 \tag{D-82}$$

In order to solve equation (D-72) for $f_{a_2}(\eta)$ it is necessary to express the optical path length τ as a function of η. This can be done with aid of the definitions of τ and η. The result is

$$\tau = \tau_{\Delta_o}\left(\frac{\eta}{\eta_{\Delta_o}}\right) + O(\epsilon^{-1}) \tag{D-83}$$

Now, equation (D-72) can be written in the form

$$2\eta^2 f''_{a_2}(\eta) - 4\eta f'_{a_2}(\eta) + 4f_{a_2}(\eta)$$

$$= -a^2 \eta_{\Delta_o} \dot{h}(0) \frac{3\left(1 + r_w\right) k_P^2 \tau_{\Delta_o}}{4\left[1 + \frac{3}{4}\left(1 - r_w\right) k_P \tau_{\Delta_o}\right]} \eta$$

The solution to this equation is

$$f_{a_2}(\eta) = \left[\left(\frac{\eta_{\Delta_1}}{\eta_{\Delta_o}}\right)^2 - 2\left(\frac{\eta_{\Delta_2}}{\eta_{\Delta_o}}\right) - A\,ln\ \eta_{\Delta_o}\right]\left(\frac{\eta}{\eta_{\Delta_o}}\right)^2$$

$$+ \left[A\,ln\ \eta_{\Delta_o}\right]\left(\frac{\eta}{\eta_{\Delta_o}}\right) + A\left(\frac{\eta}{\eta_{\Delta_o}}\right) ln\left(\frac{\eta}{\eta_{\Delta_o}}\right) \qquad \text{(D-84)}$$

where

$$A = a^2 \eta_{\Delta_o}^2 \dot{h}(0) \frac{3\left(1 + r_w\right) k_P^2 \tau_{\Delta_o}}{8\left[1 + \frac{3}{4}\left(1 - r_w\right) k_P \tau_{\Delta_o}\right]} = 3\left(\frac{\eta_{\Delta_1}}{\eta_{\Delta_o}}\right)^2 k_P \tau_{\Delta_o}$$

Also

$$\eta_{\Delta_2} = -\eta_{\Delta_o}\left(\frac{\eta_{\Delta_1}}{\eta_{\Delta_o}}\right)^2 \left[1 + \frac{3}{2} k_P\ \tau_{\Delta_o}\left(1 - ln\ \eta_{\Delta_o}\right)\right] \qquad \text{(D-85)}$$

and

$$\tau_{\Delta_2} = \frac{\eta_{\Delta_2}}{\kappa_P^{-1}(0)} + \eta_{\Delta_o} \frac{\left[\dot{\kappa}_P^{-1}(0)\right]}{\left[\kappa_P^{-1}(0)\right]^2} B_{a_2}(0)\left[1 + \frac{3}{4} k_P \tau_{\Delta_o}\right]$$

$$+ \int_o^{\epsilon\tau_{\Delta_o} + \epsilon^{1/2}\tau_{\Delta_1} + \tau_{\Delta_2}} \left[\frac{\kappa_P^{-1}\left(B_{b_o}(\xi)\right)}{\kappa_P^{-1}(0)} - 1\right] d\xi \qquad \text{(D-86)}$$

Radiative flux and standoff distance.- In chapter V, it was shown that with the substitute kernal approximation the radiant flux passing into the cold wall can be expressed in terms of the black body emissive power of the gas adjacent to the wall. Substituting the solution for $B_a(0)$ into this expression (5.5) gives

$$\frac{q_w^R}{1 - r_w} = \frac{1}{2\left[1 + \frac{3}{4}\left(1 - r_w\right) k_P \tau_{\Delta_o}\right]} \qquad \text{(D-87)}$$

The ratio of the shock standoff distance to the shock standoff distance for radiationless flow is given by the condition

$$\bar{\Delta} = \int_o^{\tau_\Delta} h(B)\kappa_P^{-1}(B)dt \qquad \text{(D-88)}$$

Expanding this expression in powers of $\epsilon^{-1/2}$ gives

$$\bar{\Delta} = \epsilon^{-1}\left\{ \eta_{\Delta_o}\left[\dot{h}(0) + h(0)\,\frac{\left(\dot{\kappa}_P^{-1}(0)\right)}{\kappa_P^{-1}(0)}\right] B_{a_2}(0)\left[1 + \frac{3}{4}\,k_P\,\tau_{\Delta_o}\right] + \int_0^{\epsilon\tau_{\Delta_o}+\epsilon^{1/2}\tau_{\Delta_1}+\tau_{\Delta_2}} h\left(B_{b_o}(\xi)\right)\kappa_P^{-1}\left(B_{b_o}(\xi)\right)d\xi \right\} \qquad \text{(D-89)}$$

APPENDIX E

LIST OF SYMBOLS

Symbol	Definition	Units
a	constant defined by equation (2.54)	none
a_n	n th-order coefficient in the perturbation expansion of the constant a	none
a^*	constant defined by equation (4.15)	none
B	black-body emissive power, $B = \frac{\sigma}{\pi} T^4$; chapter II only	erg/cm^2-ster-sec
B	nondimensional black-body emissive power; except for chapter II	none
B_λ	Planck function, defined by equation (2.11); chapter II only	erg/cm^3-ster-sec
B_λ	nondimensional Planck function; except for chapter II	none
$\bar{B}$	nondimensional black-body emissive power; chapter II only	none
$\bar{B}_\lambda$	nondimensional Planck function; chapter II only	none
B_o	$B_o(\eta) = B\left[h_o(\eta)\right]$	none
B_{λ_o}	$B_{\lambda_o}(\eta) = B_\lambda\left[h_o(\eta)\right]$	none

B_2	value of the nondimensional black-body emissive power in the interior of an optically thick shock layer	none
B_w	value of the nondimensional black-body emissive power in the gas adjacent to the wall in an optically thick shock layer	none
$\bar{B}$	constant definedin chapter V	none
$\dot{B}$	constant defined in chapter V	none
B_a	nondimensional black-body emissive power in the interior of a radiation depleted shock layer	
B_{a_n}	n th-order coefficient in the perturbation expansion of B_a	none
B_b	nondimensional black-body emissive power in the shock boundary layer in a radiation depleted shock layer	none
B_{b_n}	n th-order coefficient in the perturbation expansion of B_b	none
B^*	constant in formula (6.34)	none
b	constant defined by equation (5.26)	none
C_1	constant defined by equation (4.19)	none
C_1	constant of integration	none
C_2	constant of integration	none

c	velocity of light	cm/sec
E_n	exponential integral function of order n	none
F	nondimensional stream function defined by equation (3.31)	none
$\mathcal{F}_1$	function of h defined by equation (2.54)	none
$\mathcal{F}_2$	function of h defined by equation (2.54)	none
$\mathcal{F}_3$	function of h defined by equation (2.54)	none
f	nondimensional stream function defined by equation (2.35)	none
f_n	n th-order coefficient in the perturbation expansion of f	none
f_n^*	n th-order coefficient in the P-L-K expansion of f	none
f_a	nondimensional stream function in the interior of a radiation depleted shock	none
f_{a_n}	n th-order coefficient in the perturbation expansion of f_a	none
f_b	nondimensional stream function in the shock boundary layer in a radiation depleted shock layer	none

f_{b_n}	n th-order coefficient in the perturbation expansion of f_b	none
g	stream function; chapter II only	g/cm^2-sec
g	nondimensional stream function in the viscous boundary layer; defined by equation (2.85)	none
g_n	n th-order coefficient in the perturbation expansion of g	none
H	nondimensional enthalpy defined by equation (3.35)	none
h	static specific enthalpy; chapter II only	erg/g
h	nondimensional enthalpy; except for chapter II	none
h	Planck's constant	erg/sec
h_n	n th-order coefficient in the perturbation expansion of h, the nondimensional enthalpy	none
h_n^*	n th-order coefficient in the P-L-K expansion of h, nondimensional enthalpy	none
$h^{(n)}$	n th-order coefficient in the expansion of h, the static specific enthalpy; chapter II only	erg/g

$\bar{h}$	nondimensional enthalpy; chapter II only	none
$\bar{h}$	average value of h, the non-dimensional enthalpy; defined by equation (4.5)	none
$\bar{h}_n$	n th-order coefficient in the perturbation expansion of $\bar{h}$	none
h^*	value of h for which γ (the exponent in the correlation formula $\kappa_p(h) = Ch^\gamma$) changes	none
h_t	total enthalpy; chapter II only	erg/g
h_2	value of the nondimensional enthalpy in the interior of an optically thick shock layer	none
h_w	static specific enthalpy in the gas at wall conditions; chapter II only	erg/g
h_w	nondimensional enthalpy in the gas adjacent to the wall; except for chapter II	none
h_e	approximation to the ratio of convective heat transfer to the stagnation point in a radiating gas to that in a non-radiating gas	none
I	divergence of the radiant flux vector chapter II only	erg/cm^3-sec

I	nondimensional divergence of the radiant flux vector; except in chapter II	none
I	nondimensional divergence of the radiant flux vector; chapter II only	none
I_n	n th-order coefficient in the perturbation expansion of the nondimensional divergence of the radiant flux vector, I	none
$\tilde{I}$	nondimensional divergence of the radiant flux vector defined by equation (3.36)	none
i	nondimensional enthalpy in the viscous boundary layer; defined by equation (2.84)	none
i_n	n th-order coefficient in the perturbation expansion of i	none
J	nondimensional divergence of the radiant flux vector in the viscous boundary layer; defined by equation (2.87)	none
J_n	n th-order coefficient in the perturbation expansion of J	none

J_λ	specific intensity of radiation	erg/cm^3-ster-sec
j_λ	mass emission coefficient	erg/g-cm-ster-sec
k	Boltzmann's constant	erg/$^\circ$K
k_{eff}	effective coefficient of heat conduction including energy transport by molecular collisions and by diffusion of reacting species	erg/cm-sec-$^\circ$K
k_P	Bouguer number; $k_P = \rho_s \kappa_{P_s} \Delta_A$	none
l_i	direction cosine between the direction of a beam of intensity J_λ and the i th-direction	none
Pe	Peclét number	none
Pr	Prandtl number	none
p	pressure	dyne/cm^2
p_o	standard pressure of air, 1.013×10^6	dyne/cm^2
$p^{(n)}$	n th-order coefficient in the expansion p	dyne/cm^2
q_i	i th-component of the combined radiant and conductive heat fluxes	erg/cm^2-sec
$q_i^{(n)}$	n th-order coefficient in the expansion of q_i	erg/cm^2-sec
q^c	component of the conductive heat flux vector in the η-direction	erg/cm^2-sec

q_i^c	component of the conductive heat flux vector in the i th-direction	erg/cm^2-sec
q^R	component of the radiant heat flux vector in the η-direction	erg/cm^2-sec
q_i^R	component of the radiant heat flux vector in the i th-direction	erg/cm^2-sec
$q_{\lambda_i}^R$	component of the monochromatic radiant heat flux vector in the i th-direction	erg/cm^2-sec
q_w^R	nondimensional rate of radiant heat transfer to the wall	none
R	gas constant for air, 2.882×10^6	cm^2/sec^2-^{o}K
R_N	body nose radius	cm
R_s	shock radius in the vicinity of the stagnation streamline	cm
Re	Reynold's number	none
r	position coordinate	cm
r_{o_λ}	defined by equation (3.13)	none
r_{1_λ}	defined by equation (3.18)	none
r_w	reflectivity of the wall	none
S_λ	radiation source function	erg/cm^3-ster-sec
s	position coordinate	cm
s_λ	nondimensional variable of integration	none
T	temperature	^{o}K

T_o	standard temperature, 273.16	^oK
T_w	temperature of the wall	^oK
t_λ	nondimensional variable of integration	none
u	component of gas velocity in the r-direction	cm/sec
$u^{(n)}$	n th-order coefficient in the expansion of u	cm/sec
u_i	component of gas velocity in the i th-direction	cm/sec
V	volume	cm^3
W_∞	free-stream velocity	cm/sec
w	component of the gas velocity in the z-direction	cm/sec
$w^{(n)}$	n th-order coefficient in the expansion of w	cm/sec
x	coordinate in the transformed plane; chapter III	none
x	normalized Dorodnitsyn coordinate, $x = \eta/\eta_{\Delta_o}$; chapter IV	none
x_n^*	n th-order coefficient of the P-L-K expansion of x; chapter IV	none
x_o	value of the transformed coordinate for which $\eta = 0$; chapter III	none

y	coordinate in the transformed plane; chapter IV	none
z	position coordinate	cm
β	local angle of inclination of the bow shock from the stream direction	none
β_λ	mass extinction coefficient	cm^2/g
Γ	inverse Boltzmann number, $\Gamma = 4\sigma T_s^4 / \rho_\infty W_\infty^3$	none
γ	Euler's constant, $\gamma = 0.577216 \cdots$	none
γ_1, γ_2	exponents in the correlation formula for κ_p (equation (4.18))	none
Δ	shock standoff distance	cm
Δ_A	shock standoff distance for non-radiating shock layer	cm
$\bar{\Delta}$	ratio of shock standoff distance for radiating and nonradiating shock layer, $\bar{\Delta} = \Delta / \Delta_A$	none
δ	displacement distance for the viscous boundary layer	cm
δ	exponent in the correlation formula $B = h^\delta$	none
δ_n	n th-order coefficient in the perturbation expansion of the displacement distance, δ	cm

ϵ	radiation cooling parameter, $\epsilon = 4\sigma T_s^4 \, k_P / \rho_\infty W_\infty^3$	none
ζ	transformed nondimensional Dorodnitsyn coordinate in radiation depleted shock layer	none
ζ	transformed optical path length in optically thick shock layer	none
η	Dorodnitsyn coordinate defined by equation (2.34); chapter II only	g/cm^2
η	nondimensional Dorodnitsyn coordinate	none
$\bar{\eta}$	nondimensional Dorodnitsyn coordinate; chapter II only	none
η'	variable of integration	none
η_Δ	location of the shock in terms of the Dorodnitsyn coordinate; chapter II only	g/cm^2
η_Δ	nondimensional location of shock in terms of the Dorodnitsyn coordinate	none
$\bar{\eta}_\Delta$	nondimensional location of shock in terms of the Dorodnitsyn coordinate; chapter II only	none
η_{Δ_n}	n th-order coefficient in the perturbation expansion of η_Δ	none

η_n^*	n th-order coefficient in the P-L-K expansion of η	none
θ_n	constants defined by equations (B.11a) and (B.11b)	none
κ_λ	mass absorption coefficient; chapter II only	cm^2/g
κ_λ	nondimensional mass absorption coefficient	none
$\bar{\kappa}_\lambda$	nondimensional mass absorption coefficient; chapter II only	none
κ_P	Planck mean mass absorption coefficient; chapter II only	cm^2/g
κ_P	nondimensional Planck mean mass absorption coefficient	none
$\bar{\kappa}_P$	nondimensional Planck mean mass absorption coefficient; chapter II only	none
κ_{P_n}	n th-order coefficient in the perturbation expansion of κ_P	none
κ_R	Rosseland mean mass absorption coefficient	cm^2/g
λ	wavelength	cm
λ	boundary layer parameter, $\lambda = Pe_s^{-1/2}$	none
μ	coefficient of viscosity	dyne-sec$/cm^2$
μ'	second coefficient of viscosity	dyne-sec$/cm^2$

ξ	transformed nondimensional Dorodnitsyn coordinate in viscous boundary layer	none
ξ^*	thickness of the viscous boundary layer in terms of ξ	none
ρ	density	g/cm^3
ρ_o	standard density, 1.288×10^{-3}	g/cm^3
ρ_2	density in the interior of an optically thick shock layer	g/cm^3
$\rho^{(n)}$	n th-order coefficient in the expansion of ρ	g/cm^3
σ	Stefan-Boltzmann constant, 5.669×10^{-5}	$erg/cm^2\text{-}sec\text{-}{}^oK^4$
σ	area	cm^2
σ_λ	mass scattering coefficient	cm^2/g
σ_λ	transformed monochromatic optical path length in viscous boundary layer	none
σ_λ^*	thickness of the viscous boundary layer in terms of σ_λ	none
τ	optical path length in a gray gas; chapter II only	none
τ	normalized optical path length in a gray gas	none
$\bar{\tau}$	normalized optical path length in a gray gas; chapter II only	none

τ_λ	monochromatic optical path length; chapter II only	none
τ_λ	normalized monochromatic optical path length	none
$\bar{\tau}_\lambda$	normalized monochromatic optical path length ; chapter II only	none
$\tau_\lambda^{(s)}$	monochromatic optical path length in the s-direction	none
τ_λ^*	thickness of the viscous boundary layer in terms of τ_λ	none
τ_Δ	shock location in terms of τ	none
τ_{Δ_n}	n th-order coefficient in the perturbation expansion of τ_Δ	none
τ_{λ_Δ}	shock location in terms of τ_λ	none
τ_{ij}	component of the viscous stress tensor	$\mathrm{dyne}/\mathrm{cm}^2$
Φ_n	functions of η defined by equations (B.9a) and (B.9b)	none
ϕ_n	constants defined by equations (B.10a) and (B.10b)	none
χ	density ratio across the normal shock, $\chi = \rho_\infty/\rho_s$	none
ψ_n	constants defined by equations (B.12a) and (B.12b)	none

ω	solid angle	none
ω_1	constant defined by equation (5.22)	none
ω_2	constant defined by equation (5.30)	none

Subscripts

s	indicates value of dimensional quantity at normal shock equilibrium conditions
∞	indicates value of dimensional quantity in the free stream